Modélisation des interactions non covalentes avec des fonctionnelles non empiriques

Hanwei Li

▶ **To cite this version:**

Hanwei Li. Modélisation des interactions non covalentes avec des fonctionnelles non empiriques. Chimie théorique et/ou physique. Université Paris sciences et lettres, 2022. Français. NNT : 2022UPSLC005 . tel-04027035

HAL Id: tel-04027035
https://pastel.hal.science/tel-04027035v1

Submitted on 13 Mar 2023

HAL is a multi-disciplinary open access archive for the deposit and dissemination of scientific research documents, whether they are published or not. The documents may come from teaching and research institutions in France or abroad, or from public or private research centers.

L'archive ouverte pluridisciplinaire **HAL**, est destinée au dépôt et à la diffusion de documents scientifiques de niveau recherche, publiés ou non, émanant des établissements d'enseignement et de recherche français ou étrangers, des laboratoires publics ou privés.

PSL
UNIVERSITÉ PARIS

THÈSE DE DOCTORAT
DE L'UNIVERSITÉ PSL

Préparée à Chimie ParisTech

Modelling Non-covalent Interactions with Non-empirical Functionals

Soutenue par
Hanwei LI
Le 14 Septembre 2022

Ecole doctorale n° 388
Chimie physique et chimie analytique de Paris Centre

Spécialité
Chimie Physique

Composition du jury :

Juan-Carlos SANCHO-GARCIA Professor, University of Alicante	*Président*
Emilia SICILIA Professor, Università della Calabria	*Rapporteur*
Laurent JOUBERT Professeur, Université de Rouen	*Rapporteur*
Eric BRÉMOND Maître de conférences, Université Paris-Cité	*Examinateur*
Carlo ADAMO Professeur, Chimie ParisTech, Université PSL	*Directeur de thèse*

Chimie Paris ParisTech | PSL

Acknowledgments

Time flies and my three-year doctoral study life is coming to an end, countless people helped me during my Ph.D. time. Firstly, I would like to thank my dissertation director and supervisor, Carlo Adamo. I am extremely grateful to be his student and he continued to have faith in me over the three years. Thanks for his careful guidance from the thesis project selection, and conception to the final drafting, so that I could finally complete this dissertation. During my study, he gives me constructive advice when I met problems, and develop my critical thinking. His wealth of knowledge, rigorous academic attitude, keen academic thinking, and excellent work attitude are the role models for my lifelong learning, his academic spirit will always inspire me. Here, I would like to express my sincere thanks and best wishes to him. And I would also like to thank Dr. Eric Brémond for his continued support, invaluable guidance over the past three years. It's a great pleasure for me to work with him, his kindness, thinking calmly and patience influenced me a lot.

Thanks to my jury members, thanks them give the guidance of this thesis. Thanks to Professor Emilia's kind acceptance to be one of the jury members. Thanks to Professor Laurent Joubert, a member of my 'comite de suivi' from the first year until the end of my Ph.D., he gives me a lot of guidance and advice to make my thesis project works forward. Thanks to Professor Juan Carlos Sancho-Garcia's constructive suggestions during the thesis work.

I have enormous gratitude to all of the members of the CTM group, especially Bernardino Tirri, who helped me a lot. When I just came into the CTM group, he helped me quickly get used to the laboratory environment, taught me the basics of theory and computational operation. When I met the problems, he gave me timely help. It was with his enthusiastic help that I was able to quickly start my project. And many thanks to Laure, who has helped me a lot in my study and daily life in Paris, her optimistic character and encouragement have given me more confidence to face difficulties. Thanks to Carmen, Anna, Michele, Gabrielly, Laura, etc. influencing me with their optimism, and cheerfulness, which let me better integrate into this big CTM family. Thanks to Alistar's kind help when I met the computational problems, and thanks to Ilaria, Frederic, and Aureli's kindful help those 3 years. Gratitude to meet all of you, I have a great time during my Ph.D.

I would like to express my endless gratitude to my parents, they always help me out of difficulties and support me to go forward.

At last, many thanks China Scholarship Council (CSC) for the financial support.

Résumé

Introduction

Le concept d'interactions non covalentes (NCI) a été proposé pour la première fois par van der Waals au 19ème siècle alors qu'il travaillait sur l'amélioration de l'équation des gaz parfaits. Elle était autrefois appelée par Lehn "la chimie au-delà de la molécule" et est un type typique d'interaction faible. Contrairement à la liaison covalente classique qui conduit à la formation de molécules, la force de liaison non covalente ne partage pas d'électrons pendant le processus de formation, mais il existe une force électromagnétique changeante entre ou à l'intérieur de la molécule, ce qui conduit à la formation d'amas moléculaires. Les interactions non covalentes ne sont généralement que d'environ quelques dizaines de kilocalories par mole, cette interaction faible est facilement détruite dans des circonstances normales. Bien qu'une interaction non covalente soit très faible, la plupart des réactions impliquent un ou plusieurs types d'interactions non covalentes, l'addition ou la synergie de plusieurs liaisons non covalentes peut modifier les forces intermoléculaires de sorte que la structure associée devient très stable.

Les interactions non covalentes sont omniprésentes au cours des réactions chimiques et ont un large éventail d'impacts sur l'apparition et le développement de la pollution environnementale, la génération et les propriétés des molécules matérielles, le métabolisme et les effets des médicaments dans les sciences de la vie. Jusqu'à présent, de nombreux types d'interactions non covalentes ont été découverts, parmi lesquelles on trouve les liaisons hydrogène, les interactions C-H…π, les interactions O-H…π, les interactions S…π, les interactions d'empilement π-π, les interactions de van der Waals, les interactions hydrophobes, etc.

Bien que de nombreuses méthodes existantes aient obtenu de bons résultats dans le calcul des interactions non covalentes, ces méthodes rencontrent encore des difficultés et des défis dans les applications pratiques, qui sont résumées comme suit :

a) La difficulté des méthodes de calcul : en raison des méthodes expérimentales nécessitant beaucoup de ressources, la plupart des méthodes actuelles utilisées pour obtenir les

énergies d'interaction non covalentes sont des méthodes de calcul de chimie quantique, telles que les méthodes *ab initio* ou de la théorie de la fonctionnelle de la densité (DFT), etc. Ces méthodes exigent que les chercheurs aient une solide connaissance préalable du problème de recherche, afin de sélectionner les méthodes de calcul appropriées. Dans le même temps, la coopération de différentes méthodes et de différents ensembles de bases a une grande influence sur la précision du calcul.

b) La limite des calculs supramoléculaires : les résultats obtenus au niveau du « golden standard » CCSD(T) sont relativement précis, cependant, le coût de calcul et les ressources nécessaires sont élevés. La théorie de la fonctionnelle de la densité permet de diminuer ce coût au détriment de la précision sur les énergies d'interactions non covalentes entre les macromolécules.

c) L'absence de méthodes de calcul simultané de différents types d'interactions non covalentes : de nos jours, la plupart des méthodes de calcul sont spécialement développées pour un certain type d'interaction non covalente.

Dans ce travail de thèse, nous avons mis en place un schéma de calcul pour décrire les propriétés non covalentes en utilisant des fonctionnelles double-hybrides non empiriques dans la modélisation des interactions de dispersion présentes dans de grands systèmes moléculaires. Dans un premier temps, la réaction isodesmique servira de premier jeu de données pour tester le protocole établi, puis ce protocole sera étendu à d'autres ensembles tels que l'ensemble BSR36 et AAA, etc. Les résultats obtenus pour chaque jeu de données sera analysé et rationnalisé par les outils de chimie théorique. Dans un second temps, nous avons étendu la base DH-SVPD au système halogène afin de quantifier le plus d'atomes possible. Enfin, un benchmark de fonctionnelle a été réalisé sur les réactions organiques en plusieurs étapes, ici les réactions péricycliques. Ceci dans le but de mieux comprendre le comportement de chacune et de développer dans un futur proche une fonctionnelle qui combinerait le meilleur de chacune.

Méthodes

Dans cette thèse, nous avons utilisé la base DH-SVPD avec différents échelons des fonctionnelles. Cet ensemble de base a été développé à partir de la petite base Def2-SVPD et en optimisant les fonctions les plus diffuses (une fonction « *p* » et « *d* » pour l'atome de Carbone et une fonction « *s* » et « *p* » pour l'atome d'hydrogène) afin de minimiser l'expression suivante (Equation 1) pour le dimère de benzène :

$$\mathcal{F} = \left[\frac{(E - E^0) - (J + K)}{(E - E^0) + (J + K)}\right]^2 \qquad (1)$$

avec E l'énergie totale du dimère, J et K sont les énergies de Coulomb et d'échange correspondantes et E^0 est l'énergie totale du benzène isolé. Cette procédure conduit à l'optimisation de l'énergie d'interaction d'un dimère telle qu'exprimée dans une théorie de perturbation d'ordre zéro, sans la nécessité de données de référence externes provenant, par exemple, de l'expérience de méthodes post-HF précises, une pratique courante en chimie computationnelle. En pratique, cette procédure est basée sur une compensation d'erreur entre l'erreur de superposition d'ensemble de base (BSSE) et l'erreur d'incomplétude d'ensemble de base (BSIE). Ces erreurs sont non seulement strictement intriquées, mais agissent de manière opposée, les premières conduisant à une surestimation des énergies d'interaction dans les systèmes faiblement liés, tandis que les secondes conduisent à une sous-estimation de ces énergies.

Afin de vérifier la précision de la base HD-SVPD, les résultats calculés par la base DH-SVPD ont été comparés à ceux obtenus par les bases de Dunning, cc-pVTZ et cc-pVQZ, les bases de Karlsruhe Def2-TZVPP, Def2-QZVP, etc.

Un certain nombre d'échelons différents des fonctionnelles d'échange-corrélation ont été également considérés, semi-local (M06-L…), hybride global (M06, TPSSh, PBE0, B3LYP, CAM-B3LYP, ωB97XD14…) et double-hybride (B2PLYP, DSD-PBEP86, PBE0-DH and PBE-QIDH, revDSD-PBEP86…). Dans certains cas, des potentiels empiriques, tels que les modèles D3 et D3(BJ), ont également été ajoutés.

Résultats

Au-delà de la précision chimique pour la thermochimie des alcanes : l'approche DH*thermo*

En considérant un système hydrocarboné, nous proposons une étude sur le problème de proto-ramification des alcanes, pour lequel les alcanes ramifiés sont plus stables que les alcanes linéaires. La réaction s'écrit sous la forme :

$$(m\text{-}1)\ C_2H_6 \rightarrow C_mH_{2m+2} + (m\text{-}2)\ CH_4$$

Cette réaction est connue sous le nom *de Bond Separation Reaction* (BSR), ici, nous n'entrerons pas dans les détails sur la raison d'origine de ce problème, qui n'est pas le point principal de la présente thèse. Il convient aussi de souligner que cette réaction a été utilisée pour le benchmark des modèles DFT au fil des ans, car elle a l'avantage intrinsèque de préserver le nombre et le type de liaisons, évitant ainsi le calcul de systèmes à couche ouverte comme dans le cas des énergies d'atomisation. La plupart des approches DFT actuelles fournissent également des erreurs importantes sur la thermochimie des BSR. L'inclusion de corrections empiriques produit un effet bénéfique, mais la précision chimique n'est pas systématiquement atteinte même par les fonctionnelles DH. Il serait donc intéressant de tester notre protocole, couplant DHs et la base sur mesure DH-SVPD dans un contexte aussi difficile, puisque les effets de corrélation non locales et les interactions de dispersion, sont au cœur du développement de cette base.

En résumé, une précision sur les énergies BSR au-delà du seuil communément admis pour les applications chimiques (erreurs ≤ 1,0 kcal/mol) peut être obtenue en utilisant un protocole combinant une fonctionnelle double-hybride, comme PBE-QIDH ou B2PLYP, avec une la correction empirique D3 et un petit jeu de base de valence divisée, DH-SVPD, développé pour les interactions non covalentes. Ce protocole, nommé DH*thermo*, qui n'est pas adapté aux systèmes sélectionnés, est capable de reproduire correctement, avec des erreurs exceptionnellement faibles, à la fois les énergies de réaction et les enthalpies pour les réactions isodesmiques sélectionnées, les résultats obtenus, vérifiés sur cinq jeux de données de référence différents (deux jeux de données théoriques et trois expérimentaux), démontrent clairement sa qualité. Et le protocole DH*thermo* a l'avantage de sa simplicité intrinsèque et de sa simplicité d'utilisation.

Associer des fonctionnelles double hybrides doubles à un jeu de base sur mesure pour une thermochimie précise des hydrocarbures

Ici, nous souhaitons étendre davantage notre étude à d'autres hydrocarbures de taille moyenne compris dans des ensembles de données sélectionnés, pour lesquels des valeurs de référence précises sont disponibles. Ces ensembles (vide *infra*) ont été choisis pour montrer une plus grande diversité de situations chimiques, y compris de multiples liaisons carbone-carbone, une grande délocalisation électronique et, bien sûr, des interactions non covalentes faibles.

L'objectif est de vérifier les limites des méthodes DHs modernes dans la modélisation de la thermochimie des hydrocarbures, qui joue un rôle central en chimie expérimentale et

théorique. Ainsi, cinq ensembles différents ont été considérés comme point de référence, y compris les hydrocarbures saturés, insaturés et aromatiques

Dans les deux premiers ensembles, ADIM6 et AAA, dominés par des interactions de dispersion intermoléculaires, la combinaison des fonctionnelles PBE-QIDH avec l'ensemble de base DH-SVPD fournit essentiellement les mêmes déviations obtenues avec des ensembles de base plus grands et des potentiels empiriques. Les autres fonctionnelles double-hybride se comportent de la même manière. Cette tendance est également observée pour le jeu de données IDHC5 qui contient également des réactions d'isomérisation avec des modifications modérées des structures électroniques. Pour ces trois ensembles de données, la petite base ne peut pas être utilisée en conjonction avec un potentiel empirique, car elle conduit à une sorte de double comptage des interactions de dispersion et à une surestimation conséquente des énergies de réaction.

Passant au jeu de données PAH5, les résultats obtenus montrent que la petite base est capable de d'identifier les modifications de la structure électronique observées en passant d'un isomère à un autre. Le dernier ensemble, Cope, révèle un comportement différent avec la base DH-SVPD donnant des déviations plus élevées que la base triple-ζ. Cela pourrait être lié aux caractéristiques particulières des intermédiaires de réaction, qui n'ont pas le même nombre et le même type (double, triple) de liaisons. En effet, la base DH-SVPD fournit des résultats très précis pour les réactions dîtes de séparation des liaisons, où la thermochimie des réactions sélectionnées est évaluée avec un principe isodesmique qui conduit à la préservation du nombre et du type de liaisons intramoléculaires. La situation est encore plus complexe du fait de l'absence d'effets de dispersion pour ces réactions. Cela rend l'ensemble Cope très particulier dans le contexte de cette étude, mettant en évidence les limites de la combinaison d'une DH avec la base DH-SVPD développée dans ce travail. Cependant, il convient également de remarquer que le temps de calcul d'une fonctionnelle DH couplée à cette petite base est équivalent à celui d'une fonctionnelle DH avec une base triple-ζ, plus importante en taille. En effet l'utilisation d'un jeu de base plus petit compense largement le temps de calcul supplémentaire nécessaire pour le traitement de la partie perturbative de PBE-QIDH.

Pour éviter tout biais provenant de la nature et du nombre de données différentes des ensembles considérés, la déviation moyenne absolue (« *Mean Absolute Deviation* ») a été déterminée. Ces MAD sont simplement la moyenne mathématique de celles calculées pour les différents ensembles, c'est-à-dire leur somme divisée par 6 (en comptant la réaction et les barrières pour le Cope autrement). La première caractéristique frappante concerne les

fonctionnelles PBE0-DH et B2-PLYP, qui n'atteignent pas le seuil de 1 kcal/mol, même si une amélioration significative est constatée avec l'emploi de base plus large tel que DH-SVPD. Comme déjà discuté, toutes les foncionnelles DH comprenant une dispersion empirique couplé à un jeu de base plus large conduit à des résultat de grande précision chimique. En revanche, les combinaisons PBE-QIDH/DH-SVPD sont compétitives avec ces dernières. En bref, les valeurs les plus faibles sont obtenues avec PBE-QIDH/DH-SVPD ou en combinant PBE-QIDH-D3(BJ), DSD-PBEP86 et rev-DSDPBEP86-D3(BJ) avec une base plus large, tous ces modèles fournissant une signifie MAD autour de 0,5 kcal/mol. Il est rassurant de constater que sur un tel indicateur de performance globale, le modèle PBE-QIDH-D3(BJ)/DH-SVPD, qui est notre modèle DH*thermo* pour la thermochimie des alcanes, est parmi les plus performants, étendant ainsi son applicabilité au-delà des réactions isodesmiques.

Aborder une description précise de la réactivité moléculaire avec des fonctionnelles à double densité hybride

Dans ce travail, nous évaluons un panel de 18 fonctionnelles double hybride pour la modélisation des propriétés thermochimiques et cinétiques d'un jeu de données étendu de 449 réactions de chimie organique (868 Bond Heights (BHs) et 434 Reaction Energies (Res)) appartenant à la base de données BH9, nous montrons que les DH peuvent fournir une réponse statistiquement vérifiée et précise à la problématique de modélisation cinétique et thermochimique. Sur l'ensemble des BHs et REs, les DH paramétrés au minimum comme wB2PLYP ou B2K-PLYP, et les DH non empiriques comme PBE0-DH et PBE-QIDH réussissent à atteindre le seuil d'énergie de "précision chimique" de plus de 40 % pour les deux propriétés de manière équilibrée. Ce succès correspond à des MAD inférieures à 2,5 kcal/mol. D'autres DH hautement paramétrées wB97X-2 ou DSD-PBEP86-D3(BJ) et DSD-BLYP-D3(BJ) à l'échelle des composants de spin fournissent également une excellente estimation des propriétés REs. Leurs performances restent toutefois inférieures aux attentes probablement en raison de leur paramétrisation empirique. De plus, nous remarquons que le couplage d'une correction de dispersion empirique comme -D3(BJ) à une DH tend à détériorer sa précision. Contrairement aux fonctionnelles d'échange-corrélation semi-locales ou hybrides plus standards, nous déconseillons donc leur utilisation pour ce type d'étude.

Hybrides doubles et interactions non covalentes : jusqu'où peut-on aller ?

L'évaluation précise des interactions non covalentes faibles dans les grands systèmes moléculaires, c'est-à-dire contenant jusqu'à mille atomes, représente un défi difficile pour toute

méthode de chimie quantique. En effet, certaines approximations sont souvent introduites pour rendre abordables ces calculs. Ici, nous considérons le protocole PBE-QIDH/DH-SVPD, combinant une fonction double hybride non empirique (PBE-QIDH) couplé à une petite base (DH-SVPD) adaptée aux interactions non covalentes avec pour objectif : i) d'explorer la robustesse et la précision de ce protocole par rapport à d'autres approximations de DFT ; ii) d'illustrer comment ses performances sont affectées par les paramètres de calcul sous-jacents au calcul de l'échange exact et de la contribution coulombienne, ainsi que par le terme perturbatif. Pour cela, nous considérons trois jeux de données, à savoir S66, L7 et CiM13, incorporant des molécules de taille croissante.

Nos résultats suggèrent que le protocole PBE-QIDH/DH-SVPD est particulièrement précis pour les grands systèmes tels que ceux contenus dans l'ensemble CiM13 (jusqu'à plus de 1 000 atomes et 14 000 fonctions de base), pour lesquels l'approximation DLPNO conduit à une accélération significative de l'évaluation du terme de corrélation perturbative.

Cependant, notre analyse pointe aussi la limite de cet exercice statistique, lorsque la qualité des données de référence ne peut être facilement appréciée, du fait de la taille des complexes moléculaires impliqués, et lorsque le nombre de molécules est limité.

Liaisons halogènes et doubles fonctionnelles hybrides : une évaluation rapide avec un petit jeu de base dédié

Décrire précisément le phénomène d'interactions non covalentes de Halogen Bonding (HB) est l'un des principaux défis pour les méthodes théoriques car il doit correctement prendre en compte toutes les interactions électrostatiques non covalentes, les dispersions, les polarisations, etc. Ici, nous avons élargi la petite base DH-SVPD définie sur les atomes d'halogène en optimisant les dimères CH_4X_2 (X = F, Cl, Br, I) et CH_3ClCH_2O (pour optimiser l'atome O) extraits de X40 défini à la base de la base Def2-SVPD adapté aux interactions non covalentes. Les ensembles de base sont ensuite testés sur 3 benchmarks standards, les résultats obtenus montrent que cet ensemble de base DH-SVPD peut atteindre la soi-disant « précision chimique » (< 1,0 kcal/mol) avec la fonctionnelle PBE-QIDH sur chaque ensemble testé, fournir des résultats précis pour les énergies HB dans tous les ensembles considérés lors de l'utilisation de fonctionnelles Double Hybrid (DH), peut récupérer les performances des fonctionnelles DH dans la reproduction des énergies d'interaction de la coulée HB avec des corrections de dispersion empiriques.

Modélisation de réactions organiques en plusieurs étapes : les calculs DFT peuvent-ils produire une chimie trompeuse ?

En chimie organique multi-étapes, expliquer correctement les mécanismes de réaction et quelle étape est l'étape à vitesse déterminée est essentiel pour comprendre les mécanismes complexes et la conception nouveaux composés. L'utilisation d'approches de chimie quantique et de données expérimentales pour soutenir la faisabilité des mécanismes de réaction dans le cas de phénomènes chimiques complexes est le meilleur moyen d'améliorer l'efficacité de la synthèse. Cependant, différents calculs employant la peuvent donner des réponses différentes. Les réactions péricycliques en sont des exemples typiques et des algorithmes et méthodes spécifiques ont été développés pour suivre ces chemins réactionnels complexes et caractériser les points de bifurcation. Il est clair qu'une description fiable, même qualitative, du chemin de réaction complexe de cette réaction ambimodale prototypique représente un défi difficile pour les approches DFT. En utilisant une série de différentes fonctionnelles pour étudier la réaction ambimodale, il a été constaté que la différence d'énergie dans les réactions ambimodales est liée aux erreurs de délocalisation, c'est-à-dire la surdélocalisation non physique de la distribution électronique, est un inconvénient commun résultant de la nature approximative de l'échange -fonctionnelles de corrélation. On pourrait alors soutenir que la différence d'énergie est presque constante le long d'un chemin de réaction reliant des espèces avec le même nombre de doubles liaisons, alors qu'elle varie si les intermédiaires ont un degré de conjugaison différent.

Table of Contents

Chapter 1

Introduction and thesis framework

1.1 Introduction

The concept of non-covalent interactions (NCIs) was first proposed by van der Waals in the 19th century and it's known as weak interaction. Unlike the classical covalent bond that leads to the formation of molecules, the non-covalent bond force does not share electrons during the molecule formation process, but there is a changing electromagnetic force between or within the molecule, which leads to the formation of molecular clusters. Non-covalent interactions are generally only about a few to tens of kilocalories per mole (kcal/mol), this weak interaction is easily destroyed under normal circumstances. Although the non-covalent interaction is very weak, most of the reactions involve one or more types of non-covalent interactions, addition or synergy of multiple non-covalent bonds can change the intermolecular forces so that the associated structure becomes very stable. For example, the stable spherical structure of protein molecules and the firm double helix chain of DNA molecules are all the result of non-covalent interactions.

Non-covalent interactions are ubiquitous in the process of chemical reactions and have a wide range of impacts in many disciplines, such as the environmental pollution and protection, the generation and properties of material molecules, and drug effects in life sciences. So far, many types of non-covalent interactions have been discovered, as shown in Figure 1.1. There are hydrogen bonds, C-H…π interactions, O-H…π interactions, S…π interactions, π-π stacking interactions, van der Waals interactions, hydrophobic interactions, halogen bonds, phosphorus bonds, sulfur bonds, etc. Therefore, due to their intrinsic complexity, the understanding of NCIs is quite limited.

At present, quantum chemical methods are commonly used to theoretically study weak intermolecular interactions. Quantum chemistry is a discipline that applies the principles and methods of quantum mechanics to study chemical problems. It mainly studies the structural

properties of molecules, as well as intermolecular interactions and collisions. The basic principle of quantum chemistry is to solve the Schrödinger equation to obtain the relevant properties such as the energy of the molecule and the state of motion of its electrons.

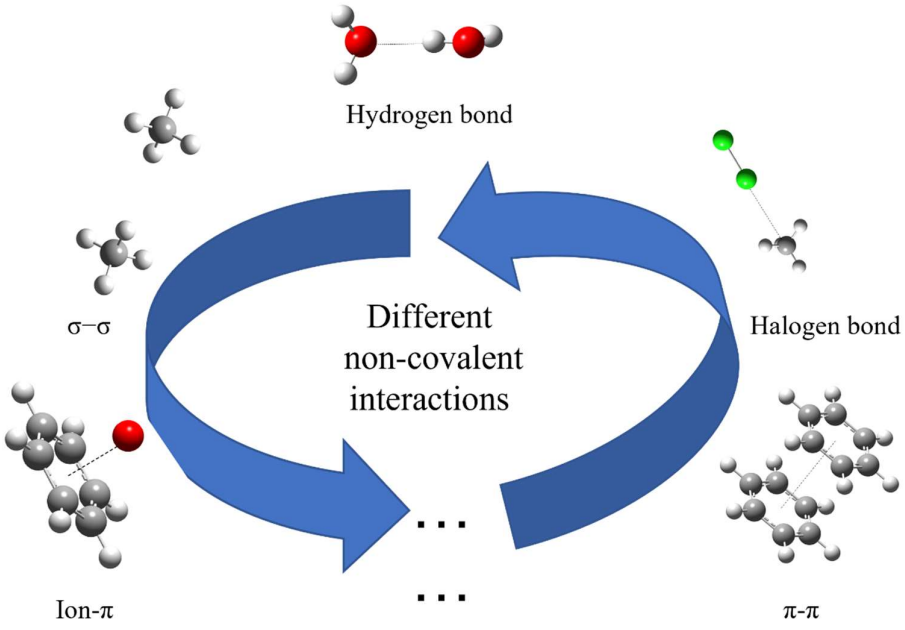

Figure 1.1 Different types of the non-covalent interactions

With the development of the quantum chemistry, the wavefunction-based methods ranging from the basic Hartree-Fock (HF) method to the "gold standard" coupled-cluster theory. In Hartree product, the electronic structure calculations for many-electron systems are considered as a product of wavefunctions of non-interacting electrons. As a consequence, this approximation gives a large difference of the computed energy from the exact energy, this energy difference is known as the correlation energy. Inclusion of the anti-symmetry principle in the HF method via Slater determinant corrects the wavefunctions and energies for the correlation between electrons having parallel spins. The electronic correlation corresponding to this is known as the Fermi correlation, while the correlation between the electrons having opposite spin is sometimes called Coulomb correlation.

Configuration interaction (CI) techniques further improve the wavefunction by representing it as a linear combination of ground and excited configuration state functions (CSFs) or Slater determinants. Another approach to account for electron correlations in many-

electron systems is to use many-body perturbation theory, Møller and Plesset proposed perturbative treatments (MP*n*) to evaluate the electronic energies. While MP*n* couldn't give the accurate results for the geometries far from the equilibrium and excited electronic states, several other methods have been proposed to improve the accuracy of such perturbative treatments, such as the coupled-cluster methods, the electron correlation is taken care of by the exponential cluster operator. The couple-cluster with single and double (triple) excitations (CCSD(T)) method incorporates a complete treatment of single and double excitations while perturbatively estimating the contribution from triples is often considered as the "gold standard" of molecular quantum chemistry.

Although the wavefunction-based methods are accurate, their implementation requires enormous computational resources even for the not large molecules. The chemical investigations can be supported theoretically by calculating the molecular structures, conformer ensembles, reaction energies, barrier heights, non-covalent interactions, and so on. Over the past few decades, Density Functional Theory (DFT) is the most often used method in many standard quantum chemistry software packages. The success of DFT can be attributed to the favorable balance between computational cost and accuracy, along with the existence of efficient algorithmic implementations widely available in modern software packages.

Currently, several available DFT methods have achieved good results in the calculation of non-covalent interactions, these methods still face some difficulties and challenges in practical applications, which are summarized as follows:

a) Difficulty of calculation methods: due to the experimental methods requiring a lot of resources, most of the current methods that have been used for obtaining non-covalent interaction energies are quantum chemical calculation methods, such as ab initio methods, density functional theory, etc. These methods require researchers to have strong prior knowledge of the research problem, so as to select suitable computational methods. At the same time, the cooperation of different methods and different basis sets has a great influence on the calculation accuracy.

b) Limitations of supramolecular calculations: the results get at the "golden standard" CCSD(T) level are relatively accurate, however, the computational cost is expensive. These calculations of supramolecules require a highly demanding computational resource, and the common hardware resources cannot satisfy these calculations. If the lower level of the density functional theory method is used, it is possible to calculate the non-covalent interactions between macromolecules at the expense of accuracy.

c) Lack of methods for simultaneous calculation of different kinds of non-covalent interactions: nowadays, most of the calculation methods are specially developed for a certain type of non-covalent interaction. For example, the DOD-PBEP86-NL method only corrects for non-local van der Waals interactions. If one quantum chemical calculation method is used to calculate different types of non-covalent interactions, the overall accuracy cannot be guaranteed.

As a result, several studies have focused on curing these problems, in DFT, one of the main contents in DFT is the choice of exchange-correlation functional approximation, which determines the accuracy of a given DFT method for a particular purpose. Such applications normally performed by choosing an appropriate functional, and, typically, a relatively large basis set. However, it is well known that this applications are unable to accurately describe dispersion forces, which are critical when modeling non-covalent interactions and chemical reactions involving large molecules due to the deficiencies of density-functional approximation and limited basis set. Based on these deficiencies, normally, here are 2 different ways to develop the DFT, like the empirical functionals, the number of functionals and the number of parameters have proliferated, and often dozens of parameters are fitted to dozens of databases, with thousands of benchmark data. While in the non-empirical functionals, the parameters are based on the physical approximations, not obtained by fitting to experimental data.

In this thesis work, we set up the computational scheme to describe the non-covalent properties by using non-empirical double-hybrid functionals in modeling dispersion interactions in large molecular systems. Once this protocol is set up, we will consider Bond Separation Reaction (BSR) as the first dataset to test, then verify the protocol in the standard benchmark BSR36 set, five medium challenging systems, thermochemical and kinetic properties of the BH9 set, and the large system CiM13 dataset those difficult systems to study. From the results we obtained, we will systematically try to explain the observed phenomena in theoretical insights. Then we carefully extend the DH-SVPD basis set to the Halogen system to quantify as many as possible the atoms.

1.2 Thesis framework

The work presented in this manuscript is organized in 8 chapters.

Chapter 2 presents a brief overview of the backgrounds and methods of the theory used in this thesis. It contains the different methods to solve the Schrödinger equation. Particularly,

a more detailed description of the Double Hybrid Density Functional Theory (DH-DFT) which is the main method used in this work.

In the 3rd chapter, the study of the thermochemistry of hydrocarbons is presented. In the beginning, the results of Bond Separation Reactions (BSR) with several functionals (global hybrid, double hybrid functionals) at different basis sets (cc-pVTZ, cc-pVQZ, and DH-SVPD basis sets) are presented. Based on the results, the DH*thermo* protocol was proposed, then followed by this protocol have been tested on 5 subsets (AAA, ADIM6, IDHC5, PAH5, and Cope). Those theoretical results are presented and discussed.

In chapter 4, we compared the DH-SVPD basis set with several DH functionals to study the thermochemistry and kinetics properties of the BH9 database. And showed that most of DHs provide a statistically robust performance to model barrier height and reaction energies in reaching the 'chemical accuracy'.

In chapter 5, we investigated PBE-QIDH this double-hybrid functionals together with DH-SVPD this tailored basis set from the medium-sized sets of S66 and L7 to the large set CiM13, explore the robustness and accuracy of PBE-QIDH/DH-SVPD this protocol.

In chapter 6, we develop the DH-SVPD basis set to the halogenated molecules based on optimized CH_4X_2 (X=F, Cl, Br, I) extracted from the X40 set. The influence of this enlargement basis set has also been investigated through both global and double hybrid functionals by testing on 3 standard benchmarks (X_2/CH_4-Bz, HXB, X40×10). The results are described in detail.

In chapter 7, we used series of functionals to study the cycloadditions of cyclopentadiene and cycloheptatriene with tropones for those [6+4] cycloaddition reactions, to find the influences of those different functionals on those reactions. The results are described in detail.

Finally, in chapter 8, we conclude and present some possible future developments, proposing a global and critical analysis of the problems that we studied, and providing some suggestions or comments for improving the related fields.

Chapter 2

Theoretical background and methods

2.1 Context

This chapter is devoted to the theoretical background of the present thesis. In the first section, a general overview concerning the Quantum Mechanics (QM) methods will be presented. After a general introduction, a detailed description of Hartree-Fock (HF) and Density Functional Theory (DFT) will be given, also introducing the Double Hybrid Functionals, the different methods to explain the non-covalent interactions also introduced.

2.2 The Schrödinger equation

Under the non-relativistic approximation, to determine the electronic structure and properties of the possible stable states of a molecule, the Schrödinger equation must be solved. The time-independent form of the Schrödinger equation is ion as follows:

$$\hat{H}\Psi = E\Psi \qquad (2.2.1)$$

$\hat{H}$ represents the Hamiltonian operator, ψ is the multi-electron wave function and E is the energy associated with the system. To solve the Schrödinger equation, it needs to find the eigenvalue E and the corresponding wavefunction ψ.

The molecular Hamiltonian operator, in atomic units, presents in this form (the numerical values of electrons mass m_e, of the reduced Planck's, constant ħ and of the Coulomb constant $e^2/4\pi\varepsilon_0$ are all equal to one):

$$\hat{H} = \hat{H}_e + \hat{H}_N + \hat{V}_{Ne} + \hat{V}_{ee} + \hat{V}_{NN} \qquad (2.2.2)$$

The first and second terms describe the kinetic energy of electrons and nuclei, respectively.

For a system containing N electrons and M nuclei, $\hat{T}_e$ and $\hat{T}_N$ can be expressed as:

$$\hat{T}_e = -\frac{1}{2}\sum_{i=1}^{N}\nabla_i^2 \qquad (2.2.3) \qquad ; \qquad \hat{T}_N = -\frac{1}{2}\sum_{A=1}^{M}\frac{\nabla_A^2}{M_A} \qquad (2.2.4)$$

Where M_A is the mass of the nuclei A and ∇^2 is the Laplacian operator.

The remaining terms $\hat{V}_{Ne}$, $\hat{V}_{ee}$ and $\hat{V}_{NN}$ are the potential energy operators of the nuclei-electron electrostatic interaction, the electronic repulsion and the nuclear repulsion, respectively. Those can be expressed as:

$$\hat{V}_{Ne} = -\sum_{i=1}^{N}\sum_{A}^{M}\frac{Z_A}{r_{iA}} \qquad (2.2.5);$$

$$\hat{V}_{ee} = \sum_{i=1}^{N}\sum_{j>i}^{N}\frac{1}{r_{ij}} \qquad (2.2.6);$$

$$\hat{V}_{NN} = \sum_{A}^{M}\sum_{A>B}^{M}\frac{Z_A Z_B}{r_{AB}} \qquad (2.2.7)$$

with r_{iA}, r_{ij} and r_{AB} are the electron i - nuclei A, electron i - electron j and nuclei A- nuclei B distances, respectively. Z_A and Z_B are the nuclear charge of the nuclei A and B.

The equation (2.2.2) can only be solved analytically in the case of a hydrogen atom in which there is only one electron, when the electron-electron repulsion term (multielectron system) is present, some approximations are needed.

2.2.1 The Born-Oppenheimer approximation

The Born-Oppenheimer approximation[1] introduces a separation between the movement of electrons and the movement of nuclei. It was accepted on the basis that nuclei have a mass at least 1836 times greater than the electron, which moves much faster than the nuclei. In practice, electronic 'relaxation' with respect to nuclear motion is instantaneous. As such, it is convenient to decouple these two motions, compute electronic energies for fixed nuclear positions, leading to a separation of the molecular Hamiltonian into the electronic Hamiltonian $\widehat{H}_{el}$ and the nuclear Hamiltonian $\widehat{H}_{nucl}$. Thus, the Hamiltonian, considering this approximation, can be written as follows:

$$\widehat{H} = \widehat{H}_{el} + \widehat{H}_{nucl} \qquad (2.2.1.1)$$

$\widehat{H}$ can be considered as the sum of an operator depending only on the electron coordinates ($\widehat{H}_{el}$) and an operator depending only on the nucleus coordinates ($\widehat{H}_{nucl}$). If we develop $\widehat{H}_{el}$ and $\widehat{H}_{nucl}$. we get:

$$\widehat{H}_{el} = -\frac{1}{2}\sum_{i}^{N} {\nabla_i}^2 - \sum_{i}^{N}\sum_{A}^{N}\frac{Z_A}{r_{iA}} + \sum_{i}^{N-1}\sum_{i>j}^{N}\frac{1}{r_{ij}} \qquad (2.2.1.2)$$

$$\widehat{H}_{nucl} = \sum_{A}^{M}\sum_{A>B}^{M}\frac{Z_A Z_B}{r_{AB}} \qquad (2.2.1.3)$$

$\widehat{H}_{\mathrm{nucl}}$ can be considered as a constant value. Now, the following electronic equation should be solved:

$$\widehat{H}_{el}\psi_{el} = E_{el}\,\psi_{el} \qquad (2.2.1.4)$$

The total energy of the system can be assimilated to electronic energy (E_{el}) to which a nuclear electrostatic repulsion contribution can be added:

$$E_{tot} = E_{el} + \sum_{A}^{M}\sum_{A>B}^{M}\frac{Z_A Z_B}{r_{AB}} \qquad (2.2.1.5)$$

Those two parts' electronic kinetic energy and nuclear repulsion can be calculated directly, while the electron-electron repulsion part could not be solved exactly for the many-electrons system. To solve this thorny problem, different approaches have been proposed. In general, it can be divided into two main types, the approaches based on the wave function, such as the Hartree-Fock method, and the other one based on the electron density, Density Functional Theory (DFT). Those two methods will be presented in detail in sections 2.3 and 2.4.

2.3 The Hartree-Fock (HF) theory

2.3.1 Context

In the Schrodinger equation, only the hydrogen molecule has an exact solution with ellipsoidal coordinates, however, it is difficult to solve the molecular system because it includes the interaction of many electrons. Hartree proposed the so-called self-consistent field method, to calculate approximate wave functions and energies for atoms and ions. Later, Hartree and Fock proposed the one-electron approximation, also known as the mean-field approximation or orbital approximation, based on the predecessor Hartree's proposition.

2.3.2 The HF approach

D. R. Hartree proposed that when considering the interaction between an electron with the other electrons, this electron is subjected to the average forces of the other electrons, which can be regarded as every single electron moving in an average potential field of other electrons. Since the wave function of every single electron is independent of each other, the overall wave function of the multi-electron system can be written as the simple product of mono-electronic wave functions Φ_i :

$$\psi(\overrightarrow{X_1}, \overrightarrow{X_2} \cdots \overrightarrow{X_N}) = \phi_1(\overrightarrow{X_1})\phi_1(\overrightarrow{\chi_2}) \cdots \phi_1(\overrightarrow{X_N}) \qquad (2.3.2.1)$$

The product of each mono-electronic wave function is known as the Hartree product. The functions ϕ_i are called spin-orbital, composed of space function $\varphi(\vec{r})$ and spin function $\sigma(s)$ $(\sigma = \alpha, \beta)$:

$$\phi(\vec{X}) = \psi_1(\vec{r})\sigma(s) \qquad (2.3.2.2)$$

The wave function obtained in this way describes the electron's classical Coulomb potential very well, however, for the wave function of the multi-electron system, since it does not meet the principle of antisymmetric of the fermion particle, the description of the exchange potential between electrons exists a significant flaw. To cure this flaw, the Slater determinant was introduced to satisfy the anti-symmetry requirements.

$$\psi(\overrightarrow{\chi_1},\overrightarrow{\chi_2},\overrightarrow{\chi_3},\cdots,\overrightarrow{\chi_N}) = \frac{1}{\sqrt{N!}}\begin{bmatrix} \phi_1(\overrightarrow{\chi_1}) & \cdots & \phi_1(\overrightarrow{\chi_N}) \\ \vdots & \ddots & \vdots \\ \phi_N(\overrightarrow{\chi_N}) & \cdots & \phi_N(\overrightarrow{\chi_N}) \end{bmatrix} \qquad (2.3.2.3)$$

Slater's determinant is an approximation for many electrons system, minimizing the energy of the Slater's determinant can find the best approximation to the wave functions, with the condition that varies the spin-orbitals under the orthonormality constraint.

$$E_{HF} = \min_{\psi_{SD} \to N} E[\psi_{SD}] \qquad (2.3.2.4)$$

By using the formalism of the Lagrange multipliers can get the minimum constant, for the sake of simplicity, here we just present the resulting equation directly.

$$\left[-\frac{1}{2}\Delta_i - \sum_{A=1}^{M}\frac{Z_A}{r_{iA}} + \sum_{j=1}^{N}(\widehat{J}_j - \widehat{K}_j)\right]\phi_i = \sum_j \lambda_{ij}\phi_j \qquad (2.3.2.5)$$

The λ_{ij} represents the Lagrange multipliers, $\hat{J}$ is the Coulomb operator, written as:

$$\hat{J}_j(\vec{x}_1) = \int \phi_j(\vec{x}_2)\frac{1}{r_{12}}\phi_j(\vec{x}_2)d\hat{x}_2 = \int \left|\phi_j(\vec{x}_2)\right|^2 \frac{1}{r_{12}}d\vec{x}_2 \qquad (2.3.2.6)$$

In the equation (2.3.2.6), mono-electronic potential instead of the bi-electronic repulsion, by averaging the electronic interaction over all the spin and space coordinates of electron 2 to get the mono-electronic potential, then times the weight of the probability $\left|\varphi_j(x_2)\right|^2 dx_2$ of finding electron 2 in volume dx_2. In this case, the total average potential acting on electron 1 from the other N − 1 electron is obtained by summation J.

$\widehat{K}$ is the exchange operator, by considering the anti-symmetry of the wave function to correct the Coulomb repulsion.

$$\widehat{K}_j(\vec{x}_1)\phi_i(\vec{x}_1) = \int \phi_j^*(\vec{x}_2)\frac{1}{r_{12}}\phi_i(\vec{x}_2)\phi_j(\vec{x}_1)d\vec{x}_2 \qquad (2.3.2.7)$$

Equation (2.3.2.5) is can be written in the other form from the equation (2.3.2.6) and (2.3.2.7), which is called the Hartree-Fock equations, can be represented as:

$$\hat{f}_i \phi_i = \varepsilon_i \phi_i \qquad (2.3.2.8)$$

ϕ_i is HF orbital, and also called the molecule orbital, ε_i is the energies of the orbital, $\hat{f}_i$ is the Fock operator, represented as:

$$\hat{f}_i = -\frac{1}{2}\Delta_i - \sum_{A=1}^{M} \frac{Z_A}{r_{iA}} + \sum_{j=1}^{N} (\widehat{J}_j - \widehat{K}_j) \qquad (2.3.2.9)$$

In the actual calculations, the HF orbitals (ϕ_i) is represented by a linear combination of single-electron basis functions: atomic orbitals, called as the Linear combination of atomic orbitals (LCAO)

2.3.3 Limit of the HF approach

Within the HF theory, the electronic correlation is partially taken into account because of the mean-field approximation. Löwdin defined a correlation energy, E_{coor}, that represents, within the limit of a complete basis set, the difference between the exact energy and the energy calculated within the HF method[2]:

$$E_{coor} = E_{exact} - E_{HF} \qquad (2.3.3.1)$$

Correlation can be considered under two different aspects:

- Static correlation, related to the use of multi-determinantal wavefunction
- Dynamic correlation, related to the movement of the electrons that are not explicitly taken into account in the mean-field approximation.

Different methods have been developed, like the post-HF methods (Configuration Interaction (CI), Multiconfigurational, Perturbative, and Coupled-Cluster methods) or the Density Functional Theory (DFT), have been proposed to introduce the correlation energy at the basis of HF theory. The post-HF methodologies, can provide very accurate results, but they cost expensive computational resources. It has not been used in our work, so it will not be presented in this manuscript. In the next section, we will introduce the DFT methods.

2.4 Density functional theory

2.4.1 Context

In the former section, the Hartree-Fock method has been introduced. In this section, we will aim at the DFT. In DFT, the energy, wave function, and various properties can be determined by the electron density ρ of the system's ground states, that is to say, the energy of an electronic system can be described by its electronic density. The first concept of density functional dates back to the work of Thomas and Fermi in 1927[3,4], then supplemented by the Dirac exchange formula to give the Thomas-Fermi-Dirac model[5,6], they regarded the kinetic and exchange energies of systems of many electrons as locally modeled by their uniform electron gas energy densities. The results only depend on the total electronic density ρ(r). It is quietly simply, however, it returns poor results, as it is well known, it does not take into account the correlation energy. In the 1950s, Slater proposed an approximation for Hartree-Fock exchange, in a form similar to the Dirac exchange[7]:

$$E_x[\rho] = \mathsf{C}_x \int \rho(\vec{r})^{4/3}\, d\vec{r} \qquad (2.4.1.1)$$

Where C_x is a constant. In 1964, Hohenberg and Kohn established that the total electron density completely and exactly determine all the ground-state properties of an *N*-electron system and the electron density at which the lowest energy can be obtained is the ground state electron density[8]. These theorems establish a framework of their application thanks to Kohn-Sham's approach[9]. The DFT and its applications elaborated by Kohn and Sham are exact methods in theory. In practice, however, approximations are necessary. In the next paragraph it will be presented the work of Kohn and Sham together with the approximations used in the DFT will be discussed as well[10–12].

2.4.2 The Kohn-Sham method

Until 1965, Kohn and Sham proposed an approach to overcome the problem of the DFT was not used for quantitative predictions[9]. Before, only the Thomas-Fermi's method (then Dirac's) was used to solve the Schrödinger equation based on electron density[5]. However, this method provides inaccurate results due to the poor description of the kinetic energy of electrons. Kohn and Sham's idea was to treat the kinetic term as accurately as possible. To do

this, they used an approach similar to that of Hartree-Fock calculations by placing themselves in a hypothesis of an average field: the electrons evolve independently of each other in an effective potential V_s generated by the nuclei and the other electrons:

$$\widehat{H} = -\frac{1}{2}\sum_{i}^{N}\Delta_i + \sum_{i}^{N} V_s(\hat{r}_i) \qquad (2.4.2.1)$$

The advantage of such method is that the kinetic energy expression of a N-electron system without interaction is accurate, by using its spin-orbitals ϕ_i, expression as follows:

$$T_s = -\frac{1}{2}\sum_{i}^{N} < \phi_i|\Delta_i|\phi_i > \qquad (2.4.2.2)$$

It contains most of the kinetic energy of the real system. In a similar way, electronic movements are uncorrelated from each other, so the exact wave function can be written as an antisymmetric product of mono-electronic wave functions (spin-orbitals ϕ_i) in the form of a Slater determinant:

$$\psi_{SD} = \frac{1}{\sqrt{N!}}\begin{bmatrix} \phi_1(\overrightarrow{\chi_1}) & \cdots & \phi_1(\overrightarrow{\chi_N}) \\ \vdots & \ddots & \vdots \\ \phi_N(\overrightarrow{\chi_N}) & \cdots & \phi_N(\overrightarrow{\chi_N}) \end{bmatrix} \qquad (2.4.2.3)$$

By analogy with the Hartree-Fock method, the spin-orbitals ϕ_i is determined by solving the equation at eigenvalues:

$$\hat{f}^{KS}\phi_i = \varepsilon_i\phi_i \qquad (2.4.2.4)$$

Where Kohn-Sham's single-electronic operator $\hat{f}^{KS}$, is defined by:

$$\hat{f}^{KS}\phi_i = -\frac{1}{2}\Delta + v_S(\hat{r}) \qquad (2.4.2.5)$$

The spin-orbitals ϕ_i is then called Kohn-Sham orbitals, or KS orbitals. The connection between the virtual system and the real system is made by choosing a fictitious potential V_s for which the electron density ρ_s defined in the followed equation to the one of the real system ρ_0.

$$\rho_s(\hat{r}) = \sum_i^N \sum_S |\phi_i(\vec{r}, s)|^2 = \rho_0(\vec{r}) \qquad (2.4.2.6)$$

The original idea of the Kohn and Sham is to separate the exact known part (classical kinetic energy T_s, equation (2.4.2.2)) from the unknown part due to the accurate kinetic energy is so difficult to get. This logic also has been applied to the universal functional:

$$F_{HK}[\rho\vec{r}] = T_s[\rho(\vec{r})] + J[\rho(\vec{r})] + E_{xc}[\rho(\overrightarrow{r})] \qquad (2.4.2.7)$$

T_s, the kinetic energy of the virtual system without interactions, and J, the Coulomb interaction, can be computed directly. All unknown terms are absorbed into the exchange-correlation energy E_{xc} :

$$E_{xc}[\rho] = (T[\rho] - T_s[\rho]) + (E_{ee}[\rho] - J[\rho]) \qquad (2.4.2.8)$$

E_{xc} contains all the corrections that are couldn't get directly: the correction to the real kinetic energy $(T[\rho] - T_s[\rho])$, the not classical effects related to the exchange (X) and correlation (C), and other possible corrections due to the self-interaction error in the expression of the Hartree potential J. After these approximations, the next step is to find the expression of the effective potential V_S to ensure the same density characterizes to the virtual and the actual systems. For the real system, the expression of the total energy is as follows:

$$E[\rho] = T_s[\rho] + J[\rho] + E_{xc}[\rho] + E_{eN}[\rho] \qquad (2.4.2.9)$$

Separate each items, it can be write in:

$$E[\rho] = -\frac{1}{2}\sum_{i}^{N}\langle\phi_i|\Delta_i|\phi_i\rangle + \frac{1}{2}\sum_{i}^{N}\sum_{j}^{N}|\phi_i(\overrightarrow{r_1})|^2\frac{1}{r_{12}}\left|\phi_j(\overrightarrow{r_2})\right|^2 + E_{xc}[\rho(\vec{r})] + \sum_{i}^{N}\int\sum_{A}^{M}\frac{Z_A}{r_{iA}}|\phi_i(\overrightarrow{r_1})|^2 d\overrightarrow{r_1} \qquad (2.4.2.10)$$

Like the Hartree-Fock method, the variational principle was applied to the expression of the $E[\rho]$ with the constraint that the spin-orbitals ϕ_i are orthonormal ($\langle\phi_i|\phi_j\rangle = \delta_{ij}$). The eigenvalue equations can be found in the resulting equations:

$$\left[-\frac{1}{2}\Delta + V_{eff}(\vec{r}_i)\right]\phi_i = \varepsilon_i\phi_i \qquad (2.4.2.11)$$

To identify the effective potential V_s to the potential V_{eff}:

$$V_s \equiv V_{eff} = \int\frac{\rho(\overrightarrow{r_2})}{r_{12}}d\overrightarrow{r_2} + V_{xc}(\overrightarrow{r_1}) - \sum_{A}^{M}\frac{Z_A}{r_{1A}} \qquad (2.4.2.12)$$

Equation (2.4.2.12) are called Kohn-Sham equations. They are dependent on spin-orbital ϕ_i through J, and in a self-consistent way solving it is mandatory. It should be noticed that they are not based on an approximated method, precisely determining the fundamental state of a system in theory can be achieved. In practice, the exactly exchange-correlation functional is unknown, so make approximations are necessary to find the correct form. The main aim of the current research in DFT is thus to develop increasingly accurate exchange-correlation functionals, more details will be shown in the next section.

Because the method of the KS has many similarities to the HF equations, the solution is made according to the same framework. Spin-orbitals are expanded as a linear combination of atomic orbitals (LCAOs), which are then expanded with a basic set of primitive functions. The KS equations form a set of pseudo-eigenvalues equations solved self-consistently. However, the evaluation of the exchange-correlation integrals differs slightly. Rather complex mathematical functions generally approach the part of exchange-correlation. Therefore, an

analytical evaluation of the integral is excluded, and the calculation codes perform a numerical quadrature integration. It consists in replacing the integral with a finite sum on a grid of points., where the value at each point is weighted by a coefficient noted here W_p:

$$\int \chi_\mu^* (\vec{r}_1) V_{xc}(\vec{r}_1) \chi_\nu(\vec{r}_1) d\vec{r_1} \approx \sum_p^P \int \chi_\mu^* (\vec{r}_p) V_{xc}(\vec{r}_p) \chi_\nu(\vec{r}_p)\, W_p \qquad (2.4.2.13)$$

In 1988, Becke introduced the frequently used integration grid, which split the molecular space into atomic contributions[13].

2.4.3 Different exchange-correlation functional

The central problem of the DFT is that the Exchange-Correlation (XC) functional is unknown, one of the main task is develop the XC approximations.

Energy-correlation functional are usually written in the following term:

$$E_{xc}\,[\rho] = \int \rho(r)\varepsilon_{xc}[\rho(r)]dr \qquad (2.4.3.1)$$

$\rho(r)$: electron density, i.e. electron per unit volume

$\varepsilon_{xc}[\rho(r)]$: exchange-correlation energy density, i.e. energy per electron density

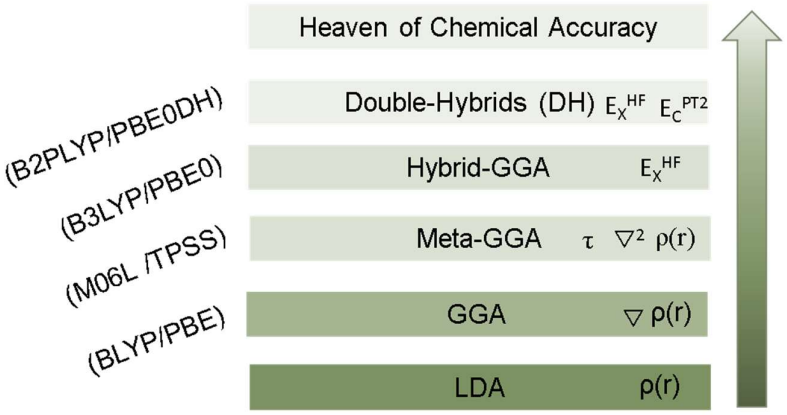

Figure 2.1 The Jacob's Ladder

Currently, although we do not know the exact form of this functional, different approximations have been made to develop this unknown exchange correlation functional. The approximations have been compared at the Jacob's ladder (Figure 2.1), roughly be divided into five rungs.

Local Density Approximation

In Local Density Approximation (LDA), only depends on the electron density, and it is the basis of many higher-rung functionals. In 1960s, a great deal of attention have been paid to the homogeneous gas of interacting electrons, then a matter of interest to see how properties of the homogeneous gas can be utilized in theoretical studies of inhomogeneous systems. Kohn and Sham proposed a set of self-consistent equations which include, in an approximate way, exchange and correlation effects in 1965[9]. The basic idea is that it is possible to estimate the exchange-correlation energy (E_{xc}) of an inhomogeneous system by using on infinitesimal portion, the results of a homogeneous electron gas with a density equal to the local density of the real system. E_{xc} is the sum of all point contributions and it yields to the exchange-correlation energy according to the equation (2.4.3.1):

In equation (2.4.3.1), ε_{xc} can be divided into exchange contributions, respectively. This division, significantly simplifies the calculations:

$$\varepsilon_{xc}[\rho(\vec{r})] = \varepsilon_x[\rho(\vec{r})] + \varepsilon_c[\rho(\vec{r})] \qquad (2.4.3.2)$$

The exchange energy of an electron in a uniform gas is exactly known from the exchange equation of Dirac[6]:

$$\varepsilon_x[\rho(\vec{r})] = -\frac{3}{4}\sqrt[3]{\frac{3\rho(\vec{r})}{\pi}} \qquad (2.4.3.3)$$

The correlation energy ε_c, on the other hand, is not known exactly. The Vosko, Wilk, and Nussair (VMN) approximation is the most commonly used. It is based on Monte-Carlo calculations of the homogenous electron gas to give an approximation expression[14]. The treatment of the open-shell system is accomplished by following the Hartree-Fock method, but it distinguishes between the spin α and β of the electrons ($\rho(\vec{r}) = \rho_\alpha(\vec{r}) + \rho_\beta(\vec{r})$). This

approach, generally called LSD (Local Spin Density), adds the flexibility to the system, typically it is possible to get more accurate results. Actually, in practice, the LDA approach improves the Hartree-Fock results, however, this approximation is only valid for systems with a constant density at each point in space, it meets problems when explain the inhomogenous systems. More elaborate functionals were later developed.

Generalized Gradient Approximation

The second rung of the Jacob's ladder corresponds to the Generalized Gradient Approximation (GGA). GGA approximation corrects the LDA through an additional density gradient correction, making the functional more flexible. It considers the inhomogeneity of density by introducing its first derivative $\nabla\rho$ in the expression of the exchange-correlation energy:

$$E_{xc}[\rho] = \int \varepsilon_{xc}(\rho(\vec{r}), \nabla_{\rho}(\vec{r}))d\vec{r} \qquad (2.4.3.4)$$

The terrm of ε_{xc} is highly variable from one function to another, however, in most cases, treat the exchange and correlation contributions separately and combine them to form the total functional. The exchange part expression is based on the exchange energy LDA, but is improved by adding an enhancement factor (F_X^{en}) and the reduced density gradient $s(\nabla\rho(\vec{r}))$, which improves the performance of the description of inhomogeneous systems:

$$E_x[\rho(\vec{r})] = \int d\vec{r}\rho_x(\vec{r})\varepsilon_x(\rho(\vec{r})F_X^{en}(s(\nabla\rho(\vec{r})) \qquad (2.4.3.5)$$

$$s(\nabla\rho(\vec{r})) = \frac{|\nabla\rho_r(\vec{r})|}{\rho^{4/3}(\vec{r})} \qquad (2.4.3.6)$$

F_X^{en} can use empirical data as the noble gas exchange energy (Becke 1988)[15], or based on physical limitations (as the PBE functional, for instance)[16]. As for the energy exchange, the correlation part usually has no immediate physical meaning, is based on experimental data (P86)[17], or it is based on physical consideration (PW91)[16].

GGA-type functionals significantly improve LDA results for lengths and binding energies. However, they never consider the static correlation, so the long-distance effects are often poorly described.

Meta-Generalized Gradient Approximation

To improve the form of the exchange-correlation potential, a new type of functionals was introduced. These functionals, called meta-Generalized Gradient Approximation (meta-GGA), it modifies an underlying GGA method by additionally taking into account the kinetic-energy density or the Laplacian of the density ($(\nabla\rho)$. It is more flexible compared to the GGAs. Although it has some improvement, this approximation still has the disadvantage of the inadequate consideration of the exchange, which contributions are much more relevant than the ones of the correlation.

Adiabatic Connection

In Kohn-Sham's model, it shows a kinetic correction in the exchange-correlation functional. In the theory of adiabatic connection, it allows to include the exchange-correlation hole, yet designed to take into account only potential term, a system of non-interacting "connected" to the actual system by gradually increasing the value of the coupling parameter λ, has been developed. The Hamilitonian can then define partially interacting systems:

$$\widehat{H_\lambda} = \hat{T} + \hat{V}_{ext,\lambda} + \lambda \sum_i \sum_{j<i} \frac{1}{r_{ij}} \qquad (2.4.3.7)$$

In λ = 0 limit, the electrons are non-interacting, corresponding no correlation energy and only the exchange is taken into account, to λ=1, it represents the real system. For each value of λ, the potential external V_{ext} adapts to maintain a constant density equal to the one of the real system.

Hybrid Density Functionals

This approach to improving the exchange-correlation functional was to have explicit dependencies on the occupied orbitals and include a fraction of exact HF exchange in the exchange part.

Initially, an exact value instead of the exchange contribution in the original functional is only an approximation to the correlation part, which is known to be relatively weak. However, the results of this method are worse due to the unsuitable of the exact exchange term with the approximations made on the correlation part. Such as, in the long-range part, if the correlation is unconsidered or explained poorly, the long-range exchange contributions will not

be offset. In general, the results are false. One method to deal with this problem is to adopt the adiabatic connection, and only the exact exchange part was introduced. Assuming that the exchange-correlation functional varied linearly with λ, Becke first proposed the half-half functional (HH)[18] :

$$E_{xc}^{HH} = \frac{1}{2}E_{xc}^{\lambda=0} + \frac{1}{2}E_{xc}^{\lambda=1} \qquad (2.4.3.8)$$

E_{xc} for $\lambda = 0$ assumes the value of the exact Hartree-Fock exchange, while for $\lambda = 1$, E_{xc} assumes the value of the approximated LSD exchange. Later, Becke introduced three semi-empirical parameters (a_{x0}, a_{x1}, a_c) into its functional system based on G2 dataset[19] to improve the performance.

$$E_{xc}^{Hybrid} = a_{x0}E_x^{LSD} + (1 - a_{x0})E_x^{HF} + a_{x1}\Delta E_x^{GGA} + E_c^{LSD} + a_c E_c^{GGA} \qquad (2.4.3.9)$$

where E_x^{HF} is obtained from Hartree-Fock theory. Such functionals that include the exact exchange in their expression are named hybrid functionals. Hybrids improve upon GGAs on the most common properties: energies, geometries, reaction barriers, and so on. However, because of the introduction of the non-local HF exchange term, they are more expensive than GGA functionals although still applicable to large systems.

Global hybrids are the hybrid functionals that contain a fixed amount of exact exchange, some of them are PBE0[20], B3LYP[21], M06[22] etc. Consequently, nonlocal processes, is unsuccessful in several applicants: the polarizability of long chains, Rydberg excited states[23] and the charge transfer excitations[24], due to the incorrectly descriptions on the long-range exchange potential behaviors, while HF approach describes quiet well. By changing the ratio of the HF part from short to long distance, range-separated exchange (RSX) uses μ being the range-separation (bohr^{-1}) threshold switching the exchange operator r_{12}^{-1} from short- to long-range regimes, the fraction of the exact exchange is introduced as a function of the interelectronic distance.

$$\frac{1}{r_{12}} = \frac{1 - [\lambda_x + (1 - \lambda_x)erf(\mu r_{12})]}{r_{12}} + \frac{\lambda_x + (1 - \lambda_x)erf(\mu r_{12})}{r_{12}} \qquad (2.4.3.10)$$

Where the first and second term account for short-range and long-range interactions, respectively. r_{12} is the electronic spatial coordinates, and erf is the error function, the μ which is determined either empirically or by using theoretical arguments, control the interplay between the long-range and short-range parts, the larger the parameter the sooner the short-range interaction vanishes.

Double-hybrid Functionals

At the fifth level of the Jacob's ladder is the double hybrid functionals (DHFs), also is the mainly functionals we used in this work.

Görling and Levy introduced a perturbation theory (GLPT) in 1993 and 1994[25,26]. In GLPT, the perturbed Hamiltonian $\hat{H}^{\lambda}$ can be write as follows:

$$\hat{H}^{\lambda} = \hat{T} + \hat{V}_{ext} + \lambda\hat{V}_{ee} + \hat{v}^{\lambda}[\rho] \qquad (2.4.3.11)$$

Where $\hat{T}$ is the kinetic-energy operator, $\hat{V}_{ext}$ is the external nuclear-electron potential, $\hat{V}_{ee}$ is the Coulomb operator, which scaled by the coupling-constant λ, connects the Kohn-Sham Hamiltonian of noninteracting electrons (λ=0) to real system (λ=1), $\hat{v}^{\lambda}$ ensures that the electron density ρ remains constant and exact for all λ.

The zeroth-order Hamiltonian is $\hat{H} = \hat{T} + v^{\lambda}[\rho]$, the perturbation is $\hat{H}' = \hat{V}_{ext} + \lambda\hat{V}_{ee} - \hat{v}^{\lambda}[\rho]$. Hence, in terms of the standard perturbation theory[27], the ground state energy of $\hat{H}^{\lambda}$ can be write:

$$E_{\lambda} = E_s^0 + \lambda E^{(1)} + \lambda^2 E^{(2)} + \lambda^3 E^{(3)} + O(\lambda^4) \qquad (2.4.3.12)$$

Where $E^{(k)}$ is the *k*th-order energy correction to E_s^0. In particular, Görling and Levy proposed that the same KS scheme should work as well in terms of KS orbitals φ_i and eigenvalues ε_i, they introduced a formally exact KS scheme based on perturbation theory, the E_{xc} is given by[25,26]:

$$E_{xc}[\rho] = E_x^{HF}[\{\varphi_i\}] + \sum_{j=2}^{\infty} E_{c,j}\left[\{\varphi_i\}, \{\varepsilon_i\}, \{v_1(r), v_2(r), \cdots v_{j-1}(r)\}\right] \qquad (2.4.3.13)$$

the second-order perturbation energy is:

$$E_{c,2} = E_c^{GL2} = \sum_{m\neq 0}^{\infty} \frac{\left|\langle \varphi_S^0 | \hat{V}_{ee} - \nu_1 | \varphi_s^i \rangle\right|^2}{E_s^0 - E_s^i} \qquad (2.4.3.14)$$

E_c^{GL} is recognized as the GL perturbation theory up to the second order, E_s^i is the expectation value of the i*th* excited determinant, E_s^0 is the energy for the ground-state, φ_s^i is the corresponding determinant, $\hat{V}_{ee}$ is the operator of electron-electron repulsion, and $\nu_1 = \sum_{i=1}^{N} \hat{v}_J(j) + \hat{v}_x(j)$, N is the number of electrons. With knowledge of the potentials $\nu_j(r)$, equation (2.4.3.13) gives the formally exact exchange-correlation energy as functional of the KS orbitals φ_i and eigenvalues ε_i, which written in the terms of KS orbital as:

$$E_{c,2} = E_c^{GL2} = \sum_i \sum_a \frac{|\langle \phi_i | \nu_x - k_x | \phi_a \rangle|^2}{\varepsilon_i - \varepsilon_a} + \frac{1}{4} \sum_{ij} \sum_{ab} \frac{\left|\langle \phi_i \phi_j | \nu_{ee} | \phi_a \phi_b \rangle\right|^2}{\varepsilon_i + \varepsilon_j - \varepsilon_a - \varepsilon_b} \qquad (2.4.3.15)$$

$\nu_{ee} = \frac{1}{|r-r'|}$ is the electron-electron repulsion operator, and the subscripts (i,j) and (a,b) denote the occupied and unoccupied KS orbitals. ν_x is the local exchange operator, k_x is the non-local exchange operator:

$$k_x \phi_p(r) = -\sum_{i(occ)} \int \frac{\phi_i^*(r')\phi_p(r')}{|r-r'|} dr' \phi_i(r) \qquad (2.4.3.16)$$

The term 'double-hybrid' was for the first time used by Truhlar and co-workers[28]. To overcome missing the important dynamic correlation in DFT, which is the key of the *ab initio* wave function theory (WFT), the double hybrid functionals were developed by mixing a part of second-order Görling and Levy perturbation theory, including the non-local virtual orbital-dependent term, which efficiently and effectively connect the DFT with WFT world.

DHFs contain the HF exchange, exchange density functional, correlation density functional, and second-order Møller-Plesset (MP2) correlation, the first three terms are calculated in a usual self-consistent hybrid KS calculation, and the last perturbative term evaluated with the previously obtained orbitals is added a posteriori.

$$E_{xc}^{DH} = a_x E_x^{HF} + (1-a_x)E_x[n] + (1-a_c)E_c[n] + a_c E_c^{MP2} \qquad (2.4.3.17)$$

$$E_c^{MP} = \frac{1}{4}\sum_{ij}\sum_{ab}\frac{\left|\langle\phi_i\phi_j\|\phi_a\phi_b\rangle\right|^2}{\varepsilon_i + \varepsilon_j - \varepsilon_a - \varepsilon_b} \qquad (2.4.3.18)$$

When the a_x, a_c are 1.00, 0.00, respectively, the DH reduces to the GH, while a_x, a_c are 0.00, 1.00, respectively, the MP2 is recovered. Normally, it thinks that the DFT correlation functionals are better to explain the short-range correlation than MP2, while MP2 is very suitable to describe the long-range correlation. Consequently, the double hybrid functionals that mix those two features should better explain the correlation part than DFTs and MP2.

Generally, the percent of the exact exchange is much larger in DH methods than the simple hybrids, because the MP2 correlation can correct for HF deficiencies. So, the kinetic barriers and diffuse orbitals can be improved. At the same time, dispersion forces (Van der Waals) can be more accurately computed because of the perturbational term (HF and DFT traditionally fail with this), although it still predicts weaker dispersion forces. Specific care must be taken in unrestricted calculations where HF introduces a high spin population. One more thing that should be considered is that calculation time, the convergence is more difficult than global hybrid functionals.

B2-PLYP

Grimme made the B2-PLYP double hybrid functional popular in 2006[29]. The functional can be expressed using a simple formula:

$$E_{xc}^{B2PLYP} = a_x E_x^{HF} + (1 - a_x)E_x^{DFT} + (1 - a_c)E_c^{DFT} + a_c E_c^{MP2} \qquad (2.4.3.19)$$

Where E_x^{DFT} and E_c^{DFT} are the DFT-exchange and correlation part, respectively, E_x^{HF} and E_c^{MP} are the HF exchange and MP2 perturbative correlation energy, both computed on the basis of DFT orbitals. In B2PLYP, B88 exchange and LYP correlation were used, the parameters a_x and a_c were calculated by parameterization against heats of formation (HOFs) of the G2/97 set consisting of 148 neutral molecules[19] at B2PLYP/[7s4p3d2f] level. The a_x and a_c are 0.53, 0.73, respectively, in B2-PLYP.

PBE-QIDH

Based on the adiabatic-connection (AC) formalism[30–33], Toulouse *et al.* introduced a family of one-parameter DHs[34–36], proposed a quadratic ($a_c=a_x^2$), and a cubic ($a_c=a_x^3$) relation

between a_x and a_c. In this formalism, it doesn't specific the exact values of the parameters, which is the key point to develop the new types of double hybrid functional.

In AC Hamiltonian, there is a coupling-constant integral between the non-interacting KS Hamiltonian (λ=0) and the exact Hamiltonian (λ=1).

$$E_{xc}[\rho] = \int_{(\lambda=0)}^{1} \omega_\alpha[\rho] d\alpha \qquad (2.4.3.20)$$

Where $\omega_\alpha[\rho]$ stands for the exchange and correlation integrand. As for the exchange and correlation energy, the exact integrand is unknown, some approximations have been developed. One of simple way is taking the integrand as a quadratic function (QI) of α:

$$\omega_\alpha[\rho] = a[\rho] + b[\rho]\alpha + c[\rho]\alpha^2 \qquad (2.4.3.21)$$

Where a and b depend on the value of λ, is the functionals of density, c is determined by upper integral limit of eq 1.

Normally, at the weak interaction limit (λ →0), the integrands trends to the exact exchange at the zeroth-order, the first-order derivative of the integrand of eq1 is the second-order Görling-Levy[26,37] (GL2) correlation energy.

$$\omega_0[\rho] = E_x^{HF}, \quad \left.\frac{\partial \omega_\alpha[\rho]}{\partial \lambda}\right|_{\lambda=0} = 2E_c^{GL} \qquad (2.4.3.22)$$

Where,

$$E_c^{GL} = E_c^{MP2} + E_c^{\Delta H} \qquad (2.4.3.23)$$

The $E_c^{\Delta HF}$ contributions almost negligible, so that

$$E_c^{GL} \approx E_c^{MP2} \qquad (2.4.3.24)$$

So,

$$a[\rho] = E_x^{HF} \qquad (2.4.3.25)$$

$$b[\rho] = 2E_c^{MP2} \qquad (2.4.3.26)$$

From Levy and Perdew[38], the integrand is expressed as:

$$\omega_\alpha[\rho] = \frac{\partial}{\partial\alpha}\left(\alpha^2 E_{xc}\left[\rho_{1/\alpha}\right]\right) \qquad (2.4.3.27)$$

$$= E_x^{DFA}[\rho] + 2E_c^{DFA}\left[\rho_{1/\alpha}\right]\alpha + \frac{\partial E_c^{DFA}\left[\rho_{1/\alpha}\right]}{\partial\alpha}\alpha^2 \qquad (2.4.3.28)$$

When the integrand behavior close to the upper limit (α→1), the integrand can be approximated by :

$$\omega_1[\rho] \approx E_x^{DFA}[\rho] + 2E_c^{DFA}[\rho] \qquad (2.4.3.29)$$

or:

$$\omega_{1,\lambda_x}[\rho] = \lambda_x E_x^{HF} + (1-\lambda_x)E_x^{DFA}[\rho] + 2E_c^{DFA}[\rho] \qquad (2.4.3.30)$$

So, we can get c term

$$c[\rho] = (\lambda_x - 1)E_x^{HF} + (1-\lambda_x)E_x^{DFA}[\rho] - 2E_c^{MP2} + 2E_c^{DFA}[\rho] \qquad (2.4.3.31)$$

The a, b and c term has been set, the eq 3 can be solve. So, the Quadratic Integrand Double-Hybrid (QIDH) has been developed, the form for this model is:

$$E_{xc}^{QIDH,\lambda_x} = \frac{\lambda_x+2}{3}E_x^{HF} + \frac{1-\lambda_x}{3}E_x^{DFA} + \frac{2}{3}E_c^{DFA} + \frac{1}{3}E_c^{MP2} \qquad (2.4.3.32)$$

Where the fraction of MP2 correlation ($a_c=a_x^3$) has a cubic dependence on the fraction of the exact HF exchange, so, $(\frac{\lambda_x+2}{3})^3 = \frac{1}{3}$. We can get the

$$\lambda_x = 3^{2/3} - 2 \qquad (2.4.3.33)$$

In PBE-QIDH, a_x is $3^{-\frac{1}{3}}$ (about 0.69), a_c is $\frac{1}{3}$, respectively.

DSD-PBEP86

In DSD-PBEP86[39], it adopted the spin-component-scaled MP2 (SCS-MP2) method[40], it's more flexibility by setting a different weight to the same- and opposite-spin MP2, same-spin MP2 reflects more long range correlation, while the opposite-spin is related to short range interactions[40,41]. Adding the dispersion correction is recommended when using the DFT methods, although DHF has been considered about the MP2 part, which is account for those interactions[42], the accuracy is not as expected as 'chemical accuracy'. When the SCS distinction and a dispersion and term are included into the double-hybrid functionals, the Dispersion corrected, Spin-component scaled Double Hybrid (DSD-DFT) was developed. The exchange-correlation term is expressed as:

$$E_{xc} = C_x E_x^{DFT} + (1 - C_x)E_x^{HF} + C_c E_c^{DFT} + C_o E_o^{MP2} + C_s E_s^{MP2} + S_6 E_D \qquad (2.4.3.34)$$

Where C_x is the amount of DFT exchange, C_c is the correlation part of the DFT, C_o and C_s is the opposite and same-spin MP2, respectively, S_6 is the D2 dispersion correction.

In DSD-PBEP86, the parameters were optimized by using six training sets, cover thermochemistry, kinetics of main group together with transition metals, and long-range interactions. And used PBE as the exchange functional, P86 as one of correlation part to get the parameters, C_x is 0.32, C_c is 0.45, C_s and C_o is 0.23, 0.51, respectively, S_6 is 0.29.

2.5 Modeling van der Waals with DFT (including empirical potentials)

2.5.1 Context

Weak interactions dominated by dispersion are important for van der Waals molecules, long-range forces, and biological systems. The "lack" of dispersion forces, often called van der Waals (vdW) forces, is one of the most significant problems in modern DFT methods, seeking for DFT-based methods which accurately account for dispersion is becoming the hottest topics in computational chemistry.

2.5.2 van der Waals Density Functional

In 1998, Kohn et al. point out that "the commonly used LDA and GGA, designed for nonuniform electron gases, fail to capture the essence of vdW energies" [43]. Mourik and Gdanitz confirmed this point by showing that the local density approximation (LDA) and some well-established GGA functionals are incapable of accounting for dispersion effects in a quantitative way[44]. However, it is valuable to extend this kind of assessment to a broader range of functionals. In particular, a new-generation of functionals called meta-GGAs or MGGAs has been developed; they incorporate kinetic energy density and are a possible area of systematic improvement [45–49]. These methods include electron correlation effects in an approximate manner, have been made great progress while not able accurate describe the dispersive interactions[50,51].

As the DFT is becoming an essential tool for computational chemistry, it will be useful to make DFT including vdW interactions, a set of corrections to the DFT energies was recently introduced, the initial of the correction is basis at the dispersion is a special kind of the electron correlation problem operating only on long-range scales. The approximation derived by Dion et al[52], known as the van der Waals density functional (vdW-DF), has recently received a great deal of attention owing to its lower degree of empiricism. It is based on nonlocal density-dependent correlation functional can fully capture the elusive vdW forces at asymptotic limit or at the intermediate distance, is a significant advance in the description of vdW forces in the DFT framework. In the original formulation, the correlation energy write as follows:

$$E_c[n] = E_c^0[n] + E_c^{NL}[n] \qquad (2.5.2.1)$$

The $E_c^0[n]$ term is the local correlation energy, which can be approximated from a standard (semi)local correlation DF. $E_c^{NL}[n]$ corresponds to a nonlocal DF correlation kernel able to fully describe the nonlocal vdW forces. $E_c^{NL}[n]$ was designed to vanish where the correlation energy comes only from the $E_c^0[n]$ term, thus to avoid double-counting effects for the correlation energy. The $E_c^{NL}[n]$ can be expressed as:

$$E_c^{NL}[n] = \frac{\hbar}{2}\iint drdr' n(r)\phi(r,r')n(r') \qquad (2.5.2.2)$$

Where $\phi(r, r')$ is the correlation kernel function that depends on two electron positions r and r'. $\phi(r, r')$ is defined that in the $|r - r'| \to \infty$ limit, E_c^{NL}[n] preserves the asymptotic limit described by the second-order perturbation theory between two finite nonoverlapping systems with the typical $-C_6^{AB}/|r - r'|^6$ form[53]. In equation (2.5.2.2), the factor of ½ is to avoid double-counting the inter- and intramolecular contributions for the nonlocal correlation energy, both r and r' integrals running over the whole space. The nonlocal term in equation (2.5.2.2) is a very general approach that requires neither dividing the system into interacting fragments nor any kind of atomic partitioning. The entire correlation functional is nonempirical and yields the correct long-rang asymptotics, where vdW forces are fully captured from a nonlocal density-dependent correlation kernel.

In 2010, Lee et al improved the vdW-DF functional, named vdW-DF2[54], where a more accurate semilocal exchange functional (PW86) was employed, and a large-*N* asymptote gradient correction was used in determining the nonlocal correlation kernel. The new vdW-DF2 shows advantages in some chemical applications, likely the intermolecular separations, binding energies for hydrogen-bonded complexes. Although both vdW-DF and vdW-DF2 versions can be considered as accurate DFs for the description of weakly interacting systems, for the jellium spheres, it couldn't provide the correct C_6 coefficients, gives poor results.

Based on the pioneering work, vdW-DF was implemented self-consistently by Vydrov and Voorhis[55]. They investigated the effect of the exchange functional used on the vdW-DF scheme, they adjusted the local and nonlocal correlation components by enhancing factor and empirical constant. In contrast to the vdW-DF, the VV09 has a simple form, incorporate with the exact HF exchange or the rPW86 exchange functional, the performances on the weak interactions systems work well. In 2010, the same authors developed the nonlocal correlation kernel VV10[56], the long-range behavior as same as the precursor VV09, the damping function for the short-range simplified a lot, which makes VV10 more computationally efficient. And the parameters of short-range region are adjustable, which is convenient to cooperate with other density functionals.

2.5.3 Empirical dispersion correction

On the other hand, there are several methodologies based on the empirical dispersion correction to account for van der Waals forces. In this way, it introduces a damped, atom-pair wise potential to a standard Kohn-Sham DFT results, namely the so-called DFT-D, the dispersion corrected DFT energy is:

$$E_{DFT-D} = E_{DFT} + E_{disp} \qquad (2.5.3.1)$$

Where E_{DFT} is the DFT energy and E_{disp} is an empirical dispersion correction. DFT is known to provide a fairly good description of the short-range correlations. In the intermediate region, both DFT and empirical correction are valid to some extent. The empirical correction is usually based on the atom pair-wise additive treatment of the dispersion energy, asymptotic formulas valid for long-range interactions. The general form for the dispersion energy is:

$$E_{disp} = -\frac{1}{2}\sum_{A\neq B}\sum_{n=6,8,10,\ldots} s_n \frac{C_n^{AB}}{R_{AB}^n} f_{damp}(R_{AB}) \qquad (2.5.3.2)$$

The sum is over all atom pairs in the system, C_n^{AB} is the averaged *n*th-order dispersion coefficient (orders *n*=6, 8, 10,…) for atom pair AB, and R_{AB} is the distance of the atoms A and B. Global (functional depended) scaling factors $s_n$can be used to adjust the correction to the repulsive behavior of the chosen exchange-correlation density functional.

The key factors in the DFT-D approaches is the damping function f_{damp}, it determines the short-range behavior of the dispersion correction, also should considered the near-singularities for small R_{AB}, avoid double counting at the intermediate distances and to adjust the empirical correction to a given functional[57]. Experience in the past few years has shown that it is just the quality of the damping function that determines the accuracy of the DFT-D method. Normally, the damping function should be continuously switches off the dispersion from the intermediate to the short distances, and its form is usually chosen by trial and error. The expression is given by

$$f_{damp}(R_{AB}) = \frac{1}{1 + 6(r_{AB}/(S_{r,n}R_0^{AB}))^{-\alpha_n}} \qquad (2.5.3.3)$$

Or

$$f_{damp}(R_{AB}) = \frac{1}{1 + e^{-\gamma(R_{AB}/S_{r,n}R_0^{AB}-1)}} \qquad (2.5.3.4)$$

Where R_0^{AB} is a cut-off radius for atom pair AB, $S_{r,n}$ is a functional dependent radii scaling factor, and γ is a parameter that determines the steepness of the function for small R_{AB}. For the R_0^{AB} values, often use the averaged empirical atomic vdW-radii. Another more complicated damping function that is used is the Tang and Toennies[58].

In generally, the fundamental question of the existing dispersion approaches is how it behaves asymptotically in the small R, normally in most of the methods, the damping function approaches to 0 when R_{AB} trends to 0 limit, named "zero-damping". While Becke and Johnson (BJ)[59,60] propose the rational damping function as follows:

$$E_{disp} = -\sum_{n=6,8} S_n \sum_{A\neq B} \frac{C_n^{AB}}{R_{AB}^n + f_n(R_{AB}^0)} \qquad (2.5.3.5)$$

The BJ- damping function defined as $f_n(R_{AB}^0) = a_1 R_{AB}^0 + a_2$, the a_1 and a_2 parameters are fitted, R_{AB}^0 defined as:

$$R_{AB}^0 = \sqrt{\frac{C_8^{AB}}{C_6^{AB}}} \qquad (2.5.3.6)$$

The BJ-damping function leads to a constant contribution of E_{disp} to the total correlation energy from each spatially close pair of atoms.

Currently, the most widely used DFT-D method called DFT-D3[61], it can be used as a general tool for compute the dispersion energy of any kind with DFT[62] with higher accuracy for arbitrary systems. In this thesis, the inclusion of 2 different dispersion corrections, named DFT-D3 (or with appended "-D3" to a functional name) to denote the original version with zero-damping and dub the variant employing BJ-damping as "DFT-D3(BJ)" (or "-D3(BJ)").

For Double-hybrid functionals, it recovers at least part of the dispersion effects through the MP2-like part, the performance still has space to improve, likely introduce the empirical dispersion corrections -D2, -D3 method. In the lower rung of the 'Jacob's Ladder', the DFT has no corrections to the long-rang distance correlation energy, in such a way, the van der Waals forces are severely underestimated, MP2 correction normally deal with the dispersion corrections in an overestimated way.

For the relevant parameters of the BJ damping function such as PBE0-DH-D3(BJ)[63] and PBE-QIDH-D3(BJ)[64] will show in the appendix.

2.6 Basis set development

The many-electron equations can be approximated by simplifying the problem to the Hartree-Fock method and adding electron correlation effects to ab initio[27].

These equations are usually represented by one-electron wavefunctions, atomic orbitals (AOs), and molecular orbitals ware developed. The equations cannot be solved directly by mathematics, normally the key to working out is using basis functions or basis sets to do iterative numerical computations to fit the radical part of the wavefunction in the Hartree–Fock method or the electronic density in the Density-Functional theory. The basis functions can be any mathematical functions that make up a complete set.

Different types of basis sets were used. Such as Slater, Gaussian, and plane-wave. Slater was the first to develop a function called Slater-type functions (STFs)[65]. STFs possess exponential decay at long range and Kato's cusp condition at short range, they behave similarly to hydrogen-like radical functions and are efficient in representing the AOs, while they are troublesome to use in the three or four centers two-electron integrals. Boys[66] developed the Gaussian-type functions (GTFs), which differ from the STFs in the exponent term. The GTFs are quadratic, three-center and four-center two-electron integrals can be easily converted into two-center two-electron integrals, so the conversion of the centers can reduce the number of calculations, which can speed up the calculations. While the same number of functions are used in linear least-squares fittings, the GTFs are less accurate than the STFs because they decay too fast when compared with the “real” radical functions (e.g., hydrogen-like orbitals). To solve this disadvantage, linear combinations of the primitive GTFs were used to form a new function. On one hand, it’s better to simulate the shape of the atomic orbital wave function, and on the other hand, it makes use of the mathematical properties of the Gaussian function to simplify the calculation. The gaussian basis set is the most widely used basis set now, different forms of the primitive Gaussian basis set with different levels of accuracy, likely used GTFs include minimum (or single-ζ) basis sets, double-ζ, triple-ζ, quadruple-ζ, and so forth, with or without polarization and diffuse functions[67].

For the different basis set families, here are some popular used:

Dunning correlation consistent set: (aug)-cc-pVnZ, …… the performance is well. It is available all to way to Rn element (pVnZ-PP). And very large basis sets have been developed (n=D, T, Q, 5), including the diffuse functions also developed.

For the People family: 6-31G*, 6-311G**, …… but it is mostly for light elements, DZP to Zn element, TZP only to K element.

The Ahlrichs/Karlsruhe family: def-TZVP, def2-QZVPP,……it's quite efficient for HF and DFT, more so than People's, the QZP quality for all elements up to Rn, it is also augmented by diffuse functions, def2-TZVPD, etc. But it is not very systematic naming, and the energy convergence is also somewhat erratic.

The top aim of the development of a basis set is to find a suitable set of different functions that can give a description of the molecular orbitals as accurately as possible, given a predefined set of functions to choose from. However, due to the finite base of the linear combination of the basis functions, there is an intrinsic error when using the quantum chemical approaches based on the expression of molecular orbitals (or density). This effect is particularly correlated with the small-medium size GTFs so that the basis set optimization is a common practice to approach the variational energy limit when using a limited number of basis functions[68]. A number of the basis sets have been developed with HF or post-HF frameworks, such as the Def2 basis of Ahlrichs and coworkers[69] or the correlation consistent basis sets of Dunning[70].

Focused on the specific aims, the basis set has been developed, such as polarizability[71], NMR[72] spectroscopic constants. And also for reproduce the weak noncovalent interactions at the post-HF level is also an interesting field[73–75].

In this thesis manuscript, the DH-SVPD basis set that we have been used is optimized from the Def2-SVPD, using the SD-Box algorithm[76] to minimize the following expression:

$$\mathrm{F} = \left[\frac{(E - \mathrm{E}^0) - (J + K)}{(E - \mathrm{E}^0) + (J + K)}\right]^2 \qquad (2.6.1)$$

E is the total energy of the molecular aggregate (dimer), J, and K are the corresponding Coulomb and exchange energies and E^0 is the total energy of the isolated fragments. Indeed, the minimization of the function basically allows for the optimization of the interaction energy of a dimer as expressed at the perturbation theory level. Therefore, the exponents of a basis set which minimizes F for a given Hamiltonian (here the Kohn−Sham Hamiltonian) will be the optimal for the description of the interaction energy. This optimization procedure does not consider any external reference data for the interaction energy, but only the perturbation energy expression of the interaction energy of a dimer.

For the applications of the DH-SVPD, it will be shown in next Chapters.

Chapter 3

Theoretical study of the thermochemistry of hydrocarbons

3.1 Introduction

Thermochemistry, that is the energy variation all along a chemical reaction, is by definition at the heart of Chemistry, as the challenges it poses to modeling are. Indeed, an accurate theoretical evaluation of reaction energies allows not only a better understanding of the microscopic phenomena underpinning the experimental observations but also the prediction of new ones. This last step forward is even more compelling if accurate methods, or at least methods for which an accurate and reproducible error bar can be defined, are developed and easily applicable. As a consequence, computational thermochemistry has been regularly developed over the past years[77–79].

Heats of formation or ionization energies, just to mention two challenges of the multifaceted thermochemistry problem, have been some of the most relevant properties on which modern approaches based on density functional theory (DFT) have been developed and/or tested since the 90s[80,81]. Also thanks to such efforts, the most recent DFT approaches provide very accurate results on many properties, including also thermochemical one[82]. If DFT methods are, at least in principle, of easy use, nevertheless they are not always able to reach the so-called chemical accuracy[83], that is an error lower than 1 kcal/mol on reaction energies[82,84,85].

Of course, sophisticated post-HF methods represent a more accurate choice, but their direct application is not always possible for larger systems. Therefore, the so-called composite models[77–79,86,87], combining different theoretical approaches, have been developed, successfully applied, and routinely used over the years (for some examples see references 77 to 79 and 86 to 87). Usually, these models are based on smart combinations of various *ab-initio*

methods, where basis set and electronic effects are treated at different levels and extrapolation schemes are assumed. If a "sub-kJ" accuracy is nowadays reached by such approaches[88], their main targets are small molecules, due to the intrinsic computational costs of the refined *ab initio* approaches considered. Indeed, more recently efforts toward larger molecules have been done, by introducing some lower-level methods and/or further extrapolations[89–92].However, the drawback of introducing some approximation in electronic models could be negligible risk of introducing errors in energy evaluations of the same magnitude of the chased accuracy.[93,94] Furthermore, composite models could be relatively complex to set-up so that their use is not straightforward if they are not already implemented in quantum-chemistry codes.

In this context, it is therefore worth coming back to the most recent developments in DFT have conducted to the definition of exchange-correlation functionals, and try to improve its performances even for large systems so to reach, at least, the chemical accuracy threshold. This step should however do preserving its strong points, that is the reasonable accuracy/computational cost ratio and the ease of use, so to allow routine applications, also by non-specialists. One of the main problems arises from the unbalanced description of both covalent and non-covalent interactions, which is need for an accurate thermochemistry, especially for species like alkanes[95]. Indeed, the addition of a pairwise classical potential, an approach firstly proposed by Yang[51] and then popularized by Grimme[96], to common DFT approaches significantly improves their performances on thermochemistry at a minimal computational cost[82].

A new class of functionals, called Double Hybrids (DH), have been developed more recently, to cure some of the difficulties encountered by more traditional DFT models. This combination of DFT, exact-like exchange and second-order Moller-Plesset (MP2) correlation represents a further step onward with respect its predecessors (their Global Hybrids) for a number of ground and excited state properties[97–102]. Such methods could even show an accuracy on thermochemistry higher than that obtained by some composite *ab-initio* models[103]. Furthermore, non-covalent interactions are better reproduced at this level of theory, albeit also in this case the further addition of empirical potentials leads to a very low deviations with respect to reference values[63,104]. As matter of fact, most of the DH approaches provides errors in the range of 1.0 to 1.5 kcal/mol on thermochemistry, even adding empirical dispersion corrections[82,103,105]. For instance, for thermochemistry, where some DHs rival in accuracy with some composite *ab-initio* models.

We have then proposed an alternative protocol for improving the description of weak interactions, based on the pairing of DHs with a property-tuned basis set, called DH-SVPD[30].

Applications to medium and large noncovalent complexes[106,107], suggest that the very good accuracies obtained by DH in conjunction with large basis sets (triple-ζ or quadruple-ζ) and empirical potential can be reached with such split-valence basis set, but at a fraction of the computational cost[106]. As for the empirical potentials, this approach does not impact the computed molecular structures[108]. Based on these encouraging results, here we propose a systematic study on the thermochemistry of the selected systems.

3.2 Computational methods

In the following, a particular attention will be devoted to the results obtained with the DH-SVPD basis set. This basis set has been developed starting from the small Def2-SVPD basis[69] and optimizing the most diffuse functions (one *p*-function and one *d*-function for C atom and one *s*-function and one *p*-function for H atom) so to minimize the following expression for the benzene dimer[109]:

$$\mathcal{F} = \left[\frac{(E - E^0) - (J + K)}{(E - E^0) + (J + K)}\right]^2 \qquad (3.2.1)$$

where E is the total energy of the dimer, J and K are the corresponding Coulomb and exchange energies and E^0 is the total energy of the isolated benzene. This procedure leads to the optimization of the interaction energy of a dimer as expressed at a zero-order perturbation theory[109], without the necessity of external reference data from, for instance, experiment of accurate post-HF methods, a common practice in Computational Chemistry. In practice, this procedure is based on an error compensation between Basis Set Superposition Error (BSSE) and Basis Set Incompleteness Error (BSIE). These errors are not only strictly entangled, but act in opposite way, the former leading to an overestimation of the interaction energies in weakly bonded systems, whereas the latter leads to an underestimation[107].

It is worth to mention that the DH-SVPD basis is significantly smaller than standard basis sets used in accurate energy evaluation. For instance, it has 10 and 30 contracted gaussian functions for H and C, respectively, while the Def2-TZVPP[69] basis foreseen 16 and 46 contracted functions which rise to 18 and 58 for the cc-pVTZ[110], just to mention two other bases considered in the following. The gain in computer resources is then evident.

A number of exchange-correlation functionals were considered in the 3.3 section, the semilocal (M06-L[111]), global hybrid (M06[22], TPSSh[49], PBE0[112], B3LYP[21], CAM-B3LYP[113],

ωB97XD[114]) and double-hybrid (B2-PLYP[29], DSD-PBEP86[39], PBE0-DH[115] and PBE-QIDH[116]) families. And added the revDSD-PBEP86[117] this double hybrid functional in the section 3.4. In some cases, empirical potentials, such as D3 and D3(BJ) models[118], were also added, with the appropriate parametrizations[57,64], giving series of DFT approaches.

3.3 Beyond chemical accuracy for alkane thermochemistry: the DH*thermo* approach

3.3.1 Context

In this section, we propose a study on the thermochemistry of alkanes, a relevant chemical family, which is still a challenge (and a benchmark) for theoretical methods. Indeed, the origin and nature of the greater stability of branched isomers with respect to their linear form, *n*-alkanes, has been largely debated in literature[95,119–126] (see for instance Refs. 95, 119-126). This problem, known as protobranching[95], has been analyzed in terms of the energetic features of isodesmic reactions, which can be written in the following form (see also Scheme 3.3.1):

$$(m\text{-}1)\ C_2H_6 \rightarrow C_mH_{2m+2} + (m\text{-}2)\ CH_4 \qquad (3.3.1)$$

This reaction is also known as Bond Separation Reaction (BSR), since the pioneering work of Pople and co-workers[127]. Without entering into details on the mentioned debate, which is not the main point of the present chapter, it should be pointed out that this reaction has been used for benchmarking DFT models over the years[122,123,125,128], since it has the intrinsic advantage of preserving the number and type of bonds, thus avoiding the calculation of open shell systems as in the case of atomization energies. Despite this feature, which at first sight could suggest an error cancellation and a consequently great accuracy, it has been suggested that a correct reproduction of the energies requires a balanced description of nonlocal correlation effects, including dispersion interactions[95]. This point of view is not, however, fully shared and problems related to the exchange energies have been also advocated in different contexts[37,40]. As a matter of fact, most of the current DFT approaches provide significant errors also on the thermochemistry of BSRs[95,124,125]. The inclusion of empirical corrections have a beneficial effect, but the chemical accuracy is not systematically reached even by DH functionals[105,123,124,128,129].

Scheme 3.3.1. Isodesmic reactions investigated in this work.

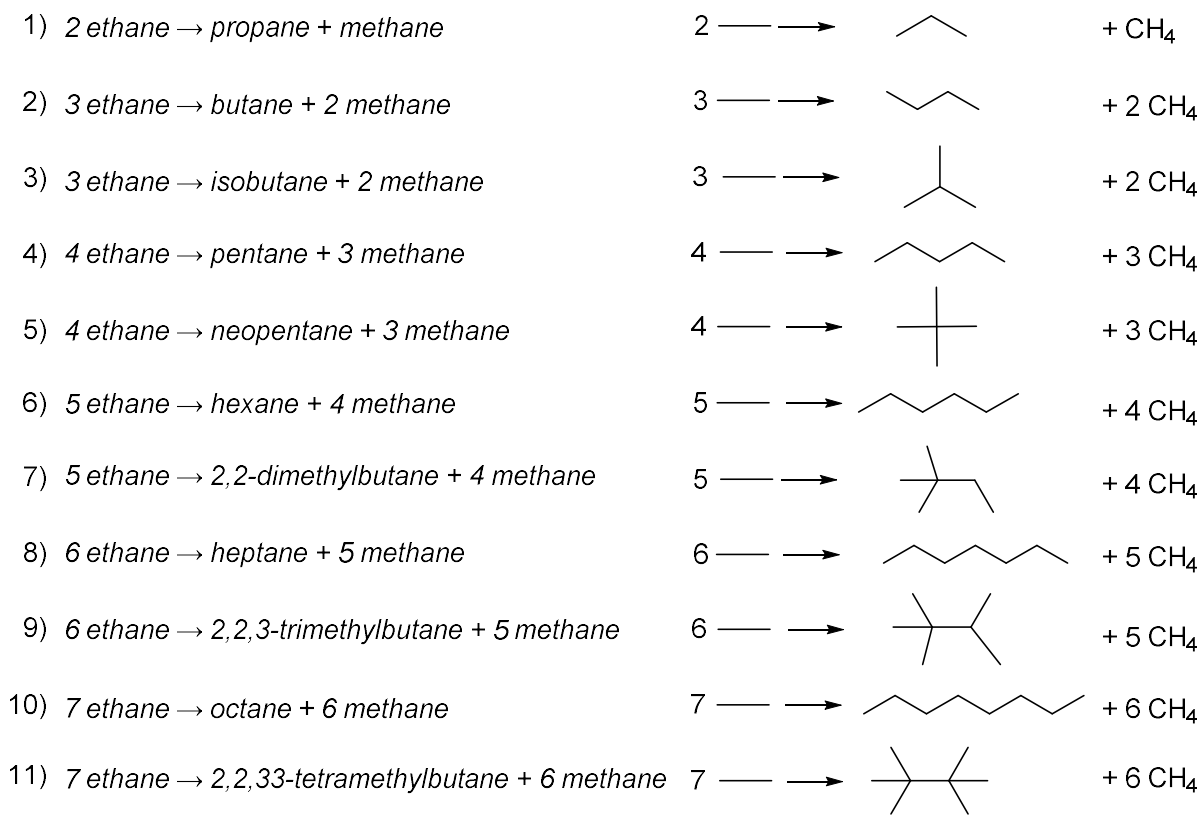

The other dataset BSR36, the reaction energies were, instead, obtained using the molecular structures retrieved from the Grimme's website[130] and routinely used for this benchmark[82]. The molecules considered in this second set are reported in Scheme 3.3.2.

It would be therefore interesting, in our opinion, to test our model coupling DHs and tailored basis set on such difficult playground, since these two concurring facets of the problem, nonlocal correlation effects and dispersion interactions, are at the heart of its development.

Scheme 3.3.2. Sketches of the molecules composing the BSR36 dataset. The set consists of saturated chains (H), rings (R) and cages (C).

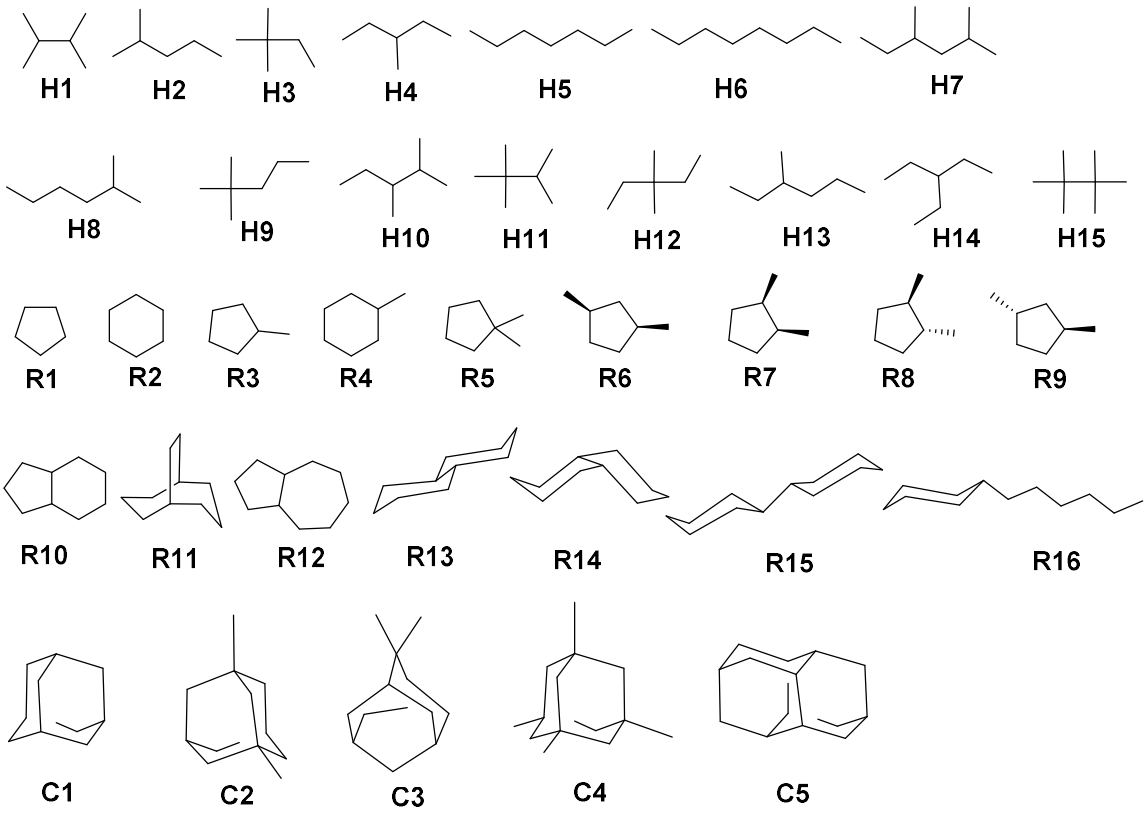

To allow a meaningful comparison with previously reported results[95], the Dunning's basis, cc-pVTZ and cc-pVQZ[110] were considered. Furthermore, these basis sets were also used for the structure optimisation of the systems belonging to the set reported in Scheme 3.3.1 (hereafter referred as *opt*BSR11 set) and the subsequent vibrational and thermochemical calculations. These data were completed with those obtained using our DH-SVPD basis set, developed using a "self-consistent" model based only on energy contributions of the monomers and dimer computed at the same DH level of theory, without requiring an external reference energies[106,109]. In practice, the DH-SVPD basis set is obtained from the original Def2-SVPD basis set, upon a constrained optimization of only one *p*-function and one *d*-function for C atom and one *s*-function and one *p*-function for H atom. All other exponents are kept fixed as those in the original basis set. The optimized exponents are reported in the supplemental material of Table S3.3.1, while an example of input for Gaussian, with the whole basis set for C and H atoms is given in Table S3.3.2.

All calculations were performed with the Gaussian program[131].

3.3.2 Results and discussion

As first step, the BSR energies for the optBSR11 dataset, were computed with the Dunning's basis, cc-pVTZ and cc-pVQZ, so to be consistent with previous works[95], and compared with the reference experimental data reported in Ref. 95. The obtained Mean Absolute Deviations (MADs) for the selected functionals are reported in Table 3.3.1. All these data include Zero Point Energy (ZPE) corrections, computed at the corresponding level of theory using the usual harmonic approximation. We believe that the limited size of our systems makes the anharmonic vibrational effects to ZPE small with respect to the other contributions, so that they are practically cancelled when the BSR energies are computed. This is fully within the philosophy of the isodesmic reaction approach.

As expected, our results do not substantially differ from the previous indications[95]: all the considered DFT approaches are not able to attain the accuracy provided by the MP2 method. Indeed, the lowest DFT error, 2.1 kcal/mol at the PBE-QIDH-D3(BJ)/cc-pVQZ level, is about three times that obtained at the MP2 level (0.7 kcal/mol, cc-pVTZ basis set). DH functionals, generally speaking, show the lowest deviations (between 2.1 and 2.9 kcal/mol) even if the M06 model, a global hybrid (GH), shows a close value (2.8 kcal/mol). This latter functional was developed also taking into account thermochemistry of main group thermochemistry as well as non-covalent interactions[111]. Smaller deviations are obtained with the inclusion of empirical potentials whose effect, as already noticed[63], is significant for B2-PLYP (−1.9 kcal/mol on MAD, from 4.6 to 2.7 kcal/mol) and lower for PBE-QIDH (−0.7 kcal/mol on MAD, from 2.9 to 2.2 kcal/mol). In particular, the DSD-PBEP86, a DH already casting a dispersion correction, is the best performer with a MAD of 1.6 kcal/mol. Finally, it should be noticed that the two correlation-consistent basis sets give similar results, with differences often around 0.1 kcal/mol and not exceeding 0.2 kcal/mol (see Table 3.3.1).

Table 3.3.1. Computed Mean Absolute Deviations (MAD, kcal/mol) for energy variations of the 11 isodesmic reactions reported in Scheme 3.3.1, computed with respect to the experimental data reported in reference 95. All theoretical values include ZPE corrections estimated at the corresponding level of theory. In parenthesis are reported the MADs computed using the experimental references values for 8 reactions (reactions 1-6, 8 and 10 of Scheme 3.3.1) taken for the Active Thermochemical Tables (ATcT)[132,133]

	DH-SVPD	cc-pVTZ	cc-pVQZ
M06-L	3.6	4.7	4.6
TPSSh	6.5	7.6	7.5
B3LYP	6.0	7.6	7.5
PBE0	4.7	5.9	5.7
M06	1.8	2.8	2.8
CAM-B3LYP	4.3	5.8	5.7
ωB97X-D	2.1	3.3	3.3
B3LYP-D3	2.6	4.1	4.0
B2PLYP	3.0	4.6	4.5
PBE0-DH	3.2	4.5	4.3
PBE-QIDH	1.4 (0.67)	2.9 (1.76)	2.8
B2PLYP-D3(BJ)	1.1	2.7	2.6
DSD-PBEP86	0.4	1.7	1.6
PBE0-DH-D3(BJ)	1.1	2.3	2.2
PBE-QIDH-D3(BJ)	0.8 (0.55)	2.2 (1.33)	2.1
DSD-PBEP86	0.4 (0.71)	1.7(1.03)	1.6
MP2[a]		0.7	

a) from reference 95

When the DH-SVPD basis set is instead considered, there is a significantly improvement of the results for all the DHs (−1.5 kcal/mol in average), so that the MP2 accuracy is practically reached for the PBE-QIDH-D3(BJ) model (0.8 vs. 0.7 kcal/mol) and even outshone by DSD-PBEP86 (0.4 kcal/mol). Other PBE-based DHs show close MADs ranging between 1.1 and 1.4 kcal/mol. Interestingly, all DHs present lower MADs when the small basis

set is considered, thus showing the validity of this basis set for the chosen property (and benchmark set).

Since the experimental data reported in Ref 95 can be somehow considered not the most updates ones, MADs have been also computed using the energy values taken from the Active Thermochemical Tables (ATcT)[132,133]. Unfortunately, we were able to retrieve only 8 out of the 11 reactions considered (reactions 1-6, 8 and 10 of Scheme 1), so that only selected functionals have been considered. The value reported in Table 3.3.1, point out not only that above discussed trends are confirmed, but also a further reduction of the deviations for the PBE-QIDH functional, with or without empirical correction. The only exception is the DSD-PBEP86 model, whose error increases considering this second set of experimental data, even if it is still below the threshold of 1kcal/mol. However, in view of the limited set, these values, albeit appealing, cannot be considered as conclusive.

The optBSR11 set is composed by two classes of reactions, leading to linear (reaction 1, 2, 4, 6, 8 and 10 in Scheme 3.3.1) and branched (reaction 3, 5, 7, 9 and 11) alkanes. It was repeatedly pointed out in literature that, for standard DFT approaches, the error proportionally increases with the chain length, at least for linear alkanes[104,124,129]. In Figure 3.3.1 are reported the BSR energy errors with respect to the experimental reference values as a function of the number of C atoms for linear and branched alkanes, computed with the DH-SVPD basis. Concerning the linear alkanes, the error clearly increases with the number of C atoms, but while the slope is large for the standard DFT approaches, such as PBE0 or B3LYP, it is significantly smaller for DHs. Indeed, the four best-performing functionals, PBE-QIDH-D3(BJ), PBE0-DH-D3(BJ), B2-PLYP-D3 and DSD-PBEP86, show remarkably a small dependency of the error upon the number of C atoms. In particular, while for TPSSh and B3LYP (the two worst functionals) the error increases as the number of carbon atoms increases, by around ~1.3 kcal/mol per atom, for PBE-QIDH-D3(BJ) an error saturation over the length of the alkyl chain is observed. Indeed, the energy difference tends to be constant: from the *n*-butane to *n*-octane the error goes from 0.17 Kcal/mol to 0.12 kcal/mol. An even flatter behavior is observed for DSD-PBEP86.

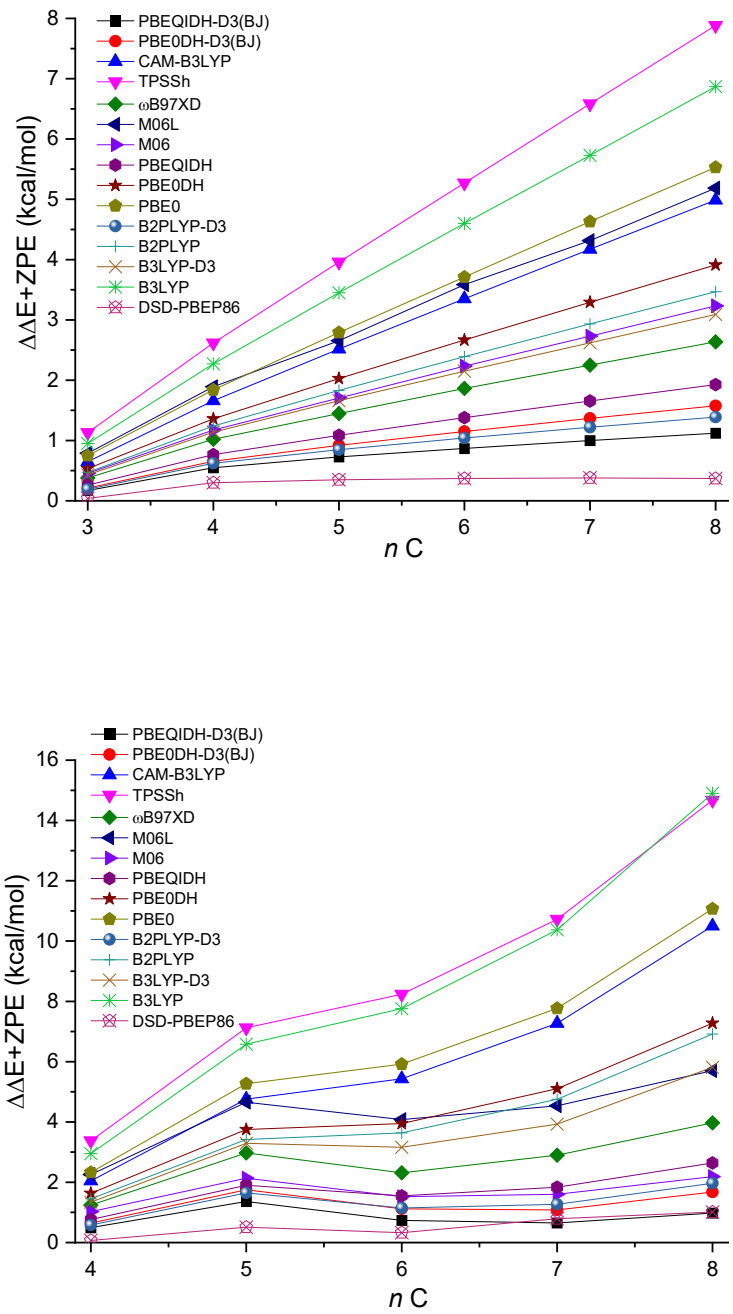

Figure 3.3.1. Errors on Bond Separation Reactions Energies (ΔE_{BSR}, kcal/mol) for the isodesmic reactions giving linear (up) and branched (down) alkanes. All the values were computed using the DH-SVPD basis set and include ZPE contributions. Experimental values from reference 95 are taken as a reference.

The plots for branched alkanes have a less regular behavior but still the errors increase with the size of the molecule for standard DFT approaches. It should be noticed that the 1,3-alkyl-alkyl interactions plays a relevant role in branched alkanes, so that the errors on their BSR energies are generally higher than those found for linear ones[95]. As before, the three mentioned functionals show an almost flat behavior, the error marginally increasing with the number of C atoms. This is already true for PBE-QIDH, but it is still improved when the empirical D3(BJ) dispersion is added. The peak observed in the curves is related to the number of the 1,3 alkyl-alkyl interactions, which is maximal for neopentane and 2,2,3,3-tetramethylbutane. The fact that the PBE-QIDH level of theory (with and without empirical correction) provides very close deviations for these systems point out its robustness.

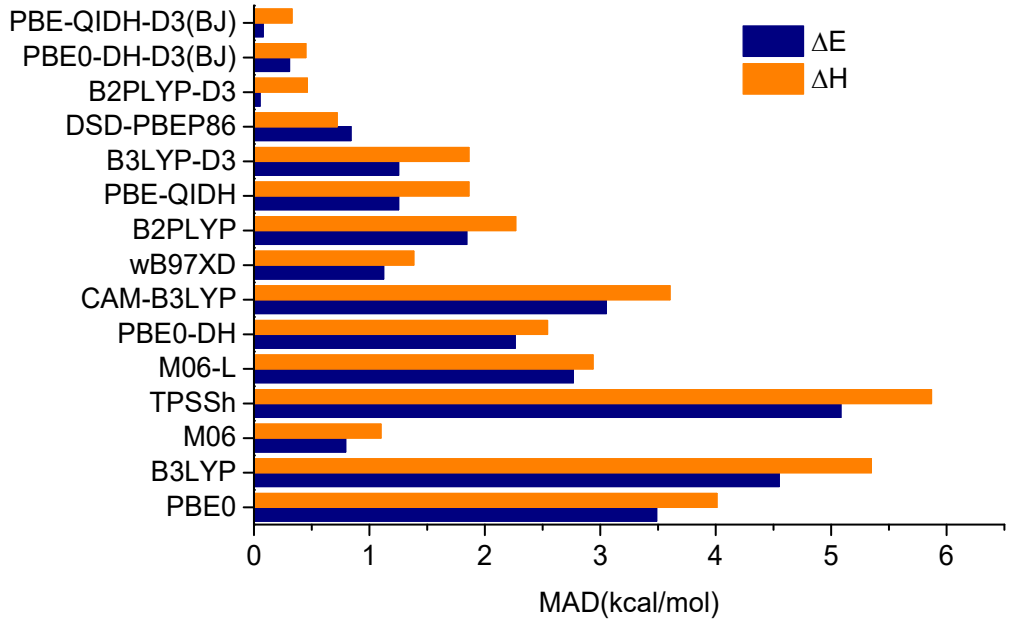

Figure 3.3.2. Mean Absolute Deviations (MADs, kcal/mol) for the relative energies (ΔE) and enthalpies (ΔH) at 298 K for the isodesmic reactions of Scheme 3.3.1. All the values were computed using the DH-SVPD basis set.

In order to corroborate (or refute) such good results, different reference energies were considered, notably those computed from the very accurate W4 and quasi-W4 atomization energies of Martin and co-workers[121] (Table S7 of Ref. 121). These energies are ZPE-uncorrected. The corresponding MADs obtained with the DH-SVPD basis are plotted in Figure 3.3.2, while the raw data are collected in Table S3.3.6. At a first sight, Figure 3.3.2 clearly shows that all the discussed trends are preserved with these new reference values, but the deviations are systematically lower by 1.0-1.5 kcal/mol than those previously discussed. Consequently, exceptionally good accuracies are observed for the best-performing functionals: a MAD of about 0.08 kcal/mol is found for PBE-QIDH-D3(BJ) and 0.05 kcal/mol is the MAD for B2-PLYP-D3. Notably, the D3 correction has a positive effect on both B2-PLYP and PBE-QIDH, decreasing the MADs from 1.8 and 0.6 kcal/mol, respectively, to the mentioned small value (< 0.1 kcal/mol). The exception is represented by the DSD-PBEP86 functionals which, however, still provides a MAD higher than the required chemical accuracy (about 0.7 kcal/mol).

When the cc-pVTZ larger basis set is instead considered, the MADs are significantly larger: 1.4 kcal/mol for PBE-QIDH-D3(BJ) and 1.6 kcal/mol for B2-PLYP-D3, just to mention the best performing functionals (see Table S3.3.7 for other results).

To double check these excellent performances, the DH-SVPD energies of the isodesmic reactions giving linear alkanes (reaction 1, 2, 4, 6 and 10 in Scheme 3.3.1) were compared with the CCSD(T)/CBS value of Grimme[124]. Considering only this limited subset, the MAD for PBE-QIDH-D3(BJ), PBE0-DH-D3(BJ) and B2PLYP-D3 are 0.24, 0.04 and 0.20 kcal/mol, respectively. The fluctuations in going from one set to another can be mainly ascribed to the difference reference for the reaction 10 (13.6 kcal/mol in the first reference set, 13.3 kcal/mol in the second). Such difference has a large weight on the final average due to the limited size of the data subset (5 reactions).

Altogether, these results suggest that the so-called “chemical accuracy” (deviations of ~ 1 kcal/mol) can be reached (and even outdo) using DHs and our DH-SVPD basis set, provided that the quality of the reference data is concomitantly assessed.

In this sense, experimental data collected from the NIST repository[134] have been already used for comparison purposes[124]. So, the MADs for the 15 functionals obtained considering the relative NIST enthalpies for the 11 isodesmic reactions are also collected in Figure 3.3.2. The obtained deviations are all intermediated between those found with the previous two sets, but still all the trends are maintained. So, the largest error (up to about 6 kcal/mol) are observed for GHs, with the only exception of M06 which, with a MAD of 1.1 is by far the best functional in its category. DHs are significantly better than their parent hybrid functionals but still their

performance are inadequate, the error being around 2.0-2.5 kcal/mol. As already observed, the inclusion of empirical potentials for dispersion leads to the lowest deviations. Here, the best performances are obtained, as before, with PBE-QIDH-D3(BJ), PBE0-DH-D3(BJ) and B2-PLYP-D3, which give 0.3, 0.4 and 0.5 kcal/mol, respectively.

It should be also remarked, as already done for the relative energies, that significantly higher deviations (MADs > 1.6 kcal/mol) are obtained at all level of theory considered with the cc-pVTZ basis set (see table S3.3.7).

As last test for our protocol, we consider the BSR36 dataset, which is de facto a standard benchmark for functionals. As it is custom in such cases, the calculations were done using standard geometries, an approach which has the clear advantage to disconnect energetic and structural factors which could affect the overall performances. Nevertheless, it is not a priori granted that both thermochemistry and structures are all well reproduced with a given functional tested (or optimized) just on one of them[135]. Indeed, the benchmark results could be misinterpreted, so that well-performing functionals are sometimes uncritically used also for structural optimizations. For these reasons we have chosen this standard set as last benchmark of our protocol.

The results obtained with selected functionals are reported in Table 3.3.2. First of all, it is reassuring the MADs computed for the BSR36 test are close to those obtained for the previous systems (see Table 3.3.1 and Table 3.3.2). There are two notable exceptions: the first is the PBE-QIDH functional which shows a MADs of 1.4 kcal/mol of the optBSR11 set and 0.4 kcal/mol for the BSR36 set with the small basis set, and the second is DSD-PBEP86, for which the two MADs are 0.4 and 2.1 kcal/mol, respectively.

These differences, which are reduced when the larger basis is considered, suggest that there is a mismatch between energetical and structural parameters for these two functionals. However, still DSD-PBEP86 can be safely used for structural optimization and related energetics in conjunction with the DH-SVPD basis set. More generally, it should be remarked that DHs casting an empirical potential, such as B2-PLYP-D3(BJ) and PBE-QIDH-D3(BJ), show MADs lower than the chemical-accuracy threshold (1 kcal/mol) when the DH-SVPD basis is considered. This is even more remarkable, since a quick look to literature clearly shows that such performances on BSR energies are rarely attained by DHs, even using modern approaches, such as ωB97-M(2)[136], or upon specific parametrization of sophisticated DHs models, like revDSD-PBEP86-D4[117].

It should be also remarked the good performance of the hybrid M06 functional which reaches a deviation of 1 kcal/mol with this same basis set.

Table 3.3.2. Computed Mean Absolute Deviations (MAD, kcal/mol) for the BSR36 data set, computed with respect to the reference values reported in reference 130, using the molecular structures retrieved from the same reference.

	DH-SVPD	Def2-QZVP
M06	1.65	3.03
M06-D3	1.02	1.70
ωB97X-D	2.41	4.29
B2-PLYP	3.08	5.79
PBE-QIDH	0.44	2.73
PBE0-DH	3.86	5.74
B2-PLYP-D3(BJ)	0.64	2.10
DSD-PBEP86	2.07	1.36
PBE-QIDH-D3(BJ)	0.86	1.48
PBE0-DH-D3(BJ)	0.33	1.86

3.3.3 Conclusion

In summary, an accuracy on BSR energies beyond the commonly-accepted threshold for chemical applications (errors ≤ 1.0 kcal/mol) can be obtained using a protocol combining a double-hybrid functional, such as PBE-QIDH or B2-PLYP, with a D3-like empirical correction and a small split-valence basis set, DH-SVPD, developed for non-covalent interactions. This protocol, which is named DH*thermo*, not further tuned on the selected systems, is able to correctly reproduce, with exceptionally low errors, both reaction energies and enthalpies for selected isodesmic reactions, a difficult benchmark where other functionals fails. Due to the intricate nature of this class of reactions and to the method-dependent analysis proposed in literature, it is not possible to clearly relate the contribution of the single component of the protocol (functional, empirical potential and basis set) to the factors affecting the BSR energies. Nevertheless, the obtained results, checked on five different references datasets (two theoretical and three experimental), clearly demonstrate its quality. Finally, the DH*thermo* has the advantage of its intrinsic simplicity and straightforward use, as showed by an input example reported in the Supplementary Material. The results are even more relevant in view of the very

good performances of the PBE-QIDH functionals for other organic reactions, such as Cope rearrangements[137].

Further tests on more challenging systems, easily affordable with our protocol, could be also envisaged provided that reliable experimental or theoretical references are available. The work is shown in section 3.4.

3.4 Pairing double hybrid functionals with a tailored basis set for accurate thermochemistry of hydrocarbons

3.4.1 Context

From the former work, we have recently found that DHs coupled to a small basis set[106,138], tailored for non-covalent interactions, reach, or even exceed, the chemical accuracy threshold for the Bond Separation Reactions (BSR), an elegant way to investigate the greater stability of branched alkanes with respect to their linear forms using the isodesmic principle[95].

Here we want to further extend our investigation to other medium-sized hydrocarbons included in selected datasets, for which accurate reference values are available. These sets (vide infra) have been chosen to show a larger diversity of chemical situations, including multiple carbon-carbon bonds, large electronic delocalization and, of course, weak noncovalent interactions. The aim is to verify the limits of modern DHs methods in modelling the thermochemistry of hydrocarbons, that plays a central role in both experimental and theoretical Chemistry. So, five different sets have been considered as benchmarks, including saturate, unsaturated and aromatic hydrocarbons. They are listed in Table 3.4.1, together with their main characteristics.

The first set is the so-called ADIM6[61], part of the very large GMTKN55 database (and its predecessors)[82], that is considered as a reference for benchmarking functionals. Indeed, structures and references energies are those reported in the original paper and retrieved from the Grimme's website[130]. It is composed by 6 six alkane dimers obtained from ethane to *n*-heptane.

The second set, called AAA (see Figure 3.4.1), has been recently introduced by Chao and collaborators[139] and it is composed by 6 dimers of *n*-alkanes (from methane to hexane) in all-trans conformation, 4 alkenes (ethene, propene, 1-butene and 1-pentene) and 4 alkynes (ethyne, propyne, 1-butyne and 1-pentyne). The interactions energies discussed in the

following were computed for the optimized structures of the dimers, using the same functional for structural and energetic evaluation. The comparison is done with the CCSD(T)/CBS values reported in the original paper. These two sets, ADIM6 and AAA, have been created to probe weak dispersive interactions.

The third set, IDHC5, concerns intramolecular dispersion interactions in hydrocarbons and it extracted by that originally proposed by Grimme[140]. It is composed by the energies of the following reactions:

1) *n*-octane → tetramethylbutane
2) *n*-undecane → hexamethylbutane
3) $C_{14}H_{30}$ (linear) → $C_{28}H_{20}$ (folded)
4) $C_{22}H_{46}$ (linear) → $C_{22}H_{46}$ (folded)
5) $C_{30}H_{62}$ (linear) → $C_{30}H_{62}$ (folded)

As it can be seen, this set is nonuniform containing two isomerization reactions (1 and 2) and three folding reactions (4, 5 and 6). The original reference data, QCISD(T) for 1, experimental for 2, and MP2 for the others, have been replaced by CCSD(T)/CBS values in order to keep consistency with the other datasets. For the sake of homogeneity, all structures were first fully optimized at the PBE0-D3(BJ) level of theory using the def2-TZVPP basis set. Then, DLPNO-CCSD(T)[141] single point energy computations were performed with the release 4.1.2 of the Orca program package[142] making use of a TightPNO convergence criteria as recommended in reference 143[143]. The complete basis set limit is finally obtained from a triple- to quadruple-ζ extrapolation based on the aug-cc-pVTZ and aug-cc-pVQZ and corresponding auxiliary basis set[110] following the scheme developed in reference 144[144].

The PAH5 set has been proposed by Karton some years ago[145]. It is composed by the following isomerization reactions involving medium-sized polycyclic aromatic hydrocarbons (PAHs, see Figure 3.4.2):

1) phenanthrene → anthracene
2) triphenylene → chrysene
3) tryphenylene → benz[a]anthracene
4) tryphenylene → benz[a]anthracene
5) tryphenylene → naphthacene

The difficulty in these large molecules is represented by the π-conjugated pattern which significantly changes in going from one isomer to the other. Also in this case, reliable CCSD(T)/CBS values are taken as references.

Finally, the last set (Cope) recently proposed by Karton, is composed by reaction energies and barrier heights for the Cope rearrangement of substituted bullvalene[137]. The reactions, sketched in Figure 3.4.3, are sigmatropic rearrangement involving a large reorganization of the electronic structure along the reaction path, even if the number and type of bond is unaffected from reactants to products. We have discarded 3 molecules from the original set, since they contain atoms (S, F and Cl) not included in the currently available DH-SVPD basis set. Also in this case, the reference values are computed at the CCSD(T)/CBS level of theory.

Even if it can be argued that these systems are medium-sized ones, they, except for the recent AAA set, are currently used in literature as representative benchmarks for DFT approaches. At the same, it should be stressed that the outcomes of any benchmark analysis, in term of accuracy and domain of applicability of tested functionals, depends on the quality of the reference values. Indeed, in validating theory against theory we face to the above-mentioned problems related to the size/computational cost ratio derived from the consideration of post-HF methods as reference. Reference values obtained at the CCSD(T)/CBS level, which is considered as the gold standard in thermochemistry[146], are already available or have been obtained at a reasonable computational cost for all the considered datasets. This is not always the case for larger systems, but this choice does not affect the legitimacy of our tests, in terms of numerical accuracy for thermochemistry, domain of applicability of the protocol and chemical analysis.

All calculations have been performed with the Gaussian 16 program[131] and the release 4.1.2 of the Orca program package[142].

Table 3.4.1. Chemical space considered in the present work.

set	type	property[a]	relative energies	single-point calculations	geom. opt.	reference data	Ref
ADIM6	hydrocarbon dimers	ΔE_{int}	6	12	NO	W1-F12	Ref[61]
AAA	hydrocarbon dimers	ΔE_{int}	7	21	YES	CCSD(T)/CBS	Ref[139]
IDHC5	isomerization and folding reactions	ΔE	5	10	NO	CCSD(T)/CBS	This work
PAH5	PAH isomers	ΔE	5	10	NO	CCSD(T)/CBS	Ref[145]
Cope	Cope rearrangements	ΔE, $\Delta E^{\neq}$	25	50	NO	CCSD(T)/CBS	Ref[147]
Total			48	103			

a) ΔE_{int} = dimerization energy; ΔE = reaction energy; $\Delta E^{\neq}$ = reaction barrier height.

3.4.2 Results and discussion

1. The ADIM6 and AAA sets

As above mentioned, these first two sets, having some overlap, have been developed for benchmarking weak interactions in terms of interaction energy (ΔE_{int}) between dimers and separated monomers. The Mean Absolute Deviations (MAD) of the selected functional obtained for the first test are reported in Table 3.4.2. Since ADIM6 is part of the larger GMTKN55, that have been widely applied to any class of known functionals (or almost), no unexpected behavior can be evidenced in the results obtained with the larger Def2-QZVP basis set. Indeed, sub-chemical accuracies can be obtained with DHs casting empirical potentials, with deviations as low as 0.1 kcal/mol (B2-PLYP-D3 and DSD-PBEP86). It should be also

noticed that the PBE-QIDH prefers, on this set, to be coupled with the D3 potential rather than the D3(BJ) one (MAD of 0.4 vs. 0.8 kcal/mol). More interesting are, however, the low MADs showed by the hybrid M06 functionals (0.3 kcal/mol) and its local counterpart, M06-L (0.2 kcal/mol), obtained without any specific corrections. The B3LYP-D3 model is also very competitive (0.5 kcal/mol). In order to give a flavor of the reached accuracies, it can be mentioned that the DLPNO-CCSD(T) approach provides on this set a MAD of 0.4 kcal/mol with respect to the same reference values[93].

By moving to the DH-SVPD basis set, a deterioration of the performances of all the DHs coupled to empirical potential can be observed, as already remarked for other systems ruled by pure dispersive interactions. This is true for both PBE- and BLYP-based functional as well as DSD-PBEP86 functionals. In contrast, the three pure DHs, B2-PLYP, PBE0-DH and PBE-QIDH, are all below the chemical- accuracy threshold, with the last functional showing a MAD value of 0.2 kcal/mol. This last value is lower than that obtained by the same functional corrected with the empirical potential and the large basis set, thus showing that one of the primary objectives in the development of the DH-SVPD basis set was reached.

All the other functionals show similar behaviors: those already providing good performances with the larger basis set are worsening (e.g. M06 or ωB97X-D), while those with more moderate performances improves their MADs up to about 50%.

The AAA set can be considered an enlargement of the previous one, containing both alkenes and alkynes, with the structures of the 14 noncovalently bounded dimers depicted in Figure 3.4.1, while the MADs for the interaction energies are reported in Table 3.4.3. In this case the structures of the dimers have been fully optimized with each single functional, so to verify the coherence between energy and structure evaluation. The trends observed for the ADIM6 dataset are globally preserved, with minor modifications, and most of the deviations are even lower than before. Indeed, all the DHs give very low MADs, between 0.1 kcal/mol (B2-PLYP-D3) and 0.4 kcal/mol (PBE0-DH-D3(BJ) and PBE-QIDH-D3(BJ)) when coupled with empirical potentials and larger basis set. Few hybrid functionals also provide very respectable performances with deviations under the 1 kcal/mol threshold. They include ωB97X-D (0.7 kcal/mol), B3LYP-D3 (0.4 kcal/mol) and, as before, M06 (0.4 kcal/mol). The local M06-L gives also a remarkable accuracy (0.3 kcal/mol). The D(0) correction seems to be more suitable for the PBE-QIDH functional than D3(BJ), since it halves the error (0.2 vs. 0.4 kcal/mol), as for the ADIM6 set (0.4 vs. 0.8 kcal/mol, see Table 3.4.2).

The performances of these dispersion-corrected functionals significantly deteriorate with the small DH-SVPD basis set, while those not including an empirical potential become competitive. Among the latter, it should be emphasized B2-PLYP (0.5 kcal/mol) and PBE-QIDH, whose value is very close to that obtained with an empirical potential and larger basis (0.2 kcal/mol, see Table 3.4.3).

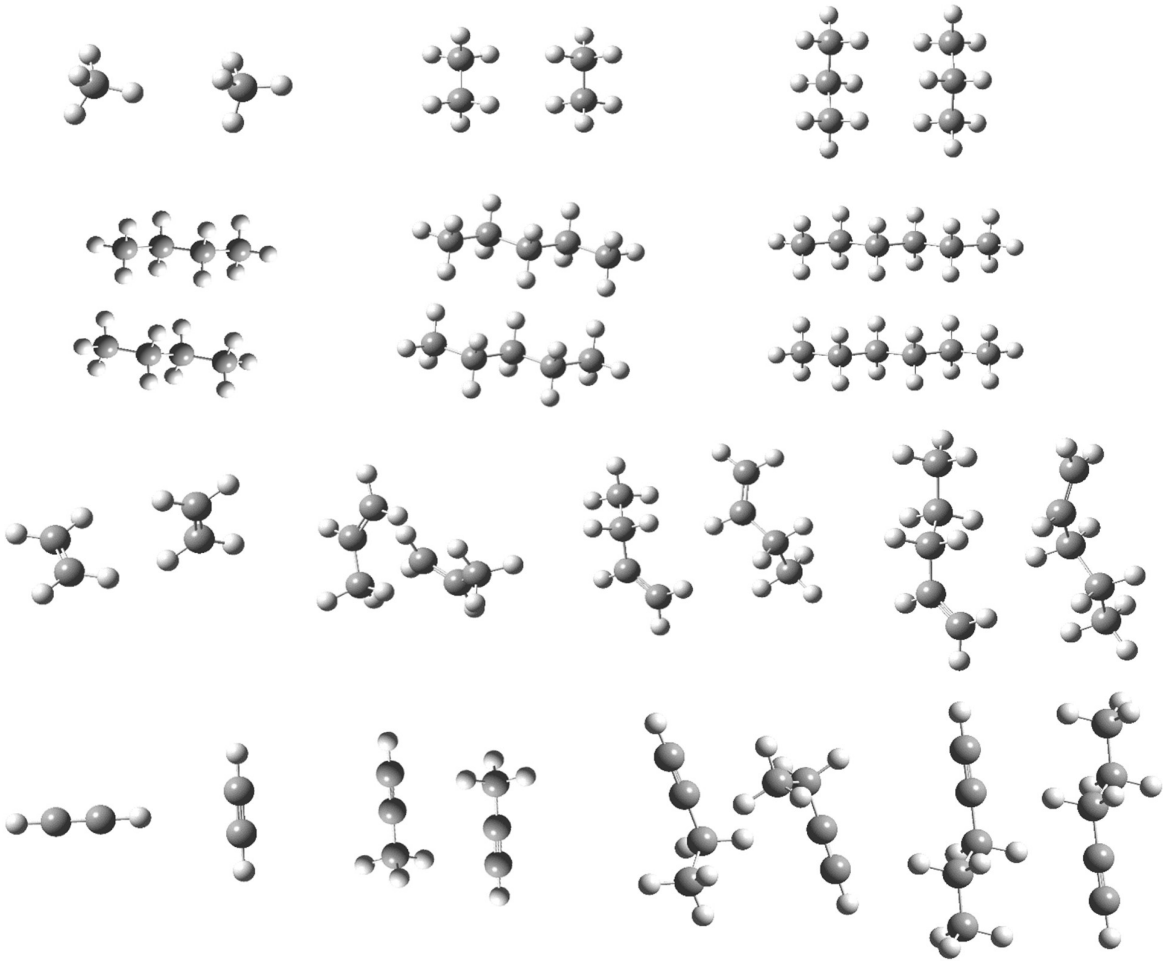

Figure 3.4.1. The optimized structures of the dimers in the AAA groups at PBE-QIDH/DH-SVPD level.

In Figure 3.4.4 are reported the intermolecular distance for three selected cases of the AAA set, namely methane, propane and ethyne dimers. There is a general agreement on the computed distances for all the considered methods, independently from the basis set and the inclusion of an empirical potential. This is particularly evident for the ethyne dimers, where all the methods predict the distance between a hydrogen atom and the mid-point of the CC bond to be about 2.8 Å. Larger variations, as a function of the DFT approach used, are observed for the larger CC distances in the two other dimers, albeit for a given functionals, the two basis sets provide very close results. Two notable exceptions are evident from the figure: B3LYP and the related CAM-B3LYP functional. In both cases, the two dimers of methane and ethane are not bound (intermolecular distance > 7Å in the plot) when the cc-pVTZ basis is considered. Of course, the two interactions energies are significantly underestimated at both the B3LYP and CAM-B3LYP levels (between −20% and −50% of the references values), but the statistical weight of these deviations on the MAD is small due to the low interaction energies (see Table S3.4.2). The DH-SVPD leads to shorter distances for both functionals, even if B3LYP also provides the largest distance for these two dimers, thus confirming its large underestimation of the dispersion interactions. Of course, the addition of an empirical potential to B3LYP gives a better description, both in term for energy and distances. However, B3LYP distances are among the most overestimated and the related energies are significantly underestimated, thus confirming a significantly overbonding character of the empirical correction[148–150].

Table 3.4.2. Computed Mean Absolute Deviations (MAD, kcal/mol) for interactions energies of the ADIM6 dataset.

	DH-SVPD	Def2-QZVP
M06-L	1.95	0.22
TPSSh	3.07	4.64
B3LYP	2.98	4.99
PBE0	1.74	3.43
M06	1.86	0.28
CAM-B3LYP	1.51	3.55
ωB97X-D	2.80	1.03
B3LYP-D3	2.47	0.46
B2-PLYP	0.70	2.90
PBE0-DH	0.95	2.76
PBE-QIDH	0.15	1.86
B2-PLYP-D3	2.06	0.14
DSD-PBEP86	2.42	0.10
revDSD-PBEP86-D3(BJ)	2.07	0.32
PBE0-DH-D3(BJ)	1.57	0.23
PBE-QIDH-D3(BJ)	1.24	0.77
PBE-QIDH-D3	1.64	0.37

Table 3.4.3. Computed Mean Absolute Deviations (MAD, kcal/mol) for the interaction energies of the AAA set. In parenthesis are reported the values obtained at with cc-pVQZ basis set.

	DH-SVPD	cc-pVTZ
M06-L	1.12	0.30
TPSSh	1.40	2.04
B3LYP	1.53	2.30
PBE0	0.91	1.75
M06	1.23	0.41
CAM-B3LYP	0.95	2.04
ωB97X-D	1.91	0.66
B3LYP-D3	1.57	0.43
B2-PLYP	0.49	1.69
PBE0-DH	0.56	1.53 (1.52)
PBE-QIDH	0.18	1.07 (1.05)
B2-PLYP-D3	1.32	0.09
DSD-PBEP86	0.44	0.23
revDSD-PBEP86-D3(BJ)	1.35	0.13
PBE0-DH-D3(BJ)	1.11	0.39
PBE-QIDH-D3(BJ)	0.80	0.39
PBE-QIDH-D3	1.08	0.16

2. IDHC5

The second set, IDHC5, it has been scarcely considered in previous benchmarks, due probably to the absence of updated reference data. To resolve this omission, the reaction energies of the reactions 1) to 5) have been computed at the CCSD(T)/CBS level. The MADs for the selected functionals are, instead, gathered in Table 3.4.4. The most striking feature among the results obtained with the larger Def2-TZVPP basis is the very good performances obtained by M06 and M06-L functionals, which complete the very good performances already observed for the ADIM6 and AAA sets. Indeed, these two models, with a MAD around 1.9

kcal/mol are the best performers among the local, GH and RSH approaches. Even the introduction of empirical potential into B3LYP, the worst performer, does not allow to reach of the chemical accuracy threshold, even if the error is reduced by an order of magnitude (from 14.9 to 2.7 kcal/mol). Pure DHs do not behave as expected, albeit significantly better that their GH counterparts, since their deviations range between 7.7 kcal/mol (B2-PLYP) and 3.7 kcal/mol (PBE-QIDH). However, the coupling with an empirical dispersion, either D3 or D3(BJ), leads to the overcoming of the 1 kcal/mol threshold for four functionals (DSD-PBEP86, revDSDPBEP86-D3(BJ), PBE0-DH-D3(BJ) and PBE-QIDH-D3(BJ)), the lowest value being 0.4 kcal/mol, obtained with the DSD-PBEP86 model.

When the smaller DH-SVPD basis set is considered, the trend already discussed for ADIM6 and AAA is also now observed, that is an increasing of the MADs for all the methods, and in particular DHs, casting an empirical potential. Indeed, the reaction energies are in these cases all overestimated, probably due to a double counting (potential + basis set) of the dispersion interactions.

This is no longer the case when the empirical correction is not considered. Indeed, a significant improvement is found for the PBE-QIDH that, as before, shows with the small DH-SVPD basis set an error comparable to that obtained with the larger basis set and empirical potential (1.1 vs. 1.0 kcal/mol). However, in this case the chemical accuracy is just marginally reached. Also, the other two pure DHs provide significantly lower (about – 40%) deviations the the DH-SVPD basis.

Table 3.4.4. Computed Mean Absolute Deviations (MAD, kcal/mol) for the reaction energies of the IDH5 set.

	DH-SVPD	Def2-TZVPP
M06-L	4.04	1.90
TPSSh	10.17	12.32
B3LYP	11.49	14.86
PBE0	7.64	10.06
M06	4.21	1.94
CAM-B3LYP	7.31	10.55
ωB97X-D	4.26	3.11
B3LYP-D3	3.13	2.66
B2-PLYP	4.75	7.72
PBE0-DH	4.62	7.05
PBE-QIDH	1.07	3.65
B2-PLYP-D3	1.87	1.34
DSD-PBEP86	3.39	0.41
revDSD-PBEP86-D3(BJ)	2.19	0.88
PBE0-DH-D3(BJ)	1.71	0.72
PBE-QIDH-D3(BJ)	1.21	1.37
PBE-QIDH-D3	1.62	0.96

3. PAH5

The PAH5 set is composed by 7 molecules, two of them are $C_{14}H_{10}$ isomers and five are $C_{18}H_{12}$ isomers. Their structures are sketched in Figure 3.4.2.

As already highlighted by Karton[145], GGA funtionals underestimate the relative energies of the reactions 6 to 10 and only GHs including either a high percent of HF exchange or a low percent and a dispersion potential significantly reduce the deviations with respect to the reference data. DHs follows the same trends, so that the MADs are bracketed between 0.7 kcal/mol (B2-PLYP) and 0.1 kcal/mol (B2GP-PLYP-D3). In all cases, the DHs provide an accuracy lower than 1 kcal/mol and, in particular, indicate triphenylene as the most stable isomer of $C_{18}H_{12}$ and anthracene as the most stable $C_{14}H_{10}$ molecule.

Figure 3.4.2. Sketches of the molecules composing the PAH5 set. Only one of the possible resonance structures is reported.

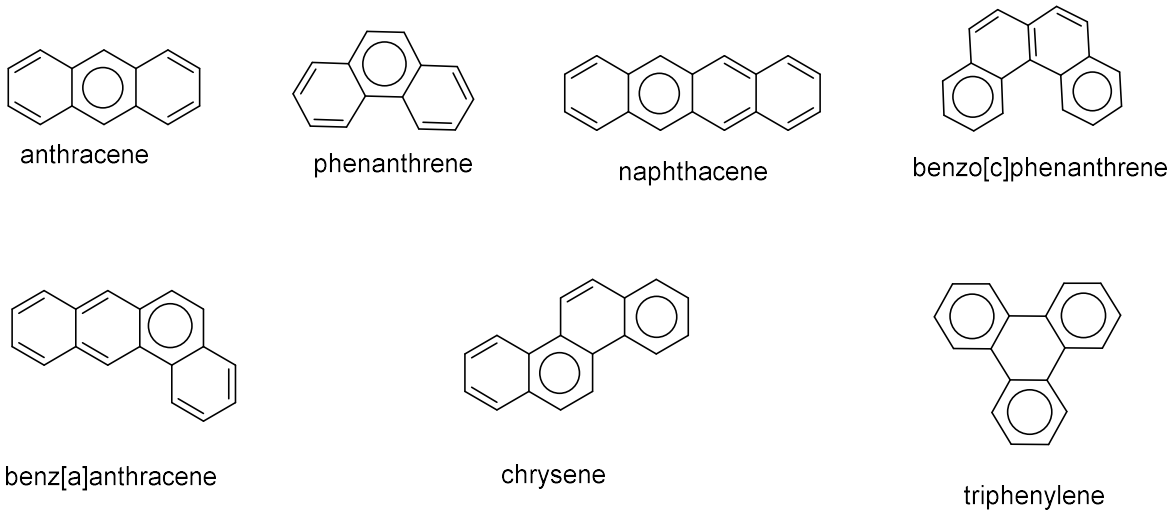

The data reported in Table 3.4.5 follows this trend. In particular, two DHs, PBE0-DH and PBE-QIDH, provide very low deviations in conjunction with the cc-pVQZ basis set (0.2 and 0.3 kcal/mol). These functionals are among the better performing functionals of their class not corrected for dispersion. The inclusion of empirical potential has a beneficial effect for B2-PLYP whose error is significantly reduced (from 0.7 to 0.2 kcal/mol), while a negative impact is obtained for the DHs casting the PBE functional. Indeed, the empirical potential, further strengthening the weak interactions, leads to an overestimation of the reaction energies with a consequent increase of the MADs. The PBE0-DH functional represents the worst case, since its error grows from 0.2 kcal/mol to 1.5 kcal/mol, if the D3(BJ) correction is added. This behavior is not surprising since empirical potentials work at their best with functional (like B3LYP) significantly underestimating weak interactions. In contrast, functionals which already somehow give an energy minimum, even if small (such as PBE0), lead to an overestimation of the interactions upon addition of classical potentials.

In going from the larger to the smaller basis set, the MADs decrease or are unchanged (± 0.05 kcal/mol). The exceptions are represented by ωB97X-D (+ 0.1 kcal/mol), B3LYP -D3 (+0.4 kcal/mol) and B2-PLYP-D3 (+0.4 kcal/mol).

In conclusion, all DHs give deviation below the chemical accuracy thresholds with both large (cc-pVQZ) and small (DH-SVPD) basis set. In most cases, the two bases provide very close deviations. However, while the DSD-PBEP86 provides the lowest MADs when coupled

to the DH-SVPD basis (0.1 kcal/mol), PBE0-DH and PBE-QIDH are not far (0.2 and 0.3 kcal/mol, respectively) without further introduction of an empirical correction.

Table 3.4.5. Computed Mean Absolute Deviations (MAD, kcal/mol) for reaction energies of the PAH5 set.

	DH-SVPD	cc-pVQZ
M06-L	0.71	0.74[a]
TPSSh	1.10	1.20[a]
B3LYP	1.38	1.48[a]
PBE0	0.68	0.79[a]
M06	0.49	0.53[a]
CAM-B3LYP	0.40	0.38[a]
ωB97X-D	0.79	0.69[a]
B3LYP-D3	1.11	0.69[a]
B2-PLYP	0.69	0.74[a]
PBE0-DH	0.21	0.24
PBE-QIDH	0.34	0.31
B2-PLYP-D3	0.57	0.22[a]
DSD-PBEP86	0.10	0.36[a]
revDSD-PBEP86-D3(BJ)	0.32	0.36
PBE0-DH-D3(BJ)	0.41	1.46
PBE-QIDH-D3(BJ)	0.50	0.45
PBE-QIDH-D3	0.42	0.36

a) Data from reference 145

4. Cope set

The last set, Cope, collects 25 reactions and transition-state energies derived from the structural reorganization of the 5 bullvalene derivatives depicted in Figure 3.4.3. These two sets of data span different energy intervals, from −22 kcal/mol to 6 kcal/mol for the reaction energies and from 42 to 66 kcal/mol for the barrier heigths. More interesting, they collect molecules different in nature, minima and transitions states, so that they reppresent a very difficul play ground for most of the DFT approaches. Indeed, few DFT methods provide a balanced description of both sets[146]. In particular, some of the functionals, such as PBE-QIDH or ωB97X-2 provides sub-chemical accuracy on both barriers and reaction energies, whereas other functionals are good only on one of these properties.

The obtained results are collected in Table 3.4.6. The first feature to be commented is that the MADs obtained for the barrier heights are larger than those calculated for the reaction energies. Indeed, several functionals are lower than the 1 kcal/mol threshold when coupled to the larger Def2-TZVPP basis set. In particular, DH performances for reaction energies range between 0.7 kcal/mol (B2-PLYP) and 0.2 kcal/mol (revDSD-PBEP86-D3(BJ)), the only exception in this family being PBE0-DH (1.0 kcal/mol). In contrast, the range is between 0.4 kcal/mol (PBE-QIDH-D3 and PBE-QIDH) and 0.9 kcal/mol (PBE0-DH) for energy barriers, with three functionals, B2-PLYP(D3), B2-PLYP and DSD-PBEP86 providing large errors (between 3.7 and 1.7 kcal/mol). The other non-DH functionals provide correct (around 1 kcal/mol) deviations for reactions barrier, while only PBE0 is close to the chemical accuracy (1.0 kcal/mol, see Table 3.4.6).

More interesting, only few functionals provide a balanced description of reaction and barrier energies, in terms of comparable deviations. They include all those casting the PBE functionals, either GH or DH), M06-L and revDSD-PBEP86-D3(BJ). For the other ones, the difference can be as high as some kcal/mol, as in the case of B2-PLYP(D3) (0.5 and 3.7 kcal/mol for the two sets, respectively) and DSD-PBEP86 (0.3 and 1.7 kcal/mol). It is also remarkable the small effect of dispersion on the computed energies, as showed by the small or even negligible variations of the MADs observed upon addition to empirical corrections. For the reaction energies there is a variation of -0.2 kcal/mol in going from B2-PLYP to B2-PLYP-D3 and a negligible difference (< 0.1 kcal/mol) for PBE-QIDH and PBE-QIDH-D3(BJ). Even smaller differences are found for barrier heights.

In going from the larger to the small basis set a significant increase of the MADs is observed. This variation is smaller and constant for the reaction energies of all DHs (around

+0.2 kcal/mol), while larger values are observed for barrier heights (between 0.2 and 0.6 kcal/mol). A similar behavior is also observed for the other classes of functionals, even if with some small variation for some functional and energies (see Table 3.4.6 for details).

Overall, two functionals provide a subchemical accuracy with the DH-SVPD basis set on both reaction energies and barrier heights, namely PBE-QIDH, with and without corrections, and revDSD-PBEP86-D3(BJ).

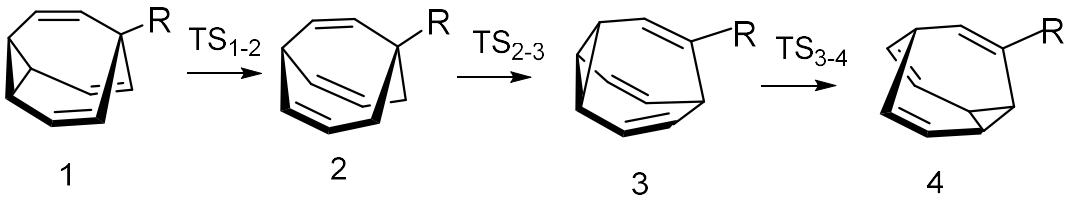

Figure 3.4.3. Schematic representation of the unimolecular rearrangements in the Cope database (R = NH_3, OH, CH_3 and CN).

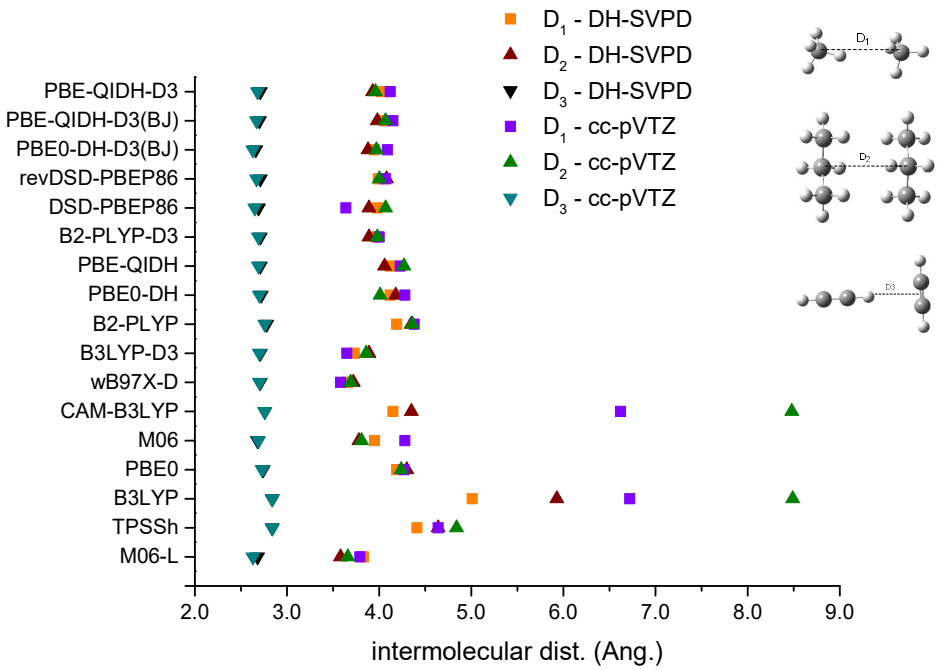

Figure 3.4.4. Values of the reported intermolecular distances (Å) for the indicated dimers, computed with the small (DH-SVPD) and larger (cc-pVTZ) basis set.

Table 3.4.6. Computed Mean Absolute Deviations (MAD, kcal/mol) for energies of the Cope set.

	Barrier Heights		Reaction Energies	
	DH-SVPD	Def2-TZVPP	DH-SVPD	Def2-TZVPP
M06-L	1.26	1.35	1.88	1.83
TPSSh	2.54	3.24	1.81	1.64
B3LYP	2.70	3.33	1.56	1.40
PBE0	0.97	1.03	1.64	1.45
M06	2.22	1.95	0.91	0.89
CAM-B3LYP	2.57	1.91	1.00	0.84
ωB97X-D	2.18	1.52	1.09	0.93
B3LYP-D3	2.88	3.52	1.13	0.98
B2-PLYP	3.05	3.56	0.9	0.74
PBE0-DH	1.41	0.86	1.22	1.04
PBE-QIDH	0.63	0.37	0.85	0.68
B2-PLYP-D3	3.14	3.65	0.66	0.50
DSD-PBEP86	1.26	1.65	0.43	0.26
revDSD-PBEP86-D3(BJ)	0.46	0.83	0.41	0.24
PBE0-DH-D3(BJ)	1.25	0.70	1.01	0.83
PBE-QIDH-D3(BJ)	0.59	0.36	0.81	0.65
PBE-QIDH-D3	0.60	0.36	0.80	0.63

3.4.3 An overview and discussion

As mentioned above, the selected datasets constitute a quite heterogeneous ensemble, where dispersion interactions are, in some cases, combined with subtle modifications of the electronic structures in such a way that they cannot be disentangled. At the same time, this difficulty concomitantly increases the interest of the selected datasets, which represent reasonably well "real-world" chemical problems where several factors rule the overall behavior. Some trends can be however evidenced from the obtained results.

In the first two sets, ADIM6 and AAA, dominated by intermolecular dispersion interactions, the combination of PBE-QIDH functionals with the DH-SVPD basis set, provides basically the same deviations obtained with larger basis sets and empirical potentials. The remaining pure DHs behaves in a similar way. This trend is also observed for the IDHC5 dataset which also contains some isomerization reactions with moderate modifications of the electronic structures. For all these three datasets, the small basis cannot be used in conjunction with an empirical potential, since it leads to a sort of double counting of dispersion interactions and a consequent overestimation of the reaction energies.

Moving to the PAH5 dataset, the obtained results show that the small basis is able to capture the modifications in the electronic structure observed in going from one isomer to another one.

The last set, Cope, reveals a different behavior with the DH-SVPD basis giving higher deviations that the triple-ζ basis, more evident in some cases. This could be related to the peculiar features of the reaction intermediates, which have not the same number and type (double, triple) of bonds. Indeed, the DH-SVPD basis set provides very accurate results for the so-called Bond Separation Reactions, where the thermochemistry of selected reactions is evaluated with an isodesmic principle which leads to the preservation of the number and type of intramolecular bonds[95]. The situation is even more complex due to the absence of dispersion effects for these reactions. This makes the Cope set very peculiar in the context of this study, well representing the limits of the pairing a DH with the tailored DH-SVPD. However, it should be also remarked that the computational time of a DHs coupled with this small basis is in practice equivalent to that of a DH with a large triple-ζ basis set, since the use of the smaller basis set largely compensates for the more computer-demanding time of the perturbative part in PBE-QIDH.

The overall trends can be better observed from the plots in Figure 3.4.5 and 3.4.6. In the first one, are reported the MADs for all the considered DHs functionals and datasets, obtained with the DH-SVPD and reference basis sets. From these data it clearly appears that the small basis provides error smaller, or at least close, to that systematically provided with the larger basis set, in absence of empirical corrections for all the datasets. The advantages in term of computational speed-up are evident. For instance, the whole computational time for the ADIM6 with the DH-SVPD basis set is only 3% of that needed for the Def2-QZVP basis (about 5 minutes of wall-clock time against 188 minutes, respectively). When the empirical corrections are added, larger bases of triple-ζ or quadruple-ζ quality are mandatory for obtaining a small deviation with respect to reference data. It should be outlined, however, that sub-chemical accuracy can be obtained with the two approaches, DH and DH-SVPD or DH+D together with a large basis set, for most of the considered sets, with the few exceptions already discussed. For these exceptions, the small basis provides a smaller deviation than the larger basis sets, even if the 1 kcal/mol threshold cannot be reached.

Finally, in Figure 3.4.6 are reported the MADs for all the DHs considered. To avoid any bias coming from the different nature and number of data the different considered set, these MADs are simply the mathematical average of those computed for the different set, that is their sum divide by 6 (counting reaction and barriers for the Cope in a different way). The first striking feature of the plot concerns two functionals, namely PBE0-DH and B2-PLYP, which do not reach the threshold of 1 kcal/mol, even if a significant improvement is found in going for the larger basis set to DH-SVPD. As already discussed, all DHs including an empirical dispersion prefer the larger basis set which lead to sub-chemical accuracies. In contrast, the PBE-QIDH/DH-SVPD combinations is competitive with these latter. In short, the lowest values are obtained with PBE-QIDH/DH-SVPD or by combining PBE-QIDH-D3(BJ), DSD-PBEP86 and rev-DSDPBEP86-D3(BJ) with a larger basis, all these models providing a mean MAD around 0.5 kcal/mol. It is reassuring than on such global performance indicator, the PBE-QIDH-D3(BJ)/DH-SVPD model, which is our *DHthermo* model for the thermochemistry of alkanes[138], is among the best performers, thus extending its applicability beyond isodesmic reactions.

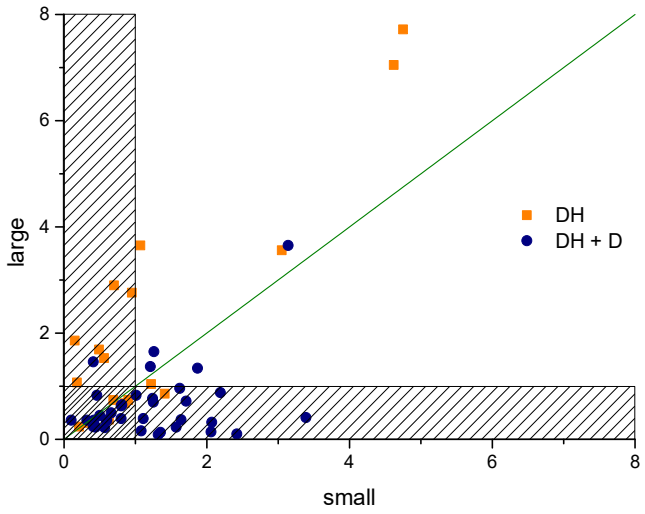

Figure 3.4.5. Mean Absolute Deviations (MAD, kcal/mol) obtained with the larger and DH-SVPD basis set) for pure and dispersion-corrected double hybrids. The shadow areas correspond to values lower than the chemical accuracy (1 kcal/mol).

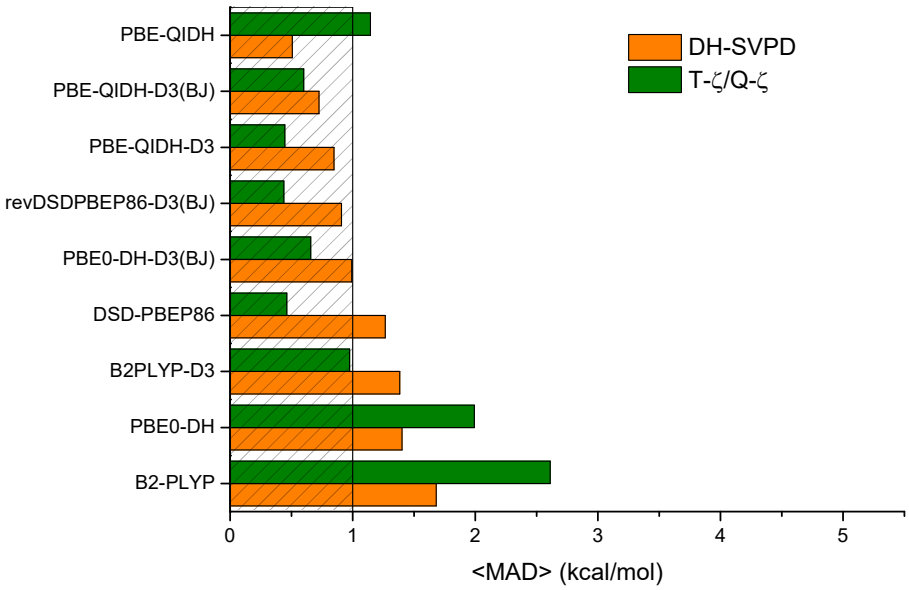

Figure 3.4.6. Average of the Mean Absolute Deviations (<MAD>, kcal/mol) computed for the considered benchmarks and double hybrids functionals. The shadow area corresponds to values lower than the chemical accuracy (1 kcal/mol).

3.4.4 conclusions

A detailed analysis of the performances of DHs coupled with the small DH-SVPD basis set, especially developed for weak noncovalent interactions, have been carried out on a series of difficult datasets. The aim is to extend the applicability domain of this computational protocol (DH + DH-SVPD basis set) while showing its reliability with respect to data obtained with larger basis sets of triple-ζ or quadruple-ζ quality and empirical pairwise potentials for modeling noncovalent interactions. The data sets were chosen so to include, beyond the mentioned noncovalent interactions, others subtle electronic effects and simple, yet challenging, reactions. The obtained results suggest that the chemical accuracy, that is deviations of less than 1 kcal/mol with respect to reference values, can be obtained with the nonempirical PBE-QIDH functionals for the 5 considered datasets, when it is coupled with the tailored DH-SVPD basis set. Globally speaking, this pairing is competitive with respect to modern semiempirical DHs, such as revDSD-PBEP86, coupled to empirical potential and large basis set. A similar positive behavior is found for all the other pure DHs functionals, where the DH-SVPD basis set leads to a significant improvement toward the chemical accuracy threshold.

Albeit this newly developed basis set is based on a compensation between two errors, that is BSSE and BSIE, the results clearly show that it is[151] transferable to both nonempirical and empirical DH, when an empirical potential is not further added. The resulting protocol is robust, fast, and simple to use, as showed by the Gaussian input example reported in the SI of Table S3.3.2.

Chapter 4

Tackling an accurate description of molecular reactivity with double hybrid density functionals

4.1 Context

From the results of the last chapter, we want to test performance of the DH-SVPD basis set together with only double-hybrid functionals in this chapter for some trick problems. Focus on this aim, we choose BH9 dataset, which include 9 different types of the reactions, 449 real-size molecular reactions (RE) and 898 barrier heights (BH) (i.e., 449 forward and 449 reverse BHs). And we explored the panel of 18 non-empirical and empirical double-hybrid density functionals for the modeling of the thermochemistry and kinetics properties of the BH9 dataset, to check the chemical accuracy if can be reached.

4.2 Introduction

Thermochemistry and kinetics rule the chemical reactivity of molecular systems. The former studies the equilibrium state between reactants and products and delivers the concept of reaction yield. The latter focuses on the path followed by the transformation of reactants into products, and particularly to the rate constant driving the reversibility of the reaction. Both fields rely on two different energy quantities that have been routinely assessed at theoretical chemistry level along the last century as the reaction and barrier height energies (RE and BH, respectively)[152]. RE is the energy variation between products (P) and reactants (R). Here dubbed ΔE_{RE}, it is defined as

$$\Delta E_{RE} = E_P - E_R$$

where E_R and E_P are the energies of the reactant and product at their minimum-energy structures, respectively. Dubbed ΔE_{BH}^{i}, the BH energy involves a third quantity, namely the energy of the transition-state (**TS**) structure E_{TS} which connects **R** and **P**. According to its definition, ΔE_{BH}^{i} characterizes a forward ($i = f$) or reverse ($i = r$) reaction

$$\Delta E_{BH}^{i} = E_{TS} - E_{min}$$

where E_{min} refers to the minimum energy structure of **R** or **P** whether a forward or reverse process is targeted.

The computation of these energy quantities requires a robust computational chemistry protocol that guarantees an homogeneous and reproducible accuracy while conserving a daily affordable cost when applied to sizable molecular systems[77–79]. Within the computational energy landscape, highly accurate ab initio composite methods (e.g., WnX)[77,153,154] are often claimed as being the 'Holy Grail' of reactivity. However, even alleviated by the domain-based local pair natural orbital (DLPNO) framework[141,155–157], their computational cost prevents them from being applied to very large molecules commonly employed in chemistry. For these reasons, electronic structure methods, and notably the Kohn-Sham variant of density-functional theory (KS-DFT), has continuously drawn attention since the middle of the 80's[8,9].

KS-DFT cost/accuracy trade-off has indeed regularly improved with the recurrent efforts done by the community to develop new and sophisticated density functional approximations (DFAs)[158,159]. The double-hybrid (DH) class of approximations is one of their modern (striking) representation[97,98,102,160]. By adding nonlocality to both the exchange and correlation energies, it systematically improves the well-known and widely used global-hybrid class of approximations[99]. The exchange-correlation energy term is now defined as:

$$E_{xc}^{DH}[\rho] = a_x E_x^{XX}[\{\phi_i\}] + (1 - a_x)E_x^{DFA}[\rho] + a_c E_c^{PT2}[\{\phi_i, \phi_a\}] + (1 - a_c)E_c^{DFA}[\rho]$$

where a_x and $(1- a_x)$ govern the fractions of nonlocal exact-like (EXX) and semilocal DFA exchange energies, respectively, which depend on the set of occupied orbitals $\{\phi_i\}$. a_c and $(1- a_c)$ denote the parts of second-order perturbation theory (PT2) correlation energy and its semilocal complementary, respectively, the former adding also a dependence on the set of virtual orbitals $\{\phi_a\}$.

In literature, the DH class of approximation and its adaptations into range-separated exchange and/or correlation[161–164], and/or spin-component-scaled variants[39,41,165–167], are often found as overperforming other exchange-correlation approximations in extensive benchmark sets probing for energy[82,101,168], structure[135,169] and density based properties[170]. On the one hand, their large fraction of EXX energy (mostly $a_x > 50\%$) helps to cancel the self-interaction error (SIE)[171,172] which spuriously contaminates elongated bonds in **TS** structures resulting in an underestimation of energy BHs. On the other hand, their PT2 energy term brings the nonlocal dynamic correlation required to accurately describe covalent bond energies, and thus REs. It is thus expected, and confirmed on some previous benchmark sets, that DHs are excellent candidates to model reactivity of molecular systems[39,41,42,173,174].

In kinetics and thermochemistry, 1.4 kcal/mol is often recalled as being the 'chemical accuracy' threshold for an accurate determination of BHs and REs[152]. At room temperature, it corresponds to an error of about one order of magnitude for equilibrium or rate constants. With the aim to identify which variant of DHs is able to reach this energy threshold for a wide variety of molecular reactions, we will thus assess these expressions on the newly developed BH9 comprehensive benchmark set for BHs and REs[175]. The dataset contains a total of 449 real-size molecular reactions and 898 barrier heights (i.e., 449 forward and 449 reverse BHs), all of them characterized by reference energies computed at the DLPNO coupled-cluster singles and doubles plus perturbative triples [CCSD(T)] level of theory at the complete basis set limit (CBS). DLPNO-CCSD(T) is indeed becoming a standard owing to its linearly-scaled computational cost and high accuracy (tenth of kcal/mol) with respect to pristine CCSD(T). It is thus an excellent compromise to obtain reference energy values for large systems like those implied in BH9.

4.3 Computational methods

All the computations are performed with the release 5.0 of Orca[176]. For each energy single point, a tight SCF convergence criteria together with the DefGrid3 integration grid are taken as default. The BH9 database is both assessed with the very large Def2-QZVPP Ahlrichs' quadruple-z[69] and small DH-SVPD split-valence[106] basis sets, the former assuring a nearly complete basis set convergence and minimizing Basis Set Superposition Errors (BSSE) while the latter assuming compensation between BSSE and Basis Set Infinite Errors (BSIE). The DH-SVPD basis set being only available for H, C, N and O, we replace it by Def2-SVPD for the missing elements[69,177]. The resolution-of-the-identity in combination with the "chain-of-

spheres' algorithm[178] (COSX) and an automatic construction of a general purpose auxiliary basis set is systematically turned on.

4.4 Results and discussion

We removed 15 entries due to the unreliable reference barrier height and reaction energies in the original publication of the BH9 dataset, they are: 41: 01_41, 45: 01_45, 47: 01_47, 197: 03_9, 204: 03_16, 205: 03_17, 207: 03_19, 263: 04_32, 264: 04_33, 265: 04_34, 271: 04_40, 306: 04_75, 311: 04_80, 317: 04_86, 319: 04_88. Thus the size of the dataset to 434 real-size molecular reactions and 868 barrier heights. The originality of BH9 is not only its extensive size which guarantees the calculation of robust error bars, but also the chemical diversity of the molecular systems (reaching 71 atoms) involved and the energy diversity of their reactions. More precisely, it probes for 9 types of reactions involved in highly important organic and biochemistry reactions. They belong to (i) radical rearrangement and addition, (ii) pericyclic, (iii) halogen atom transfer, (iv) hydrogen atom transfer, (v) hydride transfer, (vi) B- and Si- containing reactions, (vii) proton transfer, (viii) nucleophilic substitution, and (ix) nucleophilic addition.

Table 4.1 gathers the performance of a set of DHs augmented by their dispersion-corrected variants on the BH9 barrier height energy database (see Table S4.1 of Supporting Material of Chapter 4 for more detailed information about their composition). They are selected to be representative of the modern DH variety, i.e., to belong to (i) nonempirical, minimally or highly parameterized DHs (nonempirical in case its constants are identified to limit physical constraints; minimally parameterized in case it contains few empirical parameters, typically 1 to 5; and highly parameterized in case it contains more than 5 empirical parameters). (ii) global or range-separated exchange DHs, (iii) spin-component-scaled DHs, and (iv) dispersion-corrected with Grimme's -D3(BJ) model[57,184]. For the BH energy property, the total mean absolute deviations (MADs) span between 1.71 (PBE0-DH) and 4.89 kcal/mol (RSX-0DH), and the MADs calculated from subsets are relatively homogeneous with the related total MAD. We notice however that in average DHs tend to better perform on subsets (vi), (vii), and (ix), but obtain worse MADs on subset (iii).

Table 4.1. Mean absolute deviations (kcal/mol) over the 9 subsets of the BH9 barrier height energy database (868 entries) computed with the 18 double hybrids considered in this work at the Def2-QZVPP level of theory.

	Ref.	(i)	(ii)	(iii)	(iv)	(v)	(vi)	(vii)	(viii)	(ix)	total
PBE0-DH	Ref[115]	1.53	1.95	1.51	1.58	1.84	1.34	1.55	2.72	1.25	1.71
ωB2PLYP-D3(BJ)	Ref[162]	1.69	2.23	0.94	1.69	1.23	1.47	1.73	1.68	1.47	1.72
ωB2PLYP	Ref[162,168]	1.69	2.23	1.00	1.60	1.41	1.52	1.69	1.74	1.47	1.73
PBE-QIDH	Ref[116]	2.04	2.39	1.62	1.31	2.52	1.52	1.28	2.06	1.46	1.93
B2K-PLYP	Ref[174]	2.08	2.96	1.32	1.32	2.78	1.74	0.62	1.21	1.16	2.08
PBE-QIDH-D3(BJ)	Ref[64,116]	2.06	2.88	1.13	1.94	4.64	1.79	1.50	1.06	1.82	2.38
B2K-PLYP-D3(BJ)	Ref[174,179]	2.02	3.58	1.21	1.69	5.32	0.87	0.74	1.44	1.47	2.53
ωB97X-2	Ref[180]	1.98	3.95	1.77	2.22	4.49	1.35	1.38	2.02	1.67	2.80
ωB97X-2-D3(BJ)	Ref[104,180]	1.98	3.96	1.77	2.22	4.50	1.36	1.38	2.02	1.67	2.81
PBE0-DH-D3(BJ)	Ref[63,181]	1.98	2.99	1.80	3.39	4.87	2.53	1.91	0.93	2.33	2.86
DSD-PBEP86-D3(BJ)	Ref[182]	2.30	3.70	1.65	2.55	7.29	1.47	1.29	2.15	1.98	3.11
B2-PLYP	Ref[29]	1.46	5.00	2.57	1.91	3.69	2.52	1.19	1.85	2.34	3.15
RSX-QIDH-D3(BJ)	Ref[161,163,168]	3.35	5.41	3.27	1.11	1.50	2.48	1.79	3.29	3.12	3.28
RSX-QIDH	Ref[161,163]	3.34	5.35	3.52	1.06	1.82	2.52	1.71	3.58	3.07	3.32
DSD-BLYP-D3(BJ)	Ref[182]	1.92	5.12	2.19	2.76	7.73	1.36	1.07	2.73	2.27	3.68
B2-PLYP-D3(BJ)	Ref[29,183]	1.53	5.72	4.80	3.99	8.10	2.06	1.31	3.94	3.00	4.49
RSX-0DH-D3(BJ)	Ref[161,168]	3.79	7.46	4.34	0.98	5.36	3.04	1.96	5.41	3.92	4.61
RSX-0DH	Ref[161]	3.74	7.42	5.13	1.30	6.82	3.18	1.76	6.22	3.91	4.89

The best performance is reached by the PBE0-DH nonempirical global DH (1.71 kcal/mol), and by the dispersion-corrected and uncorrected variants of ωB2-PLYP, a minimally parameterized range-separated exchange (RSX) DH trained to accurately reproduce excitation energies (1.72 and 1.73 kcal/mol, respectively). They are followed by the PBE-QIDH nonempirical global DH (1.93 kcal/mol), by B2K-PLYP (2.08 kcal/mol), a minimally parameterized DH trained for kinetics purpose, and by their dispersion-corrected variants (2.38 and 2.53 kcal/mol, respectively). We find then the highly parameterized ωB97X-2 RSX-DH (2.80 kcal/mol), its dispersion corrected variant (2.81 kcal/mol), and PBE0-DH-D3(BJ) (2.86 kcal/mol). The remaining 8 DHs considered in this work provide deviations larger than 3 kcal/mol, i.e. deviations larger than 2 times the 'chemical accuracy' threshold.

Even if it seems difficult to rationalize trends between the nature of the DHs and their performances, it is easy to realize that the on-top addition of the -D3(BJ) correction systematically deteriorates, or at least marginally improves for few of them, the estimation of BH energies (Table 4.1). It is generally found an overstabilization of the TS with respect to reactants and products, leading to underestimation of BHs induced by a double counting of dispersion forces (see mean signed deviations in Table S4.2 of Supporting Materials of Chapter 4). This behavior confirms some previous investigations showing that a dispersion correction does not a fortiori improve the accuracy of nonempirical DHs[63]. However, it contradicts some others which highly recommend to systematically add it on-top of a DH[82,104].

In terms of performance/features rationalization, it is worth noting that nonempirical global DHs including between 50 to 70% of EXX, and between 10 to 35% of PT2 correlation energies, provide promising results. It is however not the case of their RSX variants. We remark also that to get an accurate measure of BH energies, minimally parameterized global DHs need to include a large fraction of EXX (70%) and PT2 correlation energies (40%) like in B2K-PLYP, while the performance of B2-PLYP (a_x = 0.53 and a_c = 0.27) remains more modest. Finally, we note the excellent performance of wB2PLYP which is the only RSX-DH able to well behave with respect to BHs.

At this point, it is also important to compare the DH performances with respect to other (non-DH) density-functional approximations reported in Ref[175]. The comparison is of course not completely strict since we removed here 30 troublemaker BHs energies from the original BH9 dataset, as before mentioned. However, it provides a (slightly overestimated) flavor of their MADs. On this line, only some global- or RSX-hybrid approximations displays MADs lower than 3 kcal/mol. Among them, we note highly parameterized density functionals from the Head-Gordon (e.g., ωB97M-V[185] and ωB97XD[114]) or Truhlar (e.g., M05-2X[186], M06-2X[22]

and MN15[187]) groups for which the BH property is an integral part of their training set, and MADs compete with the best DHs (MADs between 2.1 and 2.3 kcal/mol). Good results are also found with the CAM-B3LYP[113] minimally parameterized RSX and PBE0[20,188] nonempirical global hybrids when coupled with the XDM dispersion correction[118,189] (2.37 and 2.85 kcal/mol, respectively). Unlike with DHs (exception made with Minnesota density functionals), we notice here that the on-top addition of a dispersion correction is recommended.

Looking now at the BH9 database from the thermochemistry point of view, Table 4.2 gathers the performance of all DHs on REs. For most of the DHs, the total MADs are here better than for BHs. They span from 1.37 to 6.24 kcal/mol with a better average performance on subsets (v) and (vii) than on subset (i). The best approach is the highly parameterized ωB97X-2 range-separated exchange DH (1.37 kcal/mol). It is directly followed by the minimally parameterized DSD-PBEP86-D3(BJ) and DSD-BLYP-D3(BJ) spin-component scaled, and B2K-PLYP-D3(BJ) global DHs (1.56, 1.63 and 1.72 kcal mol^{-1}, respectively), all of them being corrected for dispersion forces. We find then the ωB2-PLYP range-separated exchange(RSX) DH (2.10 kcal mol^{-1}), and the PBE0-DH and PBE-QIDH nonempirical DHs (2.23 and 2.48 kcal mol^{-1}, respectively). The last one yielding a MAD below 3 kcal/mol is B2-PLYP-D3(BJ), a minimally parameterized DH corrected for dispersion interactions. The 6 other approaches considered in this work are above this threshold.

Except for B2K-PLYP and B2-PLYP, we notice that -D3(BJ) overcorrects REs of all DHs considered in this work. The larger improvements are of about 0.5 kcal/mol for the former and 1.4 kcal/mol for the latter. They are obtained for pericyclic reactions [subset (ii)]. Just like within the Diels-Alder reaction (DARC) testset[190], the repulsive nonbonded interactions at highly com-pressed distance ruling the reactants are overestimated, leading to their larger destabilization with respect to the product (see mean signed deviations in Table S4.3 of Supporting Material of Chapter 4). Even if this error is claimed to be closely related to SIE[190], -D3(BJ) artificially stabilizes the product and improves the estimation of the RE property. This observation is confirmed by the good performance of the ωB2-PLYP RSX-DH variant which better corrects SIE. The other subsets are revealed as less affected by the use of the *a posteriori* correction.

Table 4.2. Mean absolute deviations (kcal/mol) over the 9 subsets of the BH9 reaction energy database(434 entries) computed with the 18 double hybrids considered in this work at the Def2-QZVPP level of theory.

	References	(i)	(ii)	(iii)	(iv)	(v)	(vi)	(vii)	(viii)	(ix)	total
ωB97X-2	Ref[180]	2.51	0.91	1.90	1.89	0.62	1.33	0.52	1.47	0.96	1.37
ωB97X-2-D3(BJ)	Ref[104,180]	2.51	0.91	1.90	1.89	0.62	1.33	0.52	1.47	0.96	1.37
DSD-PBEP86-D3(BJ)	Ref[182]	2.9	1.09	1.95	2.07	0.62	1.51	0.67	1.47	1.59	1.56
DSD-BLYP-D3(BJ)	Ref[182]	2.43	1.48	1.77	2.02	1.08	1.38	0.55	1.52	1.28	1.63
B2K-PLYP-D3(BJ)	Ref[174,179]	2.27	2.06	1.72	1.83	1.30	0.92	0.48	1.17	1.12	1.72
ωB2PLYP	Ref[162,168]	2.14	3.27	1.01	1.10	1.71	1.88	0.49	1.05	2.60	2.10
ωB2PLYP-D3(BJ)	Ref[162,168]	2.15	3.33	1.01	1.10	1.70	1.99	0.49	1.06	2.66	2.13
PBE0-DH	Ref[115]	2.98	3.06	2.33	1.53	1.28	1.24	0.96	1.50	2.22	2.23
B2K-PLYP	Ref[174]	2.26	3.33	1.77	1.85	1.37	1.71	0.48	1.26	1.44	2.23
PBE-QIDH	Ref[116]	3.7	3.79	1.36	1.72	0.90	1.46	0.67	1.19	2.82	2.48
B2-PLYP-D3(BJ)	Ref[29,183]	1.87	5.06	1.48	1.44	1.40	0.99	1.03	1.7	1.77	2.64
PBE-QIDH-D3(BJ)	Ref[116,191]	3.86	4.67	1.33	1.74	0.83	2.32	0.67	1.14	3.54	2.89
PBE0-DH-D3(BJ)	Ref[115,181]	3.91	4.98	1.89	1.49	1.15	3.30	0.95	1.49	4.43	3.18
B2-PLYP	Ref[29]	2.57	7.99	1.90	1.52	1.54	3.82	1.03	1.83	3.75	4.07
RSX-QIDH	Ref[161,163]	6.11	9.92	1.37	1.56	1.29	3.33	0.61	1.12	6.09	5.06
RSX-QIDH-D3(BJ)	Ref[161,163,168]	6.14	10.07	1.37	1.56	1.28	3.56	0.61	1.14	6.22	5.14
RSX-0DH	Ref[161]	7.44	12.05	1.59	7.44	12.05	1.59	1.19	1.85	3.79	0.81
RSX-0DH-D3(BJ)	Ref[161,168]	7.54	12.51	1.55	1.21	1.83	4.55	0.81	1.54	7.36	6.24

The performance/features trade-off is less restrictive for the estimation of RE than for BH energies. Except nonempirical RSX-DHs and B2-PLYP, most of the DHs tested in this work provide excellent performances with respect to this property. This is however not the case for other density-functional approximations as semilocal or hybrids. Like for BHs, highly parameterized global and RSX hybrids from the Head-Gordon and Truhlar groups compete with the best DHs even if MADs are biased by 15 more troublemaker REs. The best performance is found for ωB97M-V (1.62 kcal/mol) and the deviations remain below 3 kcal/mol for M05-2X, M06-2X and ωB97XD. Other approximations are found less accurate than DHs.

Since the accuracy in kinetics and thermochemistry is ruled by the 'chemical accuracy' energy threshold, Figure 4.1 depicts the success of DHs in reaching it for BH and RE properties. It is calculated as the number of reactions included in the BH9 database with an absolute energy error lower than 1.4 kcal/mol divided by the total number of reactions. The higher this percentage is, the better a DH fulfills the 'chemical accuracy' criteria. At a first glance, most of the DHs investigated here gather a similar success for BH and RE properties. Only the ωB97X-2 and ωB97X-2-D3(BJ) highly, and DSD-PBEP86-D3(BJ), DSD-BLYP-D3(BJ) and B2-PLYP-D3(BJ) minimally parameterized DHs display unbalanced performance versus both properties. ωB97X-2 is by far the most successful in predicting REs (67.5%). Its parameterization is likely the source of its large success. However, it is also probably at the origin of its poor success with respect to BHs (27.4%). Similar remarks can be made for DSD-PBEP86-D3(BJ) and DSD-BLYP-D3(BJ), and in a lower extent to B2-PLYP-D3(BJ).

The other DHs provide a well balanced and more stable success versus both properties, proving that the parameterization of a DFA can give an unbalanced performance (Figure 4.1). The best DH is ωB2PLYP while the worse is B2-PLYP-D3(BJ). Their successes are of about 51.7% (41.7%) and 17.5% (42.4%) for BH (RE), respectively. In between, the B2K-PLYP minimally parameterized, and PBE0-DH and PBE-QIDH nonempirical global DHs are found as very promising with a success ranging from 45 to 49% for BH, and from 35 and to 49% for REs. The other DHs present a more moderate success positioned around 30% for both properties.

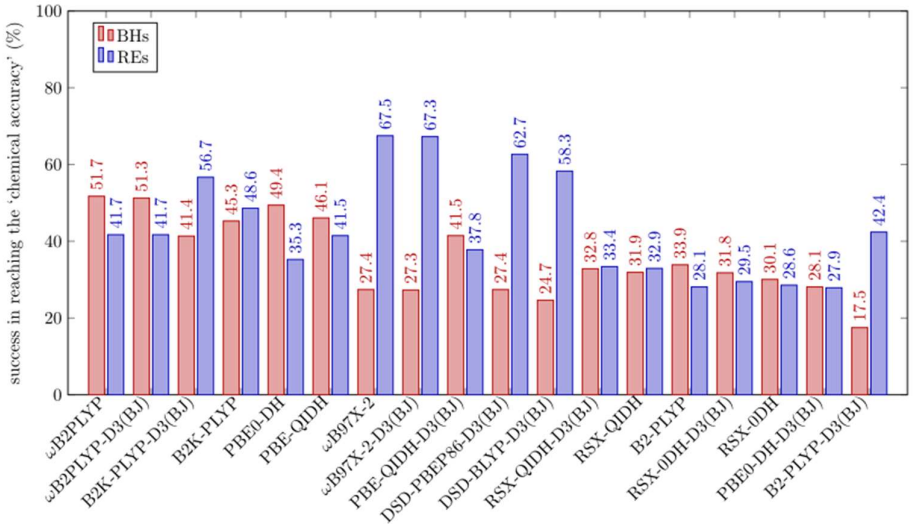

Figure 4.1. Percentage of success of each DH in reaching the 'chemical accuracy' threshold (1.4 kcal/mol) for the (red) 868 barrier height (BH) energies, and (blue) 434 reaction energies (RE). From left to right, DHs are ranked from the more to the less successful in reaching the 'chemical accuracy' threshold for bothBH and RE properties.

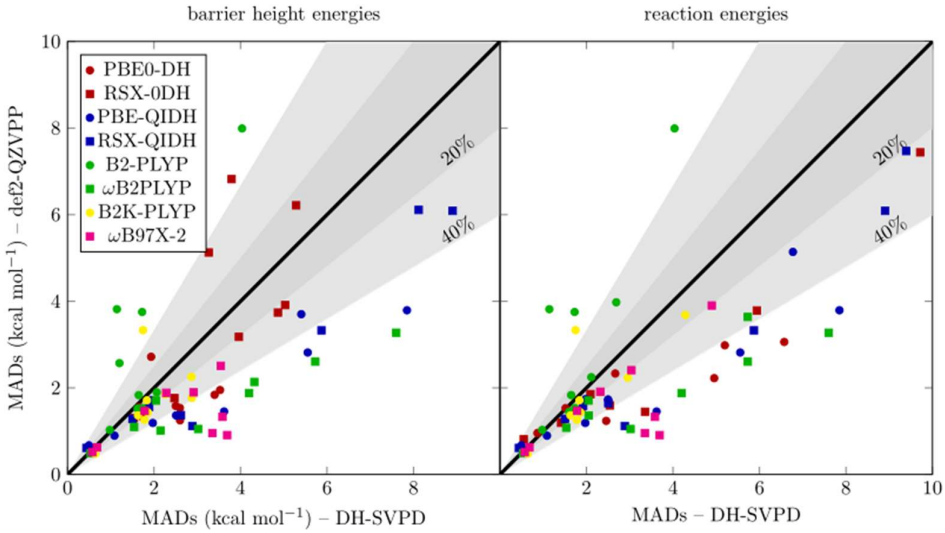

Figure 4.2. Correlation diagrams comparing the mean absolute deviations (MAD in kcal/mol) calculated over the 9 subsets of the BH9 dataset at DH-SVPD and Def2-QZVPP level of theories for (left) barrier height (BH) and (right) reaction energy (RE) properties. The thin and large gray areas depict a ±20 and ±40% error with respect to the diagonal, respectively. A lower deviation to the diagonal indicates a better performance with the Def2-QZVPP basis set.

Despite their excellent performance, DHs are often criticized for their larger computational cost with respect to more standard DFAs. It scales as O(n^5) (n referring to the size of the basis set) compared with O(n^4) for standard hybrids. Even if it is common practice to alleviate their computational effort by using the resolution-of-the-identity (RI) or similar fitting techniques, we recently developed a novel protocol able to reduce again the computational cost, and extend in the same time their domain of applicability (in terms of molecular size). Dubbed DH*thermo*[138], the protocol rests on the development of a small split-valence basis set (DH-SVPD)[106], which by error compensation between basis set superposition and basis set incompleteness errors (BSSE and BSIE, respectively), assures a good performance for a DH at a relatively cheap computational effort. Since DH*thermo* turns out to be a protocol of choice to model the thermochemistry properties of hydrocarbons[138,192,193], we investigate here its impact while assessing the kinetics and thermochemistry properties of reactions gathered into the BH9 database. Figure 4.2 compares the MADs of 8 DHs uncorrected for dispersion forces and calculated over the 9 subsets with the very large Def2-QZVPP and small DH-SVPD basis sets. At a first glance, we observe that most of the correlation points (i.e., 83% for BHs and 83% for REs) are located lower to the diagonal, i.e. that DHs better perform at def2-QZVPP level than at DH-SVPD level. However, this loss of accuracy goes well with a large saving in computational effort. For instance, the full assessment of the BH9 database costs 130.4 versus 27.5 wall-time hours on Intel Xeon Gold 6134 (3.20GHz) CPUs at Def2-QZVPP and DH-SVPD levels, respectively, that corresponds to a saving factor of 4.7.

Going deeper into details, we remark that just like dispersion corrections, the loss of accuracy provided by DH-SVPD is a consequence of an underestimation of BHs and REs (see mean signed deviations in Tables S4.4 and S4.5 of Supporting Material of Chapter 4). Over the 8 dispersion-uncorrected DHs assessed in this work, 21% (54%) of subsets are in the conic area of 20% (40%) error for the BH property. It is of about 33% (60%) for the RE property. Nevertheless, coupling DH-SVPD to a DH tends to improve the estimation of BHs for subsets (i), (iii) and (viii), and of REs for subsets (iv), (v) and (vii).

4.5 Conclusions

In summary, by assessing 868 BHs and 434 REs contained into the novel and extended BH9 database, we show that DHs can provide a statistically verified and accurate answer to the kinetics and thermochemistry modeling issue. Over the whole set of BHs and REs, minimally parameterized DHs like ωB2-PLYP or B2K-PLYP, and nonempirical DHs like PBE0-DH and

PBE-QIDH succeed to reach the 'chemical accuracy' energy threshold by more than 40% for both properties in a balanced fashion. This success corresponds to MADs lower than 2.5 kcal/mol. Other DHs like the highly parameterized ωB97X-2, or minimally parameterized DSD-PBEP86-D3(BJ) and DSD-BLYP-D3(BJ) spin-component-scaled DHs provide also an excellent estimate of RE properties. Their performance remains however lower than expected probably due to their empirical parameterization. Furthermore, we notice that coupling an empirical dispersion correction like -D3(BJ) to a DH tends to deteriorate its accuracy. Unlike with more standard semilocal or hybrid DFAs, we thus discourage their use for this type of investigation.

Chapter 5

Double hybrids and noncovalent interactions: how far can we go?

5.1 Contexts

The accurate evaluation of weak non-covalent interactions in large sets, that is containing up to thousand atoms, those molecular systems represents a difficult challenge for any quantum chemical method. Indeed, some approximations are often introduced to render affordable these calculations. Here, we consider the PBE-QIDH/DH-SVPD protocol, combining a non-empirical double hybrid functional (PBE-QIDH) with a small basis set (DH-SVPD) tailored for non-covalent interactions with a double aim: i) explore the robustness and accuracy of this protocol with respect to other Density Functional Approximations; ii) illustrate how its performances are affected by the computational parameters underlying the calculation of the exact exchange and the Coulomb contribution, as well as the perturbative term. To this end, we consider three datasets, namely S66, L7 and CiM13, incorporating molecules of increasing size.

5.2 Introduction

Double hybrids (DHs) are among the most sophisticated Density Functional Approximations (DFAs), lying on the highest rungs of the Perdew's quality ladder[97,194]. These functionals can be considered as the consecutive extension of the global hybrids (GH), introduced by Becke about thirty years ago[18]. Suggested long time ago by Ernzerhof[195], then proposed by Truhlar[28], DHs have been definitely popularized by Grimme[98]. The inclusion of a second order perturbative (PT2) contribution into the functional leads to an increase accuracy for a wide range of molecular properties, ranging from structures to thermochemistry, reaction

barriers, and electronic transitions energies[97,98,135]. Still, some of these properties are not yet obtained with the looked-for accuracy, that is the one often defined as "chemical accuracy" in some fields like thermochemistry[88]. Indeed, these properties represent a practiced and challenging playground for any (new) DFAs.

Weak non-covalent interactions are a typical example of a field calling for an improvement of methods based on Density Functional Theory (DFT)[196,197]. Here, DHs undoubtedly represent a step forward with respect to traditional DFAs, significantly reducing the errors in reference benchmarks[41,82,98,100,104]. Further improvements can be then obtained by adding empirical dispersion potentials[64,117,140]. Proposed by Yang[51] and then developed by Grimme[96], these empirical potentials represent a fast and chemically sound correction to remedy the DFA flaws on such important class of chemical interactions. They are pairwise functions, parametrized on the atoms and exchange-correlation functional considered, derived from models used for classical force fields. Notably, these corrections have a smaller impact on DHs than on traditional functionals, such as GHs, since the formers already recover a part of the noncovalent interactions through the PT2 correlation contribution[198].

Nonetheless, standard implementations of DHs are more computationally demanding than other DFAs, due to the numerical requirements of the PT2 contribution, thus limiting de facto the size of the systems that can be studied.

As usual the case in Quantum Chemistry, to overcome this problem two ways can be pursued: reducing the spanned atomic basis and/or approximating the PT2 term. In both cases, the strategy is to have a minor (negligible) degradation of the results with respect to the initial approaches. Concerning the first point, we have recently proposed a small split-valence basis set, named DH-SVPD[106], that, when coupled to DHs functionals, allows a good evaluation of noncovalent interactions. This basis set, derived from Def2-SVPD[69], was developed using an approach based on energy contributions of few reference monomers and related noncovalent dimers, computed at the same DH level of theory, and it does not require any tuning to external reference values. When coupled to our non-empirical PBE-QIDH functional[116], this basis set avoids the introduction of empirical dispersion potential, thus restoring a full non-empirical DFA approach[101]. At the same time, the small size of the basis set helps in containing the computational requirements, even for large systems, such as fullerene dimers[107]. Previous works on standard benchmarks, such as S66 and S66x8 datasets[198,199], indicate that the PBE-QIDH/DH-SVPD model has an accuracy comparable (and sometime better) than that obtained when the same functional is coupled to larger quadruple-z or triple-z basis set and empirical dispersion corrections[106,107]. This basis set is also transferable to other DHs, such as the popular

B2-PLYP [29]. A similar behavior has been found for the L7 set[200], that contains quite large molecules[106].

Starting from this solid ground, we want to further push the limit of PBE-QIDH/DH-SVPD protocol, exploring larger systems, such as those included in the CiM13 dataset recently proposed by Neese[201]. This investigation gives us the opportunity to explore the speed-up obtained by computing the PT2 contribution with methods like Resolution of Identity (RI)[202] or Domain-based Local Pair Natural Orbital (DLPNO)[141,203], and verify the accuracy of the obtained interaction energies for such very large noncovalent complexes. The quality of these approximations have been very recently discussed in the context of the CCSD(T) approach[143], but, at the best of our knowledge, never for DHs. However, their use is appropriate for accelerating the DH calculations and/or to enlarge the size of the investigated molecules. It could be argued that they are expected to have a significant positive impact also on the DHs, where the time limiting step is the evaluation of the PT2 contribution.

5.3 Methods

All the calculations were carried out with the non-empirical PBE-QIDH[116] functionals and the Orca 5.0 program[176,204,205]. For each energy single point, a tight SCF convergence criteria together with the DefGrid3 integration grid are taken as default.

Contrary to our previous works, we considered only one DFA in order to have a straightforward evaluation of the effects of the computational parameters underpinning its evaluation on the large systems considered. Several approximations for speed-up the calculations of large systems have been considered. Unless when indicated with the NORI label, the RI approximation was always considered for Coulomb and exchange integrals together with the auxiliary basis set automatically generated by Orca for the DH-SVPD basis (keyword: AUTOAUX) and making use of the chain-of-spheres approximation (RIJCOSX)[178].

Few tests using different auxiliary basis[206] did not lead to any significant variation of the obtained numerical results. The DLPNO approximation was also applied for the evaluation of the PT2 correlation. Three parameter settings, indicated with the label Loose, Normal and Tight, were selected for the latter. As suggested by these labels, these three sets correspond to an increasing level of accuracy, assured by the cutoff thresholds of the domain (TCutDo), pair natural orbitals (TCutPNO) and orbital Mulliken population (TCutMKN), as reported in Table 5.1. Details on all these approximations can be found in the original papers[141,178,203], as well as

in the Orca documentation. All the other parameters have been kept fixed to their default values.

Table 5.1. Default parameter values for the DLPNO model.

setting	$T_{cutPairs}$	T_{cutPNO}	T_{cutMKN}
loose	$1.0 \cdot 10^{-3}$	$1.0 \cdot 10^{-6}$	$1.0 \cdot 10^{-3}$
normal	$1.0 \cdot 10^{-4}$	$3.33 \cdot 10^{-7}$	$1.0 \cdot 10^{-3}$
tight	$1.0 \cdot 10^{-5}$	$1.0 \cdot 10^{-7}$	$1.0 \cdot 10^{-4}$

The DH-SVPD basis set was obtained from the original def2-SVPD basis set[69], upon a constrained optimization of one s- and one p-function for H atom and one p-f and one d-function for the C, N and O atoms. All other exponents are kept fixed to those of the original basis set Def2-SVPD. The optimized exponents of DH-SVPD are already reported in Table S3.3.1, while an example of input for Orca is given in Table S5.1.

The good results obtained coupling the DH-SVPD basis and PBE-QIDH (or other DHs) stem from a compensation between Basis Set Superposition Error (BSSE) and Basis Set Incompleteness Error (BSIE), the former overestimating the interaction energies in weakly bonded systems, the latter underestimating them[107]. A similar compensation, leading to correct estimation of interaction energies, has been observed for CCSD(T) energies when double-z basis and, to a minor extend, triple-z basis are used[207].

Several molecular sets were considered in the present paper, namely S66, L7 and CiM13[199–201]. While the first one can be clearly defined as a benchmark, in view of its significant number of systems and the general consensus on the reference energies, the other two are more a collections of large systems than real benchmark systems. Furthermore, the size of the molecules involved in these sets make difficult to have accurate reference energies, so that the reference values for their interaction energies are still matter of debate (see also infra). Here we use the DLPNO-CCSD(T) of Sancho-García and co-workers for the L7 set[208], and the CIM-DLPNO-CCSD(T)||RI-MP2 of Neese and co-workers for the CiM13 sets[201].

The first data set, from reference[208], is obtained from DLPNO-CCSD(T) value, where the default threshold of Orca for DLPNO(Tight) model have been used, together with the def2-

TZVPP basis set. Interaction energies were then extrapolated to the Complete Basis Set (CBS) limit using a two-point extrapolation[208].

The reference data for the CiM13 set were obtained using a more approximate model, based on the recently developed Cluster-in-Molecule (CIM) approach[209]. In particular, interaction energies were computed at the CIM-RI-MP2/CBS level and then corrected for the CCSD(T) correlation energy. The resulting model is denominated CIM-DLPNO-CCSD(T)||RI-MP2[201]. The basis set was of double-ζ (aug-cc-pVDZ) or triple-ζ (aug-cc-pVTZ) quality depending on the system size. The interest reader can refer to the original reference[201] for more details on the computational procedure. Here we want to stress that even if these energy values could be not at convergence with respect to different computational parameters (such as basis set or CBS extrapolation scheme) they actually represent the current state-of-the-art for the large system investigated.

As usual in this kind of analysis, the original molecular structures were considered for the three sets, that are those reported in reference 198, 200 for S66, L7 and in reference 201 for CiM13. The molecules belonging to the L7 and CiM13 sets are also sketched in Figure 5.1 and 5.2, respectively.

5.4 Results and comments

5.4.1 Medium-sized sets: S66 and L7

The first two benchmarks, S66 and L7, are largely used in literature to assess the performance of modern (and less modern) functionals. Figure 5.3 gathers the Mean Average Errors (MAEs) computed for the PBE-QIDH/DH-SVPD model, using the 4 mentioned models (RIJCOSX and the three DLPNO settings) together with the conventional DFA calculations (NORI). These MAEs are obtained with respect to the reference values computed at the CCSD(T)/CBS level of theory, using density fitting for the MP2/CBS correlation energy[199]. The numerical values are reported in Table S5.2 The S66 set is composed by relatively small molecules, containing between 6 and 24 atoms, whose weak interactions are classified as H-bonding, p-stacking, London or mixed interactions by the proposing authors[199].

First of all, it should be remarked that the computed MAEs on the whole set are equal for all the four approximations considered, all being around 0.37 kcal/mol, in agreement with our previous work[106]. The negligible variations, on the third digit, found in going from the not-approximated DFA calculations to the approximated approaches (see Table S5.2) are not worth a detailed discussion. Looking at the different subsets, the only model showing a relatively

large deviation is DLPNO(*Loose*) for the London subset, whose MAE increases of 0.1 kcal/mol with respect to the NORI value. Since this variation represent only 2% of the Mean Interaction Energy (MIE) of the S66 set (−5.5 kcal/mol), we can safely argue that our results indicate that all the 4 considered approximations can be applied on the S66 set, without any degradation of the results.

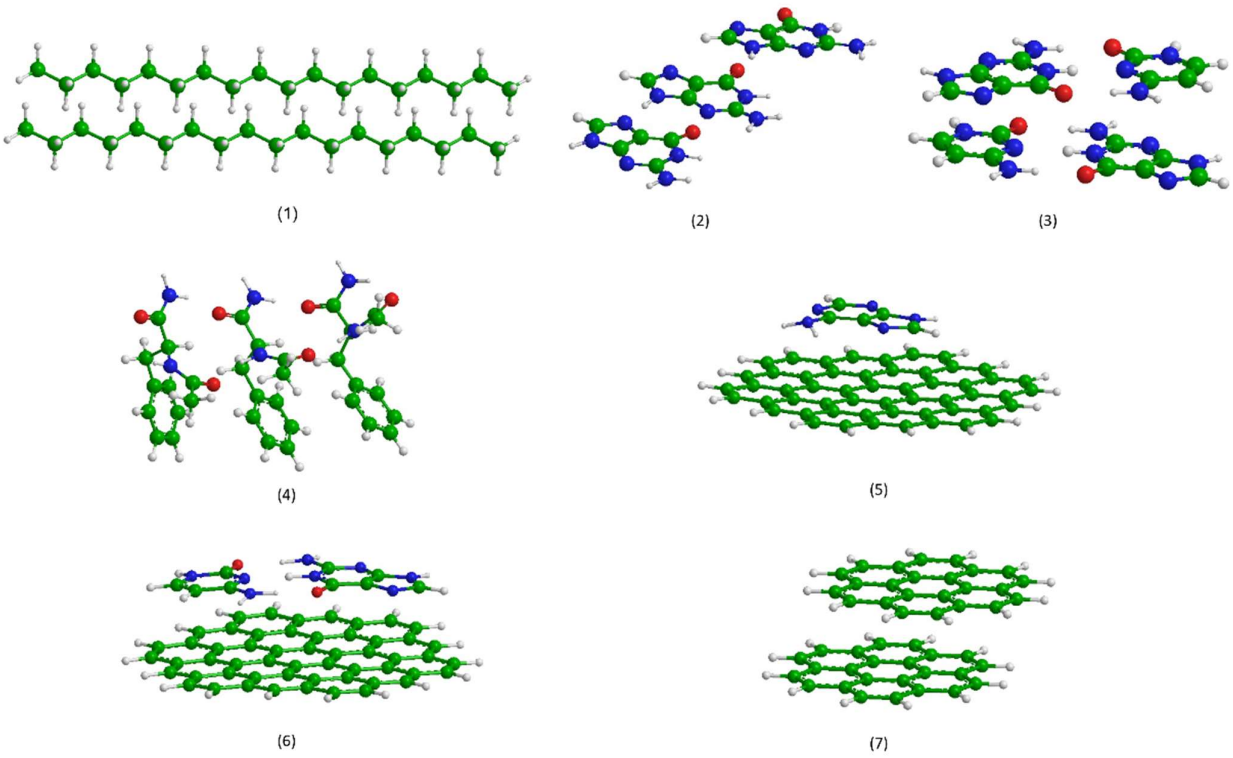

Figure 5.1. Molecular complexes in the L7 set.

A similar exercise can be carried out for the L7 set, whose molecules have between 48 and 101 atoms. The computed deviations are collected in Figure 5.4, while the numerical values are given in Table S5.3. As expected, no significant variations are observed upon the introduction of approximations of the Coulomb and exchange contributions (RIJCOX) whose MAE is very close to the reference NORI value (2.09 vs. 2.07 kcal/mol). A negligible decrease is found for the DLPNO approximation with the *Tight* setting (2.03 kcal/mol), while a significant increase is instead observed for the less severe thresholds: 2.31 kcal/mol for *Normal* and 3.10 kcal/mol for *Loose*. However, the variations with respect to NORI (+ 0.24 and + 1.03 kcal/mol, respectively) correspond to about 1% and 6% of the MIE for the L7 set (−17.4

kcal/mol). As a consequence, the DLPNO(*Loose*) setting begins to show its limits and cannot be recommended for L7.

The limited size of the benchmark set allows for a detailed analysis of the single molecules, thus revealing some interesting features. First of all, the single errors span a large energy interval, from −5.73 to +0.70 kcal/mol for the NORI model. This range is not peculiar to PBE-QIDH but other functionals, such as B3LYP-D3 and M06-2X[200], show similar behavior, thus underlining how this test can be considered difficult for any DFA. Then, it is interesting to remark that, while RIJCOSX and *Tight* and *Normal* settings are very close each others and show the trend already discussed for MAEs, an opposite behavior can be observed for the *Loose* model. Indeed, in this case the error is larger with respect to the other two settings for the molecules 1, 5, 6 and 7, while a lower error is predicted for molecules 2, 3 and 4. In other terms, the protocol DLPNO(*Loose*) has a behavior that cannot be easily predicted on the basis of the size of the system or the nature of the weak interactions involved.

Taken together, these results indicate that the DLPNO(*Loose*) protocol is not recommended for weak interactions also for PBE-QIDH (and other DHs), even if only a weight of 1/3 is introduced in the functional for the PT2 correlation.

5.4.2 Large set: CiM13

The CiM13 set, recently proposed by Neese[201], contains among the largest systems (see Figure5.2) used for analyzing the performance of DFT and post-Hartree-Fock (post-HF) methods. The number of atoms for the 13 molecules of the set, as well as the number of primitive and contracted basis functions for the DH-SVPD basis, are reported in Table 5.2. As it can be seen, the largest system is composed by about 1 thousand atoms and it already leads to 14 thousand basis functions with our small split valence basis set. Indeed, systems ***1*** to ***8*** are defined as components of the Extra-Large 8 (ExL8) set, just to stress their size[201]. It is therefore not surprising that these systems are too large for being processed without any approximation on the PT2 contribution, so that NORI results are not given and the RIJCOSX results will be considered as reference. In view of the negligible differences observed for these two models (NORI and RIJCOSX) for the S66 and L7 sets, we are confident about this choice. A similar choice was also done in reference[201], where further approximations were introduced to compute the interaction energies of ExL8 set at CCSD(T) level. Furthermore, systems **6**, **7** and **8** are even too large to be computed with the RIJCOSX model without any further approximations, so that their values have been not considered in the corresponding RIJCOSX statistics.

Table 5.2. Number of atoms, contracted and primitive functions (*f*) for the CiM13 molecules and the DH-SVPD basis set.

molecule	atoms	primitive *f*	contracted *f*
1	200	3616	1472
2	296	4240	1808
3	328	6153	2539
4	381	6150	2558
5	552	7782	3330
6	750	11166	4722
7	910	14536	6076
8	1027	14810	6306
a	126	1800	768
b	137	2198	938
c	144	2034	870
d	160	2288	976
e	174	2634	1110

Figure 5.5 reports our PBE-QIDH/DH-SVPD results, that clearly show an increase of the deviations in going from RIJCOSX to the DLPNO approximations. These variations are significative: + 22% of the MAE for *Tight*, + 36% for *Normal* and + 63% for *Loose* (see Table S5.4 for the numerical values). Indeed, the *Tight* setting correspond to a MAE of 4.13 kcal/mol, an error of 6% with respect to the MIE of the CiM13 set. Larger deviations are then found for the other settings: 4.59 kcal/mol for *Normal*, that is 7% of MIE and 5.49 kcal/mol for *Loose*, corresponding to 8% of the MIE. It should be also remarked that the difference between the MAE obtained with the RIJCOSX approximation and those computed for *Normal* and *Loose* is larger than the 1.0 kcal/mol threshold chased in thermochemistry (1.2 kcal/mol and 2.1 kcal/mol, respectively).

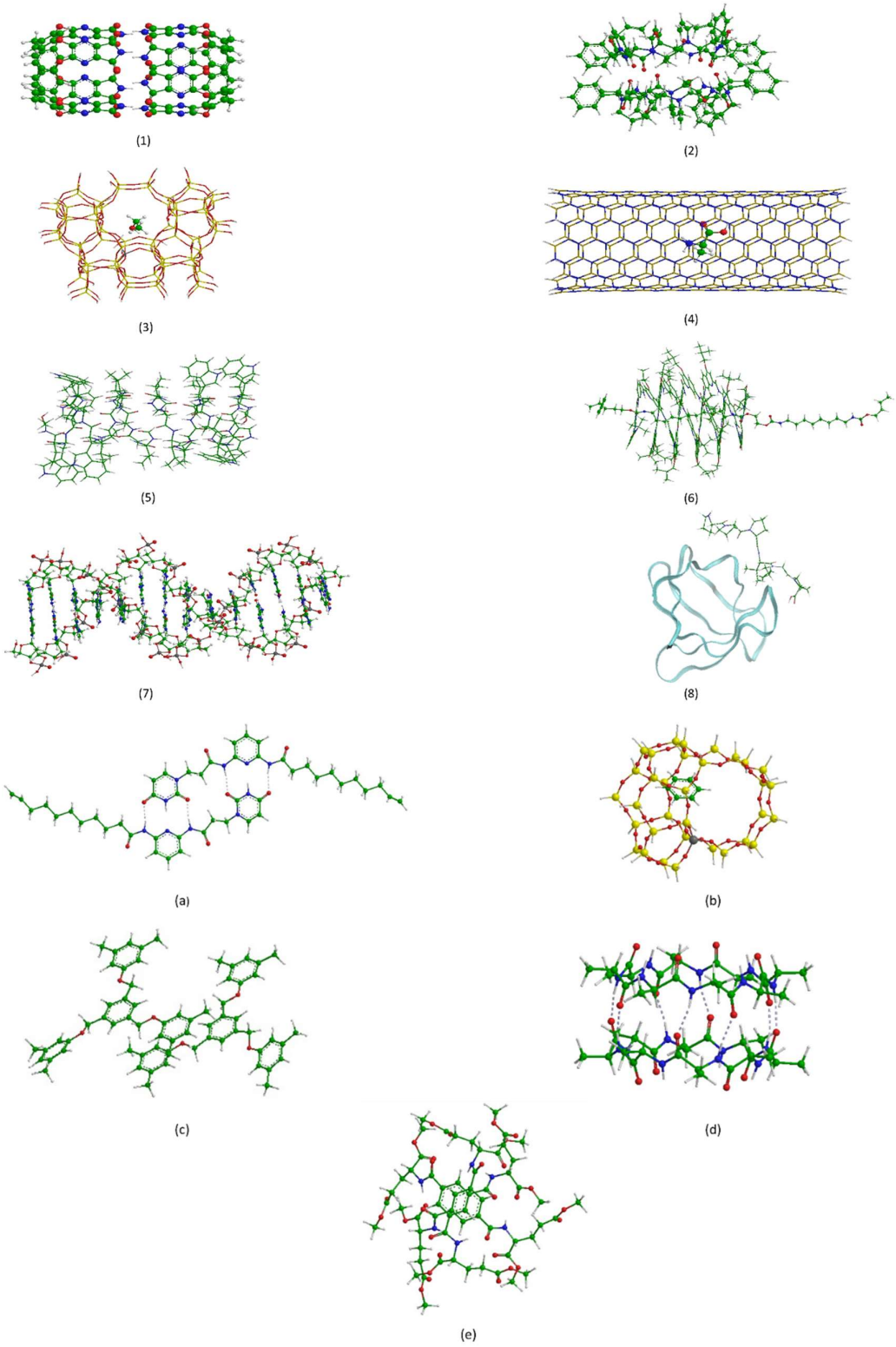

Figure 5.2. Molecular complexes in the CiM13 set.

Looking more in details for the different systems, in several cases there are significant variations of the interactions energies that are smoothed in the statistical analysis. In fact, the RIJCOSX deviations range between −10.22 kcal/mol (molecule ***2***) and +11.69 kcal/mol (molecule ***c***), corresponding to 16% and 42% of the corresponding molecular interactions energies. Similar range can be observed for *Normal* and *Tight* settings, while the largest deviation is obtained with DLPNO(Loose) for molecule ***7*** (+23.11 kcal/mol, see Figure 5.5). It is also interesting to notice that in some cases (molecules ***2***, ***3***, ***4***, ***b*** and ***d***), the deviations decrease in going from *Tight* to *Loose*, thus suggesting some error compensations.

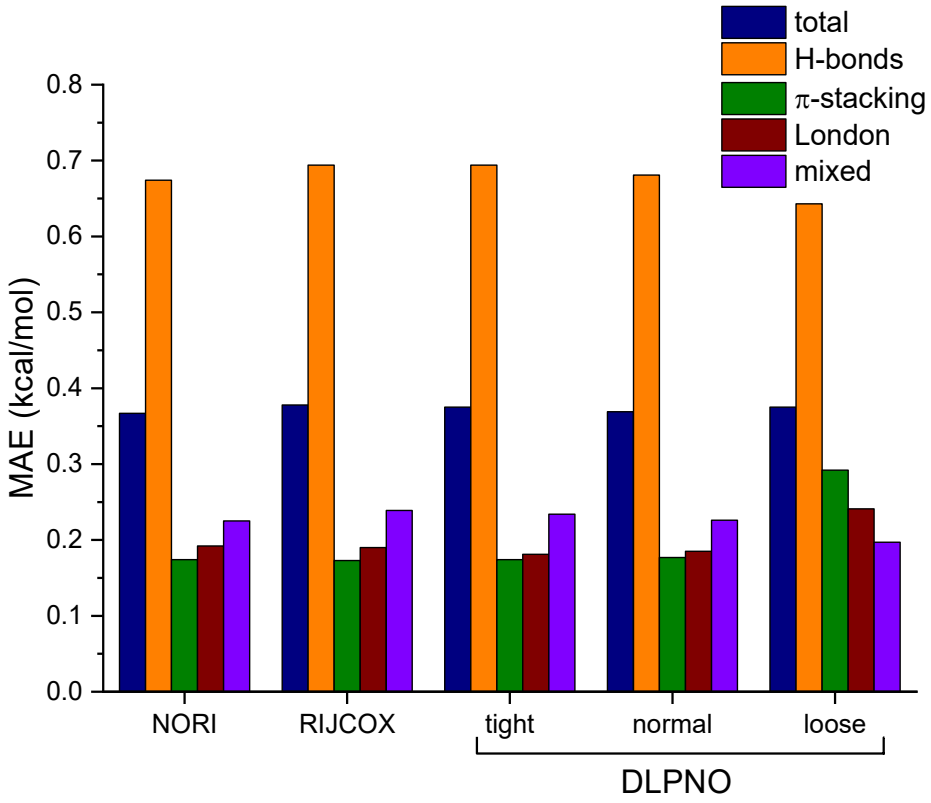

Figure 5.3. Mean Absolute Errors (MAE, kcal/mol) for the interaction energies of the S66 set, computed with the PBE-QIDH/SVPDH model and different approaches for the PT2 contribution. The terms *Loose*, *Normal* and *Tight* define the set of parameters used in the DLPNO approximation.

Before to comment the accuracy of the PBE-QIDH/DH-SVPD protocol with respect to other DFAs, a short summary on the above results is in order. This outline is reported in Figure 5.6 where all the MAEs for the three sets are collected. From these data, it is clear that the errors for the S66 are not affected by the different approximations. A negligible increase can be found for L7 set and the DLPNO(*Normal*) model, while the first signs of degradation appear with the *Loose* settings. This degradation is more evident with the last set, CiM13, whose MAEs systematically increase in going from RIJCOSX to the different settings for the DLPNO approximation. Despite such disappointing situation, it is still remarkable that such large systems can be computed at a reasonable computer effort and with errors that can be defined as acceptable even if far from the pursued chemical accuracy.

It is worth, at this point, a comment on the speed-up obtained with the different approximations. This point will not discussed in details since (clock)time is strongly depending on the computer architecture, so that results are difficult to generalize and they can be easily misinterpreted. It is well known that RIJCOSX allows for a significant reduction of computer time and, indeed, the time for the L7 set is, in average, 40% of the standard one (NORI). More involved is the situation when the different DLPNO setting are considered. As reported in literature[210], DLPNO is not recommended for small- and medium-sized molecules. Indeed we found that it provides, for the L7 set, in average a comparable computational time with respect to RIJCOSX, but without any predictable tendency. Since the observed behavior is strongly system-dependent and the dataset is limited, these data will be not further discussed. Moving to CiM13 a more regular behavior is observed, as can be remarked from Figure 5.7, where the MAEs are reported as function of the fraction of time with respect to the RIJCOSX calculations. The speed-up is evident, the DLPNO model providing, in average, between 20% and 27% of the reference RIJCOSX time. This time reduction has a linear relationship with the MAEs: faster time corresponds to less-stringent thresholds and higher deviations. However, the gain in speed from *Tight* to *Loose* (+7%) is not enough to justify the high loss in accuracy (+ 40% on MAE, see Figure 5.7). As a consequence the *Tight* settings should be considered for all the calculations.

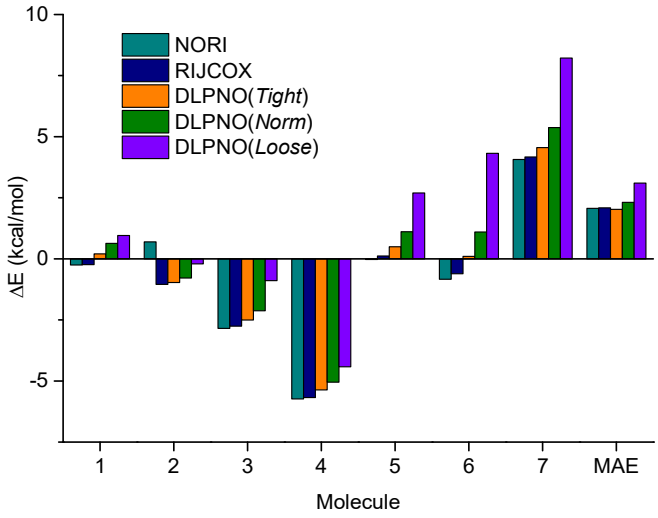

Figure 5.4. Errors (ΔE, kcal/mol) and Mean Absolute Errors (MAE, kcal/mol) for the interaction energies of the L7 set, computed with the PBE-QIDH/SVPDH model and different approaches for the PT2 contribution. The terms *Loose*, *Normal* and *Tight* define the set of parameters used in the DLPNO approximation.

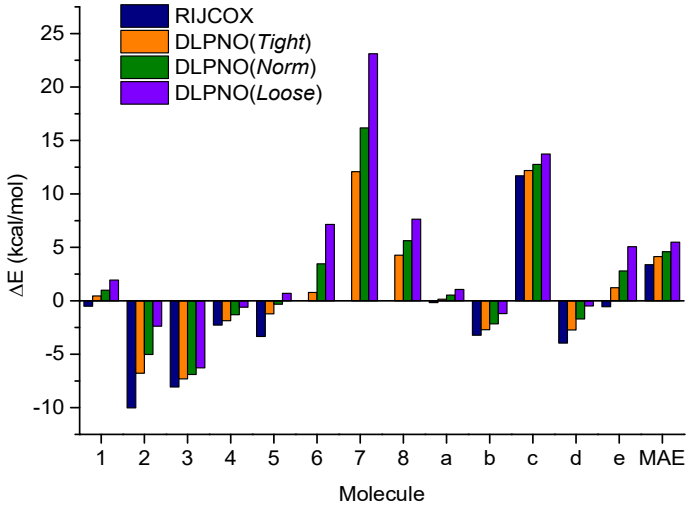

Figure 5.5. Errors (ΔE, kcal/mol) and Mean Absolute Errors (MAE, kcal/mol) for the interaction energies of the CiM13 set, computed with the PBE-QIDH/SVPDH model and different approaches for the PT2 contribution. The terms *Loose*, *Normal* and *Tight* define the set of parameters used in the DLPNO approximation.

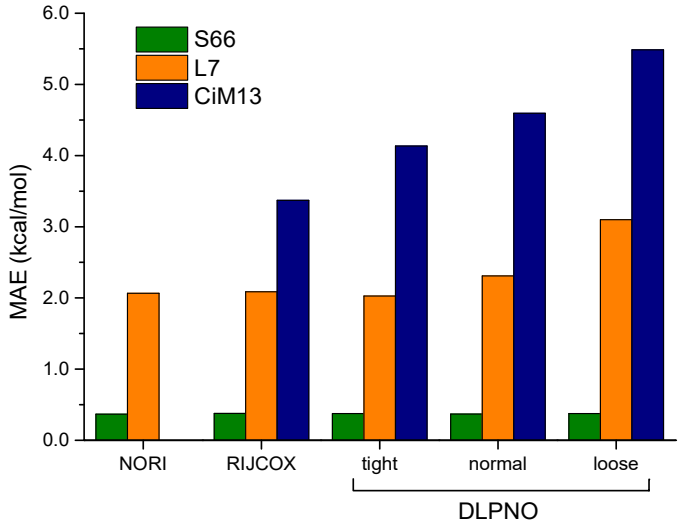

Figure 5.6. Mean Absolute Errors (MAE, kcal/mol) for the interaction energies of the S66, L7 and CiM13 sets, computed with the PBE-QIDH/SVPDH model and different approaches for the PT2 contribution. The terms *Loose*, *Normal* and *Tight* define the set of parameters used in the DLPNO approximation.

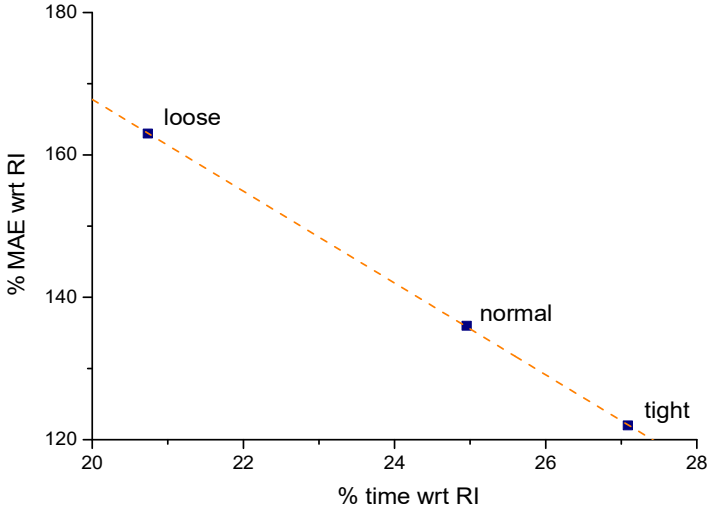

Figure 5.7. Scaling of the Mean Absolute Errors with the computer time relative to the RI calculations (%) computed for the CiM13 set and different DLPNO parameters.

Table 5.3. Interaction energies (kcal/mol) for the molecules 1 to 7 of the CiM3 dataset, the corresponding Mean Average Errors (MAEs, kcal/mol), Root Mean Square Deviations (RMSDs, kcal/mol) and largest error (max, kcal/mol) with the concerned molecule indicated in parenthesis. Except for the PBE-QIDH/DH-SVPD values, all the data are from references[201,211]

functional	**1**	**2**	**3**	**4**	**5**	**6**	**7**	MAE	RMSD	max
B3LYP	-50.47	-18.14	-24.78	-0.03	-17.39	-4.90	-263.49	49.13	67.79	152.59 (***7***)
M06-2X	-72.38	-64.69	-36.02	-14.74	-36.16	-59.51	-354.88	13.06	24.35	61.2 (***7***)
M06-L	-70.38	-69.63	-36.54	-15.95	-37.39	-67.75	-366.72	10.19	19.29	49.36 (***7***)
B3LYP-D3(BJ)	-74.31	-76.69	-43.82	-21.74	-45.42	-82.81	-423.31	6.43	7.10	-8.64 (***1***)
B97-D3(BJ)	-63.09	-69.30	-43.55	-22.88	-40.22	-71.09	-405.15	6.21	6.92	10.93 (***7***)
M06-2X-D3(0)	-76.34	-79.42	-39.44	-20.12	-44.87	-84.06	-392.22	8.73	11.48	23.86 (***7***)
M06-L-D3(0)	-74.60	-85.39	-40.25	-21.76	-46.64	-93.84	-406.33	9.31	11.26	-15.76 (***2***)
PW6B95-D3(BJ)	-68.70	-71.51	-39.84	-20.52	-40.98	-75.93	-381.14	7.71	13.69	34.94 (***7***)
ωB97X-D	-69.33	-78.41	-41.18	-23.84	-44.03	-79.78	-411.78	5.06	6.67	-8.78 (***2***)
B3LYP-D4	-76.33	-72.99	-42.94	-20.41	-44.86	-76.25	-417.91	4.81	5.43	-10.66 (***1***)
M06-L-D4	-75.73	-84.99	-40.62	-21.93	-46.24	-90.84	-408.47	8.70	10.44	-15.36 (***2***)
PW6B95-D4	-72.10	-69.25	-37.86	-16.69	-40.60	-68.33	-377.18	8.56	15.41	10.47 (***6***)
B3LYP-D4-MBD	-76.65	-73.31	-43.05	-20.44	-45.02	-76.52	-419.00	5.06	5.65	-10.98 (***1***)
PBE-QIDH[a]	-69.66	-70.39	-43.86	-19.70	-41.35	-78.02	-404.00	4.36	5.99	12.08 (***7***)
CIM-RI-MP2/CBS[b]	-70.02	-71.25	-37.77	-19.53	-43.09	-88.50	-422.60	4.26	5.45	-9.70 (***6***)
Reference[b]	-70.11	-63.61	-36.55	-17.83	-40.13	-78.80	-416.08			

a) This work, using the DH-SVPD basis set and the DLPNO(*Tight*) approximation; b) from Table 5 of reference[201];

5.4.3 A comparison with literature data

As last step in this investigation, it is worth to compare the obtained results on the three data sets with those of other functionals. As above mentioned, the PBE-QIDH/DH-SVPD protocol has been already tested in literature on the S66 and L7 datasets, showing very good performances. In particular, it provides on the S66 set results that are close to those obtained with a dedicated protocol such as DSD-PBEP86/Def2-QZVP (0.78 kcal/mol) but better than standard B2-PLYP/Def2-QZVP (1.61kcal/mol) or mPW2PLYP (1.71 kcal/mol)[208].

More complex is the situation for the L7 set where a consensus on the reference energies has not been reached. Indeed, at least two sets of reference energy values have been proposed, one based on QCISD(T)/CBS protocol by Hobza et co-worker[200] and another one by Sancho-García and co-workers, derived from DLPNO(*Tight*)-CCSD(T)/CBS calculations[208]. More recent sophisticated Quantum Monte-Carlo calculations show a significant discrepancy with respect to a LNO-CCSD(T)/CBS model, as large as 29% of the interaction energy for the system ***2*** or 16% for system ***3*** of the L7[47]. This point has been deeply discussed in a very recent article of Lao and co-workers[48], that also proposed revised values of the DLPNO(*Tight*)-CCSD(T)/CBS calculations. This incertitude affects the error assessment for DFAs, variations in the reference values leading to different statistics. For instance, the PBE-QIDH/DH-SVPD shows a MAE of 1.25 kcal/mol if the QCISD(T)/CBS values are considered, 1.18 kcal/mol for the Lao's CCSD(T) reference[212] and 2.3 kcal/mol with respect to the FN-DMC values of Tkatchenko and co-workers[210].

Concerning recent DFA approaches, it is worth to mention the ωB97M-V or the parent B97M-V functionals that give a MAE of 0.63 and 0.24 kcal/mol, respectively[94]. Not far are PW6B95-D3(BJ) with a MAE of 0.79 kcal/mol and B2-PLYP-D3(BJ) with 0.95 kcal/mol. The best performance can be ascribed (at the moment) to the PBE0 functional, developed by Adamo and Barone[20], coupled with the D4 dispersion[213] (PBE0-D4), with an impressive MAD of 0.15 kcal/mol[94]. Higher values are obtained with the more traditional B3LYP-D3(BJ) (1.76 kcal/mol) and M06-2X (3.39 kcal/mol)[201]. The MAE of about 2.0 kcal/mol obtained with PBE-QIDH/DH-SVPD is comparable to these latter values.

More involved is, instead, the situation for the CiM13 set, which was only considered in a single study before[211]. In this work, Truhlar and co-workers, considered 7 systems taken from the CiM13 (molecules ***1*** to ***7*** in Figure 5.2) in order to show that an accurate reproduction of noncovalent interactions in large systems is possible at DFT level. The MAEs, obtained for selected functionals for this subset are collected in Table 5.3. The lowest deviations are

obtained for functionals casting empirical dispersions, such as B3LYP-D4 (4.81 kcal/mol) and ωB97X-D (5.06 kcal/mol). Higher deviations are obtained for the uncorrected models, such as M06-L (10.19 kcal/mol) and M06-2X (13.06 kcal/mol). It should be also remarked the (relatively) poor performance of the PW6B95-D3(BJ) functional (7.71 kcal/mol) that was among the best performers on the L7 set.

Our PBE-QIDH/DH-SVPD protocol provides the lowest error among the functionals listed in Table 5.3, with a MAE of 4.36 kcal/mol. Similar trends are obtained if the Root Mean Square Deviations (RMSD) are considered, even if B3LYP-D4 is now better than PBE-QIDH/DH-SVPD (5.53 vs. 5.99 kcal/mol, respectively). These results are even more noteworthy, considering the non-empirical nature of the PBE-QIDH functional and the absence of an empirical potential. Furthermore, this MAE is close to that provided by the CIM-RI-MP2 model, 4.26 kcal/mol[201], that is almost as computing demanding as a DH (using RI). Interestingly, the systems showing the largest errors (last column of Table 5.3) are not the same for all the functionals and not even the largest, thus pointing out the heterogeneity of the molecular set.

It should be also noticed that the reference values are obtained with the CIM-DLPNO-CCSD(T)||RI-MP2 level of theory, a method that contains the Cluster-In-Molecule (CIM) approximation on the top of the DLPNO model[44]. The resulting approach is even faster than the DLPNO, but the quality of the reference data is weakened by the introduced approximation.

Indeed, a MAE of 0.9 kcal/mol is found for the CIM-DLPNO-CCSD(T)||RI-MP2 model with respect to the parent DLPNO-CCSD(T) approach, if the energy of molecules ***a*** to ***e*** of Figure 5.2 are considered (taking all the data from Table 4 of reference[201]). Conversely, the MAE of PBE-QIDH/DH-SVPD for these 5 molecules using the CIM-DLPNO-CCSD(T)||RI-MP2 references is 4.34 kcal/mol, a value to be compared to 3.80 kcal/mol obtained for the MAE with respect to the DLPNO-CCSD(T) values.

Extrapolating similar differences for the larger molecules ***1*** to ***8*** for which DLPNO-CCSD(T) reference are not available, a lower MAE than the actual one (4.36 kcal/mol) could be expected for PBE-QIDH/DH-SVPD. This example well illustrates the difficulty that can be encountered for not having well-assessed reference energies easily available.

More in general, it should also be noticed that for most of the functionals the MAE shows an steep increase with the size of the molecules. For instance, the MAEs for B3LYP-D3(BJ) are 0.38, 0.70 and 6.43 kcal/mol, for S66, L7 and CiM13 sets, respectively. A similar behaviour can be evidenced for M06-2X (0.26, 4.81, 13.06 kcal/mol) and PW6B95-D3(BJ) (0.19, 0.79, 7.71 kcal/mol) for the three sets (respectively). For DLPNO(Tight)-PBE-QIDH,

these values are 0.38, 2.03 and 4.36 kcal/mol, in the same order. The different nature of the functionals, the inclusion (or not) of empirical dispersion and the limited number of molecules in the sets do not allow for a deeper analysis on the physics behind this behaviour. However, the closer range obtained for PBE-QIDH is reassuring and could be an indication of a lower dependence on the system size, due a balanced treatment of the correlation effects on the weak interactions.

5.5 Discussion and conclusions

The above reported results well illustrate how efficient models and algorithms are pushing upward the computational limits in Density Functional Theory, but, at the same time, unveil underlying numerical problems.

From one side, these tests support the robustness of the PBE-QIDH/DH-SVPD protocol, based on a double hybrid functional and a basis set specifically developed for weak interactions. The very good results obtained for the CiM13 set, highly competitive with respect to others derived from empirical functionals, nicely illustrates this point. This protocol is fully nonempirical, since the functional does not contain parameters fitted on given properties and/or systems, and the basis set has been defined self-consistently without using external energy references.

These results have been obtained using different approximations for the evaluation of the exchange and Coulomb integrals, and second-order perturbative term (PT2) in the exchange-correlation functional, that allow the calculation of the large systems considered. In this case the DLPNO(*Tight*) model, on the top of the RI approximation, is that recommended also for double hybrids. Lower computational thresholds, like those present in the *Normal* and *Loose* settings, provide less accurate interactions energies, especially for (very) large systems.

Nonetheless, if the look-for chemical accuracy is easily reached by several DFAs for the S66 and L7 sets, apparently this is not the case for the large molecules of the CiM13 set. This unwelcome result depends however from different factors. The limited number of molecules in the two sets make difficult any robust statistical analysis, so that these sets can be considered more as a collection of (extra) large molecules than a real benchmark (like S66). Furthermore, the significantly deviations observed between computed and reference data point out a great inhomogeneity of the chemical interactions, that further weakens the statistics. In other terms, the sets are composed by few systems, ruled in a different manner by (subtle) chemical effects.

For these reasons, not necessarily related to the quality of the tested functionals, the results obtained on small benchmark sets, like S66, cannot be safely extrapolated to larger systems.

This already complex situation is even worsened by the intrinsic difficulties arising from the post-HF calculations. Indeed, the approximations required to allow the evaluation of the interaction energies at a reliable level of theory, such as CCSD(T), affect the results for the large molecules of the CiM13 and, to a minor extent, of the L7 sets.

The picture emerging clearly shows the problems that can be encountered in the needed step of assessing the quality of any (new) DFT model, but, at the same time, it shows the significant progress made by quantum chemical models and algorithms in treating molecule of growing size and interaction chemical interest, so to one of in Quantum Chemistry modeling.

Chapter 6

Halogen Bonds and double hybrid functionals: a quick evaluation with a dedicated small basis set

6.1 Contexts

For the former work, we tested a series of benchmark of the hydrocarbon systems, in this chapter, we would like to extend the hydrocarbon system to the halogen system. As we all know, precisely describe the phenomenon of noncovalent interactions of Halogen Bonding (HB) is one of the main challenges for theoretical methods since it must be properly account for all non-covalent electrostatics, dispersions, polarisations, and so on. Here we enlarged the small DH-SVPD basis set to the halogen atoms by optimized the CH_4X_2 (X=F, Cl, Br, I) and CH_3ClCH_2O (for optimize O atom) dimers extracted from X40 set at the basis of Def2-SVPD basis set, suited for noncovalent interactions. The basis set are then tested on 3 standard benchmarks based on this extended DH-SVPD basis set together with the PBE-QIDH functional to evaluate the performance.

6.2 Introduction

Noncovalent interactions play important roles in many physical and chemical properties[214–218]. A molecule that includes halogen atoms can induce different types of noncovalent interactions[219], it has attracted a lot of attention in many different fields, especially in biochemistry and material chemistry[219–223]. The Halogen Bonding (HB) is a key role in those noncovalent interactions, it is well known that HB is an interaction of electrophilic region and nucleophilic region[218]. The halogen atoms are regard as Lewis acid or electronic acceptor to attract the Lewis base, it is opposite to that halogen atoms are negatively charged. The Politzer et al.[215,217,224,225] have introduced the σ-hole to express the positive charge on the halogen

surface. Normally, the halogen bonding interaction can be presented as R–X…Y, where X is halogen atoms, Y is usually represented by an electron-rich atom such as oxygen, nitrogen, sulfur or by a X-donor group, the σ-hole is the positive region along the extension of the R–X bond.

This phenomenon of halogen bonding has been the subject of numerous computational chemistry methods due to the experiment is hard to measure the interaction energies in the noncovalent complexes[226]. However, the Halogen Bonding interactions are quietly weak, the interaction potentials are quite soft, as a consequence, only the Quantum Computational Methods (QCM) who take into account the accurate correlation energies can give reliable results[227]. Indeed, much more efforts toward this weak interactions have been done[225,227–229], by introducing some lower-level methods and/or further extrapolations, like the CCSD(T)/CBS [216]method with a complete basis set (CCSD(T)/CBS) which includes the single and double electron excitations iteratively and triple electron excitation perturbatively, provide a highly accurate description to noncovalent interactions, it always has been considered as the "golden standards". However, it needs an expensive computer resource, also not always possible to use it in the large systems. Furthermore, they are not always completed in quantum-chemistry codes, so it is not easy if you want to use it directly.

Among all of the methods to describe the electronic properties, Density Functional Theory (DFT) has shown a satisfactory accuracy in the ground-state properties at low computational cost since 1990s[80,230]. However, DFT methods are not enough to calculate the noncovalent interactions due to the weak interactions, improve its performances so to reach, at least, the chemical accuracy threshold is necessary. Thanks to further efforts[22,57,231–235], a new type of functional called Double Hybrid (DH) came into being, developed from their parent hybrid functionals while is better than it[236]. It takes into account the second-order perturbation (MP2) computed in basis of Kohn-Sham orbitals to the unknown exchange-correlation energy term[26,37], which gives a balanced description of noncovalent and covalent interactions[237,238]. So, further improvement has been achieved in accuracy for noncovalent interaction. As a matter of fact, even better results can be gained, also seldom can reach the sub-chemical accuracy[239].

The choice of the basis set is a major parameter to influence the ratio of accuracy/computational cost. There are two intrinsic errors in the basis set, the Basis Set Superposition Error (BSSE) and the Basis Set Incompleteness Error (BSIE), the former is blamed for the over binding of van der Waals complexes, the latter is known for the finite basis functions[240]. Normally, the molecular orbitals are a linear combination of finite basis functions in all quantum chemical approaches. So, in general, partial optimized the finite basis functions

to reach the vibrational energies limit is a common practice to develop basis set[241–243], hope to better reproduce weak noncovalent interactions. In those bases, the DH-SVPD[244] basis set takes advantage of the BSSE and BSIE to recover the correct description of the energetics in the weakly interacting systems using DHs[244].

In former work, we have been proposed an alternative protocol for improving the description of weak interactions, based on the pairing of DHs with DH-SVPD. Applications to medium and large hydrocarbon noncovalent complexes[107,108,138], suggest that the very good accuracies obtained by DH in conjunction with large basis sets (triple-ζ or quadruple-ζ) and empirical potential can be reached with such split-valence DH-SVPD basis set, but at a fraction of the computational cost[244].

Based on these promising results, here we propose a systematic study on the optimization of halogen atoms on X40 set[245], which is still a challenge (and a benchmark) for theoretical methods, hope to give more accurate interaction energies of HB systems, indeed, the origin and nature of the HB is indistinctly. In this work, we extended the basis set DH-SVPD on halogen atoms, tailored with DH functionals, a direct comparison of results obtained from the large basis set with empirical dispersion, DH-SVPD basis set could improve the evaluation of interaction energies in this halogen noncovalent systems. And it validated on the X_2/CX_4-Benzene[246] and HXB[239] sets, provide a solid foundation for its general application. The aim of our study is to provide a robust, transferable, and reproducible protocol (PBE-QIDH+DH-SVPD) which able to reach or even beyond the chemical accuracy threshold for HB at low computational cost without adding any computational parameters.

6.3 Computational Details

Before, we have used eq 6.1 to develop an optimized basis set, called DH-SVPD[244], starting from the small Def2-SVPD[247] basis set. Optimizing the most diffuse functions (one *p*-function and one *d*-function for Halogen atoms and O atom) so to minimize the following expression[109].

$$\left[\frac{(E-E^0)-(J+K)}{(E-E^0)+(J+K)}\right]^2 \qquad (6.1)$$

This equation can be used as a criterion for the optimization of the exponent of an atom basis set tailored for the reproduction of weak-interaction energies. In this equation, E is the

total energy of the dimer, J and K are the corresponding Coulomb and Exchange energies and E^0 is the total energy of the isolated fragments. Indeed, this optimization procedure just premeditated the interaction energy of a dimer as expressed at the perturbation theory[109], doesn't consider any external reference data for the interaction energy.

Now, we used the same way to optimize the halogen atoms, to develop the DH-SVPD basis set, aim at extend the use of DH-SVPD basis set. The quality and the transferability of this basis were then verified on the X_2/CX_4-Benzene[246], HXB[239] data sets. Intermolecular energy profiles were explored for the X40×10 set[248]. The calculations were also carried out with Def2-TZVPP[206,247], casting empirical dispersion together with density functionals for comparison purposes.

For the double hybrid models, beyond the nonempirical PBE-based functionals, PBE0-DH[115] and PBE-QIDH[116], the semi-empirical BLYP-based functionals B2-PLYP[29] and DSD-PBEP86[39], revDSD-PBEP86[249] have been considered. In some cases, these functionals have been coupled with D3 or D3(BJ) dispersion corrections[118], the main trends in double functionals developments are covered.

To complete our analysis, we have also considered M06-L[111], a local approach particularly performant on weak interactions, 6 global hybrids, namely M06[22], TPSSh[49], PBE0[112], B3LYP[21], APF[250] and the functional of APF with dispersion correction APF-D[250]. Other 2 range-separated hybrids, that is CAM-B3LYP[113], ωB97X[235], also together with the dispersion corrections[233].

In such ways, albeit considering a limited number of models, the most representative functional families are represented. And also in some cases, the functionals will together with D3 dispersion corrections[57,64,118,234].

All calculations were performed with the program Gaussian 16[131].

6.4 Results and Discussion

6.4.1 Basis set optimization

6.4.1.1 The Basis set optimized exponents

As mentioned in the computational details, this basis set is an enlargement of DH-SVPD, is also optimized from the Def2-SVPD basis set. The optimized exponents are collected in the supporting information Table S6.1 together with the original Def2-SVPD basis set.

The C, H, N exponents had been optimized in the former work[244], we just directly use the exponents of C, H and N, these optimizations were implemented by considering 5 reactions in PBE-QIDH energies at their equilibrium geometries as reported in the X40 set[245]. The first 4 CH_4X_2 (X=F, Cl, Br, I) reactions and the 13th CH_3ClCH_2O (for optimize the O atom) reaction extracted from X40 dataset[245].

Not unexpectedly, most of the optimized exponents are greater than the originals, thus leading to more contracted functions, consequently, a reduced Basis Set Superposition Errors (BSSE)[244], leading to more accurate results.

6.4.1.2 The results of basis set optimization

We chose the Reactions 1, 5, 7, 9, 11, 12 of X40 set[245], which include the F atom; Reactions 2, 6, 8, 10, 22, 40 of X40 set, include the Cl atom; Reactions 3, 14, 17, 20, 23, 27, 29 of X40 set include Br atom; Reactions 4, 24, 28, 30 of X40 set include I atom and Reactions13 to 21 include O atom, for the comparison purpose. In the Table S6.3, are collected the details of MADs for all the reactions mentioned before of F, Cl, Br, I, O.

Those Reactions, to avoid any bias coming from the different nature and number of the reactions, these MADs are simply the mathematical average of those computed for the different reactions, that is their sum divided by 5 (correspond to the F, Cl, Br, I, O those five different types of reactions). The average of Mean Absolute Deviations (MAD) of the selected double hybrid functionals obtained are reported in Table 6.1.

Table 6.1. The average Mean Absolute Deviations (MAD) for the interaction energies of the reactions 1, 5, 7, 9, 11, 12 include F atom, reactions 2, 6, 8, 10, 22, 40 include Cl atom, reactions 3, 14, 17, 20, 23, 27, 29 include Br atom, reactions 04, 24, 28,30 include I atom in the X40 set. (Units: kcal/mol)

	DH-SVPD	Def2-TZVPP	Def2-TZVPP+D3
revDSD-PBEP86	0.24	0.60	0.16
PBE-QIDH	0.29	0.55	0.19
B2-PLYP	0.49	1.13	0.18
PBE0-DH	0.58	1.18	0.23
DSD-PBEP86	0.68	1.26	0.34

Compared the interaction energies errors of DH-SVPD, Def2-TZVPP and the functionals corrected by empirical dispersions coupled with Def2-TZVPP. No unexpected behavior can be evidenced in the results obtained with the larger Def2-TZVPP basis set. In most cases, the interaction energies in the Def2-TZVPP basis set together with all tested functionals are overestimated, sub-chemical accuracies can be obtained with DHs casting empirical potentials, the excellent results' deviations are lower than 0.2 kcal/mol (revDSD-PBEP86, PBE-QIDH and B2-PLYP) in this large basis set. By moving to the optimized basis set DH-SVPD, the reduction of interaction errors lead to a significant improvement (more details see the supporting information of Table S6.3). Indeed, the interaction energies in the DH-SVPD basis set are closer to the reference data CCSD(T)/CBS[245]. The pure DHs are all below the chemical-accuracy threshold, with the PBE-QIDH functional showing a MAD value of 0.29 kcal/mol, is very comparable to the same functional corrected with the empirical potential and the large basis set, 0.19 kcal/mol, thus showing that one of the primary objectives in the development of the DH-SVPD basis set to halogen atoms was reached. All other tested DHs follow this trend, and in the tested functionals, revDSD-PBEP86 functional gives the lowest MAD 0.24 kcal/mol, makes no differences to the MAD of PBE-QIDH functional, 0.29kcal/mol.

Considering this obtained basis set's effectuality and transferability, we validated it with other DHs and hybrid functionals as described in the following text.

6.4.2 Validation on two standard benchmarks: X_2/CX_4- Benzene and HXB sets

The first validation is the X_2/CX_4-Benzene (X=Cl, Br) data set developed by Kim and co-workers a few years ago[246]. This data set is composed of 10 X-π interaction energies of X_2 and CX_4 with benzene, including 3 low energy conformers X_2-Bz and 2 low energy conformers CX_4-Bz (X=Cl, Br). The detail of this system is in Figure 6.1, the details of the statistics reported in Table S6.4. As expected, the DH functionals show less deviations than the global hybrid (GH), between 0.8 kcal/mol to 2.0 kcal/mol except M06 and ωB97X those two functionals at the Def2-TZVPP basis set. Those latter two functionals considering the noncovalent interactions and long-range corrected when was developed. When adding the empirical dispersions, significantly smaller deviations can be obtained, the B2-PLYP, PBE0-DH and DSD-PBEP86 those 3 functionals even can reach the chemical accuracy while without the empirical exponentials beyond the chemical threshold. The best two functionals of revDSD-

PBEP86 and PBE-QIDH, both deviations decrease over 0.60 kcal/mol. The global hybrid functionals show similar performances, the deviations have been decreased. Moving to the DH-SVPD basis set, the DHs performances notably improved, starting discussion from the PBE-QIDH results, the data reported in Table 6.2 clearly show a significant improvement in performance for this functional when using the optimized basis (DH-SVPD), with mean absolute deviation (MAD) decreasing from 0.81 kcal/mol (Def2-TZVPP) to 0.41 kcal/mol (-50%). Of note, the gap between results obtained using the empirical dispersion correction (Def2-TZVPP+D3) and those obtained using the optimized DH-SVPD basis set is significantly decrease for the PBE-QIDH functional. Indeed, the MAD of PBE-QIDH/DH-SVPD (0.41 kcal/mol) to be compared to a MAD of 0.19 kcal/mol computed with PBE-QIDH-D3(BJ) approach with the Def2-TZVPP basis set. More interestingly, the error obtained with the PBE-QIDH functional and the large basis set Def2-TZVPP is significantly larger than that computed with the Def2-TZVPP+D3 (0.81 vs 0.19 kcal/mol) or the optimized basis (0.41 kcal/mol). To check the transferability of the basis set, four more DHs functionals were considered and the obtained results are collected in Table 6.2. For all the DHs, the same trend of PBE-QIDH can be found. Indeed, the error significantly decreasing in going from Def2-TZVPP to the optimized DH-SVPD, with variations ranging from -67%(revDSD-PBEP86) to -34% (DSD-PBEP86), and revDSD-PBEP86 gives the lowest deviations in all DHs with DH-SVP basis set. These results suggest that particular attention must be paid to choose of the basis set to be used when those empirical corrections are used with DHs, as already reported in the literature[251].

The performance of the optimized DH-SVPD basis and those evaluated with the larger Def2-TZVPP basis and empirical corrections show a good agreement. For instance, the MAD values obtained at the DSD-PBEP86 level are 1.26 and 0.55 kcal/mol for these two basis sets. Interestingly, in going from the Def2-TZVPP to the DH-SVPD basis, a systematic error decrease is observed not including dispersion corrections, the largest error is observed with the Def2-TZVPP basis for all functionals. To avoid the redundant discussions, interested readers can see the details in the Table 6.2 and Table S6.4 in the supporting materials.

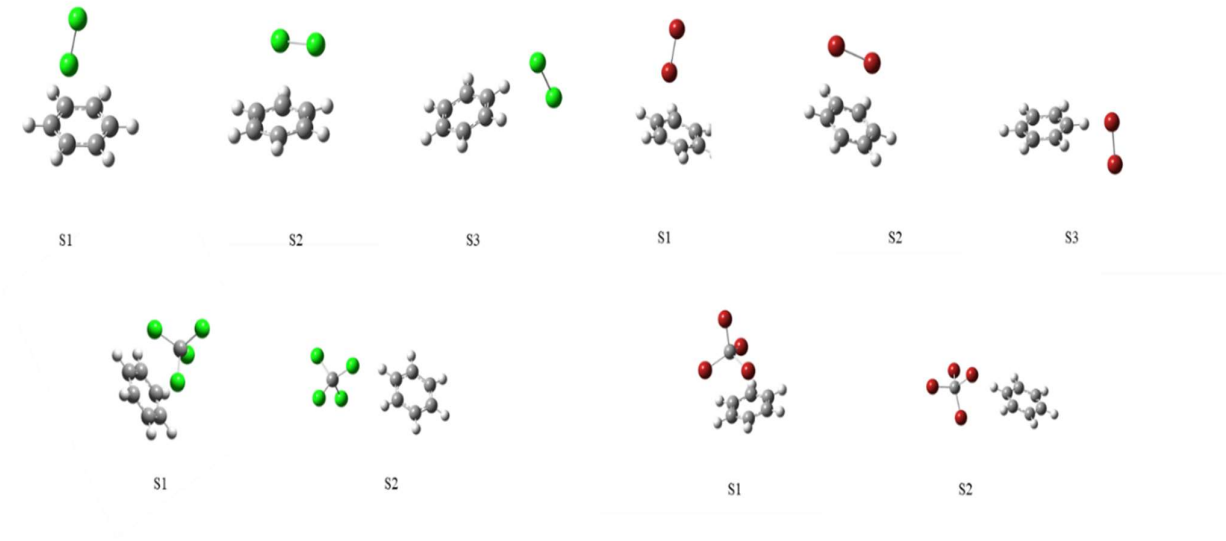

Figure 6.1. The conformers of X_2-Bz and CX_4-Bz (X = Cl, Br). The 3 conformers of Cl_2-Bz takes the Optimized Geometries at MP2/aVTZ level, 3 conformers of Br_2-Bz Optimized Geometries at BSSE-MP2/aVTZTZ geometry with optimized CCSD(T)/aVTZ Br_2-Bz distance, 2 conformers of CCl_4-Bz Optimized Geometries at BSSE-MP2/aVTZ geometry with optimized CCSD(T)/aVTZ Br_2-Bz distance, 2 conformers of CBr_4-Bz Optimized Geometries at BSSE-MP2/aVTZ geometry with optimized CCSD(T)/aVTZ Br_2-Bz distance. Atomic colour codes: C, gray; Cl, green; Br, red; H, white. All those Optimized Geometries from Ref 246.

In hybrid functionals also provide very respectable performances with deviations under the 1 kcal/mol threshold. Such as M06 and ωB97X, the MAD are 0.44 kcal/mol and 0.32 kcal/mol in DH-SVPD basis set, respectively, provide smaller MADs than the same functional together with the Def2-TZVPP basis set. This trend also shows in the other functionals which value beyond the chemical accuracy threshold. While the hybrid functionals together with empirical dispersion in the larger Def2-TZVPP basis set, can reach the chemical accuracy except for TPSSh functional.

Concerning the computational time, the hybrid functional together with empirical dispersion in the larger basis set is 3times (For example: the calculation time of M06-D3/Def2-TZVPP is almost 3.5 times to the PBE-QIDH/DH-SVPD).

The results of the second validation collect in Table 6.3, the MADs computed for the HXB data set. It contains 8 π-π complexes, two types of complexes are represented in the database: $C_6X_6…C_2X_2$ and $C_6X_6…C_2X_4$ (X=F and Cl). The reference energies were computed

at CCSD(T)/MP2(CBS) level [239]. The detail of this system is in Figure 6.2, the details of the statistics reported in Table S6.5.

Table 6.2. The average Mean Absolute Deviations (MAD) for the interaction energies of the X_2/CH_4-Bz set. (Units: kcal/mol)

	DH-SVPD	Def2-TZVPP	Def2-TZVPP+D3
revDSD-PBEP86	0.29	0.87	0.21
PBE-QIDH	0.41	0.81	0.19
PBE0-DH	0.75	1.62	0.32
B2-PLYP	0.83	1.71	0.37
DSD-PBEP86	1.26	1.91	0.55
B3LYP	2.82	3.42	0.5
APF	2.15	2.87	0.68
PBE0	1.47	2.21	0.30
M06	0.44	0.53	0.29
M06L	1.34	1.70	0.87
TPSSh	9.13	12.33	1.70
CAM-B3LYP	7.82	10.59	0.90
ωB97X	0.32	0.36	0.30

As the first general trend should be commented is that the MADs obtained for the HXB set are higher than those already discussed for the X_2/CX_4-Benzene set. In fact, no double functionals can reach the chemical accuracy at the large basis set Def2-TZVPP. While in the GHs, the only unexceptional is the hybrid functional M06L, which MAD is lower than the chemical threshold (1kcal/mol). Remarkably, there is a largely systematic error decrease for all the functionals that are un-corrected with empirical dispersions in going from the Def2-TZVPP to DH-SVPD basis set, PBE-QIDH functional with variations ranging from Def2-TZVPP (2.12 kcal/mol) to DH-SVPD (0.79 kcal/mol) basis set. In other words, a reduction of −62.7% is observed when the optimized basis set is used. All the other general trends have already discussed for the X_2/CX_4-Benzene are also occurred in this HXB set, also the results obtained with this optimized basis set DH-SVPD are comparable to those obtained with the larger basis

and dispersion corrections. For instance, PBE-QIDH has a MAD of 0.79 kcal/mol with the DH-SVPD basis set and a MAD of 0.32 kcal/mol when large basis set coupled with the empirical dispersion correction. The largest difference is found for PBE0-DH, showing a MAD of 1.70 kcal/mol for DH-SVPD and 0.08 kcal/mol for Def2-TZVPP with the D3(BJ) correction.

Table6.3. The average Mean Absolute Deviations (MAD) for the interaction energies of the HXB dataset. (Units: kcal/mol)

	DH-SVPD	Def2-TZVPP	Def2-TZVPP+D3
PBE-QIDH	0.79	2.12	0.32
revDSD-PBEP86	0.84	2.20	0.11
B2-PLYP	1.11	3.85	0.27
PBE0-DH	1.70	4.16	0.08
DSD-PBEP86	2.71	4.82	0.84
B3LYP	5.8	7.95	0.16
APF	5.00	7.05	1.47
PBE0	3.66	5.77	0.82
M06	0.46	1.65	0.54
M06L	0.83	0.79	0.49
TPSSh	5.35	7.43	0.29
CAM-B3LYP	3.45	5.68	0.34
ωB97X	0.28	1.91	0.95

Should be mentioned, PBE-QIDH gives the closet results to the references data than other considered functionals, it is the functional used for basis set optimization, but in all other cases, the performance also uncommonly improved. In this sense, suggesting that the DH-SVPD basis has a very good transferability to other DHs which leads to improve numerical performances for all the considered functionals not empirically corrected for dispersions. This is also demonstrated in the former dataset X_2/CX_4-Benzene.

Generally, the DH-SVPD also shows better results than the larger basis set Def2-TZVPP in hybrid functionals. The functionals of M06L, M06 and ωB97X perform better than other GHs, also discussed in the before mentioned.

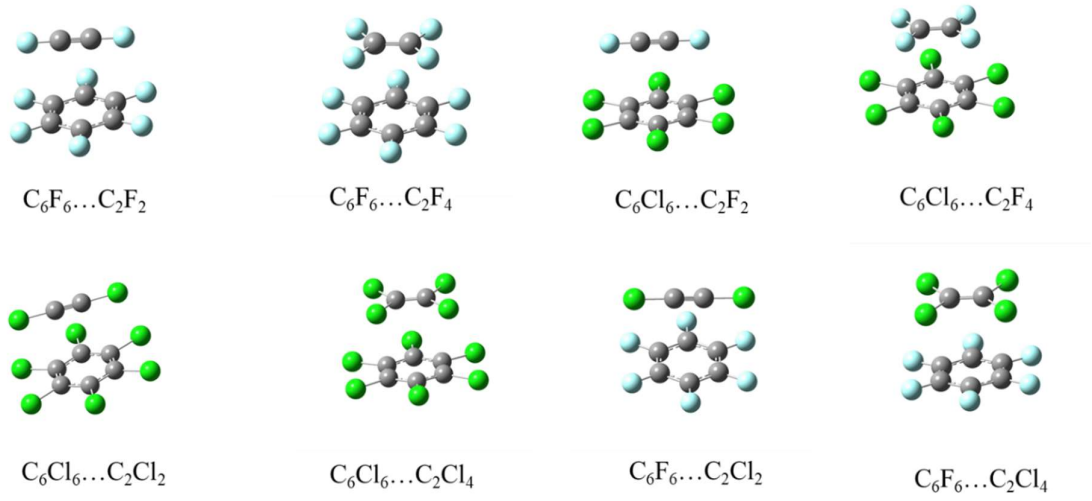

Figure 6.2. The structures of the complexes in the HXB dataset, the optimized structures of complexes from Ref 239.

6.4.3 Exploring energy profiles: X40×10 Data Set.

So far, we have investigated the quality of the DH-SVPD basis set at a given equilibrium structure in the referred halogen systems[245], as normally do in the standard benchmarks of DFT approaches. However, this approach does not involve the rearrangement of the molecule structures, aside from the dimer at the equilibrium distance r_e. To check this point, we have investigated the X40×10 data set[252]. This set collected 10 data points: four compressed dimers (at $0.80r_e$, $0.85r_e$, $0.90\ r_e$, $0.95\ r_e$) and five stretched dimers (at $1.05r_e$, $1.10r_e$, $1.25r_e$, $1.50r_e$, $2.00r_e$), it recommended interaction energies was used in the Gold2 and Silver2 those two levels of theory as reference data[252]. Due to the optimized process aimed at the dispersion forces, especially for noncovalent interactions, we just calculated the first 24 reactions in the X40 set, used different DH functionals with DH-SVPD basis set. The obtained results are collected in Table 6.4.

It is not unexpected that the errors of obtained in the double-hybrids functionals coupling with the empirical dispersions at the optimized basis set DH-SVPD are larger than the pure double-hybrids functionals, probably due to the double counting of the empirical dispersion corrections (DH-SVPD basis set + empirical dispersion potentials), as before

reported [244]. Overall, all the pure DHs provide a sub-chemical accuracy with the DH-SVPD basis set on those 24 reactions extracted from X40×10 set. Even the errors are larger in the DHs + empirical dispersion corrections, the chemical accuracy also reached. The MAD of the revDSD-PBEP86 functional shows the least error, 0.25 kcal/mol, among the tested functionals. The performance of PBE-QIDH functional also deserve to be mentioned, 0.28 kcal/mol, very close to the best one.

Table 6.4. The average Mean Absolute Deviations (MAD) for the interaction energies of the X40×10 dataset. (Units: kcal/mol)

	DH-SVPD
revDSD-PBEP86	0.25
revDSD-PBEP86-D3(BJ)	0.69
PBE-QIDH	0.28
PBE-QIDH-D3(BJ)	0.63
PBE0-DH	0.29
PBE0-DH-D3(BJ)	0.75
B2-PLYP	0.42
B2-PLYP-D3	0.57
DSD-PBEP86	0.76
DSD-PBEP86-D3	0.86

To have a clear picture of the functionals influence, Figure 6.3 shows the interaction energies at the 10 points for the first 4 reactions in the X40 set (those 4 reactions are the optimized reactions for F, Cl, Br, I atoms, respectively). In this figure, it clearly shows that the DSD-PBEP86 functional has a large difference with the Ref data in those 4 reactions. Interestingly, in most cases, B2-PLYP and PBE0-DH functionals are overestimate the interaction energies in those 4 reactions, while PBE-QIDH, revDSD-PBEP86, DSD-PBEP86 those 3 functionals underestimate the interactions. In the first 2 reactions, we can find that the B2-PLYP functional closer to the Ref data than the other functionals, especially the distance beyond $1.1r_e$, probably due to the halogen bond interaction strengths are weak in which dimers include F and Cl atoms. While in the reactions 3 and 4 which include Br, I atoms, respectively, the best two functionals PBE-QIDH and revDSD-PBEP86 almost arrive the references data,

show a very small or even negligible errors, should be mentioned that the MAD of B2-PLYP (0.51 kcal/mol) in the reaction 4 (include I atom) is 10 times to the PBE-QIDH functional 0.05 kcal/mol. It should be note that in those 4 total reactions, the average MAD of PBE-QIDH functional is 0.14 kcal/mol, is smaller than 0.24 kcal/mol to the B2-PLYP functional, decrease almost 67% than the DSD-PBEP86 functional (0.41 kcal/mol) (more details see the supporting information Table S6.6).

To be briefly, the optimized basis set accuracy is beyond the larger basis set for all tested functionals without empirical dispersions, PBE-QIDH/DH-SVPD even reach the accuracy of large basis set with empirical dispersions at same functionals.

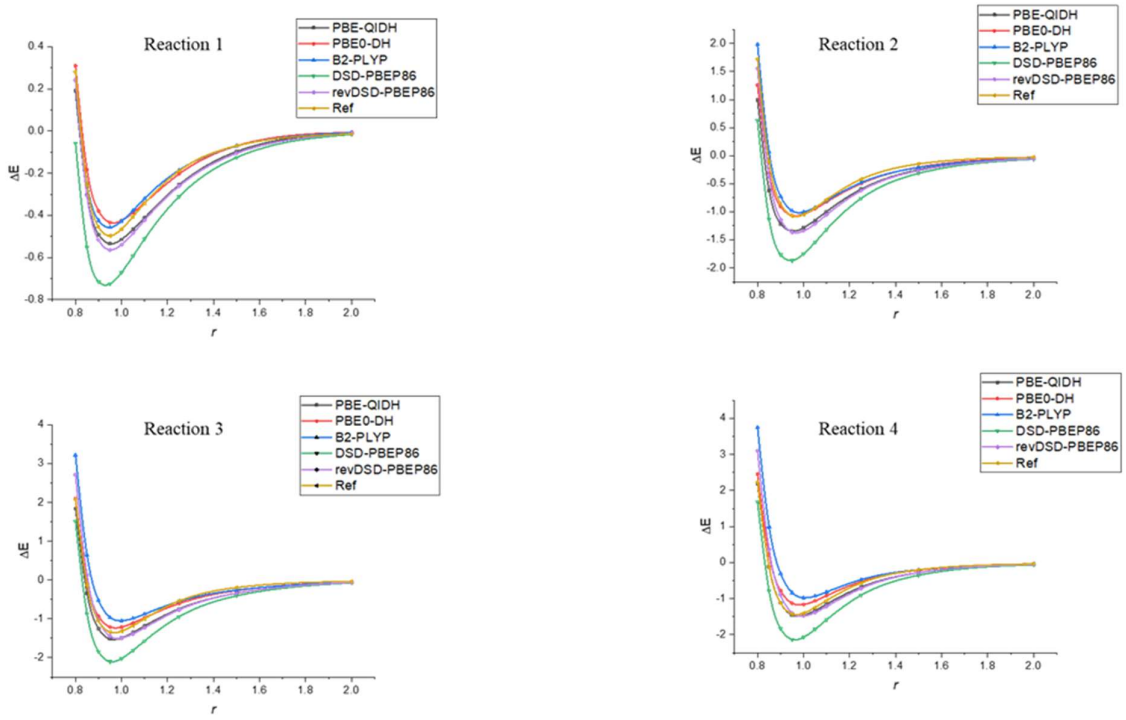

Figure 6.3. Potential energy profiles computed for the first four reactions extracted from X40×10 set. The Reference value taken from Ref 253.

6.5 Conclusions

Enlargement of the DH-SVPD basis set to halogen atoms, together uses with double-hybrid functionals has been developed. The aim is to extend the applications of DH-SVPD basis set to halogen bonding interactions, to give more accurate interaction energies. The DH-SVPD basis set takes advantage of Basis Set Superposition Errors and Basis Set Incompleteness Errors, these errors compensations are transferable and robust, as shown that the results obtained on different systems, including the challenging X_2/CX_4-Benzene, HXB, X40×10 sets, with several double hybrid functionals. The obtained results suggest that when the PBE-QIDH functional is considered, as former work showed, the results can be obtained beyond the chemical accuracy (errors < 1.0 kcal/mol) with respect to the reference values, and similar performance is found for all tested double hybrid functionals, the results are comparable to the same double-hybrid functionals with empirical dispersion at large basis set.

This protocol PBE-QIDH/DH-SVPD model, suitable for noncovalent interactions, also including the HB interactions, can be used directly without any other parameters, as showed a Gaussian input example Table S6.2 reported in the Supporting Information.

Chapter 7

Modeling multi-step organic reactions

7.1 Context

The former work is based on the optimized basis set DH-SVPD with double-hybrid functionals to identify the accurancy. However, the selection of the different density functionals also have influence to the results what we wanted to study. At here, we studied the multi-step organic chemistry, because correctly explaining the reaction mechanisms and which step is the rate-determined step is vital to understanding intricate mechanisms and designing new compounds. This work has used different density functionals to calculate the structures of intermediate and transition states to see the intrinsic properties of the functionals.

7.2 Introduction

Understanding which are the reaction mechanisms behind complex chemical transformations is a challenging task often accomplished proposing reasonable paths in agreement with a large number of experimental data and thus enabling to discriminate between mechanisms possibly occurring[253–255]. Using density functional theory to explain and predict the reaction paths and chemical properties are become popular to cure the restriction of experimental methods. This endorsement rests on the development (and availability) of robust and accurate theoretical approaches allowing to predict reactions path with high precision in energy for relatively large chemical systems.

These requirements, need for their use for experimentally relevant cases, have become more and more stringent over the year not only for energetic predictions but for an increasing number of properties. For instance, the concept of "chemical accuracy", that can be exemplified as an accuracy comparable to the best one obtained by experiments, was initially reserved to computational thermochemistry[83], but it has been extended in recent years to other properties,

such as excitations energies and bond lengths[169,256]. Ideally, in the case of a robust method this high accuracy should be attainable also for systems containing tenths, if not hundreds, of atoms, what is sometime defined as "real-world" systems, that is systems of interest for chemists.

Focusing on the prediction of reactivity features, while recent developments allow to describe the thermochemistry of systems containing up to a thousands of atoms at refined post-Hartree-Fock level (HF)[201], they are still computationally demanding to allow to screen a very large and different number of reactions profiles making approaches based on Density Functional Theory (DFT) still those offering the best compromise between accuracy and system size. Albeit exact in principle, DFT has the major drawbacks that the electronic energy is actually approximated by introducing a term for the (so-called) exchange-correlation energy, derived by a functional of the electron density[194]. As a consequence, the quality of the results depends on the functional used, and, in general, it cannot be easily assessed a priori.

An heuristic approach has taken hold over the years, based on a systematic benchmarking of any exchange-correlation functional on a set of well-assessed (molecular) properties, providing a quantitative estimate of the error of each functional and thus allowing to assess their qualities and to help the user in making an advised choice. To this end, a great variety of specific datasets have been developed for an increasing number of molecular properties. The common practice is then to define as best-performers those functionals providing, in statistical terms (i.e. average), the smallest deviation with respect to reference data (as for instance data coming from wave function correlated methods).

Among these datasets, those concerning reactivity have not surprisingly attracted a special attention. Assessments of DFT functionals in predicting differences in energy between reactants and products (thermochemistry) and differences in energy between transition states and corresponding reactants and/or products (kinetics) represents a significant part of the currently available DFT benchmarks. The reactions considered in standard benchmarks are simple one-step reactions, characterized by a single energy difference between reactant(s) and product(s) and one (forward) or two (forward and reverse) barriers. Furthermore, calculations are carried out at fixed geometrical structures, in order to better evidence the effects stemming from the differences in the predicted energies avoiding to sum-up errors related to erroneous structural predictions which are tested via different benchmark sets.

The most known family of benchmarks is the GMTKNXX (XX=24, 30, 55) family[82,257,258], composed by a large number of subsets each of them probing interaction or reaction (barriers and stabilities) energies of interest for applications in Chemistry. For instance, barriers and energy differences for Diels-Alder, Bond-Separation or Pericyclic

reactions are included in these sets[82].

This procedure assumes a full transferability of the performance obtained for the reactivity datasets to the reactions of interest. Such assumption is valid only if all the reaction intermediates and transition states occurring along the reaction pathways studied are actually statistically well and ideally equally represented in the benchmark dataset used which is clearly far to be the case for all complex multistep reactions occurring in real chemistry life.

Actually if a complex mechanism occurs via subsequent transformations, even if a given functional will not be able to provide an equally accurate description of all intermediates and transition states only the predicted kinetics will be quantitatively affected but not the overall chemical prediction. Nonetheless for complex reactions involving a possible bifurcation along the reaction path or in the case of competing reactions a functional predicting with different accuracy different intermediates or transition states may lead to the prediction of a qualitatively wrong (i.e. different) chemical product thus leading to severe problems in the use of computational approaches to disclose chemical reactivity[259].

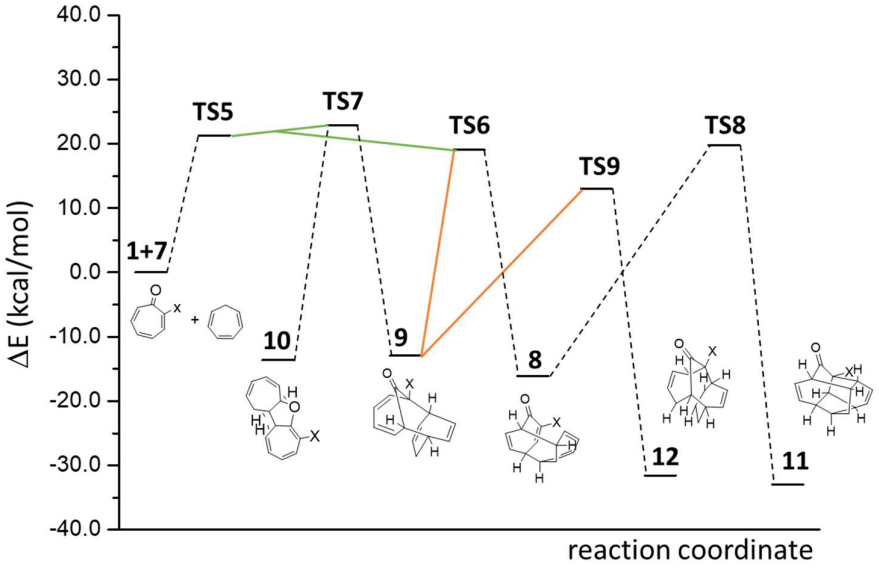

Figure 7.1. Energy profile for the ambimodal reaction, including the sketches of the stable reaction intermediates. The energies have been computed at the CCSD(T) level in reference 261.

Among the reactions that cannot be described in a "classical" way where reactants and products are connected through a series of intermediates sequentially connected by transition states (TSs) there are the ambimodal reactions. These reactions are characterized by a TS connected to several products, after a bifurcation of the reaction path[260,261]. Pericyclic reactions are a typical examples[261,262] and specific algorithms and methods have been developed to follow these complex reaction paths and to characterize the bifurcation points[263,264].

7.3 Results and discussions

Fistly, from the work of Houck and co-workers, they have proposed an ambimodal mechanism for the cycloaddition of cyclopentadiene and cycloheptatriene with tropone, sketched in Figure 7.1[265]. The bifurcation occurring after the first TS (TS5) leads to two other TSs, TS6 and TS7, connecting reactants (1 and 7) either with product 11 only or to products 12 and 11 in the case of TS7. Indeed, in the case of the population of TS7 the complexity of the reaction mechanism is increased by another possible bifurcation occurring after population of the intermediate 9, which leads to the product 12 via TS9 and to product 11 via TS8 following the same reaction path of those obtained after population of TS6.

With this complex energy landscape, the accuracy in the prediction of the observed product type and ratio will depend on the ability of each DFT method to accurately assess the energies of the different reaction intermediates, including the TSs that rule the competition of the different reaction channels. These latter correspond to different class of chemical transformations: the step from 9 to 8 is a Cope interconversion, from 9 to 10 a Claisen rearrangement, while products 12 and 11 are obtained via Diels-Alder type reactions.

DFT approaches have been benchmarked for all these type of reactions using specific benchmark sets. For instance, the energies of the Cope rearrangements (barrier and reaction energies) are expected to be predicted with a good accuracy (errors of 1 to 2 kcal/mol) by PBE-QIDH, as double hybrid functionals (DH) and by several global hybrid (GH) functionals, such as ωB97X-V and M06-2X, just to mention some among the functional that will also be discussed in the following[137]. In contrast, B2-PLYP and DSD-PBEP86, two popular DHs, or PBE0, M11 and B3LYP, three GHs, are expected to provide larger errors on this type of reactions (error larger than 4 kcal/mol). Conversely, the reaction energies for Diels-Alder reactions are correctly reproduced by DSD-PBEP86, M06-2X and PBE-QIDH (error of 2 kcal/mol or less), while ωB97X-V, PBE-QIDH and M11 are in relative difficulty (3 to 5 kcal/mol)[82]. Finally, energy barriers for pericyclic reactions are correctly reproduced by DSD-

PBEP86, B2-PLYP, PBE-QIDH, M06-2X and ωB97X-M (< 2 kcal/mol), while higher errors (> 2.0 kcal/mol) are expected for ωB97X-V and M11[82,116,266].

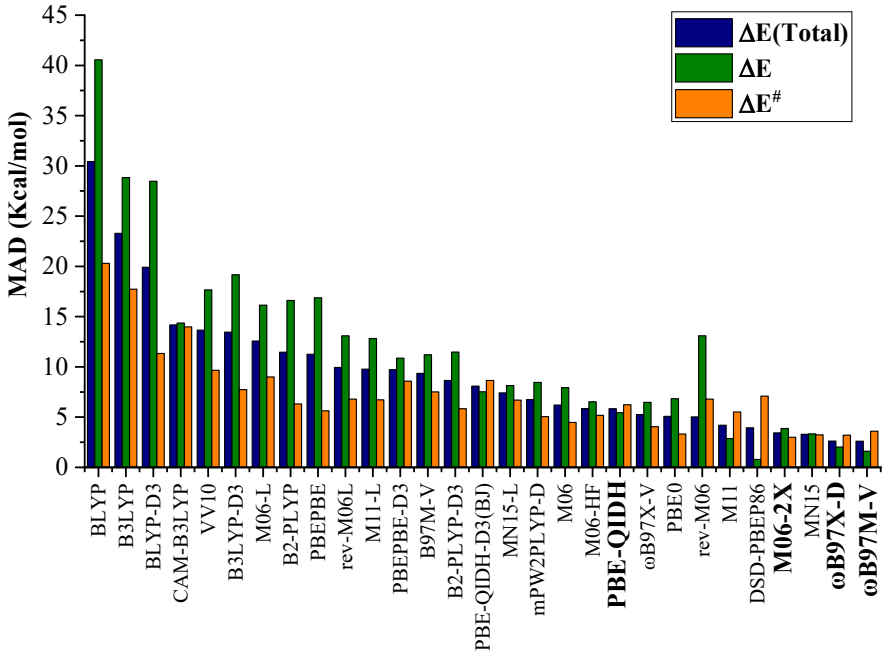

Figure 7.2. Mean Absolute Errors (MAEs, kcal/mol)) on the relative energies (ΔE), reaction barriers ($\Delta E^{\#}$) and total molecules (Total).

It is thus clear that an even qualitative reliable description of the complex reaction path of this prototypical ambimodal reaction represents an hard challenge for DFT approaches. Indeed, here we want to show how the functional's choice determines the predicted products of the reaction mechanism, as a consequence due to uneven accuracy along the different competing reaction pathways. In other words, we will first show how different DFT approaches differently affect competitive reaction channels, due to unequal errors in the predicted kinetic (energy barriers) and thermochemistry (energy differences). Next, we will explain and qualitatively correlate computed behaviors to known drawbacks differentially affecting by construction the exchange-correlation functionals applied.

To this end, we have computed the energy profile for the cycloaddition of cyclopentadiene and cycloheptatriene with tropone as well as its chlorine and oxo-methyl derivatives, using 28 functionals asshowed in the Figure7.1. All the calculations have been performed with the Gaussian Development Version (GDV)[267] and the aug-cc-pvtz basis set[268].

More details on the computational parameters are given in the Table S7.I. Accurate reference data (CCSD(T)/cc-pVQZ) data have been retrieve from the original paper of Houk and collaborators together with the corresponding structures obtained at ωB97X-D/def2-TZVP level of theory. 18 Following the traditional approach in evaluating functional performance, in Figure 7.2 are reported the Mean Absolute Errors (MAEs) for the mentioned functionals considering the relative stabilities of all intermediates (ΔE in Figure 7.2) and reaction barriers ($\Delta E^{\#}$ in Figure 7.2). Corresponding raw data are collected in supporting information (Table S7.2).

The difficulty of the playground chosen is clearly evidenced by the relative high deviations found: the most accurate functionals, ωB97X-D and ωB97M-V, have a MAE of 2.6 kcal/mol, while higher values are obtained for MN15 (3.3 kcal/mol), M06-2X (3.4 kcal/mol), DSD-PBEP86 (3.9 kcal/mol) and MN11 (4.2 kcal/mol). The other functionals follow, up to 30.4 kcal/mol (BLYP). If it is indeed reassuring that the best-performer functionals are also well-ranked in standard benchmarks, like those included in the large GMTKN55 set[82] or the most recent BH9 set[175,269], even if with lower errors. This is not the case for other DFT approaches, such as B2-PLYP or CAM-B3LYP[269]. We also like to briefly notice two points: i) the role of dispersion corrections is actually not crucial, since no clear trend can be evidenced comparing errors obtained for functionals with and without corrections (i.e. PBE and B3LYP vs. PBE-D3 and B3LYP-D3); ii) only few functionals, namely CAM-B3LYP, PBE-QIDH, M06-2X and MN15[262], give comparable errors on stabilities and barriers, while all the others are more accurate on barriers, with the notable exception of DSD-PBEP86.

These results well illustrate the difficulty of a-priori estimation of the accuracy that can be expected for functional making use in an uncritical way of the results provided by standard benchmarks for this complex ambimodal reaction.

Starting from this general picture, we now look more into the details of the different reaction steps, starting from the most-usual energy signature, the relative stability of final products (11 and 12) with respect to the reactants (1+7). These energy differences, collected in Figure 7.3, span over a large range: from 18.0 to −46.0 kcal/mol. If the general trend is close to that already discussed for the global MAEs, a striking feature appears: the positive energy predicted by BLYP and B3LYP. Basically, these two functionals envisage that products are less stable than reactants, thus indicating an endothermic reaction. The addition of an empirical potential, allowing to include the effect of noncovalent interactions, to BLYP and B3LYP (leading to BLYP-D and B3LYP-D3, respectively) stabilize the products giving a

(qualitatively) correct thermochemistry (exothermic reaction). This is role of dispersion is also evident for other functionals like PBEPBE and B2-PLYP where the same corrections further stabilize the products and improves the agreement with the reference CCSD(T) values.

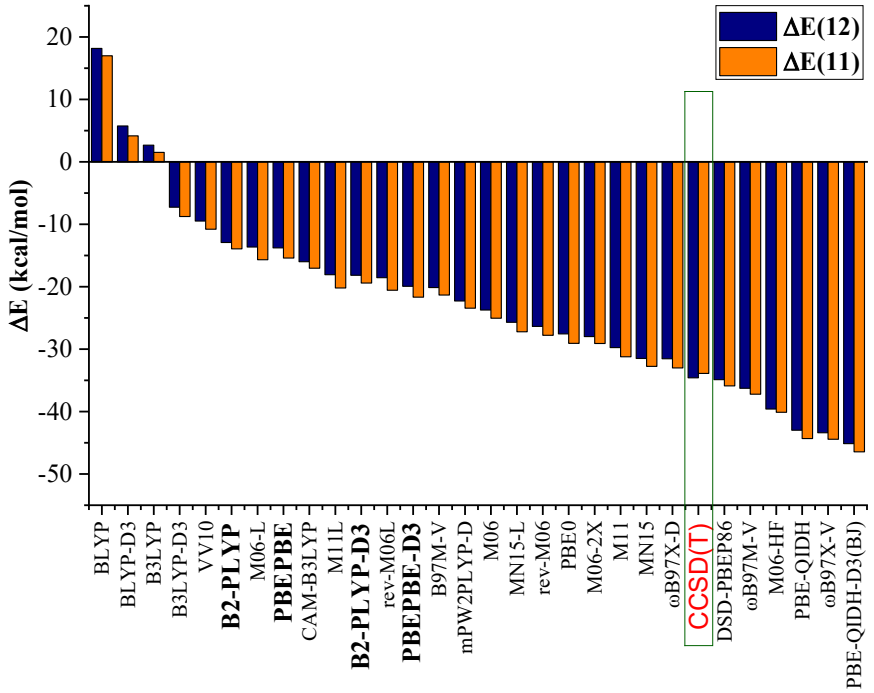

Figure 7.3. Relative energies (ΔE, kcal/mol) of the product **11** and **12** with respect to the reactants **1**+**7**.

A similar behavior is observed for the relative stabilities of the reactions intermediates, 10, 9 and 8 with respect to reactants (1+7), with BLYP and B3LYP functionals predicting largely destabilized intermediates in Figure 7.4 (more details see S7.3). Most of the other functionals correctly reproduce the general trends on relative energies, albeit with (minor) differences concerning the stability order.

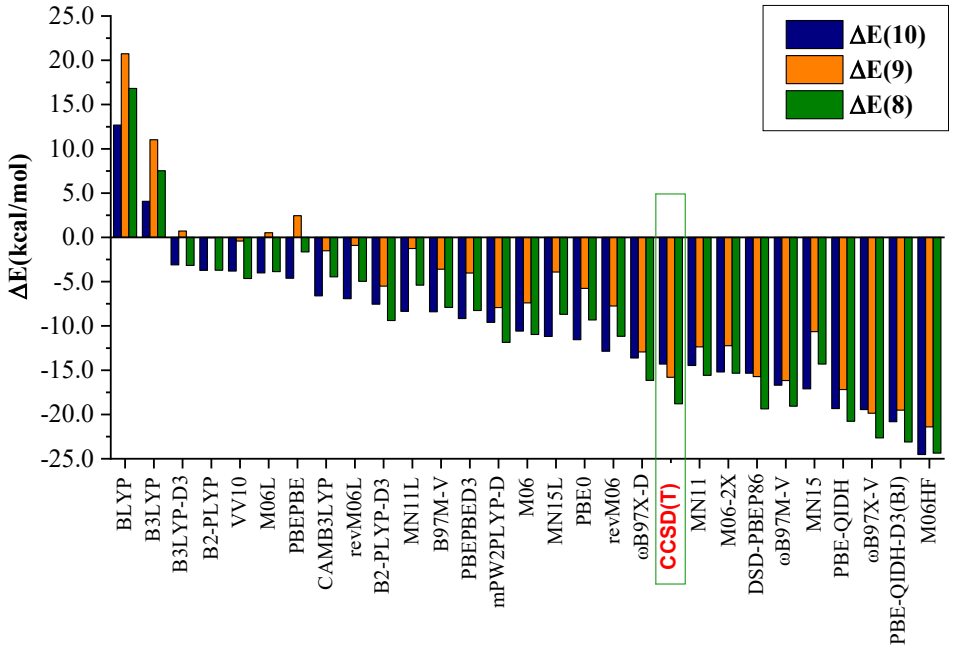

Figure 7.4. Relative energies (ΔE, kcal/mol) of the intermediates 8, 9, 10 with respect to the reactants **1**+**7**.

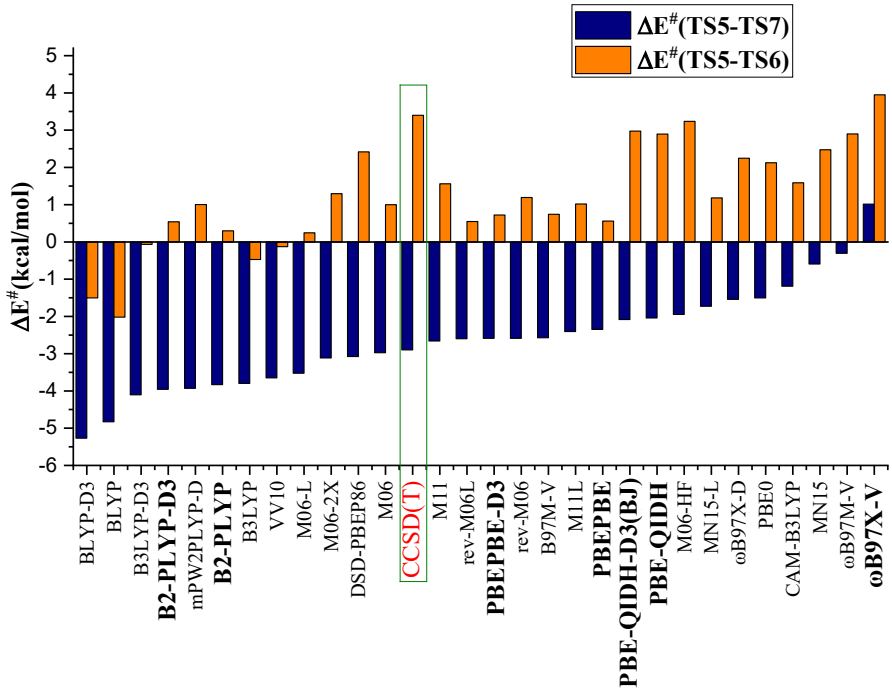

Figure 7.5. Energy differences ($\Delta E^{\#}$, kcal/mol) between **TS5** and **TS7** or **TS6**. Positive values indicates that **TS5** is higher than TS6 or TS7, negative values indicate the opposite.

From this first example, it is already clear that a specific drawback of some functionals, here the poor description of noncovalent interactions, leads not only to significant errors on the reaction energies but also on the nature (endo vs exo-thermic) of the reaction.

Nonetheless, the most relevant feature that is important to predict when aiming at describing this ambimodal reaction is the relative stability of the TSs, that is ruling the access to the different reaction channels. In Figure 7.5 are reported the energy differences between TS5, TS6 and TS7 that quantitatively determine the first bifurcation in these ambimodal reaction. Several functionals are in good (semi)-quantitative agreement with the CCSD(T) data, especially on $\Delta E^{\#}$(TS5-TS7), while more scattered are the values for $\Delta E^{\#}$(TS5-TS6). Among the approaches providing a good compromise on the evaluation of these two relative barrier energies, DSD-PBEP86, MN11, PBE-QIDH, ωB9XD and M06-HF can be mentioned. Few functionals predict a different order in stabilities: BLYP, B3LYP and, to a minor extend, B3LYP-D3 suggest TS5 as more stable than TS6, while for ωB97X-V TS7 is higher in energy than TS5. It is interesting also to notice the negligible effects of the dispersion corrections, in clear contrast with the behavior observed for the energy minima. Basically, with the notable exception of BLYP and B3LYP, all functionals correctly predict the ambimodal nature of the reactions, albeit with a different weight for the two possible reaction paths.

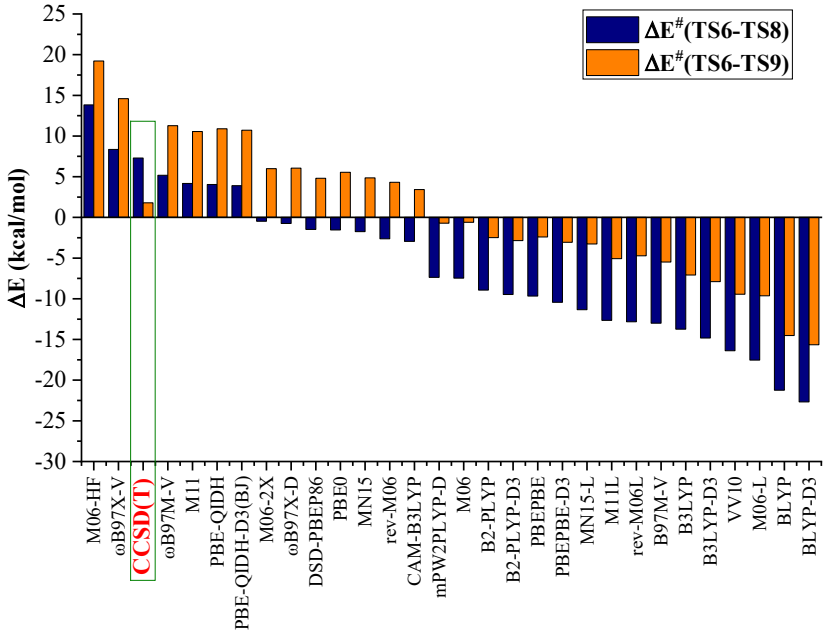

Figure 7.6. Energy differences ($\Delta E^{\#}$, kcal/mol) between **TS6** and **TS8** or **TS9**. Positive values indicates that **TS6** is higher than **TS8** or **TS9**, negative values indicate the opposite.

Figure 7.6 collects the differences in energy between the TS6 and TS9, that rule the second possible bifurcation with two reaction paths leading to the products 11 and 12, respectively. About half of the considered functionals are in (semi-) quantitative agreement with the CCSD(T) results, that indicates TS6 higher in energy than TS9. Among these, we can find the already mentioned M06-HF, ωB97X-V, ωB97M-V, PBE-QIDH as well as M11. Among those providing an opposite view, with the TS9 higher than TS6, we can find VV10, B97MV, rev-M06L and MN15L, just to mention those having the largest deviations. The analysis of the relative energy of the TS6 and TS8, determining the rate-determining step after the intermediate 9 on the path leading to product 11 (see Figure 7.1), shows even larger differences between the functionals. Indeed only 5 functionals, namely M06-HF, ωB97X-V, ωB97M-V, PBE-QIDH and M11, give a qualitative correct picture of the reactions with the TS6 higher in energy than TS8, while for all the others, the rate determine step is the second TS (TS8).

In summary, among all the considered functionals, only three, namely M06-HF, ωB97M-V and PBE-QIDH are able to provide a balance energetics of the ambimodal reactions.

Beyond this necessary and detailed numerical analysis of the errors, in order to provide more general guidelines on functional choice it would be of greater interest to understand the physical origin of these divergent behaviors. The different nature of the functionals make this task not straightforward, but apparently not all these discrepancy can be ascribed exclusively to the ability of the functional in reproducing weak interactions as for the relative stabilities of the reactants and products. Indeed, small variations are observed for the relative stabilities of the TSn upon addition of empirical potential, as can be easily seen by comparing the close energies provided by a given functional with and without empirical corrections for dispersion (e.g. BLYP vs. BLYP-D3). Analogously the amount of Hartree-Fock exchange, often evoked as a source of amelioration in functional behavior, do not correlate, at a first sight, with all the observed errors since functionals giving even qualitatively wrong predictions for barriers, such as B3LYP, B2-PLYP or M06, cast between 22% and 57 % of HF exchange.

A plausible explanation can be found looking with Chemist's eyes to the structures of the reactions intermediates, characterized by four double bonds for 9 and 8 and two for 12 and 11 (see Figure 7.1). This difference in the number of double bonds suggests a different degree of electronic conjugation in the intermediates. Delocalization error (ΔE), that is the unphysical overdelocalization of electronic distribution[190], is a common drawback arising from the approximate nature of the exchange-correlation functionals. It could be then argued that the ΔE

is almost constant along a reaction path connecting species with the with the same number of double bonds, while it varies if the intermediates have a diverse degree of conjugations. In other term, ΔE is (almost) constant in going from 9 to 8, since the number of double bonds is preserved, while it varies from 9 to 12 or from 8 to 11 where this number changes.

For a given functional an measure of its ΔE can be qualitatively given by the difference between the ionization potential of a single He atom and that of a cluster formed of well-separated He atoms (He-He distance equal to 10 Å)[270]. Functionals suffering ΔE provide low ionization energies for the cluster, due to the artificial delocalization of the positive charge in the cationic species[271].

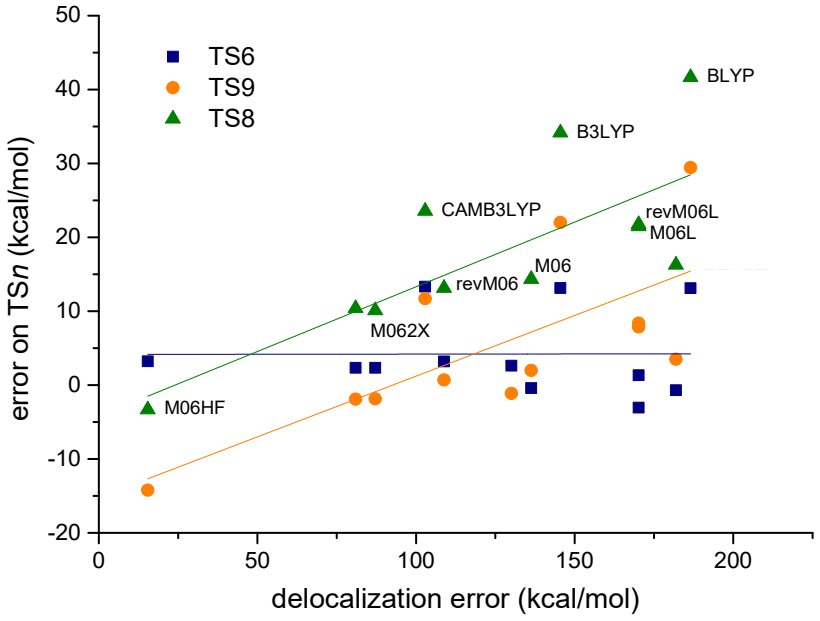

Figure 7.7. Computed error on **TS6**, **TS9** and **TS8** (error on *TSn*, kcal/mol) as function of the delocalization error for a cluster of well-separated He atoms (He-He distance equal to 10 Å). Some functionals are explicitly indicated for **TS8** (see text for discussion).

In Figure 7.7 the errors of TS6, TS8, and TS9 energies are reported as a function of the ΔE values computed for all the different functional. While the energy error for TS6 does not significantly depend on ΔE, this is not true for TS8 and TS9, whose energies qualitatively correlates with an increase of the ΔE error although the slope may depend on the functional

form. Indeed, it is noteworthy that the functionals showing highest error on TS energies and highest slope cast the BLYP functionals (BLYP, B3LYP and CAM-B3LYP, see Figure 7.6). An almost linear relationship between ΔE and errors on TS can be evidenced for the M06 family (M06L, M06, M06-2X and M06-HF). In both cases the trend is ruled by the quantity of HF exchange: larger contribution correspond to lower errors on both ΔE and TS energies. However this trend cannot be generalized, as mentioned, due to the different nature of the other considered functionals.

All the trends here discussed in the case on the unsubstituted tropone are valid for its chloro- or methoxy derivatives in Figure 7.8 (2-chlorotropone) and Figure 7.9 (2-methoxytropone), respectively, as it can be inferred from the energy values reported, for the whole set of considered functionals (see more details inTable S7.4). Of course, variations in the values energy values of the single steps are observed, due to the substituents effect, but the general trends and conclusions drawn for tropone still hold.

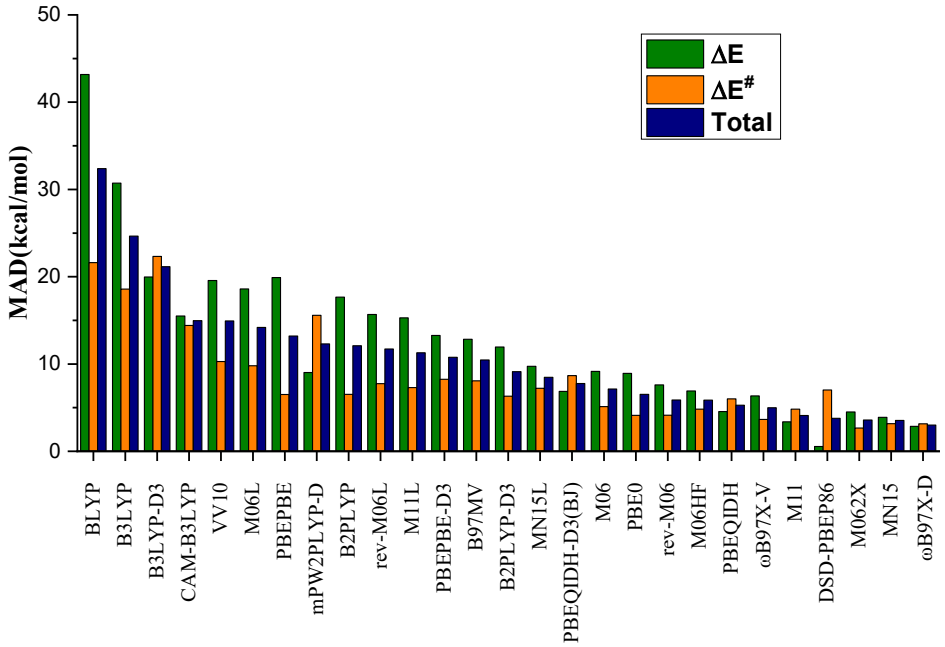

Figure 7.8. Mean Absolute Errors (MAEs, kcal/mol)) on the relative energies (ΔE), reaction barriers ($\Delta E^{\#}$) and total molecules (Total) for 2-chlorotropone.

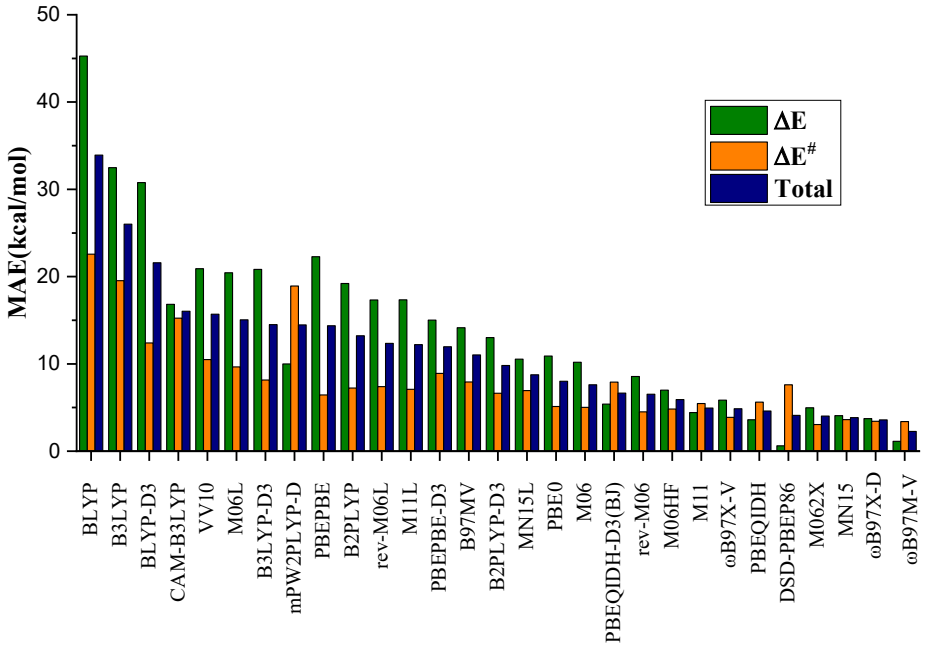

Figure 7.9. Mean Absolute Errors (MAEs, kcal/mol) on the relative energies (ΔE), reaction barriers ($\Delta E^{\#}$) and total molecules (Total) for 2-methoxytropone.

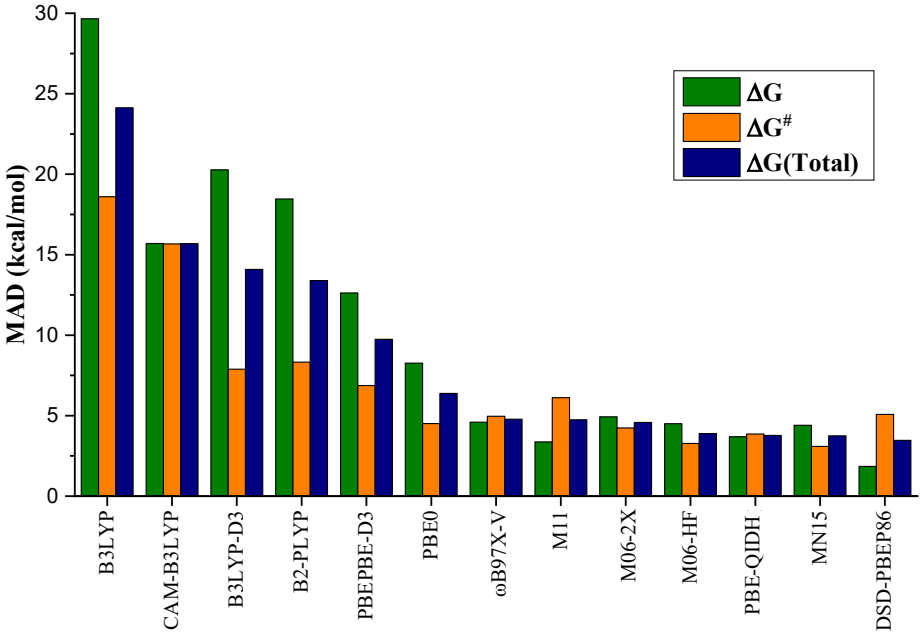

Figure 7.10. Mean Absolute Errors (MAEs, kcal/mol) on the relative Gibbs energies on tropone.

As last check we have investigated the effect of structural parameters on the computed energies by optimizing all the reaction intermediates, including minima and transitions energies, for selected functionals. This procedure allow to evaluated also the reaction enthalpies (ΔH and ΔH#) and Gibbs free energies (ΔG and ΔG#, see Figure 7.10). Also in this case, all the discussed trends are kept upon the consideration of relaxed molecular structures, thermal and entropic effects. These data are, therefore, not discussed in details and we refer the interest reader to the values reported in Table S7.5 for details.

7.4 Conclusion

The above reported results well illustrate that different density functional give different energies difference in ambimodal reactions. This difference is related with the delocalization errors, that is the unphysical overdelocalization of electronic distribution, is a common drawback arising from the approximate nature of the exchange-correlation functionals. It could be then argued that the ΔE is almost constant along a reaction path connecting species with the same number of double bonds, while it varies if the intermediates have a diverse degree of conjugations.

From a more theoretical point of view, the drawbacks of all the other functionals can be traced back to the well-known problem related to the reproduction of dispersion interactions and to the so-called Delocalization Error. Based on analysis of the reaction intermediates, a skilled Chemist user could, at least in principle, identify critical situations and foresee the onset of these errors.

Last but not least, our work also shows the limits of the use of common benchmark sets, testing separately the behavior of each functional on specific properties and reactions, when aiming at describing competing reactions paths and the necessity of a careful analysis (possibly using diagnostic indicators) of the functional behaviors all along the different reaction paths. The systematic benchmark of exchange-correlation functionals for a specific – single – property has been instrumental in the establishment of DFT as a method of choice for many applications, including reactivity. However, it must be realized that real Chemistry applications may be a much more complex problem requiring an accurate and balanced description of several different properties and of competing mechanisms.

Chapter 8

General conclusions and perspectives

The objective of this thesis was to devise, construct and apply the DH*thermo* protocol (PBE-QIDH-D3(BJ) + DH-SVPD Basis set) to investigate different benchmarks, specifically the non-covalent interactions in the hydrocarbon systems, and then extend the hydrocarbon system to the halogen systems.

To do so, we made use of DH*thermo* protocol firstly to study the proto-branching problem of the alkanes, in which the branched alkanes are more stable than the linear alkanes, this reaction is known as Bond Separation Reaction (BSR), demonstrated that this protocol is able to correctly reproduce, with exceptionally low errors (beyond chemical accuracy, less than 1 kcal/mol), both reaction energies and enthalpies for selected BSRs. The obtained results, checked on five different references datasets (two theoretical and three experimental), clearly demonstrate its quality. And the DH*thermo* has the advantage of its intrinsic simplicity and straightforward use.

In a secondary study, further extend our investigation to other 5 medium-sized different difficult hydrocarbons systems to study. As already discussed, all Double-hybrid functionals (DHs) including an empirical dispersion prefer the larger basis set which lead to sub-chemical accuracies. In contrast, the PBE-QIDH/DH-SVPD combinations is competitive with these latter. It is reassuring than on such global performance indicator, the PBE-QIDH-D3(BJ)/DH-SVPD model, which is our *DHthermo* model for the thermochemistry of alkanes is among the best performers, thus extending its applicability beyond BSRs.

Extending the study to more complicated systems, BH9, by using DH together with DH-SVPD basis set. Over the whole BH9 systems, minimally parameterized DHs like ωB2-PLYP or B2K-PLYP, and nonempirical DHs like PBE0-DH and PBE-QIDH succeed to reach

the ‘chemical accuracy’ energy threshold by more than 40% for both kinetics and thermochemistry properties in a balanced fashion.

The following study was investigated by evaluating of weak non-covalent interactions in large, that is containing up to thousand atoms, molecular systems. Here, the PBE-QIDH/DH-SVPD protocol, is particularly accurate for large systems CiM13 set (up to more than 1,000 atoms and 14,000 basis functions), for which the DLPNO approximation leads to a significant speed-up for the evaluation of the perturbative correlation term. However, the limited quality of the reference data for the quite large molecular complex is still a block to developing and identifying the new methods.

The results in the hydrocarbon system is so promising that we can safely extend to the halogen systems, the obtained results show that this DH-SVPD basis set can reach the so-called “chemical accuracy” (< 1.0 kcal/mol) with the PBE-QIDH functional on each tested halogen sets, providing accurate results for Halogen Bonding (HB) energies in all the considered sets when using DH functionals, can recover the performances of DH functionals in reproducing interaction energies of HB casting with empirical dispersion corrections.

Overall the results, correctly predicting and modeling the non-covalent interactions by DH*thermo* protocol have made a further step to improve the accuracy. While for quite a large system, with more than thousands of atoms, the limit of the quality of the precise reference data is still a tough problem. The DH*thermo* protocol is based on the DH functionals together with a tailored basis set to cure the Basis set Superposition and Incompletness Errors, espically for the weak interactions, however, we should realize that the unphysical overdelocalization of electronic distribution, is a common drawback arising from the approximate nature of the exchange-correlation functional, called Delocalization Errors. In Chapter 7, preliminary work about explore the instricit properties of the ambimodal reaction has been done, it is clear that an even qualitative reliable description of the complex reaction path of this prototypical ambimodal reaction represents an hard challenge for DFT approaches, the further step for how to cure this Delocalization Errors can put on schedule.

Chapter 9

Appendix: supplementary materials

Supporting materials of Chapter 3

Table S3.3.1. Optimized exponents of the DH-SVPD basis set. These exponents replace the corresponding exponents of the original Def2-SVPD basis set, which are also reported for comparison. All other exponents are kept as in the original basis set.

atom	function	def2-SVPD	DH-SVPD	function	def2-SVPD	DH-SVPD
H	s	0.1219496200	0.4617867850	P	0.117040991	0.079134024
C	p	0.1526861380	0.1508036550	d	0.117131851	0.322929479
N	p	0.2195434803	0.1918861474	d	0.166977081	0.309544326
O	p	0.0690022764	0.0989212321	d	0.179920243	0.237375243

Table S3.3.2. Example input for Gaussian code, reporting the optimized DH-SVPD basis set for C and H atoms.

<table>
<tr><td>%chk=hexane.chk
%mem=200GB
%nproc=32
#P PBEQIDH/gen opt freq

Hexane opt + freq

0 1
C -3.44438117 3.35712493 -1.99207046
H -3.08770833 3.86152312 -1.11841895
H -3.08770833 3.86152312 -2.86572196
H -4.51438117 3.35713811 -1.99207046
C -2.93106546 1.90519277 -1.99207046
H -3.28773626 1.40079530 -1.11841771
H -3.28774033 1.40079387 -2.86572072
C -1.39106546 1.90517380 -1.99207404
H -1.03439495 2.40787452 -2.86670432
H -1.03439034 2.41126819 -1.11940496
C -0.87775046 0.45324413 -1.98925490
H -1.23479072 -0.05297863 -2.86170019
H -1.23405637 -0.04932690 -1.11440150
C 0.66224940 0.45322386 -1.98990158
H 1.01928880 0.95946340 -1.11746568
H 1.01855553 0.95577849 -2.86476430
C 1.17556440 -0.99870576 -1.98705550
H 0.81852159 -1.50494561 -2.85948982
H 2.24556431 -0.99871985 -1.98750795
H 0.81926107 -1.50125964 -1.11219121</td><td></td></tr>
<tr><td>-H 0
s 3 1.00
13.010701000 0.19682158000e-01
1.9622572000 0.13796524000
0.44453796000 0.47831935000
p 1 1.00
0.80000000000 1.0000000</td><td>Standard def2-SVPD exponents and coefficients for H atom</td></tr>
<tr><td>s 1 1.00
0.4617867850E+00 0.1000000000E+01
p 1 1.00
0.7913402419E-01 0.1000000000E+01
****</td><td>DH-SVPD optimized exponents for H atom</td></tr>
<tr><td>-C 0
s 5 1.00
1238.4016938 0.54568832082e-02
186.29004992 0.40638409211e-01
42.251176346 0.18025593888
11.676557932 0.46315121755
3.5930506482 0.44087173314
s 1 1.00
0.40245147363 1.0000000
s 1 1.00
0.13090182668 1.0000000
s 1 1.00
0.67053540256e-01 1.0000000
p 3 1.00
9.4680970621 0.38387871728e-01
2.0103545142 0.21117025112
0.54771004707 0.51328172114
d 1 1.00
0.80000000000 1.0000000</td><td>Standard def2-SVPD exponents and coefficients for C atom</td></tr>
<tr><td>p 1 1.00
0.1508036550E+00 0.1000000000E+01
d 1 1.00
0.3229294790E+00 0.1000000000E+01</td><td>DH-SVPD optimized exponents for C atom</td></tr>
</table>

Table S3.3.3. Relative energies (kcal/mol) for the considered isodesmic reactions, obtained with the DH-SVPD basis set. In parenthesis are reported the relative errors with respect to the experimental data of reference[95].

1. 2ethane→propane+methane 2. 3ethane→butane+2methane 3. 3ethane→isobutane+2methane	4. 3ethane→pentane+3methane 5. 4ethane→neopentane+3methane 6. 5ethane→hexane+4methane	7. 5ethane→22-dimethylbutane+4methane 8. 6ethane→heptane+5methane 9. 6ethane→223trimethylbutane+5methane	10. 7ethane→octane+6methane 11. 7ethane→2233tetramethylbutane+6methane

	B3LYP	*B3LYP-D3*	*B2-PLYP*	*B2-PLYP-D3*	*PBE0*	*PBE0-DH*	*PBE-QIDH*	*M06*	*M06L*	*ωB97X-D*	*TPSSh*	*CAM-B3LYP*	*PBE0-DH-D3(BJ)*	*PBE-QIDH-D3(BJ)*	*DSD-PBEP86*
1	-2.22 (+0.95)	-2.74 (+0.43)	-2.70 (+0.47)	-2.98 (+0.19)	-2.42 (+0.75)	-2.64 (+0.53)	-2.91 (+0.26)	-2.71 (+0.46)	-2.38 (+0.79)	-2.79 (+0.38)	-2.04 (+1.13)	-2.52 (+0.65)	-2.96 (+0.21)	-3.00 (+0.17)	-3.13 (+0.04)
2	-4.48 (+2.27)	-5.61 (+1.14)	-5.51 +1.24)	-6.13 (+0.62)	-4.91 (+1.84)	-5.39 (+1.36)	-5.99 (+0.77)	-5.58 (+1.17)	-4.86 (+1.89)	-5.73 (+1.02)	-4.13 (+2.62)	-5.09 (+1.66)	-6.10 (+0.65)	-6.20 (+0.55)	-6.45 (+0.30)
3	-5.51 (+2.95)	-7.12 (+1.34)	-7.01 (+1.45)	-7.88 (+0.58)	-6.13 (+2.33)	-6.83 (+1.63)	-7.70 (+0.76)	-7.44 (+1.02)	-6.20 (+2.26)	-7.22 (+1.24)	-5.08 (+3.38)	-6.42 (+2.04)	-7.81 (+0.65)	-7.96 (+0.50)	-8.39 (0.07)
4	-6.71 (+3.45)	-8.50 (+1.66)	-8.33 (+1.83)	-9.31 (+0.85)	-7.37 (+2.79)	-8.13 (+2.03)	-9.07 (+1.09)	-8.46 (+1.70)	-7.50 (+2.66)	-8.71 (+1.45)	-6.20 (+3.96)	-7.64 (+2.52)	-9.24 (+0.92)	-9.43 (+0.73)	-9.81 (0.35)
5	-8.61 (+6.58)	-11.90 (+3.29)	-11.77 (+3.42)	-13.54 (+1.65)	-9.92 (+5.27)	-11.44 (+3.75)	-13.29 (+1.90)	-13.05 (+2.14)	-10.54 (+4.65)	-12.22 (+2.97)	-8.07 (+7.12)	-10.43 (+4.76)	-13.44 (+1.75)	-13.83 (+1.36)	-14.68 (0.51)
6	-8.99 (+4.60)	-11.44 (+2.15)	-11.20 (+2.39)	-12.55 (+1.04)	-9.88 (+3.71)	-10.92 (+2.67)	-12.21 (+1.38)	-11.36 (+2.23)	-10.00 (+3.59)	-11.73 (+1.86)	-8.32 (+5.27)	-10.24 (+3.35)	-12.44 (+1.15)	-12.72 (+0.87)	-13.22 (0.37)
7	-9.02 (+7.76)	-13.62 (+3.16)	-13.14 (+3.64)	-15.63 (+1.15)	-10.86 (+5.92)	-12.83 (+3.95)	-15.23 (+1.55)	-15.26 (+1.52)	-12.70 (+4.08)	-14.47 (+2.31)	-8.54 (+8.24)	-11.35 (+5.43)	-15.66 (+1.12)	-16.05 (+0.73)	-17.11 (-0.33)
8	-11.29 (+5.73)	-14.40 (+2.62)	-14.09 (+2.93)	-15.80 (+1.22)	-12.39 (+4.63)	-13.73 (+3.29)	-15.36 (+1.66)	-14.29 (+2.73)	-12.71 (+4.31)	-14.77 (+2.25)	-10.44 (+6.58)	-12.85 (+4.17)	-15.65 (+1.37)	-16.02 (+1.00)	-16.64 (+0.38)
9	-9.24 (+10.37)	-15.68 (+3.93)	-14.86 (+4.75)	-18.34 (+1.27)	-11.84 (+7.77)	-14.51 (+5.10)	-17.77 (+1.84)	-18.01 (+1.60)	-15.07 (+4.54)	-16.71 (+2.90)	-8.89 (+10.72)	-12.34 (+7.27)	-18.53 (+1.08)	-18.96 (+0.65)	-20.40 (-0.79)
10	-13.58 (+6.87)	-17.36 (+3.09)	-16.98 (+3.47)	-19.06 (+1.39)	-14.92 (+5.53)	-16.54 (+3.91)	-18.52 (+1.93)	-17.22 (+3.23)	-15.26 (+5.19)	-17.81 (+2.64)	-12.57 (+7.88)	-15.46 (+4.99)	-18.87 (+1.58)	-19.33 (+1.12)	-20.08 (+0.37)
11	-8.23 (+14.90)	-17.32 (+5.81)	-16.22 (+6.91)	-21.16 (+1.97)	-12.06 (+11.07)	-15.85 (+7.28)	-20.49 (+2.64)	-20.94 (+2.19)	-17.43 (+5.70)	-19.16 (+3.97)	-8.46 (+14.67)	-12.63 (+10.50)	-21.45 (+1.68)	-22.15 (+0.98)	-24.14 (-1.01)
MAD	6.04	2.60	2.96	1.08	4.69	3.23	1.43	1.82	3.60	2.09	6.51	4.30	1.10	0.79	0.41

Table S3.3.4. Relative energies (kcal/mol) for the considered isodesmic reactions, obtained with the cc-pVTZ basis set. In parenthesis are reported the relative errors with respect to the experimental data of reference[95].

	B3LYP	*B3LYP-D3*	*B2-PLYP*	*B2-PLYP-D3*	*PBE0*	*PBE0-DH*	*PBE-QIDH*	*M06*	*M06L*	*ωB97X-D*	*TPSSh*	*CAM-B3LYP*	*PBE0-DH-D3(BJ)*	*PBEQIDH-D3(BJ)*	*DSD-PBEP86*
1	-1.91 (1.26)	-2.44 (+0.73)	-2.38 (+0.79)	-2.67 (+0.50)	-2.18 (+0.99)	-2.39 (+0.78)	-2.63 (+0.54)	-2.46 (+0.71)	-2.10 (+1.07)	-2.51 (+0.66)	-1.80 (+1.37)	-2.23 (+0.94)	-2.71 (+0.46)	-2.72 (+0.45)	-2.81 (+0.36)
2	-3.88 (2.87)	-5.02 (+1.73)	-4.87 (+1.88)	-5.50 (+1.25)	-4.45 (+2.30)	-4.90 (+1.85)	-5.42 (+1.33)	-5.21 (+1.54)	-4.41 (+2.34)	-5.24 (+1.51)	-3.69 (+3.06)	-4.54 (+2.21)	-5.61 (+1.14)	-5.64 (+1.11)	-5.79 (+0.96)
3	-4.66 (3.80)	-6.29 (+2.17)	-6.16 (+2.30)	-7.04 (+1.42)	-5.49 (+2.97)	-6.18 (+2.28)	-6.97 (+1.49)	-6.83 (+1.63)	-5.56 (+2.90)	-6.54 (+1.92)	-4.48 (+3.98)	-5.64 (+2.82)	-7.17 (+1.29)	-7.23 (+1.23)	-7.53 (+0.93)
4	-5.80 (4.36)	-7.60 (+2.56)	-7.34 (+2.82)	-8.33 (+1.83)	-6.66 (+3.50)	-7.37 (+2.79)	-8.18 (+1.98)	-7.84 (+2.32)	-6.74 (+3.42)	-7.95 (+2.21)	-5.52 (+4.64)	-6.80 (+3.36)	-8.48 (+1.68)	-8.54 (+1.62)	-8.75 (+1.41)
5	-7.26 (7.93)	-10.57 (+4.62)	-10.41 (+4.78)	-12.20 (+2.99)	-8.97 (+6.22)	-10.45 (+4.74)	-12.12 (+3.07)	-12.42 (+2.77)	-9.76 (+5.43)	-11.19 (+4.00)	-7.17 (+8.02)	-9.21 (+5.98)	-12.47 (+2.72)	-12.66 (+2.53)	-13.30 (+1.89)
6	-7.75 (5.84)	-10.21 (+3.38)	-9.84 (+3.75)	-11.19 (+2.40)	-8.91 (+4.68)	-9.88 (+3.71)	-10.98 (+2.61)	-10.58 (+3.01)	-9.04 (+4.55)	-10.70 (+2.89)	-7.40 (+6.19)	-9.09 (+4.50)	-11.40 (+2.19)	-11.48 (+2.11)	-11.77 (+1.82)
7	-7.04 (9.74)	-11.66 (+5.12)	-11.13 (+5.65)	-13.63 (+3.15)	-9.39 (+7.39)	-11.28 (+5.50)	-13.44 (+3.34)	-14.18 (+2.60)	-11.48 (+5.30)	-12.88 (+3.90)	-7.17 (+9.61)	-9.51 (+7.27)	-14.13 (+2.65)	-14.26 (+2.52)	-15.04 (+1.74)
8	-9.71 (7.31)	-12.85 (+4.17)	-12.34 (+4.68)	-14.07 (+2.95)	-11.17 (+5.85)	-12.39 (+4.63)	-13.78 (+3.24)	-13.25 (+3.77)	-11.40 (+5.62)	-13.47 (+3.55)	-9.27 (+7.75)	-11.39 (+5.63)	-14.33 (+2.69)	-14.44 (+2.58)	-14.78 (+2.24)
9	-6.33 (13.28)	-12.89 (+6.72)	-12.00 (+7.61)	-15.50 (+4.11)	-9.68 (+9.93)	-12.30 (+7.31)	-15.24 (+4.37)	-16.36 (+3.25)	-13.15 (+6.46)	-14.48 (+5.13)	-6.91 (+12.70)	-9.69 (+9.92)	-16.35 (+3.26)	-16.43 (+3.18)	-17.49 (+2.12)
10	-11.68 (8.77)	-15.48 (+4.97)	-14.86 (+5.59)	-16.96 (+3.49)	-13.43 (+7.02)	-14.91 (+5.54)	-16.59 (+3.86)	-15.99 (+4.46)	-13.73 (+6.72)	-16.24 (+4.21)	-11.15 (+9.30)	-13.69 (+6.76)	-17.27 (+3.18)	-17.40 (+3.05)	-17.81 (+2.64)
11	-4.51 (18.62)	-13.65 (+9.48)	-12.48 (+10.65)	-17.42 (+5.71)	-9.26 (+13.87)	-13.01 (+10.12)	-17.19 (+5.94)	-18.83 (+4.30)	-15.12 (+8.01)	-16.27 (+6.86)	-5.94 (+17.19)	-9.13 (+14.00)	-18.62 (+4.51)	-18.83 (+4.30)	-20.31 (+2.82)
MAD	7.62	4.15	4.59	2.71	5.88	4.48	2.89	2.76	4.71	3.35	7.62	5.76	2.34	2.24	1.72

Table S3.3.5. Relative energies (kcal/mol) for the considered isodesmic reactions, obtained with the cc-pVQZ basis set. In parenthesis are reported the relative errors with respect to the experimental data of reference[95].

	B3LYP	*B3LYP-D3*	*B2-PLYP*	*B2-PLYP-D3*	*PBE0*	*PBE0-DH*	*PBE-QIDH*	*M06*	*M06L*	*ωB97X-D*	*TPSSh*	*CAM-B3LYP*	*PBE0-DH-D3(BJ)*	*PBE-QIDH-D3(BJ)*	*DSD-PBEP86*
1	-1.94 (+1.23)	-2.46 (+0.71)	-2.41 (+0.76)	-2.70 (+0.47)	-2.21 (+0.96)	-2.42 (+0.75)	-2.66 (+0.51)	-2.51 (+0.66)	-2.15 (+1.02)	-2.51 (+0.66)	-1.84 (+1.33)	-2.25 (+0.92)	-2.74 (+0.43)	-2.75 (+0.42	-2.84 (+0.33)
2	-3.93 (+2.82)	-5.08 (+1.67)	-4.94 (+1.81)	-5.56 (+1.19)	-4.51 (+2.24)	-4.96 (+1.79)	-5.49 (+1.26)	-5.22 (+1.53)	-4.45 (+2.30)	-5.25 (+1.50)	-3.75 (+3.00)	-4.57 (+2.18)	-5.67 (+1.08)	-5.71 (+1.04)	-5.86 (+0.89)
3	-4.75 (+3.71)	-6.37 (+2.09)	-6.24 (+2.22)	-7.12 (+1.34)	-5.59 (+2.87)	-6.26 (+2.20)	-7.05 (+1.41)	-6.97 (+1.49)	-5.77 (+2.69)	-6.55 (+1.91)	-4.57 (+3.89)	-5.69 (+2.77)	-7.26 (+1.20)	-7.32 (+1.14)	-7.61 (+0.85)
4	-5.87 (+4.29)	-7.67 (+2.49)	-7.43 (+2.73)	-8.42 (+1.74)	-6.76 (+3.40)	-7.46 (+2.70)	-8.28 (+1.88)	-7.91 (+2.25)	-6.84 (+3.32)	-7.94 (+2.22)	-5.61 (+4.55)	-6.85 (+3.31)	-8.58 (+1.58)	-8.64 (+1.52)	-8.85 (+1.31)
5	-7.42 (+7.77)	-10.74 (+4.45)	-10.55 (+4.64)	-12.34 (+2.85)	-9.16 (+6.03)	-10.59 (+4.60)	-12.25 (+2.94)	-12.38 (+2.81)	-9.82 (+5.37)	-11.23 (+3.96)	-7.38 (+7.81)	-9.32 (+5.87)	-12.61 (+2.58)	-12.79 (+2.40)	-13.40 (+1.79)
6	-7.85 (+5.74)	-10.31 (+3.28)	-9.96 (+3.63)	-11.32 (+2.27)	-9.05 (+4.54)	-10.00 (+3.59)	-11.11 (+2.48)	-10.62 (+2.97)	-9.14 (+4.45)	-10.71 (+2.88)	-7.52 (+6.07)	-9.16 (+4.43)	-11.53 (+2.06)	-11.62 (+1.97)	-11.90 (+1.69)
7	-7.22 (+9.56)	-11.84 (+4.94)	-11.28 (+5.50)	-13.79 (+2.99)	-9.60 (+7.18)	-11.45 (+5.33)	-13.59 (+3.19)	-14.06 (+2.72)	-11.50 (+5.28)	-12.90 (+3.88)	-7.40 (+9.38)	-9.63 (+7.15)	-14.30 (+2.48)	-14.41 (+2.37)	-15.16 (+1.62)
8	-9.83 (+7.19)	-12.97 (+4.05)	-12.50 (+4.52)	-14.22 (+2.80)	-11.33 (+5.69)	-12.54 (+4.48)	-13.95 (+3.07)	-13.33 (+3.69)	-11.54 (+5.48)	-13.46 (+3.56)	-9.42 (+7.60)	-11.47 (+5.55)	-14.49 (+2.53)	-14.61 (+2.41)	-14.95 (+2.07)
9	-6.55 (+13.06)	-13.12 (+6.49)	-12.18 (+7.43)	-15.71 (+3.90)	-9.96 (+9.65)	-12.52 (+7.09)	-15.44 (+4.17)	-16.28 (+3.33)	-13.25 (+6.36)	-14.47 (+5.14)	-7.20 (+12.41)	-9.84 (+9.77)	-16.57 (+3.04)	-16.63 (+2.98)	-17.65 (+1.96)
10	-11.82 (+8.63)	-15.62 (+4.83)	-15.04 (+5.41)	-17.14 (+3.31)	-13.63 (+6.82)	-15.09 (+5.36)	-16.79 (+3.66)	-16.05 (+4.40)	-13.88 (+6.57)	-16.24 (+4.21)	-11.33 (+9.12)	-13.79 (+6.66)	-17.45 (+3.00)	-17.60 (+2.85)	-18.00 (+2.45)
11	-4.84 (+18.29)	-13.97 (+9.16)	-12.71 (+10.42)	-17.67 (+5.46)	-9.65 (+13.48)	-13.26 (+9.87)	-17.39 (+5.74)	-18.71 (+4.42)	-15.04 (+8.09)	-16.16 (+6.97)	-6.35 (+16.78)	-9.33 (+13.80)	-18.93 (+4.20)	-19.07 (+4.06)	-20.41 (+2.92)
MAD	7.48	4.01	4.46	2.57	5.71	4.34	2.76	2.75	4.63	3.35	7.45	5.67	2.20	2.11	1.62

Table S3.3.6. Relative energies (ΔE), including also ZPE correction (ΔE + ZPE) and enthalpies (ΔH) at 298 K for the isodesmic reactions of Scheme 3.3.1, computed with the DH-SVPD basis set. All the values were computed using the DH-SVPD basis set.

Reactions	*PBE-QIDH-D3(BJ)*			*PBE0-DH-D3(BJ)*			*B2-PLYP-D3*			*B3LYP-D3*		
	Δ(E+ZPVE)	ΔE	ΔH	Δ(E+ZPVE)	ΔE	ΔH	Δ(E+ZPVE)	ΔE	ΔH	Δ(E+ZPVE)	ΔE	ΔH
1	-3.03	-2.24	-2.72	-2.94	-2.16	-2.68	-2.96	-2.23	-2.71	-2.73	-2.03	-2.48
2	-6.25	-4.52	-5.50	-6.07	-4.36	-5.41	-6.10	-4.50	-5.45	-5.59	-4.07	-4.95
3	-8.00	-5.98	-7.32	-7.78	-5.78	-7.17	-7.84	-5.99	-7.26	-7.09	-5.35	-6.52
4	-9.49	-6.83	-8.29	-9.20	-6.57	-8.11	-9.27	-6.78	-8.20	-8.46	-6.09	-7.40
5	-13.87	-10.43	-12.79	-13.38	-10.00	-12.41	-13.49	-10.39	-12.56	-11.85	-8.97	-10.95
6	-12.79	-9.15	-11.11	-12.39	-8.79	-10.84	-12.49	-9.09	-10.97	-11.39	-8.15	-9.89
7	-16.10	-11.74	-14.49	-15.60	-11.31	-14.17	-15.57	-11.60	-14.19	-13.56	-9.87	-12.22
8	-16.10	-11.49	-13.94	-15.59	-11.03	-13.59	-15.73	-11.41	-13.76	-14.33	-10.22	-12.39
9	-19.03	-13.55	-17.05	-18.45	-13.06	-16.64	-18.26	-13.28	-16.53	-15.61	-10.92	-13.88
10	-19.42	-13.82	-16.77	-18.80	-13.27	-16.34	-18.98	-13.73	-16.55	-17.28	-12.29	-14.89
11	-22.23	-15.66	-20.05	-21.37	-14.97	-19.40	-21.08	-15.19	-19.19	-17.25	-11.75	-15.37

Reactions	*PBE-QIDH*			*B2-PLYP*			*PBE0-DH*			*DSD-PBEP86*		
	Δ(E+ZPVE)	ΔE	ΔH	Δ(E+ZPVE)	ΔE	ΔH	Δ(E+ZPVE)	ΔE	ΔH	Δ(E+ZPVE)	ΔE	ΔH
1	-2.898	-2.105	-2.637	-2.686	-1.931	-2.425	-2.625	-1.837	-2.363	-3.13	-2.37	-2.87
2	-5.961	-4.233	-5.297	-5.484	-3.840	-4.821	-5.369	-3.653	-4.704	-6.45	-4.79	-5.78
3	-7.665	-5.637	-7.060	-6.980	-5.060	-6.372	-6.800	-4.785	-6.190	-8.39	-6.45	-7.78
4	-9.037	-6.368	-7.940	-8.297	-5.745	-7.204	-8.100	-5.450	-7.002	-9.81	-7.24	-8.71
5	-13.237	-9.795	-12.268	-11.724	-8.488	-10.750	-11.392	-7.974	-10.413	-14.68	-11.40	-13.71
6	-12.163	-8.519	-10.616	-11.156	-7.672	-9.615	-10.881	-7.264	-9.332	-13.22	-9.71	-11.68
7	-15.169	-10.798	-13.743	-13.090	-8.981	-11.666	-12.783	-8.449	-11.350	-17.11	-12 .96	-15.68
8	-15.303	-10.681	-13.300	-14.030	-9.610	-12.027	-13.673	-9.087	-11.669	-16.64	-12 .19	-14.64
9	-17.703	-12.205	-15.901	-14.798	-9.603	-12.972	-14.450	-8.974	-12.618	-20.40	-15.21	-18.62
10	-18.450	-12.841	-15.987	-16.916	-11.549	-14.460	-16.473	-10.910	-14.008	-20.08	-14 .68	-17.61
11	-20.409	-13.836	-18.442	-16.151	-10.007	-14.158	-15.790	-9.275	-13.796	-24.14	-17.95	-22.18

Reactions	*PBE0*			*B3LYP*			*M06*			*TPSSh*			*M06-L*		
	Δ(E+ZPVE)	ΔE	ΔH	ΔE+ZPVE	ΔE	ΔH	Δ(E+ZPVE)	ΔE	ΔH	Δ(E+ZPVE)	ΔE	ΔH	Δ(E+ZPVE)	ΔE	ΔH
1	-2.410	-1.649	-2.147	-2.211	-1.480	-1.949	-2.703	-1.980	-2.448	-2.032	-1.302	-1.758	-2.372	-1.571	-2.104
2	-4.889	-3.232	-4.226	-4.457	-2.865	-3.796	-5.555	-3.965	-4.898	-4.117	-2.518	-3.433	-4.840	-3.193	-4.174
3	-6.108	-4.164	-5.495	-5.490	-3.636	-4.880	-7.406	-5.553	-6.822	-5.063	-3.183	-4.418	-6.178	-4.190	-5.564
4	-7.337	-4.774	-6.239	-6.684	-4.210	-5.595	-8.422	-5.895	-7.321	-6.175	-3.709	-5.057	-7.475	-4.754	-6.346
5	-9.881	-6.585	-8.893	-8.572	-5.462	-7.592	-13.001	-10.070	-12.121	-8.035	-4.810	-6.983	-10.494	-7.122	-9.506
6	-9.839	-6.335	-8.299	-8.953	-5.576	-7.418	-11.311	-7.850	-9.752	-8.286	-4.913	-6.711	-9.965	-6.338	-8.387
7	-10.818	-6.640	-9.377	-8.980	-5.029	-7.553	-15.198	-11.355	-13.821	-8.510	-4.412	-6.993	-12.649	-8.254	-11.171
8	-12.342	-7.906	-10.341	-11.241	-6.952	-9.252	-14.232	-9.815	-12.211	-10.394	-6.126	-8.351	-12.655	-7.922	-10.587
9	-11.792	-6.473	-9.921	-9.200	-4.140	-7.315	-17.939	-13.144	-16.245	-8.852	-3.628	-6.891	-15.015	-9.552	-13.213
10	-14.857	-9.477	-12.398	-13.531	-8.329	-11.086	-17.148	-11.784	-14.660	-12.518	-7.337	-10.009	-15.204	-9.512	-12.672
11	-12.011	-5.671	-9.968	-8.199	-2.279	-6.162	-20.859	-15.227	-19.013	-8.425	-2.162	-6.256	-17.358	-10.789	-15.384

Reactions	*CAM-B3LYP*			*ωB97X-D*		
	Δ(E+ZPVE)	ΔE	ΔH	ΔE+ZPVE	ΔE	ΔH
1	-2.511	-1.756	-2.250	-2.780	-2.004	-2.520
2	-5.07	-3.428	-4.411	-5.71	-4.036	-5.040
3	-6.39	-4.477	-5.786	-7.19	-5.285	-6.611
4	-7.61	-5.061	-6.525	-8.68	-6.079	-7.591
5	-10.39	-7.180	-9.423	-12.17	-8.937	-11.235
6	-10.20	-6.714	-8.665	-11.68	-8.142	-10.138
7	-11.30	-7.242	-9.888	-14.41	-10.157	-12.964
8	-12.80	-8.379	-10.804	-14.71	-10.225	-12.716
9	-12.29	-7.164	-10.474	-16.64	-11.584	-14.930
10	-15.40	-10.044	-12.954	-17.74	-12.307	-15.283
11	-12.58	-6.520	-10.602	-19.08	-12.909	-17.163

Table S3.3.7. Relative energies (ΔE), including also ZPE correction (ΔE + ZPE) and enthalpies (ΔH) at 298 K for the isodesmic reactions of Scheme 3.3.1, computed with the cc-pVTZ basis set.

Reactions	*B2-PLYP*			*PBE-QIDH*			*PBE-QIDH-D3(BJ)*		
	Δ(E+ZPVE)	ΔE	ΔH	Δ(E+ZPVE)	ΔE	ΔH	Δ(E+ZPVE)	ΔE	ΔH
1	-2.374	-1.613	-2.103	-2.62	-1.82	-2.35	-2.71	-1.909	-2.440
2	-4.855	-3.208	-4.178	-5.40	-3.67	-4.72	-5.62	-3.883	-4.938
3	-6.139	-4.183	-5.509	-6.94	-4.88	-6.31	-7.21	-5.145	-6.577
4	-7.310	-4.759	-6.198	-8.15	-5.47	-7.03	-8.50	-5.829	-7.386
5	-10.372	-6.990	-9.358	-12.07	-8.50	-11.07	-12.61	-9.040	-11.609
6	-9.797	-6.321	-8.230	-10.93	-7.28	-9.35	-11.44	-7.790	-9.862
7	-11.082	-6.896	-9.617	-13.39	-8.96	-11.92	-14.20	-9.781	-12.734
8	-12.295	-7.882	-10.255	-13.73	-9.10	-11.68	-14.38	-9.754	-12.340
9	-11.948	-6.662	-10.026	-15.18	-9.62	-13.28	-16.37	-10.809	-14.466
10	-14.800	-9.445	-12.300	-16.53	-10.91	-14.01	-17.33	-11.719	-14.818
11	-12.435	-6.107	-10.317	-17.12	-10.48	-15.06	-18.75	-12.144	-16.700

Reactions	*B2-PLYP-D3*			*PBE0*			*B3LYP*		
	Δ(E+ZPVE)	ΔE	ΔH	Δ(E+ZPVE)	ΔE	ΔH	Δ(E+ZPVE)	ΔE	ΔH
1	-2.657	-1.918	-2.395	-2.169	-1.422	-1.91	-1.906	-1.185	-1.639
2	-5.479	-3.873	-4.818	-4.43	-2.805	-3.77	-3.86	-2.298	-3.194
3	-7.012	-5.123	-6.410	-5.47	-3.553	-4.87	-4.65	-2.800	-4.025
4	-8.296	-5.804	-7.204	-6.63	-4.127	-5.55	-5.78	-3.352	-4.678
5	-12.149	-8.902	-11.188	-8.94	-5.620	-7.96	-7.23	-4.044	-6.230
6	-11.149	-7.749	-9.608	-8.88	-5.456	-7.35	-7.72	-4.414	-6.169
7	-13.575	-9.527	-12.158	-9.35	-5.218	-7.92	-7.01	-3.052	-5.562
8	-14.018	-9.697	-12.017	-11.13	-6.783	-9 .14	-9.68	-5.472	-7.666
9	-15.443	-10.332	-13.597	-9.64	-4.412	-7.75	-6.30	-1.310	-4.404
10	-16.891	-11.646	-14.425	-13.38	-8.111	-10.93	-11.63	-6.530	-9.156
11	-17.354	-11.308	-15.362	-9.22	-2.975	-7.13	-4.49	-1.527	-2.334

Reactions	*B3LYP-D3*			*PBE0-DH-D3(BJ)*			*PBE0-DH*		
	Δ(E+ZPVE)	ΔE	ΔH	Δ(E+ZPVE)	ΔE	ΔH	Δ(E+ZPVE)	ΔE	ΔH
1	-2.430	-1.746	-2.176	-2.701	-1.924	-2.433	-2.377	-1.594	-2.108
2	-5.00	-3.511	-4.359	-5.59	-3.901	-4.916	-4.88	-3.183	-4.206
3	-6.27	-4.532	-5.685	-7.15	-5.151	-6.523	-6.15	-4.141	-5.527
4	-7.57	-5.250	-6.503	-8.45	-5.846	-7.340	-7.34	-4.719	-6.227
5	-10.53	-7.576	-9.613	-12.42	-8.978	-11.418	-10.41	-6.934	-9.401
6	-10.17	-7.002	-8.662	-11.36	-7.805	-9.792	-9.84	-6.263	-8.269
7	-11.62	-7.920	-10.252	-14.07	-9.808	-12.623	-11.24	-6.922	-9.780
8	-12.79	-8.756	-10.829	-14.27	-9.766	-12.246	-12.34	-7.807	-10.312
9	-12.84	-8.104	-11.012	-16.28	-10.895	-14.376	-12.25	-6.781	-10.326
10	-15.42	-10.513	-12.992	-17.20	-11.728	-14.701	-14.85	-9.350	-12.354
11	-13.60	-7.950	-11.602	-18.54	-12.168	-16.498	-12.96	-6.429	-10.878

Reactions	*M06-L*			*M06*			*ωB97X-D*		
	Δ(E+ZPVE)	ΔE	ΔH	Δ(E+ZPVE)	ΔE	ΔH	Δ(E+ZPVE)	ΔE	ΔH
1	-2.090	-1.350	-1.819	-2.448	-1.780	-2.201	-2.501	-94.559	-2.243
2	-4.391	-2.803	-3.714	-5.19	-3.651	-4.540	-5.22	-98.160	-4.551
3	-5.540	-3.624	-4.920	-6.80	-5.057	-6.240	-6.51	-135.332	-5.916
4	-6.714	-4.192	-5.586	-7.81	-5.465	-6.739	-7.92	-192.046	-6.835
5	-9.717	-6.366	-8.722	-12.37	-9.392	-11.485	-11.14	-194.493	-10.190
6	-9.003	-5.589	-7.427	-10.54	-7.280	-9.017	-10.66	-249.792	-9.125
7	-11.436	-7.180	-9.931	-14.12	-10.398	-12.762	-12.83	-251.210	-11.390
8	-11.360	-6.981	-9.300	-13.20	-9.102	-11.234	-13.41	-307.547	-11.422
9	-13.095	-7.935	-11.248	-16.30	-11.703	-14.597	-14.43	-307.884	-12.640
10	-13.672	-8.376	-11.141	-15.93	-10.920	-13.497	-16.18	-365.300	-13.717
11	-15.056	-8.755	-13.001	-18.75	-13.379	-16.903	-16.21	-364.460	-14.220

Reactions	*TPSSh*			*CAM-B3LYP*			*DSD-PBEP86*		
	Δ(E+ZPVE)	ΔE	ΔH	Δ(E+ZPVE)	ΔE	ΔH	Δ(E+ZPVE)	ΔE	ΔH
1	-1.797	-1.067	-1.515	-2.225	-1.482	-1.959	-2.809	-2.039	-2.538
2	-3.68	-2.085	-2.981	-4.52	-2.908	-3.852	-5.788	-4.121	-5.109
3	-4.46	-2.563	-3.794	-5.62	-3.715	-5.000	-7.531	-5.548	-6.899
4	-5.50	-3.056	-4.356	-6.77	-4.272	-5.674	-8.754	-6.177	-7.632
5	-7.15	-3.837	-6.075	-9.17	-5.894	-8.181	-13.297	-9.868	-12.279
6	-7.37	-4.030	-5.774	-9.05	-5.644	-7.504	-11.768	-8.247	-10 .195
7	-7.14	-3.031	-5.600	-9.48	-5.418	-8.039	-15.036	-10 .805	-13.567
8	-9.23	-5.004	-7.159	-11.34	-7.014	-9.327	-14.783	-10.319	-12.736
9	-6.88	-1.666	-4.862	-9.65	-4.540	-7.762	-17.491	-12.188	-15.593
10	-11.11	-5.976	-8.578	-13.63	-8.385	-11.154	-17.808	-12.393	-15.289
11	-5.91	0.387	-3.647	-9.09	-2.998	-7.020	-20.315	-14.016	-18.255

Table S3.4.1. The binding energies (ΔE, kcal/mol) and errors (Er, kcal/mol) of the dimers in the AAA groups with the DH-SVPD basis set .

Functionals	*PBE-QIDH*		*PBE-QIDHD3(0)*		*PBE-QIDHD3(BJ)*		*PBE0-DH*		*PBE0-DH-D3(BJ)*		*B2-PLYP*		*B2-PLYPD3(0)*		*DSD-PBEP86*		*revDSD-PBEP86D3(BJ)*	
	ΔE	Er	ΔE	Er	ΔE	Er	ΔE	Er	ΔE	Er	ΔE	Er	ΔE	Er	ΔE	Er	ΔE	Er
Butane	-3.07	-0.26	-4.40	-1.58	-3.66	-0.84	-2.21	0.61	-4.80	-1.98	-2.42	0.40	-4.81	-1.99	-3.13	-0.31	-4.80	-1.98
Butene.	-2.32	0.00	-3.35	-1.02	-3.10	-0.78	-1.64	0.69	-3.64	-1.32	-1.67	0.66	-3.61	-1.29	-2.60	-0.28	-3.64	-1.32
Butyne.	-3.32	0.11	-4.34	-0.92	-4.13	-0.71	-2.62	0.81	-4.56	-1.14	-2.60	0.83	-4.41	-0.99	-2.70	0.72	-4.56	-1.14
Ethane	-1.47	-0.09	-2.09	-0.70	-1.85	-0.46	-1.13	0.26	-2.29	-0.90	-1.10	0.28	-2.26	-0.87	-1.34	0.05	-2.29	-0.90
Ethene	-1.22	0.26	-1.71	-0.24	-1.53	-0.05	-0.97	0.51	-1.83	-0.35	-0.83	0.65	-1.83	-0.35	-1.00	0.47	-1.83	-0.35
Ethyne.	-1.68	-0.15	-1.88	-0.36	-1.85	-0.33	-1.56	-0.04	-1.95	-0.42	-1.44	0.09	-1.92	-0.39	-0.55	0.97	-1.95	-0.42
Hexane.	-4.84	-0.33	-6.94	-2.43	-6.39	-1.89	-3.37	1.13	-7.58	-3.07	-3.85	0.66	-7.69	-3.18	-5.12	-0.61	-7.58	-3.07
Methane	-0.59	-0.06	-0.79	-0.26	-0.71	-0.18	-0.50	0.03	-0.87	-0.34	-0.47	0.06	-0.82	-0.29	-0.42	0.11	-0.87	-0.34
Pentane	-3.96	-0.30	-5.66	-2.00	-5.19	-1.53	-2.82	0.84	-6.20	-2.54	-3.19	0.47	-6.27	-2.61	-4.06	-0.40	-6.20	-2.54
Pentene.	-3.37	-0.20	-4.74	-1.57	-4.46	-1.29	-2.36	0.81	-5.09	-1.92	-2.54	0.63	-5.02	-1.85	-3.66	-0.49	-5.09	-1.92
Pentyne	-4.25	0.20	-5.62	-1.17	-5.35	-0.90	-3.21	1.24	-5.91	-1.46	-3.18	1.27	-5.81	-1.36	-3.82	0.63	-5.91	-1.46
Propane	-2.19	-0.18	-3.10	-1.09	-2.80	-0.79	-1.64	0.37	-3.41	-1.40	-1.76	0.25	-3.39	-1.39	-2.10	-0.09	-3.41	-1.40
Propene.	-2.39	-0.18	-3.24	-1.02	-2.98	-0.77	-1.82	0.40	-3.36	-1.15	-1.71	0.50	-3.22	-1.01	-2.07	0.14	-3.36	-1.15
Propyne	-2.60	-0.26	-3.11	-0.76	-3.03	-0.69	-2.30	0.05	-3.23	-0.89	-2.16	0.18	-3.25	-0.91	-1.44	0.91	-3.23	-0.89
MAD		0.18		1.08		0.80		0.56		1.11		0.49		1.32		0.44		1.35

Functionals	*M06-L*		*TPSSh*		*B3LYP*		*PBE0*		*M06*		*CAM-B3LYP*		*ωB97X-D*		*B3LYP-D3*	
	ΔE	Er	ΔE	Er	ΔE	Er	ΔE	Er	ΔE	Er	ΔE	Er	ΔE	Er	ΔE	Er
Butane	-4.86	-2.04	-1.22	1.60	-1.26	1.56	-1.75	1.07	-4.91	-2.09	-1.82	0.99	-5.79	-2.97	-5.19	-2.37
Butene.	-3.24	-0.92	-0.80	1.52	-0.68	1.64	-1.25	1.08	-3.42	-1.10	-1.17	1.15	-4.13	-1.81	-3.87	-1.55
Butyne.	-4.13	-0.70	-1.66	1.76	-1.46	1.96	-2.26	1.16	-4.60	-1.17	-2.12	1.31	-5.05	-1.63	-4.63	-1.21
Ethane	-2.03	-0.64	-0.73	0.66	-0.61	0.78	-0.92	0.47	-1.92	-0.53	-0.93	0.45	-2.63	-1.24	-2.45	-1.06
Ethene	-1.44	0.04	-0.51	0.96	-0.45	1.03	-0.82	0.65	-1.55	-0.07	-0.74	0.74	-2.04	-0.56	-2.04	-0.56
Ethyne.	-1.19	0.34	-1.22	0.31	-1.13	0.40	-1.52	0.01	-1.44	0.09	-1.44	0.08	-1.88	-0.35	-2.03	-0.50
Hexane.	-7.95	-3.44	-1.73	2.77	-1.48	3.02	-2.56	1.95	-8.09	-3.58	-2.71	1.79	-9.25	-4.74	-8.23	-3.72
Methane	-0.61	-0.08	-0.35	0.18	-0.38	0.15	-0.47	0.06	-0.52	0.01	-0.44	0.09	-0.88	-0.35	-0.88	-0.35
Pentane	-6.31	-2.65	-1.50	2.17	-1.28	2.38	-2.20	1.46	-6.46	-2.80	-2.32	1.34	-7.50	-3.84	-6.75	-3.09
Pentene.	-4.69	-1.52	-1.24	1.93	-1.00	2.17	-1.81	1.36	-4.93	-1.76	-1.79	1.38	-5.72	-2.55	-5.29	-2.12
Pentyne	-5.52	-1.07	-1.81	2.64	-1.55	2.90	-2.59	1.86	-5.87	-1.42	-2.40	2.05	-6.54	-2.09	-5.97	-1.52
Propane	-3.38	-1.37	-0.94	1.07	-0.96	1.05	-1.35	0.66	-3.31	-1.30	-1.39	0.62	-4.02	-2.01	-3.71	-1.70
Propene.	-2.94	-0.73	-0.93	1.28	-0.71	1.50	-1.46	0.76	-3.06	-0.85	-1.35	0.87	-3.72	-1.51	-3.39	-1.18
Propyne	-2.54	-0.20	-1.60	0.74	-1.46	0.88	-2.15	0.20	-2.80	-0.46	-1.98	0.36	-3.41	-1.06	-3.46	-1.11
MAD		1.12		1.40		1.53		0.91		1.23		0.95		1.91		1.57

Table S3.4.2. The binding energies(ΔE, kcal/mol) and errors (Er, kcal/mol) of the dimers in the AAA groups obtained with the cc-pVTZ basis set.

Functionals	*PBE-QIDH*		*PBE-QIDH-D3(0)*		*PBE-QIDH-D3(BJ)*		*PBE0-DH*		*PBE0-DH-D3(BJ)*		*B2P-LYP*		*B2-PLYP-D3(0)*		*DSD-PBEP86*		*revDSD-PBEP86*	
	ΔE	Er	ΔE	Er	ΔE	Er	ΔE	Er	ΔE	Er	ΔE	Er	ΔE	Er	ΔE	Er	ΔE	Er
Butane	-1.28	1.54	-2.56	0.26	-2.18	0.64	-0.70	2.12	-2.73	0.09	-0.55	2.27	-2.78	0.04	-2.98	-0.16	-2.61	0.21
Butene.	-1.34	0.99	-2.28	0.04	-2.03	0.30	-0.90	1.43	-2.47	-0.15	-0.74	1.58	-2.45	-0.13	-2.65	-0.33	-2.33	0.00
Butyne.	-2.33	1.09	-3.32	0.10	-3.12	0.31	-1.78	1.64	-3.62	-0.19	-1.59	1.84	-3.41	0.02	-3.76	-0.33	-3.40	0.02
Ethane	-0.57	0.82	-1.17	0.22	-0.93	0.46	-0.35	1.04	-1.26	0.13	-0.20	1.19	-1.25	0.14	-1.37	0.02	-1.21	0.18
Ethene	-0.97	0.51	-1.47	0.01	-1.29	0.19	-0.74	0.74	-1.61	-0.14	-0.58	0.90	-1.62	-0.14	-1.71	-0.23	-1.54	-0.07
Ethyne.	-1.41	0.12	-1.61	-0.09	-1.59	-0.06	-1.33	0.20	-1.79	-0.27	-1.15	0.37	-1.65	-0.12	-1.73	-0.21	-1.64	-0.11
Hexane.	-2.11	2.40	-4.16	0.35	-3.63	0.88	-1.11	3.39	-4.42	0.09	-0.96	3.55	-4.60	-0.09	-4.82	-0.32	-4.22	0.28
Methane	-0.20	0.33	-0.38	0.15	-0.30	0.23	-0.15	0.38	2.77	3.30	-0.05	0.48	-0.37	0.16	-0.54	-0.01	-0.38	0.15
Pentane	-1.67	1.99	-3.34	0.32	-2.87	0.79	-0.90	2.76	-3.55	0.11	-0.74	2.92	-3.68	-0.01	-3.88	-0.22	-3.40	0.26
Pentene.	-1.81	1.36	-3.09	0.08	-2.83	0.34	-1.17	2.00	-3.33	-0.16	-1.02	2.15	-3.23	-0.06	-3.56	-0.39	-3.15	0.02
Pentyne	-2.90	1.55	-4.25	0.20	-3.98	0.47	-2.11	2.34	-4.59	-0.14	-1.90	2.55	-4.47	-0.02	-4.85	-0.40	-4.37	0.08
Propane	-0.84	1.16	-1.75	0.25	-1.46	0.55	-0.48	1.52	-1.89	0.12	-0.34	1.67	-1.89	0.11	-2.06	-0.05	-1.80	0.20
Propene.	-1.45	0.77	-2.27	-0.06	-2.02	0.19	-1.05	1.16	-2.43	-0.21	-0.84	1.37	-2.25	-0.04	-2.53	-0.31	-2.27	-0.06
Propyne	-1.93	0.41	-2.44	-0.10	-2.36	-0.01	-1.70	0.65	-2.72	-0.38	-1.45	0.90	-2.53	-0.19	-2.65	-0.31	-2.44	-0.10
MAD		1.07		0.16		0.39		1.53		0.39		1.69		0.09		0.23		0.13

Functionals	*M06-L*		*TPSSh*		*B3LYP*		*PBE0*		*M06*		*CAM-B3LYP*		*ωB97X-D*		*B3LYP-D3*	
	ΔE	Er	ΔE	Er	ΔE	Er	ΔE	Er	ΔE	Er	ΔE	Er	ΔE	Er	ΔE	Er
Butane	-3.19	-0.37	-0.23	2.59	0.00	2.82	-0.42	2.40	-3.42	-0.60	-0.19	2.63	-4.15	-1.33	-3.37	-0.55
Butene.	-2.46	-0.14	-0.48	1.84	-0.18	2.15	-0.76	1.56	-2.66	-0.34	-0.48	1.84	-3.19	-0.86	-2.82	-0.50
Butyne.	-3.36	0.07	-1.05	2.38	-0.76	2.66	-1.50	1.92	-3.45	-0.03	-1.23	2.19	-4.13	-0.70	-3.81	-0.38
Ethane	-1.16	0.23	-0.15	1.24	0.00	1.39	-0.25	1.13	-1.08	0.31	-0.16	1.22	-1.15	0.24	-1.04	0.35
Ethene	-1.26	0.22	-0.35	1.12	-0.07	1.40	-0.62	0.86	-1.32	0.16	-0.51	0.97	-1.82	-0.35	-1.81	-0.34
Ethyne.	-1.07	0.45	-1.03	0.50	-0.88	0.65	-1.30	0.22	-1.12	0.40	-1.14	0.39	-1.57	-0.05	-1.79	-0.26
Hexane.	-5.39	-0.89	-0.29	4.22	0.00	4.50	-0.60	3.90	-5.88	-1.38	0.00	4.50	-5.79	-1.28	-5.47	-0.97
Methane	-0.41	0.12	-0.10	0.43	0.00	0.53	-0.15	0.38	-0.15	0.38	0.00	0.53	-0.57	-0.04	-0.57	-0.04
Pentane	-4.40	-0.74	-0.26	3.41	-0.01	3.66	-0.52	3.14	-4.57	-0.91	0.00	3.66	-4.46	-0.80	-4.42	-0.76
Pentene.	-3.45	-0.28	-0.49	2.68	-0.15	3.02	-0.84	2.33	-3.67	-0.50	-0.51	2.66	-4.39	-1.22	-3.87	-0.70
Pentyne	-4.51	-0.06	-1.12	3.33	-0.50	3.95	-1.68	2.77	-4.58	-0.13	-1.11	3.34	-4.98	-0.53	-4.39	0.06
Propane	-2.16	-0.15	-0.16	1.85	0.00	2.01	-0.31	1.70	-2.19	-0.18	0.00	2.01	-2.78	-0.77	-2.23	-0.23
Propene.	-2.18	0.03	-0.49	1.72	-0.18	2.03	-0.83	1.38	-2.22	-0.01	-0.60	1.62	-2.88	-0.66	-2.58	-0.37
Propyne	-1.82	0.53	-1.11	1.24	-0.87	1.48	-1.59	0.75	-1.92	0.43	-1.33	1.02	-2.76	-0.41	-2.82	-0.47
MAD		0.30		2.04		2.30		1.75		0.41		2.04		0.66		0.43

Table S3.4.3. The binding energies(ΔE, kcal/mol) and errors (Er, kcal/mol) of the dimers in the ADIM6 datasets obtained with the DH-SVPD basis set.

		Functionals	*PBE-QIDH*	*PBE-QIDH-*	*PBE-QIDH-*	*PBE0-DH*	*PBE0DH-*	*B2-PLYP*	*B2PLYP-*	*DSD-*	*revDSD-*
		ΔE	Er	ΔE	Er	ΔE	Er	ΔE	Er	ΔE	Er	ΔE	Er	ΔE	Er	ΔE	Er	ΔE	Er
AM2.	*AD2.*	1.47	0.13	2.05	0.71	1.83	0.49	1.12	-0.22	2.05	0.71	1.10	-0.24	2.12	0.78	1.00	1.00	2.22	0.88
AM3.	*AD3.*	2.11	0.12	2.98	0.99	2.72	0.73	1.51	-0.48	2.97	0.98	1.58	-0.41	3.19	1.20	1.45	1.45	3.24	1.25
AM4.	*AD4.*	3.05	0.16	4.35	1.46	3.97	1.08	2.13	-0.76	4.29	1.40	2.33	-0.56	4.65	1.76	2.12	2.12	4.72	1.83
AM5.	*AD5.*	3.96	0.18	5.64	1.86	5.18	1.40	2.72	-1.06	5.54	1.76	3.05	-0.73	6.12	2.34	2.74	2.74	6.13	2.35
AM6.	*AD6.*	4.77	0.17	6.87	2.27	6.32	1.72	3.21	-1.39	6.75	2.15	3.64	-0.96	7.47	2.87	3.35	3.35	7.46	2.86
AM7.	*AD7.*	5.69	0.14	8.12	2.57	7.55	2.00	3.73	-1.82	7.97	2.42	4.24	-1.31	8.95	3.40	3.87	3.87	8.82	3.27
MAD			0.15		1.64		1.24		0.95		1.57		0.70		2.06		2.42		2.07

Functionals		*M06-L*		*TPSSh*		*B3LYP*		*PBE0*		*M06*		*CAM-B3LYP*		*ωB97X-D*		*B3LYP-D3*	
		ΔE	Er	ΔE	Er	ΔE	Er	ΔE	Er	ΔE	Er	ΔE	Er	ΔE	Er	ΔE	Er
AM2.	*AD2.*	1.91	0.57	0.34	-1.00	0.25	-1.09	0.89	-0.45	1.68	0.34	0.93	-0.41	2.36	1.02	0.97	0.97
AM3.	*AD3.*	3.12	1.13	0.30	-1.69	0.26	-1.73	1.09	-0.90	2.99	1.00	1.18	-0.81	3.58	1.59	1.46	1.46
AM4.	*AD4.*	4.54	1.65	0.36	-2.53	0.41	-2.48	1.50	-1.39	4.39	1.50	1.67	-1.22	5.29	2.40	2.16	2.16
AM5.	*AD5.*	5.91	2.13	0.37	-3.41	0.52	-3.26	1.86	-1.92	5.87	2.09	2.14	-1.64	6.91	3.13	2.83	2.83
AM6.	*AD6.*	7.38	2.78	0.30	-4.30	0.50	-4.10	2.11	-2.49	7.32	2.72	2.45	-2.15	8.57	3.97	3.46	3.46
AM7.	*AD7.*	8.98	3.43	0.10	-5.45	0.35	-5.20	2.29	-3.26	9.05	3.50	2.73	-2.82	10.26	4.71	3.96	3.96
MAD			1.95		3.07		2.98		1.74		1.86		1.51		2.80		2.47

Table S3.4.4. The binding energies(ΔE, kcal/mol) and errors (Er, kcal/mol) of the dimers in the ADIM6 datasets obtained with the Def2-QZVP basis set.

Functionals		*PBE-QIDH*		*PBE-QIDH-*		*PBE-QIDH-D3(BJ)*		*PBE0-DH*		*PBE0-DH-D3(BJ)*		*B2-PLYP*		*B2-PLYP-D3(0)*		*DSD-PBEP86*		*revDSD-PBEP86D3(BJ)*	
		ΔE	Er	ΔE	Er	ΔE	Er	ΔE	Er	ΔE	Er	ΔE	Er	ΔE	Er	ΔE	Er	ΔE	Er
AM2.	*AD2.*	0.60	-0.74	1.19	-0.15	0.96	-0.38	0.31	-1.03	1.24	-0.10	0.16	-1.18	1.19	-0.15	0.02	0.02	1.21	-0.13
AM3.	*AD3.*	0.88	-1.11	1.75	-0.24	1.49	-0.50	0.39	-1.60	1.85	-0.14	0.26	-1.73	1.87	-0.12	0.04	0.04	1.79	-0.20
AM4.	*AD4.*	1.27	-1.62	2.57	-0.32	2.19	-0.70	0.52	-2.37	2.68	-0.21	0.38	-2.51	2.70	-0.19	0.07	0.07	2.61	-0.28
AM5.	*AD5.*	1.68	-2.10	3.36	-0.42	2.90	-0.88	0.68	-3.10	3.50	-0.28	0.53	-3.25	3.61	-0.17	0.09	0.09	3.41	-0.37
AM6.	*AD6.*	2.04	-2.56	4.14	-0.46	3.59	-1.01	0.77	-3.83	4.31	-0.29	0.63	-3.97	4.45	-0.15	0.17	0.17	4.20	-0.40
AM7.	*AD7.*	2.52	-3.03	4.95	-0.60	4.39	-1.16	0.94	-4.61	5.18	-0.37	0.76	-4.79	5.48	-0.07	0.17	0.17	5.02	-0.53
MAD			1.86		0.37		0.77		2.76		0.23		2.90		0.14		0.09		0.32

Functionals		*M06-L*		*TPSSh*		*B3LYP*		*PBE0*		*M06*		*CAM-B3LYP*		*ωB97X-D*		*B3LYP-D3*	
		ΔE	Er	ΔE	Er	ΔE	Er	ΔE	Er	ΔE	Er	ΔE	Er	ΔE	Er	ΔE	Er
AM2.	*AD2.*	1.24	-0.10	-0.38	-1.72	-0.63	-1.97	0.12	-1.22	0.97	-0.37	0.03	-1.31	1.57	0.23	0.09	0.09
AM3.	*AD3.*	2.03	0.04	-0.67	-2.66	-0.96	-2.95	0.04	-1.95	1.92	-0.07	-0.07	-2.06	2.48	0.49	0.25	0.25
AM4.	*AD4.*	3.03	0.14	-1.05	-3.94	-1.39	-4.28	-0.03	-2.92	2.87	-0.02	-0.15	-3.04	3.70	0.81	0.36	0.36
AM5.	*AD5.*	3.93	0.15	-1.42	-5.20	-1.79	-5.57	-0.07	-3.85	3.90	0.12	-0.20	-3.98	4.91	1.13	0.52	0.52
AM6.	*AD6.*	4.98	0.38	-1.83	-6.43	-2.27	-6.87	-0.20	-4.80	4.96	0.36	-0.34	-4.94	6.17	1.57	0.69	0.69
AM7.	*AD7.*	6.05	0.50	-2.30	-7.85	-2.77	-8.32	-0.30	-5.85	6.27	0.72	-0.43	-5.98	7.52	1.97	0.84	0.84
MAD			0.22		4.64		4.99		3.43		0.28		3.55		1.03		0.46

Table S3.4.5. Reaction energies (ΔE, kcal/mol) and errors (Er, kcal/mol) for the IDHC5 set obtained with the DH-SVPD basis set.

Functionals	*PBE-QIDH*		*PBE-QIDHD3(0)*		*PBE-QIDHD3(BJ)*		*PBE0-DH*		*PBE0-DH-D3(BJ)*		*B2-PLYP*		*B2-PLYPD3(0)*		*DSD-PBEP86*		*revDSD-PBEP86D3(BJ)*	
	ΔE	Er	ΔE	Er	ΔE	Er	ΔE	Er	ΔE	Er	ΔE	Er	ΔE	Er	ΔE	Er	ΔE	Er
Reaction1	-0.97	0.36	-1.96	-0.63	-1.82	-0.49	1.66	3.00	-1.68	-0.35	1.77	3.10	-1.31	0.02	-3.24	-1.91	-2.43	-1.10
Reaction2	9.94	0.94	8.00	-1.00	8.09	-0.91	14.63	5.64	8.17	-0.83	14.88	5.89	9.18	0.19	5.57	-3.43	7.04	-1.96
Reaction3	3.52	0.09	2.59	-0.85	2.63	-0.81	4.48	1.04	2.43	-1.00	4.40	0.96	2.38	-1.06	2.00	-1.43	2.31	-1.12
Reaction4	1.97	1.64	-1.92	-2.25	-1.19	-1.52	5.80	5.47	-2.27	-2.60	5.97	5.64	-2.91	-3.23	-3.80	-4.13	-2.41	-2.74
Reaction5	-0.62	2.32	-6.31	-3.38	-5.29	-2.35	5.02	7.96	-6.71	-3.77	5.21	8.15	-7.81	-4.87	-8.99	-6.05	-6.95	-4.02
MAD		1.07		1.62		1.21		4.62		1.71		4.75		1.87		3.39		2.19

Functional	*M06-L*		*TPSSh*		*B3LYP*		*PBE0*		*M06*		*CAM-B3LYP*		*ωB97XD*		*B3LYP-D3*	
	ΔE	Er	ΔE	Er	ΔE	Er	ΔE	Er	ΔE	Er	ΔE	Er	ΔE	Er	ΔE	Er
Reaction1	-1.34	0.00	5.36	6.69	6.50	7.83	3.87	5.20	-3.53	-2.20	3.67	5.01	-0.50	0.84	0.84	2.17
Reaction2	7.58	-1.42	20.06	11.06	23.42	14.42	18.48	9.48	6.23	-2.76	18.59	9.59	9.92	0.92	12.86	3.86
Reaction3	1.31	-2.13	5.77	2.33	6.20	2.77	5.21	1.78	1.62	-1.82	5.22	1.79	1.52	-1.92	2.42	-1.02
Reaction4	-6.65	-6.98	12.74	12.41	13.51	13.18	9.13	8.80	-5.60	-5.93	8.53	8.20	-6.88	-7.20	-3.12	-3.45
Reaction5	-12.63	-9.69	15.40	18.34	16.29	19.23	9.98	12.92	-11.29	-8.35	9.04	11.98	-13.35	-10.41	-8.07	-5.13
MAD		4.04		10.17		11.49		7.64		4.21		7.31		4.26		3.13

Table S3.4.6. Reaction energies (ΔE, kcal/mol) and errors (Er, kcal/mol) for the IDHC5 set obtained with the Def2-TZVPP basis set.

Functionals	*PBE-QIDH*		*PBE-QIDH-D3(0)*		*PBE-QIDH-D3(BJ)*		*PBE0-DH*		*PBE0-DH-D3(BJ)*		*B2-PLYP*		*B2-PLYPD3(0)*		*DSD-PBEP86*		*revDSD-PBEP86-D3(BJ)*	
	ΔE	Er	ΔE	Er	ΔE	Er	ΔE	Er	ΔE	Er	ΔE	Er	ΔE	Er	ΔE	Er	ΔE	Er
Reaction1	0.16	1.50	-0.82	0.51	-0.69	0.64	2.69	4.02	-0.65	0.68	3.20	4.53	0.26	1.59	-1.87	-0.54	-1.01	0.32
Reaction2	11.86	2.86	9.92	0.92	10.01	1.02	16.41	7.41	9.94	0.95	17.40	8.40	11.91	2.91	7.91	-1.08	9.48	0.48
Reaction3	4.59	1.16	3.66	0.22	3.70	0.27	5.48	2.05	3.43	0.00	5.60	2.17	3.58	0.14	3.20	-0.23	3.54	0.11
Reaction4	5.51	5.18	1.62	1.29	2.34	2.02	9.18	8.85	1.11	0.78	9.90	9.57	1.22	0.89	0.21	-0.12	1.72	1.39
Reaction5	4.62	7.56	-1.08	1.86	-0.05	2.89	9.96	12.90	-1.77	1.17	11.00	13.94	-1.75	1.19	-3.03	-0.09	-0.82	2.12
MAD		3.65		0.96		1.37		7.05		0.72		7.72		1.34		0.41		0.88

Functional	*M06-L*		*TPSSh*		*B3LYP*		*PBE0*		*M06*		*CAM-B3LYP*		*ωB97X-D*		*B3LYP-D3*	
	ΔE	Er	ΔE	Er	ΔE	Er	ΔE	Er	ΔE	Er	ΔE	Er	ΔE	Er	ΔE	Er
Reaction1	-0.12	1.21	6.23	7.56	8.39	9.72	4.95	6.28	-2.37	-1.04	5.39	6.73	0.91	2.24	2.73	4.06
Reaction2	9.65	0.66	21.46	12.46	26.74	17.74	20.34	11.35	8.47	-0.53	21.67	12.67	12.35	3.35	16.18	7.18
Reaction3	2.54	-0.90	6.64	3.21	7.40	3.96	6.19	2.76	2.54	-0.89	6.41	2.97	2.51	-0.92	3.61	0.18
Reaction4	-2.62	-2.94	15.84	15.51	17.80	17.47	12.48	12.15	-2.68	-3.01	12.70	12.37	-3.37	-3.70	1.16	0.84
Reaction5	-6.75	-3.81	19.90	22.84	22.48	25.41	14.81	17.75	-7.16	-4.22	15.05	17.99	-8.30	-5.36	-1.89	1.05
MAD		1.90		12.32		14.86		10.06		1.94		10.55		3.11		2.66

Table S3.4.7. Reaction energies (ΔE, kcal/mol) and errors (Er, kcal/mol) for the PAH5 set obtained with the DH-SVPD basis set.

Functional	*PBE-QIDH*		*PBE-QIDH-D3(0)*		*PBE-QIDH-D3(BJ)*		*PBE0-DH*		*PBE0-DH-D3(BJ)*		*B2-PLYP*		*B2-PLYPD3(0)*		*DSD-PBEP86*		*revDSD-PBEP86-D3(BJ)*	
	ΔE	Er	ΔE	Er	ΔE	Er	ΔE	Er	ΔE	Er	ΔE	Er	ΔE	Er	ΔE	Er	ΔE	Er
Reaction1	6.41	0.41	6.46	0.46	6.50	0.51	6.17	0.17	6.42	0.42	5.59	0.41	5.71	0.29	6.01	0.01	5.84	0.16
Reaction2	0.53	0.02	0.60	0.10	0.67	0.17	0.27	0.23	0.59	0.09	-0.04	0.54	0.08	0.42	0.43	0.08	0.28	0.22
Reaction3	3.61	0.24	3.73	0.36	3.84	0.47	3.11	0.26	3.69	0.32	2.51	0.86	2.73	0.64	3.35	0.02	3.06	0.31
Reaction4	6.11	0.14	6.06	0.08	6.11	0.13	6.23	0.25	6.22	0.25	5.69	0.29	5.50	0.48	5.61	0.36	5.55	0.43
Reaction5	13.56	0.89	13.75	1.08	13.90	1.24	12.80	0.13	13.65	0.99	11.30	1.37	11.65	1.02	12.66	0.01	12.19	0.48
MAD	0.34		0.42		0.50		0.21		0.41		0.69		0.57		0.09		0.32	

Functional	*M06-L*		*TPSSh*		*B3LYP*		*PBE0*		*M06*		*CAM-B3LYP*		*ωB97X-D*		*B3LYP-D3*	
	ΔE	Er	ΔE	Er	ΔE	Er	ΔE	Er	ΔE	Er	ΔE	Er	ΔE	Er	ΔE	Er
Reaction1	5.44	0.56	5.20	0.80	5.10	0.90	5.63	0.37	5.75	0.25	6.29	-0.29	6.68	-0.68	5.33	0.67
Reaction2	0.01	0.49	-0.26	0.77	-0.56	1.07	-0.11	0.61	0.12	0.38	0.35	0.15	0.89	-0.39	-0.30	0.80
Reaction3	2.63	0.74	2.02	1.35	1.51	1.86	2.36	1.01	2.62	0.75	3.06	0.31	3.92	-0.55	1.98	1.39
Reaction4	6.05	-0.08	5.82	0.15	5.79	0.19	6.00	-0.02	5.89	0.09	6.83	-0.85	6.64	-0.66	5.47	0.51
Reaction5	10.97	1.70	10.25	2.42	9.75	2.92	11.27	1.40	11.69	0.98	13.08	-0.41	14.35	-1.69	10.48	2.18
MAD		0.71		1.10		1.38		0.68		0.49		0.40		0.79		1.11

Table S3.4.8. Reaction energies (ΔE, kcal/mol) and errors (Er, kcal/mol) for the PAH5 set obtained with the cc-pVQZ basis set.

Functional	*PBE-QIDH*		*PBE-QIDH-D3(0)*		*PBE-QIDH-D3(BJ)*		*PBE0-DH*		*PBE0-DH-D3(BJ)*		*revDSD-PBEP86-D3(BJ)*	
	ΔE	Er	ΔE	Er	ΔE	Er	ΔE	Er	ΔE	Er	ΔE	Er
Reaction1	6.39	-0.39	6.44	-0.44	6.49	-0.49	6.15	-0.15	6.40	-0.40	5.83	0.17
Reaction2	0.43	0.07	0.51	-0.01	0.57	-0.07	0.17	0.33	6.20	-5.70	0.18	0.32
Reaction3	3.48	-0.11	3.61	-0.24	3.72	-0.35	2.96	0.41	3.54	-0.17	2.95	0.42
Reaction4	6.23	-0.26	6.18	-0.20	6.22	-0.25	6.21	-0.24	6.20	-0.23	5.72	0.25
Reaction5	13.39	-0.72	13.58	-0.91	13.74	-1.07	12.61	0.05	13.47	-0.80	12.03	0.64
MAD		0.31		0.36		0.45		0.24		1.46		0.36

Table S3.4.9. Reaction energies (ΔE, kcal/mol) and errors (Er, kcal/mol) for the Cope set obtained with the DH-SVPD basis set.

	Functionals	*PBE-QIDH*					*PBE-QIDH-D3(0)*					*PBE-QIDH-D3(BJ)*				
		Barrier Heights			Reaction Energies		Barrier Heights			Reaction Energies		Barrier Heights			Reaction Energies	
		ΔE	Er		ΔEr	Er	ΔE	Er		ΔE	Er	ΔE	Er		ΔE	Er
H	TS	16.32	-1.21				TS	16.26	-1.15			TS	16.24	-1.12		
CH3	TS1-2	15.64	1.12	2	-0.28	-0.28	TS1-2	15.59	1.07	2	-0.27	-0.26	TS1-2	15.57	1.05	2	-0.26	-0.26
	TS2-3	15.96	-0.59	3	-1.55	-0.68	TS2-3	15.93	-0.56	3	-1.47	-0.61	TS2-3	15.91	-0.54	3	-1.50	-0.63
	TS3-4	14.53	-0.53	4	-1.26	-0.59	TS3-4	14.56	-0.56	4	-1.16	-0.49	TS3-4	14.51	-0.50	4	-1.19	-0.52
NH3	TS1-2	14.87	0.85	2	-1.08	0.62	TS1-2	14.81	0.78	2	-1.09	0.64	TS1-2	14.81	0.78	2	-1.06	0.61
	TS2-3	11.40	0.11	3	-5.37	1.56	TS2-3	11.37	0.14	3	-5.31	1.50	TS2-3	11.39	0.12	3	-5.34	1.53
	TS3-4	10.54	0.26	4	-4.58	1.22	TS3-4	10.56	0.24	4	-4.49	1.13	TS3-4	10.50	0.30	4	-4.53	1.17
CN	TS1-2	16.45	-1.08	2	-2.88	0.56	TS1-2	16.39	-1.02	2	-2.87	0.55	TS1-2	16.38	-1.01	2	-2.86	0.54
	TS2-3	10.09	-0.25	3	-6.19	1.09	TS2-3	10.07	-0.22	3	-6.13	1.03	TS2-3	10.05	-0.21	3	-6.14	1.04
	TS3-4	11.33	-0.36	4	-5.05	0.88	TS3-4	11.34	-0.36	4	-4.99	0.81	TS3-4	11.31	-0.33	4	-4.98	0.81
OH	TS1-2	17.30	1.47	2	0.86	0.50	TS1-2	17.26	1.42	2	0.85	0.52	TS1-2	17.23	1.40	2	0.87	0.50
	TS2-3	15.25	0.22	3	-1.92	1.11	TS2-3	15.20	0.17	3	-1.89	1.08	TS2-3	15.22	0.19	3	-1.91	1.10
	TS3-4	14.09	0.12	4	-3.94	1.08	TS3-4	14.08	0.11	4	-3.87	1.01	TS3-4	14.03	0.07	4	-3.91	1.05
MAD			0.63			0.85			0.60			0.80			0.59			0.81

	PBE0-DH						*PBE0-DH-D3(BJ)*						*B2-PLYP*					
	Barrier Heights			Reaction Energies			Barrier Heights			Reaction Energies			Barrier Heights			Reaction Energies		
	ΔE	Er		ΔE	Er		ΔE	Er		ΔE	Er		ΔE	Er		ΔE	Er	
TS	17.49	-2.38				TS	17.13	-2.02				TS	12.68	2.43				
TS1-2	16.85	2.33	2	-0.43	-0.42	TS1-2	16.56	2.04	2	-0.29	-0.28	TS1-2	11.99	-2.53	2	-0.38	-0.37	
TS2-3	16.82	-1.45	3	-2.01	-1.14	TS2-3	16.68	-1.31	3	-1.71	-0.84	TS2-3	12.21	3.16	3	-1.70	-0.84	
TS3-4	15.22	-1.21	4	-1.73	-1.06	TS3-4	15.20	-1.20	4	-1.34	-0.68	TS3-4	10.68	3.33	4	-1.47	-0.80	
TS1-2	16.05	2.02	2	-1.21	0.75	TS1-2	15.78	1.75	2	-1.10	0.65	TS1-2	11.32	2.70	2	-1.03	0.57	
TS2-3	11.81	0.29	3	-5.94	2.13	TS2-3	11.86	0.35	3	-5.72	1.91	TS2-3	8.17	3.34	3	-5.38	1.57	
TS3-4	11.11	0.31	4	-5.13	1.77	TS3-4	11.03	0.24	4	-4.84	1.48	TS3-4	6.87	3.93	4	-4.65	1.29	
TS1-2	17.65	-2.28	2	-3.05	0.73	TS1-2	17.37	-2.00	2	-2.94	0.62	TS1-2	12.80	2.57	2	-2.98	0.66	
TS2-3	10.67	-0.83	3	-6.67	1.56	TS2-3	10.59	-0.75	3	-6.41	1.30	TS2-3	6.25	3.60	3	-6.60	1.49	
TS3-4	12.01	-1.04	4	-5.51	1.34	TS3-4	11.95	-0.97	4	-5.18	1.01	TS3-4	7.20	3.78	4	-5.41	1.23	
TS1-2	18.43	2.59	2	0.74	0.62	TS1-2	18.15	2.31	2	0.81	0.56	TS1-2	13.60	2.23	2	0.96	0.40	
TS2-3	15.83	0.80	3	-2.39	1.58	TS2-3	15.78	0.75	3	-2.28	1.47	TS2-3	12.14	2.89	3	-1.65	0.84	
TS3-4	14.76	0.80	4	-4.34	1.48	TS3-4	14.57	0.60	4	-4.17	1.31	TS3-4	10.75	3.21	4	-3.63	0.77	
MAD		1.41			1.22			1.25			1.01			3.05			0.90	

	B2-PLYPD3(0)					*DSD-PBEP86*					*revDSD-PBEP86-D3(BJ)*					
	Barrier Heights			Reaction Energies			Barrier Heights			Reaction Energies			Barrier Heights			Reaction Energies	
	ΔE	Er		ΔE	Er		ΔE	Er		ΔE	Er		ΔE	Er		ΔE	Er
TS	12.39	2.72				TS	14.12	0.99				TS	14.97	0.15			
TS1-2	11.78	-2.74	2	-0.19	-0.18	TS1-2	13.49	-1.03	2	-0.13	-0.12	TS1-2	14.33	-0.19	2	-0.18	-0.17
TS2-3	12.23	3.14	3	-1.30	-0.43	TS2-3	14.08	1.29	3	-1.09	-0.22	TS2-3	14.87	0.50	3	-1.14	-0.28
TS3-4	10.83	3.18	4	-1.01	-0.34	TS3-4	12.80	1.21	4	-0.80	-0.13	TS3-4	13.58	0.43	4	-0.87	-0.21
TS1-2	11.08	-2.95	2	-0.92	-0.46	TS1-2	12.80	-1.23	2	-0.85	-0.39	TS1-2	13.64	-0.39	2	-0.86	-0.40
TS2-3	8.19	-3.33	3	-5.06	-1.25	TS2-3	10.09	-1.43	3	-4.68	-0.87	TS2-3	10.73	-0.78	3	-4.60	-0.79
TS3-4	6.95	-3.85	4	-4.27	-0.91	TS3-4	9.05	-1.75	4	-3.95	-0.59	TS3-4	9.94	-0.85	4	-3.91	-0.56
TS1-2	12.55	2.82	2	-2.90	0.58	TS1-2	14.30	1.07	2	-2.65	0.33	TS1-2	15.14	0.23	2	-2.62	0.30
TS2-3	6.12	3.72	3	-6.44	1.33	TS2-3	8.40	1.44	3	-5.74	0.63	TS2-3	9.18	0.66	3	-5.65	0.54
TS3-4	7.10	3.88	4	-5.20	1.02	TS3-4	9.51	1.47	4	-4.61	0.44	TS3-4	10.39	0.59	4	-4.58	0.41
TS1-2	13.38	-2.45	2	1.00	0.37	TS1-2	15.10	-0.74	2	1.01	0.36	TS1-2	15.88	0.04	2	0.98	0.38
TS2-3	12.11	-2.93	3	-1.38	0.57	TS2-3	13.75	-1.28	3	-1.37	0.56	TS2-3	14.46	-0.57	3	-1.31	0.50
TS3-4	10.79	-3.18	4	-3.29	0.44	TS3-4	12.49	-1.48	4	-3.35	0.50	TS3-4	13.37	-0.60	4	-3.30	0.44
		3.14			0.66			1.26			0.43			0.46			0.41

	Functionals	*M06-L*					*TPSSh*						*B3LYP*				
		Barrier Heights			Reaction Energies			Barrier Heights			Reaction Energies			Barrier Heights			Reaction Energies	
		ΔE	Er		ΔEr	Er		ΔE	Er		ΔE	Er		ΔE	Er		ΔE	Er
H	TS	16.70	-1.59				TS	13.90	1.21				TS	13.58	1.53			
CH3	TS1-2	16.16	1.64	2	-0.52	-0.52	TS1-2	13.28	-1.24	2	-0.76	-0.75	TS1-2	12.92	-1.60	2	-0.64	-0.63
	TS2-3	15.31	0.06	3	-2.57	-1.70	TS2-3	12.67	2.70	3	-2.68	-1.81	TS2-3	12.56	2.81	3	-2.51	-1.64
	TS3-4	13.91	0.10	4	-2.12	-1.46	TS3-4	10.95	3.05	4	-2.39	-1.73	TS3-4	10.73	3.28	4	-2.29	-1.62
NH3	TS1-2	15.60	1.57	2	-0.76	0.31	TS1-2	12.61	1.42	2	-1.28	0.82	TS1-2	12.22	1.81	2	-1.29	0.83
	TS2-3	9.88	1.63	3	-7.04	3.23	TS2-3	8.20	3.32	3	-6.62	2.81	TS2-3	7.96	3.56	3	-6.40	2.59
	TS3-4	9.34	1.46	4	-6.02	2.66	TS3-4	6.88	3.91	4	-5.78	2.43	TS3-4	6.72	4.08	4	-5.63	2.27
CN	TS1-2	16.81	-1.44	2	-3.72	1.40	TS1-2	14.00	1.37	2	-3.56	1.24	TS1-2	13.72	1.65	2	-3.34	1.02
	TS2-3	8.17	1.67	3	-8.43	3.32	TS2-3	6.12	3.72	3	-8.01	2.90	TS2-3	6.13	3.71	3	-7.55	2.44
	TS3-4	9.64	1.34	4	-6.86	2.69	TS3-4	7.17	3.81	4	-6.57	2.39	TS3-4	7.13	3.85	4	-6.28	2.11
OH	TS1-2	17.64	1.81	2	1.02	0.35	TS1-2	14.86	0.98	2	0.70	0.66	TS1-2	14.42	1.41	2	0.77	0.60
	TS2-3	13.82	1.21	3	-3.40	2.59	TS2-3	12.09	2.94	3	-3.06	2.25	TS2-3	12.27	2.76	3	-2.38	1.57
	TS3-4	13.07	0.89	4	-5.22	2.36	TS3-4	10.58	3.38	4	-4.81	1.95	TS3-4	10.89	3.08	4	-4.22	1.36
MAD			1.26			1.88			2.54			1.81			2.70			1.56

	PBE0						*M06*						*CAM-B3LYP*					
	Barrier Heights			Reaction Energies			Barrier Heights			Reaction Energies			Barrier Heights			Reaction Energies		
	ΔE	Er		ΔE	Er		ΔE	Er		ΔE	Er		ΔE	Er		ΔE	Er	
TS	16.28	-1.17				TS	18.26	-3.15				TS	18.57	-3.45				
TS1-2	15.66	1.15	2	-0.57	-0.56	TS1-2	17.74	3.23	2	-0.06	-0.05	TS1-2	17.92	3.41	2	-0.43	-0.43	
TS2-3	15.28	0.09	3	-2.45	-1.58	TS2-3	17.69	-2.32	3	-1.59	-0.72	TS2-3	17.93	-2.56	3	-2.02	-1.16	
TS3-4	13.55	0.46	4	-2.16	-1.50	TS3-4	16.44	-2.43	4	-1.29	-0.63	TS3-4	16.21	-2.21	4	-1.82	-1.15	
TS1-2	14.88	0.85	2	-1.34	0.88	TS1-2	17.01	2.98	2	-0.71	0.25	TS1-2	17.16	3.13	2	-1.14	0.68	
TS2-3	10.16	1.35	3	-6.61	2.80	TS2-3	12.19	0.68	3	-5.58	1.77	TS2-3	12.66	1.14	3	-5.75	1.94	
TS3-4	9.23	1.56	4	-5.76	2.40	TS3-4	12.27	1.47	4	-4.79	1.44	TS3-4	12.29	1.49	4	-5.04	1.68	
TS1-2	16.42	-1.05	2	-3.26	0.94	TS1-2	18.47	-3.10	2	-3.03	0.71	TS1-2	18.76	-3.39	2	-2.77	0.45	
TS2-3	8.96	0.88	3	-7.35	2.24	TS2-3	10.97	-1.13	3	-6.72	1.62	TS2-3	11.93	-2.09	3	-6.24	1.14	
TS3-4	10.13	0.85	4	-6.08	1.90	TS3-4	12.73	-1.75	4	-5.53	1.35	TS3-4	13.31	-2.33	4	-5.26	1.08	
TS1-2	17.19	1.36	2	0.62	0.75	TS1-2	19.19	3.36	2	1.21	0.16	TS1-2	19.42	3.58	2	0.96	0.40	
TS2-3	14.19	0.84	3	-3.00	2.19	TS2-3	16.27	1.24	3	-1.98	1.17	TS2-3	17.22	2.19	3	-1.82	1.01	
TS3-4	12.97	1.00	4	-4.80	1.94	TS3-4	15.95	1.98	4	-3.96	1.10	TS3-4	16.34	2.37	4	-3.71	0.85	
MAD		0.97			1.64			2.22			0.91			2.57			1.00	

	ωB97X-D						*B3LYP-D3*				
	Barrier Heights			Reaction Energies			Barrier Heights			Reaction Energies	
	ΔE	Er		ΔE	Er		ΔE	Er		ΔE	Er
TS	18.26	-3.15				TS	13.06	2.05			
TS1-2	17.67	3.15	2	-0.40	-0.39	TS1-2	12.52	-2.00	2	-0.33	-0.33
TS2-3	17.61	-2.24	3	-1.90	-1.03	TS2-3	12.56	2.81	3	-1.83	-0.96
TS3-4	16.13	-2.13	4	-1.56	-0.89	TS3-4	10.96	3.04	4	-1.47	-0.80
TS1-2	16.87	2.84	2	-1.16	0.70	TS1-2	11.77	2.26	2	-1.12	0.66
TS2-3	12.27	0.76	3	-5.73	1.92	TS2-3	7.96	3.56	3	-5.85	2.04
TS3-4	12.07	1.27	4	-4.93	1.57	TS3-4	6.85	3.95	4	-4.95	1.59
TS1-2	18.42	-3.05	2	-2.87	0.55	TS1-2	13.26	2.11	2	-3.23	0.91
TS2-3	11.59	-1.75	3	-6.29	1.19	TS2-3	5.87	3.97	3	-7.27	2.17
TS3-4	13.05	-2.08	4	-5.22	1.05	TS3-4	6.94	4.03	4	-5.91	1.74
TS1-2	19.08	3.25	2	0.68	0.68	TS1-2	14.03	1.80	2	0.82	0.55
TS2-3	16.19	1.16	3	-2.47	1.66	TS2-3	12.17	2.86	3	-1.93	1.12
TS3-4	15.42	1.45	4	-4.28	1.42	TS3-4	10.92	3.05	4	-3.62	0.76
MAD		2.18			1.09			2.88			1.13

Table S3.4.10. Reaction energies (ΔE, kcal/mol) and errors (Er, kcal/mol) for the Cope set obtained with the Def2-TZVPP basis set.

	Functionals	*PBE-QIDH*					*PBE-QIDH-D3(0)*					*PBE-QIDHD3(BJ)*				
		Barrier Heights			Reaction Energies		Barrier Heights			Reaction Energies		Barrier Heights			Reaction Energies	
		ΔE	Er		ΔEr	Er	ΔE	Er		ΔE	Er	ΔE	Er		ΔE	Er
H	TS	15.70	-0.58				TS	15.63	-0.52			TS	15.61	-0.50		
CH3	TS1-2	15.06	0.54	2	-0.10	-0.10	TS1-2	15.01	0.49	2	-0.09	-0.08	TS1-2	14.99	0.47	2	-0.08	-0.07
	TS2-3	15.50	-0.13	3	-1.44	-0.57	TS2-3	15.47	-0.10	3	-1.37	-0.50	TS2-3	15.45	-0.08	3	-1.39	-0.53
	TS3-4	14.01	-0.01	4	-1.19	-0.52	TS3-4	14.04	-0.04	4	-1.08	-0.41	TS3-4	13.99	0.02	4	-1.12	-0.45
NH3	TS1-2	14.43	0.40	2	-0.76	0.31	TS1-2	14.36	0.34	2	-0.78	0.32	TS1-2	14.36	0.34	2	-0.75	0.29
	TS2-3	11.19	0.32	3	-5.14	1.33	TS2-3	11.17	0.35	3	-5.08	1.27	TS2-3	11.19	0.33	3	-5.11	1.30
	TS3-4	10.10	0.70	4	-4.46	1.10	TS3-4	10.12	0.68	4	-4.37	1.01	TS3-4	10.06	0.74	4	-4.41	1.05
CN	TS1-2	15.89	-0.52	2	-2.66	0.34	TS1-2	15.84	-0.47	2	-2.65	0.33	TS1-2	15.83	-0.46	2	-2.65	0.32
	TS2-3	9.72	0.12	3	-6.02	0.91	TS2-3	9.69	0.15	3	-5.96	0.85	TS2-3	9.68	0.16	3	-5.97	0.86
	TS3-4	10.87	0.10	4	-4.87	0.70	TS3-4	10.88	0.10	4	-4.81	0.63	TS3-4	10.85	0.13	4	-4.80	0.63
OH	TS1-2	16.64	0.81	2	1.21	0.15	TS1-2	16.60	0.76	2	1.20	0.17	TS1-2	16.57	0.74	2	1.22	0.15
	TS2-3	14.85	0.19	3	-1.86	1.05	TS2-3	14.80	0.23	3	-1.83	1.02	TS2-3	14.82	0.21	3	-1.85	1.04
	TS3-4	13.53	0.44	4	-3.93	1.08	TS3-4	13.52	0.45	4	-3.86	1.01	TS3-4	13.47	0.49	4	-3.91	1.05
MAD			0.37			0.68			0.36			0.63			0.36			0.65

		PBE0-DH						*PBE0-DHD3(BJ)*						*B2-PLYP*				
		Barrier Heights			Reaction Energies			Barrier Heights			Reaction Energies			Barrier Heights			Reaction Energies	
		ΔE	Er		ΔE	Er		ΔE	Er		ΔE	Er		ΔE	Er		ΔE	Er
H	TS	16.75	-1.63				TS	16.38	-1.27				TS	12.05	3.07			
CH3	TS1-2	16.13	1.62	2	-0.26	-0.25	TS1-2	15.84	1.33	2	-0.12	-0.12	TS1-2	11.39	-3.13	2	-0.24	-0.23
	TS2-3	16.25	-0.88	3	-1.88	-1.01	TS2-3	16.12	-0.75	3	-1.58	-0.71	TS2-3	11.69	3.68	3	-1.64	-0.78
	TS3-4	14.60	-0.60	4	-1.62	-0.95	TS3-4	14.59	-0.58	4	-1.24	-0.57	TS3-4	10.13	3.88	4	-1.41	-0.74
NH3	TS1-2	15.47	1.44	2	-0.94	0.48	TS1-2	15.19	1.16	2	-0.83	0.37	TS1-2	10.87	3.16	2	-0.71	0.25
	TS2-3	11.46	0.05	3	-5.70	1.89	TS2-3	11.52	0.01	3	-5.48	1.67	TS2-3	7.97	3.54	3	-5.06	1.25
	TS3-4	10.57	0.23	4	-4.98	1.63	TS3-4	10.49	0.31	4	-4.69	1.34	TS3-4	6.54	4.26	4	-4.40	1.05
CN	TS1-2	16.96	-1.59	2	-2.86	0.53	TS1-2	16.69	-1.32	2	-2.74	0.42	TS1-2	12.22	3.15	2	-2.86	0.54
	TS2-3	10.18	-0.33	3	-6.50	1.39	TS2-3	10.09	-0.25	3	-6.23	1.13	TS2-3	5.76	4.08	3	-6.51	1.40
	TS3-4	11.43	-0.46	4	-5.32	1.14	TS3-4	11.37	-0.39	4	-4.99	0.81	TS3-4	6.67	4.31	4	-5.27	1.10
OH	TS1-2	17.64	1.80	2	1.05	0.31	TS1-2	17.36	1.52	2	1.12	0.25	TS1-2	12.93	2.90	2	1.26	0.11
	TS2-3	15.33	0.30	3	-2.27	1.46	TS2-3	15.28	0.25	3	-2.16	1.35	TS2-3	11.69	3.34	3	-1.54	0.73
	TS3-4	14.16	0.19	4	-4.26	1.40	TS3-4	13.96	0.01	4	-4.09	1.23	TS3-4	10.24	3.73	4	-3.57	0.71
MAD			0.86			1.04			0.70			0.83			3.56			0.74

		B2-PLYPD3(0)					*DSD-PBEP86*					*revDSD-PBEP86-D3(BJ)*				
		Barrier Heights			Reaction Energies		Barrier Heights			Reaction Energies		Barrier Heights			Reaction Energies	
		ΔE	Er		ΔE	Er	ΔE	Er		ΔE	Er	ΔE	Er		ΔE	Er
H	TS	11.76	3.35				TS	13.59	1.52			TS	14.45	0.67		
CH3	TS1-2	11.18	-3.34	2	-0.05	-0.04	TS1-2	13.01	-1.51	2	0.05	0.05	TS1-2	13.86	-0.66	2	0.00	0.01
	TS2-3	11.72	3.65	3	-1.24	-0.37	TS2-3	13.70	1.67	3	-1.01	-0.14	TS2-3	14.51	0.86	3	-1.06	-0.19
	TS3-4	10.27	3.73	4	-0.95	-0.28	TS3-4	12.36	1.65	4	-0.73	-0.07	TS3-4	13.15	0.85	4	-0.80	-0.14
NH3	TS1-2	10.63	-3.40	2	-0.60	-0.14	TS1-2	12.46	-1.57	2	-0.49	-0.04	TS1-2	13.32	-0.71	2	-0.50	-0.05
	TS2-3	7.99	-3.52	3	-4.74	-0.93	TS2-3	10.02	-1.50	3	-4.37	-0.56	TS2-3	10.67	-0.84	3	-4.29	-0.48
	TS3-4	6.62	-4.18	4	-4.02	-0.67	TS3-4	8.78	-2.02	4	-3.75	-0.39	TS3-4	9.70	-1.10	4	-3.71	-0.35
CN	TS1-2	11.97	3.40	2	-2.79	0.47	TS1-2	13.83	1.54	2	-2.47	0.15	TS1-2	14.69	0.68	2	-2.45	0.13
	TS2-3	5.63	4.21	3	-6.35	1.25	TS2-3	8.07	1.77	3	-5.60	0.50	TS2-3	8.86	0.98	3	-5.51	0.41
	TS3-4	6.57	4.41	4	-5.06	0.89	TS3-4	9.12	1.86	4	-4.45	0.28	TS3-4	10.01	0.97	4	-4.42	0.25
OH	TS1-2	12.72	-3.12	2	1.29	0.07	TS1-2	14.54	-1.30	2	1.36	0.00	TS1-2	15.33	-0.51	2	1.34	0.03
	TS2-3	11.65	-3.38	3	-1.27	0.46	TS2-3	13.43	-1.60	3	-1.29	0.48	TS2-3	14.16	-0.87	3	-1.22	0.41
	TS3-4	10.27	-3.70	4	-3.23	0.37	TS3-4	12.03	-1.93	4	-3.34	0.49	TS3-4	12.93	-1.04	4	-3.28	0.42
MAD		MAD	3.65			0.50			1.65			0.26			0.83			0.24

	Functionals	*M06-L*					*TPSSh*						*B3LYP*					
		Barrier Heights			Reaction Energies			Barrier Heights			Reaction Energies			Barrier Heights			Reaction Energies	
		ΔE	Er		ΔEr	Er		ΔE	Er		ΔE	Er		ΔE	Er		ΔE	Er
H	TS	16.31	-1.19				TS	13.06	2.05				TS	12.83	2.29			
CH3	TS1-2	15.79	1.28	2	-0.46	-0.46	TS1-2	12.44	-2.07	2	-0.64	-0.63	TS1-2	12.18	-2.34	2	-0.56	-0.55
	TS2-3	14.92	0.45	3	-2.60	-1.74	TS2-3	11.98	3.39	3	-2.57	-1.70	TS2-3	11.90	3.47	3	-2.47	-1.60
	TS3-4	13.50	0.50	4	-2.18	-1.51	TS3-4	10.23	3.77	4	-2.30	-1.63	TS3-4	10.04	3.97	4	-2.23	-1.56
NH3	TS1-2	15.37	1.34	2	-0.59	0.13	TS1-2	11.90	2.13	2	-1.06	0.60	TS1-2	11.62	2.41	2	-1.02	0.57
	TS2-3	9.55	1.97	3	-6.97	3.16	TS2-3	7.75	3.77	3	-6.33	2.52	TS2-3	7.60	3.92	3	-6.05	2.24
	TS3-4	9.00	1.80	4	-6.01	2.65	TS3-4	6.29	4.50	4	-5.58	2.23	TS3-4	6.29	4.50	4	-5.34	1.99
CN	TS1-2	16.42	-1.05	2	-3.61	1.28	TS1-2	13.22	2.15	2	-3.42	1.10	TS1-2	13.00	2.37	2	-3.29	0.97
	TS2-3	7.85	2.00	3	-8.41	3.30	TS2-3	5.49	4.35	3	-7.86	2.75	TS2-3	5.47	4.37	3	-7.50	2.40
	TS3-4	9.17	1.81	4	-6.83	2.66	TS3-4	6.48	4.50	4	-6.38	2.21	TS3-4	6.44	4.54	4	-6.16	1.99
OH	TS1-2	17.15	1.32	2	1.27	0.10	TS1-2	13.97	1.87	2	0.93	0.43	TS1-2	13.63	2.21	2	0.99	0.38
	TS2-3	13.45	1.58	3	-3.44	2.63	TS2-3	11.47	3.56	3	-2.89	2.08	TS2-3	11.69	3.34	3	-2.20	1.39
	TS3-4	12.67	1.30	4	-5.17	2.31	TS3-4	9.93	4.04	4	-4.67	1.81	TS3-4	10.34	3.62	4	-4.05	1.20
MAD			1.35			1.83			3.24			1.64			3.33			1.40

		PBE0						*M06*						*CAM-B3LYP*				
		Barrier Heights			Reaction Energies			Barrier Heights			Reaction Energies			Barrier Heights			Reaction Energies	
		ΔE	Er		ΔE	Er		ΔE	Er		ΔE	Er		ΔE	Er		ΔE	Er
H	TS	15.48	-0.36				TS	17.98	-2.87				TS	17.79	-2.67			
CH3	TS1-2	14.88	0.36	2	-0.42	-0.41	TS1-2	17.53	3.01	2	0.07	0.08	TS1-2	17.16	2.64	2	-0.33	-0.33
	TS2-3	14.65	0.72	3	-2.30	-1.44	TS2-3	17.56	-2.19	3	-1.46	-0.59	TS2-3	17.28	-1.91	3	-1.96	-1.09
	TS3-4	12.89	1.11	4	-2.04	-1.37	TS3-4	16.31	-2.31	4	-1.16	-0.49	TS3-4	15.52	-1.52	4	-1.74	-1.07
NH3	TS1-2	14.22	0.19	2	-1.08	0.63	TS1-2	16.94	2.91	2	-0.43	0.03	TS1-2	16.55	2.52	2	-0.86	0.40
	TS2-3	9.77	1.74	3	-6.32	2.51	TS2-3	11.92	0.41	3	-5.64	1.83	TS2-3	12.28	0.76	3	-5.43	1.62
	TS3-4	8.69	2.10	4	-5.55	2.19	TS3-4	11.92	1.12	4	-4.86	1.50	TS3-4	11.82	1.02	4	-4.78	1.42
CN	TS1-2	15.66	-0.29	2	-3.11	0.79	TS1-2	18.19	-2.82	2	-2.93	0.61	TS1-2	18.02	-2.65	2	-2.72	0.40
	TS2-3	8.37	1.47	3	-7.19	2.09	TS2-3	10.81	-0.96	3	-6.64	1.54	TS2-3	11.26	-1.41	3	-6.20	1.09
	TS3-4	9.48	1.50	4	-5.88	1.71	TS3-4	12.47	-1.50	4	-5.41	1.23	TS3-4	12.60	-1.62	4	-5.13	0.96
OH	TS1-2	16.34	0.51	2	0.88	0.48	TS1-2	18.82	2.99	2	1.47	-0.10	TS1-2	18.58	2.75	2	1.20	0.17
	TS2-3	13.63	1.41	3	-2.82	2.01	TS2-3	15.86	0.83	3	-2.24	1.43	TS2-3	16.63	1.60	3	-1.64	0.83
	TS3-4	12.36	1.60	4	-4.64	1.79	TS3-4	15.45	1.48	4	-4.10	1.24	TS3-4	15.76	1.80	4	-3.57	0.71
MAD			1.03			1.45			1.95			0.89			1.91			0.84

		ωB97X-D						*B3LYP-D3*				
		Barrier Heights			Reaction Energies			Barrier Heights			Reaction Energies	
		ΔE	Er		ΔE	Er		ΔE	Er		ΔE	Er
H	TS	17.49	-2.38				TS	12.31	2.81			
CH3	TS1-2	16.93	2.41	2	-0.26	-0.25	TS1-2	11.78	-2.74	2	-0.25	-0.24
	TS2-3	17.01	-1.64	3	-1.78	-0.91	TS2-3	11.90	3.47	3	-1.79	-0.92
	TS3-4	15.49	-1.48	4	-1.46	-0.79	TS3-4	10.27	3.73	4	-1.41	-0.74
NH3	TS1-2	16.26	2.23	2	-0.90	0.44	TS1-2	11.17	2.86	2	-0.86	0.40
	TS2-3	11.79	0.27	3	-5.52	1.71	TS2-3	7.60	3.92	3	-5.50	1.69
	TS3-4	11.48	0.68	4	-4.79	1.43	TS3-4	6.43	4.37	4	-4.66	1.31
CN	TS1-2	17.70	-2.33	2	-2.75	0.43	TS1-2	12.55	2.83	2	-3.18	0.86
	TS2-3	11.00	-1.15	3	-6.18	1.07	TS2-3	5.22	4.62	3	-7.23	2.12
	TS3-4	12.38	-1.41	4	-5.07	0.89	TS3-4	6.25	4.72	4	-5.79	1.62
OH	TS1-2	18.24	2.41	2	0.94	0.43	TS1-2	13.24	2.60	2	1.04	0.33
	TS2-3	15.58	0.55	3	-2.35	1.54	TS2-3	11.59	3.44	3	-1.75	0.94
	TS3-4	14.79	0.82	4	-4.17	1.31	TS3-4	10.37	3.60	4	-3.45	0.60
MAD			1.52			0.93			3.52			0.98

Table S3.4.11. DLPNO-CCSD(T) reaction energies (kcal/mol) computed with the aug-cc-pVTZ and aug-cc-pVQZ basis sets and extrapolated at complete basis set limit according to a two point extrapolation scheme (alpha = 5.79 and beta = 3.05).

	aug-cc-pVTZ	*aug-cc-pVQZ*	*CBS*
n-*octane→tetramethylbutane*	-2.491	-1.807	-1.331
n-*undecane→hexamethylbutane*	6.419	7.951	8.996
$C_{14}H_{30}$ *(linear)→*$C_{28}H_{20}$ *(folded)*	1.951	2.836	3.434
$C_{22}H_{46}$ *(linear)→*$C_{22}H_{46}$ *(folded)*	-2.407	-0.776	0.328

Supporting materials of Chapter 4

Table S4.1 Definition of the double-hybrid density functionals used herein. The s_6, s_8, a_1 and a_2 parametersenter in the composition of the -D3(BJ) dispersion correction

	a_x	μ $(bohr^{-1})$	a_c (c_{SS}/c_{OS})	s_6	s_8	a_1	a_2	*Ref.*
PBE0-DH	1/2	–	1/8	0.840	0.095	0.000	6.102	Ref[115]
PBE0-DH-D3(BJ)	1/2	–	1/8					Ref[63,115]
RSX-0DH	1/2	0.33	1/8					Ref[161]
RSX-0DH-D3(BJ)	1/2	0.33	1/8	0.858	3.126	-0.235	11.798	Ref[161,168]
B2-PLYP	1/2	–	0.27					Ref[29]
B2-PLYP-D3(BJ)	1/2	–	0.27	0.640	0.914	0.306	5.057	Ref[29,183]
ωB2PLYP	1/2	0.3	0.27					Ref[162]
ωB2PLYP-D3(BJ)	1/2	0.3	0.27	0.691	0.000	1.499	6.257	Ref[162,168]
ωB97X-2	1/2	0.3	(0.53/0.45)					Ref[180]
ωB97X-2-D3(BJ)	1/2	0.3	(0.53/0.45)	0.547	0.000	3.52	7.795	Ref[104,180]
PBE-QIDH	$3^{-1/3}$	–	1/3					Ref[116]
PBE-QIDH-D3(BJ)	$3^{-1/3}$	–	1/3	0.610	0.566	0.114	7.538	Ref[116,191]
RSX-QIDH	$3^{-1/3}$	0.27	1/3					Ref[161,163]
RSX-QIDH-D3(BJ)	$3^{-1/3}$	0.27	1/3	0.820	0.000	0.750	8.178	Ref[161,163,168]
DSD-PBEP86-D3(BJ)	0.69	–	(0.22/0.52)	0.480	0.000	0.000	5.600	Ref[182]
DSD-BLYP-D3(BJ)	0.71	–	(0.40/0.47)	0.570	0.000	0.000	5.400	Ref[182]
B2K-PLYP	0.72	–	0.42					Ref[174]
B2K-PLYP-D3(BJ)	0.72	–	0.42	0.640	0.152	0.000	7.314	Ref[174,179]

Table S4.2 Mean signed and mean absolute deviations (MSD and MAD, respectively, in kcal/mol) overthe 9 subsets of the BH9 barrier height energy database (868 entries) computed with the Def2-QZVPP basis set.

		(i)	*(ii)*	*(iii)*	*(iv)*	*(v)*	*(vi)*	*(vii)*	*(viii)*	*(ix)*	*total*
PBE0-DH	MSD	0.26	0.47	0.77	-0.76	-0.14	0.61	-1.25	2.38	-0.34	0.17
	MAD	1.53	1.95	1.51	1.58	1.84	1.34	1.55	2.72	1.25	1.71
PBE0-DH-D3(BJ)	MSD	-0.26	-1.41	-1.7	-3.39	-4.86	-2.09	-1.91	-0.38	-1.32	-2.05
	MAD	1.98	2.99	1.8	3.39	4.87	2.53	1.91	0.93	2.33	2.86
RSX-0DH	MSD	2.53	6.78	5.13	0.55	6.04	1.61	-1.56	6.22	2.69	4.07
	MAD	3.74	7.42	5.13	1.3	6.82	3.18	1.76	6.22	3.91	4.89
RSX-0DH-D3(BJ)	MSD	2.44	6.46	4.34	-0.11	4.53	0.77	-1.76	5.41	2.49	3.5
	MAD	3.79	7.46	4.34	0.98	5.36	3.04	1.96	5.41	3.92	4.61
B2-PLYP	MSD	-0.77	-3.81	-2.35	-1.28	-3.17	1.14	-0.62	-1.19	-1.91	-2.15
	MAD	1.46	5	2.57	1.91	3.69	2.52	1.19	1.85	2.34	3.15
B2-PLYP-D3(BJ)	MSD	-1.29	-5.69	-4.8	-3.99	-8.01	-1.6	-1.28	-3.94	-2.88	-4.4
	MAD	1.53	5.72	4.8	3.99	8.1	2.06	1.31	3.94	3	4.49
ωB2-PLYP	MSD	1.41	1.91	0.57	-1.41	0.92	1.12	-1.44	0.97	0.63	0.77
	MAD	1.69	2.23	1	1.6	1.41	1.52	1.69	1.74	1.47	1.73
ωB2-PLYP-D3(BJ)	MSD	1.4	1.87	0.45	-1.51	0.62	1.02	-1.48	0.83	0.6	0.68
	MAD	1.69	2.23	0.94	1.69	1.23	1.47	1.73	1.68	1.47	1.72
ωB97X-2	MSD	1.04	-3.95	-1.61	-2.17	-4.46	-0.71	-1.35	-2.01	-1.67	-2.41
	MAD	1.98	3.95	1.77	2.22	4.49	1.35	1.38	2.02	1.67	2.8
ωB97X-2-D3(BJ)	MSD	1.04	-3.95	-1.61	-2.17	-4.47	-0.71	-1.35	-2.02	-1.67	-2.41
	MAD	1.98	3.96	1.77	2.22	4.5	1.36	1.38	2.02	1.67	2.81
PBE-QIDH	MSD	1.4	-0.84	1.35	-0.85	-2.52	0.28	-1.24	1.73	-0.49	-0.39
	MAD	2.04	2.39	1.62	1.31	2.52	1.52	1.28	2.06	1.46	1.93
PBE-QIDH-D3(BJ)	MSD	1.23	-1.46	0.31	-1.9	-4.64	-0.84	-1.5	0.62	-0.83	-1.25
	MAD	2.06	2.88	1.13	1.94	4.64	1.79	1.5	1.06	1.82	2.38
RSX-QIDH	MSD	2.57	2.64	3.51	-0.42	0.89	0.59	-1.61	3.54	1.14	1.64
	MAD	3.34	5.35	3.52	1.06	1.82	2.52	1.71	3.58	3.07	3.32
RSX-QIDH-D3(BJ)	MSD	2.54	2.54	3.25	-0.64	0.3	0.38	-1.69	3.25	1.07	1.45
	MAD	3.35	5.41	3.27	1.11	1.5	2.48	1.79	3.29	3.12	3.28
DSD-PBEP86-D3(BJ)	MSD	1.44	-3.69	-1.35	-2.48	-7.27	-0.98	-1.27	-2.15	-1.95	-2.63
	MAD	2.3	3.7	1.65	2.55	7.29	1.47	1.29	2.15	1.98	3.11
DSD-BLYP-D3(BJ)	MSD	0.83	-5.1	-2.06	-2.71	-7.68	-0.96	-1	-2.73	-2.23	-3.33
	MAD	1.92	5.12	2.19	2.76	7.73	1.36	1.07	2.73	2.27	3.68
B2K-PLYP	MSD	1.36	-2.66	0.54	-0.13	-2.69	1.42	-0.2	0.05	-0.94	-0.9
	MAD	2.08	2.96	1.32	1.32	2.78	1.74	0.62	1.21	1.16	2.08
B2K-PLYP-D3(BJ)	MSD	1.13	-3.52	-0.75	-1.48	-5.28	0.01	-0.53	-1.35	-1.39	-2.02
	MAD	2.02	3.58	1.21	1.69	5.32	0.87	0.74	1.44	1.47	2.53

Table S4.3 Mean signed and mean absolute deviations (MSD and MAD, respectively, in kcal/mol) over the 9 subsets of the BH9 reaction energy database (434 entries) computed with the Def2-QZVPP basis set.

		(i)	*(ii)*	*(iii)*	*(iv)*	*(v)*	*(vi)*	*(vii)*	*(viii)*	*(ix)*	*total*
PBE0-DH	MSD	-2.98	-1.61	-1.51	-0.25	-0.72	0.11	-0.01	-0.51	-1.88	-1.2
	MAD	2.98	3.06	2.33	1.53	1.28	1.24	0.96	1.5	2.22	2.23
PBE0-DH-D3(BJ)	MSD	-3.91	-4.73	-1.27	-0.25	-0.57	-3.15	-0.06	-0.44	-4.25	-2.67
	MAD	3.91	4.98	1.89	1.49	1.15	3.3	0.95	1.49	4.43	3.18
RSX-0DH	MSD	-7.44	-11.34	-0.69	0.02	-0.65	-3.31	-0.09	0.04	-6.97	-5.24
	MAD	7.44	12.05	1.59	1.19	1.85	3.79	0.81	1.45	6.97	6
RSX-0DH-D3(BJ)	MSD	-7.54	-11.81	-0.64	0.01	-0.62	-4.16	-0.09	0.04	-7.36	-5.49
	MAD	7.54	12.51	1.55	1.21	1.83	4.55	0.81	1.54	7.36	6.24
B2-PLYP	MSD	2.48	7.49	-1.04	-0.49	-1.14	3.37	0.37	-0.65	3.75	2.86
	MAD	2.57	7.99	1.9	1.52	1.54	3.82	1.03	1.83	3.75	4.07
B2-PLYP-D3(BJ)	MSD	1.62	4.47	-0.79	-0.5	-0.98	0.11	0.33	-0.63	1.47	1.43
	MAD	1.87	5.06	1.48	1.44	1.4	0.99	1.03	1.77	1.77	2.64
ωB2-PLYP	MSD	-2.1	-2.99	-0.05	-0.27	-1.27	-1.28	0.21	-0.2	-2.58	-1.62
	MAD	2.14	3.27	1.01	1.1	1.71	1.88	0.49	1.05	2.6	2.1
ωB2-PLYP-D3(BJ)	MSD	-2.1	-2.99	-0.05	-0.27	-1.27	-1.28	0.21	-0.2	-2.58	-1.62
	MAD	2.14	3.27	1.01	1.1	1.71	1.88	0.49	1.05	2.6	2.1
ωB97X-2	MSD	-0.34	0.59	0.7	-0.28	-0.17	-0.62	0.24	-0.8	-0.46	0.05
	MAD	2.51	0.91	1.9	1.89	0.62	1.33	0.52	1.47	0.96	1.37
ωB97X-2-D3(BJ)	MSD	-0.34	0.58	0.7	-0.28	-0.17	-0.62	0.24	-0.8	-0.47	0.05
	MAD	2.51	0.91	1.9	1.89	0.62	1.33	0.52	1.47	0.96	1.37
PBE-QIDH	MSD	-3.44	-3.46	-0.06	-0.14	-0.61	-0.98	0	-0.55	-2.77	-1.83
	MAD	3.7	3.79	1.36	1.72	0.9	1.46	0.67	1.19	2.82	2.48
PBE-QIDH-D3(BJ)	MSD	-3.66	-4.4	0.01	-0.15	-0.55	-2.23	-0.01	-0.53	-3.48	-2.29
	MAD	3.86	4.67	1.33	1.74	0.83	2.32	0.67	1.14	3.54	2.89
RSX-QIDH	MSD	-6.11	-9.38	0.35	0.01	-0.62	-3.15	-0.08	-0.24	-6.09	-4.32
	MAD	6.11	9.92	1.37	1.56	1.29	3.33	0.61	1.12	6.09	5.06
RSX-QIDH-D3(BJ)	MSD	-6.14	-9.54	0.37	0.01	-0.61	-3.39	-0.08	-0.23	-6.22	-4.39
	MAD	6.14	10.07	1.37	1.56	1.28	3.56	0.61	1.14	6.22	5.14
DSD-PBEP86-D3(BJ)	MSD	-0.71	-0.39	0.68	-0.21	-0.26	-0.99	0.22	-0.73	-1.2	-0.38
	MAD	2.9	1.09	1.95	2.07	0.62	1.51	0.67	1.47	1.59	1.56
DSD-BLYP-D3(BJ)	MSD	0.13	0.9	0.8	-0.31	-0.88	-0.9	0.23	-0.56	-0.42	0.12
	MAD	2.43	1.48	1.77	2.02	1.08	1.38	0.55	1.52	1.28	1.63
B2K-PLYP	MSD	0.69	3.06	0.56	-0.29	-1.24	1.43	0.23	-0.49	1.34	1.12
	MAD	2.26	3.33	1.77	1.85	1.37	1.71	0.48	1.26	1.44	2.23
B2K-PLYP-D3(BJ)	MSD	0.34	1.72	0.67	-0.3	-1.16	-0.2	0.22	-0.46	0.33	0.47
	MAD	2.27	2.06	1.72	1.83	1.3	0.92	0.48	1.17	1.12	1.72

Table S4.4 Mean signed and mean absolute deviations (MSD and MAD, respectively, in kcal/mol) over the 9 subsets of the BH9 barrier height energy database (868 entries) computed with the DH-SVPD basis set.

		(i)	*(ii)*	*(iii)*	*(iv)*	*(v)*	*(vi)*	*(vii)*	*(viii)*	*(ix)*	*total*
PBE0-DH	MSD	0.53	0.71	-1.21	-2.46	-3.39	-0.64	-1.59	1.46	-0.73	-0.7
	MAD	2.6	3.53	1.72	2.5	3.4	1.71	1.66	1.93	2.6	2.76
PBE0-DH-D3(BJ)	MSD	0.01	-1.17	-3.68	-5.1	-8.12	-3.34	-2.24	-1.3	-1.71	-2.93
	MAD	3.06	5.07	3.7	5.12	8.13	4.12	2.33	2.01	3.76	4.72
RSX-0DH	MSD	2.79	8.65	3.18	-1.18	2.79	0.33	-1.99	5.18	2.29	3.71
	MAD	4.87	11.08	3.27	1.53	3.79	3.96	2.47	5.29	5.03	5.89
RSX-0DH-D3(BJ)	MSD	2.7	8.33	2.39	-1.84	1.27	-0.51	-2.19	4.37	2.09	3.14
	MAD	4.92	11.28	2.54	2.14	2.79	4.6	2.67	4.53	5.2	5.95
B2-PLYP	MSD	-0.56	-3.9	-4.37	-2.94	-6.8	-0.3	-0.88	-2.05	-2.31	-3.18
	MAD	0.91	4.01	4.38	2.98	6.85	1.29	1.1	2.1	2.43	3.35
B2-PLYP-D3(BJ)	MSD	-1.08	-5.77	-6.81	-5.66	-11.64	-3.04	-1.53	-4.8	-3.29	-5.42
	MAD	1.27	5.8	6.81	5.68	11.71	3.41	1.66	4.81	3.38	5.5
ωB2-PLYP	MSD	1.62	1.86	-1.43	-3.09	-2.68	-0.36	-1.78	0.03	0.15	-0.26
	MAD	2.37	4.26	2.02	3.29	2.72	2.71	2.44	2.04	2.89	3.21
ωB2-PLYP-D3(BJ)	MSD	1.61	1.82	-1.55	-3.19	-2.98	-0.45	-1.82	-0.12	0.12	-0.35
	MAD	2.38	4.3	2.12	3.39	3.01	2.8	2.48	2.07	2.92	3.29
ωB97X-2	MSD	1.16	-3.89	-3.96	-3.85	-8.31	-2.22	-1.4	-3.28	-2.1	-3.48
	MAD	2.23	4.25	4.09	3.99	8.33	2.93	1.53	3.35	2.27	4.05
ωB97X-2-D3(BJ)	MSD	1.16	-3.9	-3.97	-3.86	-8.32	-2.23	-1.4	-3.28	-2.1	-3.48
	MAD	2.23	4.25	4.09	3.99	8.34	2.93	1.53	3.35	2.27	4.06
PBE-QIDH	MSD	1.53	-1.51	-1.11	-2.65	-6.19	-1.13	-1.4	0.34	-0.94	-1.7
	MAD	2.79	4.68	1.78	2.74	6.19	2.48	1.63	1.32	2.84	3.53
PBE-QIDH-D3(BJ)	MSD	1.37	-2.12	-2.16	-3.7	-8.32	-2.25	-1.67	-0.77	-1.27	-2.56
	MAD	2.89	5.19	2.49	3.79	8.32	3.47	1.89	1.73	3.19	4.29
RSX-QIDH	MSD	2.71	2.52	1.07	-2.27	-2.76	-0.82	-1.84	2.09	0.68	0.5
	MAD	4.19	7.44	1.92	2.53	2.82	3.82	2.33	2.48	4.45	4.47
RSX-QIDH-D3(BJ)	MSD	2.68	2.42	0.81	-2.49	-3.35	-1.04	-1.92	1.8	0.61	0.31
	MAD	4.21	7.51	1.84	2.74	3.37	4	2.41	2.28	4.52	4.59
DSD-PBEP86-D3(BJ)	MSD	1.47	-3.54	-3.98	-4.31	-11.34	-2.6	-1.38	-3.58	-2.46	-3.77
	MAD	2.55	4.53	4.11	4.5	11.35	3.25	1.6	3.7	2.84	4.64
DSD-BLYP-D3(BJ)	MSD	0.54	-6.66	-6.34	-6.31	-14.88	-4.47	-1.54	-6	-3.4	-6.1
	MAD	2.32	6.77	6.34	6.49	14.94	5.06	2.14	6.08	3.75	6.56
B2K-PLYP	MSD	1.47	-2.82	-1.92	-1.87	-6.56	-0.11	-0.32	-1.24	-1.4	-2.06
	MAD	2.27	3.01	2.29	2.25	6.57	1.3	1.13	1.72	1.68	2.76
B2K-PLYP-D3(BJ)	MSD	1.24	-3.68	-3.22	-3.22	-9.14	-1.52	-0.65	-2.64	-1.85	-3.18
	MAD	2.24	3.88	3.39	3.52	9.17	2.43	1.48	2.97	2.2	3.8

Table S4.5. Mean signed and mean absolute deviations (MSD and MAD, respectively, in kcal/mol) overthe 9 subsets of the BH9 reaction energy database (434 entries) computed with the DH-SVPD basis set.

		(i)	*(ii)*	*(iii)*	*(iv)*	*(v)*	*(vi)*	*(vii)*	*(viii)*	*(ix)*	*total*
PBE0-DH	MSD	-5.2	-6.14	-0.04	-0.16	-0.83	-2.41	-0.06	0.17	-4.86	-3.11
	MAD	5.2	6.57	2.67	1.52	1.5	2.46	0.87	1.88	4.95	3.91
PBE0-DH-D3(BJ)	MSD	-6.12	-9.26	0.2	-0.17	-0.68	-5.67	-0.11	0.25	-7.23	-4.58
	MAD	6.12	9.62	2.37	1.61	1.34	5.69	0.87	2.27	7.29	5.38
RSX-0DH	MSD	-9.72	-19.3	0.87	0.13	-0.78	-5.9	-0.18	0.63	-10.01	-8.26
	MAD	9.72	20.16	2.54	1.41	2.09	5.94	0.55	3.35	10.01	9.42
RSX-0DH-D3(BJ)	MSD	-9.82	-19.78	0.92	0.12	-0.74	-6.75	-0.18	0.64	-10.4	-8.52
	MAD	9.82	20.62	2.5	1.43	2.07	6.78	0.55	3.44	10.4	9.67
B2-PLYP	MSD	0.36	3.31	0.45	-0.42	-1.39	0.69	0.34	0.25	0.69	1.04
	MAD	1.2	4.04	2.06	1.62	1.73	1.14	0.98	1.65	1.73	2.36
B2-PLYP-D3(BJ)	MSD	-0.5	0.29	0.7	-0.43	-1.22	-2.56	0.3	0.26	-1.59	-0.38
	MAD	1.28	2.04	1.82	1.66	1.62	2.75	0.94	2.08	2.54	1.89
ωB2-PLYP	MSD	-4.32	-7.29	1.5	-0.17	-1.52	-4	0.16	0.61	-5.73	-3.48
	MAD	4.32	7.6	2.15	1.54	2.04	4.2	0.53	3.02	5.73	4.38
ωB2-PLYP-D3(BJ)	MSD	-4.33	-7.35	1.51	-0.17	-1.52	-4.12	0.16	0.62	-5.79	-3.52
	MAD	4.33	7.67	2.15	1.54	2.04	4.32	0.53	3.04	5.79	4.42
ωB97X-2	MSD	-2.14	-2.88	2.26	-0.19	-0.29	-3.27	0.29	0.12	-3.18	-1.46
	MAD	3.54	3.69	2.92	2.28	0.68	3.58	0.57	1.78	3.35	2.88
ωB97X-2-D3(BJ)	MSD	-2.14	-2.88	2.26	-0.19	-0.29	-3.27	0.29	0.12	-3.18	-1.46
	MAD	3.54	3.69	2.92	2.28	0.68	3.59	0.57	1.78	3.35	2.88
PBE-QIDH	MSD	-5.39	-7.46	1.5	-0.04	-0.7	-3.57	0.01	0.17	-5.54	-3.52
	MAD	5.41	7.85	2.51	1.94	1.09	3.62	0.49	1.97	5.55	4.49
PBE-QIDH-D3(BJ)	MSD	-5.61	-8.39	1.57	-0.06	-0.63	-4.82	0.01	0.19	-6.25	-3.98
	MAD	5.63	8.76	2.49	1.96	1.03	4.91	0.49	2.1	6.26	4.96
RSX-QIDH	MSD	-8.12	-13.47	1.96	0.11	-0.71	-5.76	-0.09	0.43	-8.9	-6.04
	MAD	8.12	14.11	2.62	1.89	1.5	5.87	0.44	2.89	8.9	7.25
RSX-QIDH-D3(BJ)	MSD	-8.15	-13.62	1.97	0.11	-0.7	-6	-0.09	0.44	-9.03	-6.12
	MAD	8.15	14.26	2.63	1.89	1.5	6.13	0.44	2.92	9.03	7.33
DSD-PBEP86-D3(BJ)	MSD	-2.6	-4.31	2.2	-0.12	-0.36	-3.67	0.26	0.11	-4.01	-2.05
	MAD	4	5.32	2.97	2.5	0.76	3.96	0.75	1.86	4.29	3.6
DSD-BLYP-D3(BJ)	MSD	-2.44	-5.34	2.52	-0.23	-0.95	-5.93	0.23	0.37	-4.95	-2.64
	MAD	3.71	5.57	3.09	2.54	1.31	6.31	0.69	2.58	5.34	4
B2K-PLYP	MSD	-1.22	-0.93	2.11	-0.21	-1.43	-1.23	0.26	0.34	-1.48	-0.58
	MAD	2.87	1.75	2.88	2.27	1.63	1.84	0.64	1.78	1.86	2.04
B2K-PLYP-D3(BJ)	MSD	-1.56	-2.26	2.22	-0.22	-1.34	-2.86	0.24	0.36	-2.49	-1.23
	MAD	3.09	2.59	2.9	2.28	1.58	3.14	0.63	1.96	2.85	2.51

Supporting materials of Chapter 5

Table S5.1. Example input for Orca code, reporting the optimized DH-SVPD basis set for C, O, N and H atoms

```
! RKS TightSCF PBE-QIDH RIJCOSX AutoAux DEFGRID3
%method
  UseFinalGrid False
  end
%mp2
  RI true
  end
*xyz 0 1
  AT  x.xxxxxx y.yyyyyy z.zzzzzz
end
%basis
  NewGTO 1
  S   3
    1   13.010701000           0.19682158000e-01
    2    1.9622572000          0.13796524000
    3    0.44453796000          0.47831935000
  S   1
    1  0.4617867850E+00    0.1000000000E+01
  P   1
    1    0.80000000000          1.0000000
  P   1
    1  0.7913402419E-01    0.1000000000E+01
  end
  NewGTO 6
  S   5
    1 1238.4016938            0.54568832082e-02
    2  186.29004992           0.40638409211e-01
    3   42.251176346          0.18025593888
    4   11.676557932          0.46315121755
    5    3.5930506482          0.44087173314
  S   1
    1    0.40245147363          1.0000000
  S   1
    1    0.13090182668          1.0000000
  S   1
    1    0.67053540256e-01           1.0000000
  P   3
    1    9.4680970621          0.38387871728e-01
    2    2.0103545142          0.21117025112
    3    0.54771004707          0.51328172114
  P   1
    1  0.1508036550E+00    0.1000000000E+01
  D   1
    1    0.80000000000          1.0000000
  D   1
    1  0.3229294790E+00    0.1000000000E+01
  end
  NewGTO 7
  S   5
    1 1712.8415853           -0.53934125305e-02
    2  257.64812677           -0.40221581118e-01
    3   58.458245853          -0.17931144990
    4   16.198367905          -0.46376317823
    5    5.0052600809          -0.44171422662
  S   1
    1    0.58731856571          1.0000000
  S   1
    1    0.18764592253          1.0000000
  S   1
    1    0.96171241529e-01           1.0000000
```

```
 P   3
   1   13.571470233           -0.40072398852e-01
   2    2.9257372874          -0.21807045028
   3    0.79927750754          -0.51294466049
 P   1
   1  0.1918861474E+00    0.1000000000E+01
 D   1
   1    1.0000000000           1.0000000
 D   1
   1  0.3095443259E+00    0.1000000000E+01
 end
 NewGTO 8
 S   5
   1 2266.1767785           -0.53431809926e-02
   2  340.87010191          -0.39890039230e-01
   3   77.363135167          -0.17853911985
   4   21.479644940          -0.46427684959
   5    6.6589433124          -0.44309745172
 S   1
   1    0.80975975668          1.0000000
 S   1
   1    0.25530772234          1.0000000
 S   1
   1    0.76572453250e-01            1.0000000
 P   3
   1   17.721504317           0.43394573193e-01
   2    3.8635505440          0.23094120765
   3    1.0480920883          0.51375311064
 P   1
   1    0.27641544411          1.0000000
 P   1
   1  0.9892123211E-01    0.1000000000E+01
 D   1
   1    1.2000000000           1.0000000
 D   1
   1  0.2373752428E+00    0.1000000000E+01
 end
end
```

Table S5.2. Mean Absolute Errors (MAE, kcal/mol) for the interaction energies of the S66 set, computed with the PBE-QIDH/SVPDH model and different settings for the PT2 contribution. The terms loose, normal and tight define the set of parameters used in the DLPNO approximation.

Hydrogen Bonding	*NORI*	*RIJCOX*	*Tight*	*Normal*	*Loose*
01_Water-Water	-5.53	-5.547	-5.547	-5.545	-5.541
02_Water-MeOH	-6.28	-6.297	-6.291	-6.288	-6.281
03_Water-MeNH2	-7.894	-7.917	-7.914	-7.911	-7.898
04_Water-Peptide	-8.751	-8.768	-8.777	-8.766	-8.747
05_MeOH-MeOH	-6.403	-6.415	-6.412	-6.406	-6.392
06_MeOH-MeNH2	-8.451	-8.467	-8.464	-8.457	-8.436
07_MeOH-Peptide	-8.933	-8.946	-8.937	-8.922	-8.884
08_MeOH-Water	-5.556	-5.573	-5.571	-5.569	-5.56
09_MeNH2-MeOH	-3.332	-3.339	-3.336	-3.331	-3.309
10_MeNH2-MeNH2	-4.608	-4.623	-4.619	-4.613	-4.58
11_MeNH2-Peptide	-5.687	-5.697	-5.684	-5.664	-5.614
12_MeNH2-Water	-8.255	-8.279	-8.277	-8.274	-8.264
13_Peptide-MeOH	-6.706	-6.725	-6.718	-6.697	-6.661
14_Peptide-MeNH2	-8.273	-8.299	-8.299	-8.274	-8.238
15_Peptide-Peptide	-9.174	-9.194	-9.2	-9.164	-9.073
16_Peptide-Water	-5.498	-5.522	-5.526	-5.515	-5.488
17_Uracil-Uracil_BP	-18.224	-18.264	-18.248	-18.222	-18.082
18_Water-Pyridine	-7.699	-7.713	-7.707	-7.7	-7.674
19_MeOH-Pyridine	-8.213	-8.221	-8.213	-8.201	-8.167
20_AcOH-AcOH	-21.116	-21.137	-21.169	-21.153	-21.103
21_AcNH2-AcNH2	-17.227	-17.254	-17.261	-17.245	-17.2
22_AcOH-Uracil	-21.027	-21.059	-21.077	-21.056	-20.978
23_AcNH2-Uracil	-20.407	-20.442	-20.446	-20.426	-20.357
MAD	0.674	0.694	0.694	0.681	0.643
pi-stacking					
24_Benzene-Benzene_pi-pi	-2.513	-2.521	-2.504	-2.466	-2.185
25_Pyridine-Pyridine_pi-pi	-3.941	-3.946	-3.941	-3.904	-3.649
26_Uracil-Uracil_pi-pi	-10.701	-10.714	-10.675	-10.618	-10.218
27_Benzene-Pyridine_pi-pi	-3.326	-3.332	-3.32	-3.284	-3.008
28_Benzene-Uracil_pi-pi	-5.653	-5.666	-5.638	-5.591	-5.237
29_Pyridine-Uracil_pi-pi	-7.063	-7.071	-7.039	-6.993	-6.671
30_Benzene-Ethene	-1.191	-1.194	-1.188	-1.176	-1.058
31_Uracil-Ethene	-3.327	-3.331	-3.32	-3.302	-3.128
32_Uracil-Ethyne	-3.648	-3.65	-3.642	-3.629	-3.479
33_Pyridine-Ethene	-1.722	-1.724	-1.72	-1.71	-1.609
MAD	0.174	0.173	0.174	0.177	0.292
London					
34_Pentane-Pentane	-3.899	-3.89	-3.835	-3.738	-3.612
35_Neopentane-Pentane	-2.973	-2.969	-2.937	-2.883	-2.733

36_Neopentane-Neopentane	-2.449	-2.437	-2.418	-2.408	-2.232
37_Cyclopentane-Neopentane	-2.692	-2.682	-2.666	-2.633	-2.449
38_Cyclopentane-Cyclopentane	-2.82	-2.826	-2.815	-2.765	-2.57
39_Benzene-Cyclopentane	-3.633	-3.642	-3.625	-3.574	-3.386
40_Benzene-Neopentane	-3.314	-3.32	-3.306	-3.266	-3.131
41_Uracil-Pentane	-5.17	-5.169	-5.14	-5.056	-4.782
42_Uracil-Cyclopentane	-4.199	-4.204	-4.188	-4.13	-3.855
43_Uracil-Neopentane	-3.813	-3.815	-3.796	-3.758	-3.507
44_Ethene-Pentane	-1.89	-1.889	-1.871	-1.838	-1.784
45_Ethyne-Pentane	-1.65	-1.648	-1.633	-1.614	-1.524
46_Peptide-Pentane	-4.223	-4.219	-4.187	-4.119	-3.966
MAD	0.192	0.19	0.181	0.185	0.241
Mixed					
47_Benzene-Benzene_TS	-2.905	-2.922	-2.906	-2.878	-2.768
48_Pyridine-Pyridine_TS	-3.855	-3.866	-3.853	-3.832	-3.724
49_Benzene-Pyridine_TS	-3.444	-3.463	-3.449	-3.425	-3.334
50_Benzene-Ethyne_CH-pi	-3.166	-3.184	-3.177	-3.158	-3.116
51_Ethyne-Ethyne_TS	-1.664	-1.665	-1.663	-1.645	-1.637
52_Benzene-AcOH_OH-pi	-5.132	-5.165	-5.158	-5.144	-5.073
53_Benzene-AcNH2_NH-pi	-4.496	-4.513	-4.499	-4.485	-4.388
54_Benzene-Water_OH-pi	-3.693	-3.717	-3.714	-3.709	-3.662
55_Benzene-MeOH_OH-pi	-4.498	-4.527	-4.52	-4.505	-4.433
56_Benzene-MeNH2_NH-pi	-3.396	-3.418	-3.408	-3.395	-3.313
57_Benzene-Peptide_NH-pi	-5.676	-5.704	-5.705	-5.664	-5.533
58_Pyridine-Pyridine_CH-N	-4.475	-4.48	-4.479	-4.468	-4.409
59_Ethyne-Water_CH-O	-3.197	-3.204	-3.202	-3.198	-3.19
60_Ethyne-AcOH_OH-pi	-5.12	-5.127	-5.124	-5.117	-5.095
61_Pentane-AcOH	-2.828	-2.827	-2.807	-2.773	-2.671
62_Pentane-AcNH2	-3.437	-3.436	-3.416	-3.375	-3.273
63_Benzene-AcOH	-3.92	-3.93	-3.917	-3.894	-3.771
64_Peptide-Ethene	-2.997	-3.002	-2.997	-2.977	-2.914
65_Pyridine-Ethyne	-4.504	-4.507	-4.494	-4.484	-4.451
66_MeNH2-Pyridine	-4.398	-4.406	-4.398	-4.378	-4.278
MAD	0.225	0.239	0.234	0.226	0.197
Total_MAD	0.367	0.378	0.375	0.369	0.375

Table S5.3. Mean Absolute Errors (MAE, kcal/mol) for the interaction energies of the L7 set, computed with the PBE-QIDH/SVPDH model and different settings for the PT2 contribution. The terms loose, normal and tight define the set of parameters used in the DLPNO approximation.

	Loose	*Normal*	*NORI*	*RIJCOX*	*Tight*	*Ref*
01_octadecane	-10.685	-11.006	-11.892	-11.877	-11.439	-11.64
02_guanine	-1.887	-2.465	-0.985	-2.724	-2.649	-1.68
03_GCbasepairstack	-14.101	-15.335	-16.057	-15.963	-15.713	-13.21
04_phenylalanineresidues	-27.228	-27.857	-28.543	-28.488	-28.176	-22.81
05_circumcoroneneadenine	-15.283	-16.873	-18.005	-17.862	-17.483	-17.98
06_circumcoroneneGCbasepair	-25.544	-28.761	-30.694	-30.468	-29.758	-29.86
07_coronene	-16.59	-19.436	-20.74	-20.642	-20.257	-24.81
MAD	3.1	2.31	2.065	2.087	2.027	

Table S5.4. Mean Absolute Errors (MAE, kcal/mol) for the interaction energies of the CiM13 set, computed with the PBE-QIDH/SVPDH model and different settings for the PT2 contribution. The terms loose, normal and tight define the set of parameters used in the DLPNO approximation.

	RIJCOX	*Tight*	*Normal*	*Loose*	*Ref*
1.capsule	-70.623	-69.659	-69.122	-68.176	-70.11
2.Cyc-Pep-2	-73.632	-70.39	-68.632	-65.989	-63.61
3.Ethanol-H-ZSM5	-44.62	-43.859	-43.451	-42.825	-36.55
4.ALA-BN	-20.101	-19.699	-19.133	-18.431	-17.83
5.gramicidin	-43.474	-41.352	-40.448	-39.437	-40.13
6.helix-rod		-78.021	-75.338	-71.656	-78.8
7.DNA		-404.004	-399.903	-392.962	-416.08
8.Protein-Ligand		-31.433	-30.082	-28.068	-35.7
a.UDPy	-43.974	-43.648	-43.272	-42.738	-43.8
b.ben-ZSM5	-15.576	-15.056	-14.505	-13.546	-12.35
c.dendrimer	-16.24	-15.749	-15.172	-14.197	-27.93
d.Cyc-Pep	-80.189	-78.957	-77.934	-76.716	-76.23
e.AB3-Peptide	-74.084	-72.312	-70.744	-68.466	-73.53
MAD	3.371	4.134	4.594	5.486	

Supporting materials of Chapter 6

Table S6.1. Optimized exponents of the extended DH-SVPD basis set. These exponents replace the corresponding exponents of the original Def2-SVPD basis set, which are also reported for comparison. All other exponents are kept as in the original basis set.

atom	*function*	*Def2-SVPD*	*DH-SVPD*	*Function*	*Def2-SVPD*	*DH-SVPD*
H	s	0.1219496200	0.4617867850	p	0.11704099050	0.0791340242
O	p	0.0690022764	0.1002414005	d	0.17992024323	0.2980692020
C	p	0.1526861380	0.1508036550	d	0.11713185140	0.3229294790
N	p	0.2195434803	0.1918861474	d	0.16697708112	0.3095443259
F	p	0.0833721480	0.0854206753	d	0.22301361948	0.3931878448
Cl	p	0.0500462711	0.0362164934	d	0.12284803390	0.1415660314
Br	p	0.0396368418	0.0396207960	d	0.096543342393	0.0965970655
I	p	0.0297955070	0.0343088335	d	0.077987255180	0.0794553835

Table S6.2. Example input for Gaussian codes.

```
%CHK=01_methane-F2.chk
%MEM=100GB
%Nprocs=32
#P PBEQIDH/gen INT=ultrafine SCF=tight

01_methane-F2

0 1
 C   -0.099779142  -0.049213106  -0.049809806
 H   -0.812383509   0.769437899  -0.053814782
 H   -0.386626161  -0.773928179   0.705768112
 H    0.890551861   0.333663823   0.175221084
 H   -0.089826477  -0.524172039  -1.025860985
 F   -1.055049793  -3.072557852  -0.601705876
 F   -1.471602008  -4.387243371  -0.835378773

-H    0
s   3   1.00
     13.010701000          0.19682158000e-01                Standard Def2-SVPD exponents and coefficient for H atom
      1.9622572000         0.13796524000
      0.44453796000        0.47831935000
s   1   1.00
    0.4617867850E+00    0.1000000000E+01                   DH-SVPD optimized exponents for H atom
p   1   1.00
      0.80000000000        1.0000000                        Standard Def2-SVPD exponents and coefficient for H atom
p   1   1.00
    0.7913402419E-01    0.1000000000E+01
****                                                       DH-SVPD optimized exponents for H atom
-C    0
s   5   1.00
    1238.4016938          0.54568832082e-02
     186.29004992         0.40638409211e-01
      42.251176346        0.18025593888
      11.676557932        0.46315121755
       3.5930506482       0.44087173314
s   1   1.00
      0.40245147363        1.0000000
s   1   1.00
      0.13090182668        1.0000000
s   1   1.00
      0.67053540256e-01          1.0000000
p   3   1.00
      9.4680970621         0.38387871728e-01                Standard Def2-SVPD exponents and coefficient for C atom
      2.0103545142         0.21117025112
      0.54771004707        0.51328172114
p   1   1.00                                               DH-SVPD optimized exponents for C atom
    0.1508036550E+00    0.1000000000E+01
d   1   1.00
      0.80000000000        1.0000000                        Standard Def2-SVPD exponents and coefficient for C atom
d   1   1.00
    0.3229294790E+00    0.1000000000E+01
****                                                       DH-SVPD optimized exponents for C atom
F    0
S   5   1.00
    2894.8325990          -0.53408255515D-02
     435.41939120         -0.39904258866D-01
      98.843328866        -0.17912768038
      27.485198001        -0.46758090825
       8.5405498171       -0.44653131020
S   1   1.00
      1.0654578038         1.0000000
S   1   1.00
      0.33247346748        1.0000000
S   1   1.00
      0.98097752264D-01    1.0000000
P   3   1.00
     22.696633924          -0.45212874436D-01
      4.9872339257         -0.23754317067                   Standard Def2-SVPD exponents and coefficient for F atom
      1.3491613954         -0.51287353587
P   1   1.00
      0.34829881977        1.0000000
P   1   1.00
      0.08542067525771294    1.0000000                     DH-SVPD optimized exponents for F atom
D   1   1.00
      1.4000000            1.0000000                       Standard Def2-SVPD exponents and coefficient for F atom
D   1   1.00
      0.3931878448448497     1.0000000                     DH-SVPD optimized exponents for F atom
****
```

Table S6.3. The interaction energies errors (Er, kcal/mol) and Mean Absolute Energies (MAD) of the reactions 1, 5, 7, 9, 11, 12 include F atom, reactions 2, 6, 8, 10, 22, 40 include Cl atom, reactions 3, 14, 17, 20, 23, 27, 29 include Br atom, reactions 04, 24, 28,30 include I atom in the X40 set. (Units: kcal/mol)

	PBE-QIDH			*B2-PLYP*			*DSD-PBEP86*			*B3LYP*			*PBE0-DH*			*revDSD-PBEP86*		
F	DH-SVPD	Def2-TZVPP	Def2-TZVPP+D3	DH-SVPD	Def2-TZVPP	Def2-TZVPP+D3	DH-SVPD	Def2-TZVPP	Def2-TZVPP+D3	DH-SVPD	Def2-TZVPP	Def2-TZVPP+D3	DH-SVPD	Def2-TZVPP	Def2-TZVPP+D3	DH-SVPD	Def2-TZVPP	Def2-TZVPP+D3BJ
01_methane-F2	-0.04	0.21	0.15	0.03	0.23	-0.07	0.24	0.41	0.02	0.32	0.42	-0.16	0.06	0.25	0.06	-0.07	0.19	0.07
05_fluorometh	0.07	0.35	0.18	0.31	0.58	-0.02	0.21	0.44	-0.11	0.81	1.04	-0.22	0.24	0.48	-0.04	-0.02	0.30	-0.03
07_trifluorom	0.06	0.32	0.14	0.24	0.53	-0.03	0.25	0.43	-0.10	0.77	0.98	-0.24	0.25	0.44	-0.04	-0.03	0.27	-0.03
09_fluorometh	-0.09	0.26	0.14	0.02	0.33	-0.14	0.02	0.26	-0.02	0.50	0.68	-0.23	0.11	0.36	0.04	-0.16	0.24	0.04
11_benF3-ben	-0.16	1.56	-0.02	1.70	3.14	-0.15	2.57	3.69	-0.98	5.44	6.52	0.03	1.86	3.31	-0.21	-0.17	1.60	-0.38
12_benF6-ben	-0.58	1.56	-0.17	1.39	3.33	-0.42	2.58	3.99	-1.23	5.74	7.22	-0.13	1.81	3.58	-0.36	-0.59	1.68	-0.55
MAD	0.17	0.71	0.13	0.62	1.36	0.14	0.98	1.54	0.41	2.26	2.81	0.17	0.72	1.40	0.13	0.17	0.71	0.18

	PBE-QIDH			*B2-PLYP*			*DSD-PBEP86*			*B3LYP*			*PBE0-DH*			*revDSD-PBEP86*		
Cl	DH-SVPD	Def2-TZVPP	Def2-TZVPP+D3	DH-SVPD	Def2-TZVPP	Def2-TZVPP+D3	DH-SVPD	Def2-TZVPP	Def2-TZVPP+D3	DH-SVPD	Def2-TZVPP	Def2-TZVPP+D3	DH-SVPD	Def2-TZVPP	Def2-TZVPP+D3	DH-SVPD	Def2-TZVPP	Def2-TZVPP+D3BJ
02_methane-Cl2	-0.26	0.35	0.15	0.07	0.61	-0.14	0.23	0.64	-0.14	0.70	1.10	-0.27	0.01	0.52	-0.07	-0.29	0.34	-0.03
06_chloromethа	0.02	0.50	0.24	0.35	0.84	0.03	0.25	0.63	-0.10	1.02	1.44	-0.20	0.29	0.70	-0.02	-0.09	0.45	0.01
08_trichlorome	-0.26	0.56	0.13	0.14	1.02	-0.02	0.17	0.78	-0.23	1.13	1.82	-0.34	0.19	0.86	-0.15	-0.47	0.49	-0.08
10_chloromethа	-0.25	0.46	0.24	0.05	0.71	0.00	0.05	0.60	-0.01	0.70	1.21	-0.11	0.03	0.64	0.05	-0.31	0.44	0.09
22_benCl-Nm3	-0.89	0.49	-0.04	-0.30	0.88	-0.31	0.27	1.26	-0.41	0.95	1.86	-0.41	-0.28	0.94	-0.25	-0.89	0.48	-0.19
40_methanol-ch	-0.57	0.26	-0.01	-0.08	0.56	-0.40	0.18	0.78	-0.34	0.84	1.23	-0.54	-0.18	0.49	-0.29	-0.49	0.36	-0.15
MAD	0.38	0.44	0.14	0.17	0.77	0.15	0.19	0.78	0.20	0.89	1.44	0.31	0.16	0.69	0.14	0.42	0.43	0.09

	PBE-QIDH			*B2-PLYP*			*DSD-PBEP86*			*B3LYP*			*PBE0DH*			*revDSDPBEP86*		
Br	DH-SVPD	Def2TZVPP	Def2TZVPP+D3	DHSVPD	Def2-TZVPP	Def2-TZVPP+D3	DHSVPD	Def2-TZVPP	Def2-TZVPP+D3	DHSVPD	Def2-TZVPP	Def2-TZVPP+D3	DHSVPD	TZVPP	TZVPP+D3	DH-SVPD	Def2-TZVPP	Def2-TZVPP+D3 BJ
03_methane-Br2.	-0.22	0.29	0.03	0.26	0.67	-0.28	0.32	0.71	-0.28	0.97	1.29	-0.38	0.07	0.52	-0.23	-0.20	0.31	-0.14
14_bromomethane	0.07	0.47	0.21	0.50	0.78	-0.12	0.69	0.92	-0.15	1.25	1.40	-0.14	0.37	0.70	-0.07	0.06	0.46	0.00
17_F3bromometha	-0.24	0.53	0.26	0.29	0.86	0.07	0.29	0.83	-0.02	1.07	1.47	0.10	0.11	0.75	-0.05	-0.11	0.62	0.14
20_benBr-aceton	0.01	0.75	0.28	0.65	1.19	0.02	0.98	1.39	-0.08	1.81	2.11	0.03	0.56	1.13	0.03	0.01	0.76	0.13
23_benBr-Nm3	-0.63	0.79	0.09	0.37	1.54	-0.11	1.18	2.24	-0.35	2.02	2.96	-0.09	0.19	1.45	-0.22	-0.45	0.93	-0.02
27_CH3Br-ben	0.02	0.82	0.09	1.00	1.58	-0.13	1.32	1.80	-0.32	2.65	1.59	-0.57	0.84	1.50	-0.05	-0.01	0.79	-0.05
29_CF3Br-ben	-0.28	0.80	0.00	1.02	1.80	-0.20	1.11	1.80	-0.36	2.92	4.29	1.16	0.67	1.57	-0.23	-0.12	0.94	-0.05
MAD	0.21	0.64	0.14	0.58	1.20	0.13	0.84	1.39	0.22	1.81	2.16	0.35	0.40	1.09	0.13	0.14	0.69	0.08

	PBE-QIDH			*B2-PLYP*			*DSD-PBEP86*			*B3LYP*			*PBE0-DH*			*revDSD-PBEP86*		
I	DH-SVPD	Def2-TZVPP	Def2-TZVPP+D3	DH-SVPD	Def2-TZVPP	Def2-TZVPP+D3	DH-SVPD	Def2-TZVPP	Def2-TZVPP+D3	DH-SVPD	Def2-TZVPP	Def2-TZVPP+D3	DH-SVPD	Def2-TZVPP	Def2-TZVPP+D3	DH-SVPD	Def2-TZVPP	Def2-TZVPP+D3 BJ
04_methane-I2	-0.14	0.23	-0.10	0.40	0.71	-0.30	0.38	0.67	-0.39	1.14	1.43	-0.35	0.18	0.51	-0.37	-0.13	0.26	-0.24
24_benI-Nm3	-1.16	0.41	-0.53	0.37	1.67	-0.40	1.17	2.50	-0.95	2.41	3.54	-0.19	-0.18	1.26	-1.06	-0.71	0.80	-0.51
28_CH3I-ben	-0.12	0.66	-0.31	1.17	1.71	-0.37	1.33	1.90	-0.64	3.05	3.45	-0.32	0.82	1.52	-0.43	-0.06	0.71	-0.31
30_CF3I-ben	-0.46	0.58	-0.48	1.17	1.92	-0.43	1.00	1.85	-0.75	3.27	3.88	-0.32	0.58	1.53	-0.74	-0.16	0.84	-0.38
MAD	0.47	0.47	0.36	0.78	1.50	0.37	0.97	1.73	0.68	2.47	3.07	0.30	0.44	1.20	0.65	0.26	0.65	0.36

	PBE-QIDH			*B2-PLYP*			*DSD-PBEP86*			*B3LYP*			*PBE0-DH*			*revDSD-PBEP86*		
O	DH-SVPD	Def2-TZVPP	Def2-TZVPP+D3	DH-SVPD	Def2-TZVPP	Def2-TZVPP+D3	DH-SVPD	Def2-TZVPP	Def2-TZVPP+D3	DH-SVPD	Def2-TZVPP	Def2-TZVPP+D3	DH-SVPD	Def2-TZVPP	Def2-TZVPP+D3	DH-SVPD	Def2-TZVPP	Def2-TZVPP+D3 BJ
13	-0.22	0.39	0.18	0.05	0.59	-0.15	0.19	0.64	-0.12	0.70	1.06	-0.25	0.03	0.54	-0.06	-0.28	0.35	-0.01
14	0.11	0.47	0.21	0.54	0.78	-0.12	0.68	0.92	-0.15	1.26	1.40	-0.14	0.39	0.70	-0.07	0.11	0.46	0.00
15	-0.13	0.32	-0.03	0.43	0.73	-0.20	0.51	0.84	-0.36	1.23	1.42	-0.18	0.19	0.56	-0.40	-0.06	0.36	-0.19
16	-0.40	0.43	0.20	-0.01	0.64	-0.08	-0.01	0.58	-0.07	0.71	1.15	-0.12	-0.11	0.59	-0.05	-0.35	0.45	0.05
17	-0.19	0.53	0.26	0.32	0.86	0.07	0.28	0.83	-0.02	1.06	1.47	0.10	0.12	0.75	-0.05	-0.06	0.62	0.14
18	-0.55	0.29	-0.06	0.13	0.77	-0.05	-0.13	0.57	-0.30	0.93	1.43	0.01	-0.22	0.52	-0.50	-0.30	0.49	-0.11
19	-0.27	0.55	0.17	0.16	0.85	-0.11	0.44	0.96	-0.16	1.16	1.59	-0.16	0.19	0.84	-0.03	-0.35	0.50	-0.01
20	0.05	0.75	0.28	0.69	1.19	0.02	0.98	1.39	-0.08	1.81	2.11	0.03	0.58	1.13	0.03	0.07	0.76	0.13
21	-0.27	0.50	-0.09	0.54	1.08	-0.14	0.70	1.20	-0.38	1.71	2.06	-0.12	0.28	0.89	-0.43	-0.13	0.61	-0.13
MAD	0.24	0.47	0.16	0.32	0.83	0.10	0.43	0.88	0.18	1.17	1.52	0.12	1.17	1.52	0.12	0.19	0.51	0.09

Table S6.4. The errors (Er, kcal/mol) and MAD in the X_2/CH_4-Bz set. (Units: kcal/mol)

kcal/mol	*PBE-QIDH*			*B2PLYP*			*DSDPBEP86*			*B3LYP*		
	DH-SVPD	Def2-TZVPP	Def2-TZVPP+D3BJ	DH-SVPD	Def2-TZVPP	Def2-TZVPP+D3	DH-SVPD	Def2-TZVPP	Def2-TZVPP+D3	DH-SVPD	Def2-TZVPP	Def2-TZVPP+D3
Cl2Bz												
S1	0.64	-0.59	0.08	-0.39	-1.45	0.36	-1.27	-2.08	0.52	-2.12	-2.87	0.42
S2	1.58	0.35	-0.05	-0.84	-1.79	0.24	-1.30	-1.92	0.46	-2.85	-3.51	0.35
S3	0.19	0.90	-0.04	-0.46	-1.00	0.36	-0.68	-0.94	0.38	-1.70	-2.01	0.55
MAD	0.80	0.61	0.06	0.56	1.42	0.32	1.09	1.65	0.45	2.23	2.80	0.44
Br2Bz												
S1	1.19	0.10	0.95	-0.37	-1.16	0.90	-1.49	-2.28	1.31	-2.23	-2.92	0.79
S2	-0.06	-0.99	0.10	-1.59	-2.15	0.37	-1.84	-2.36	0.54	-3.89	-4.23	0.48
S3	0.17	-0.55	0.10	-0.68	-1.15	0.51	-0.72	-1.12	0.49	-2.08	-2.35	0.70
MAD	0.48	0.55	0.38	0.88	1.49	0.60	1.35	1.92	0.78	2.73	3.17	0.66
CCl4Bz												
S1	0.20	-1.36	-0.13	-1.05	-2.48	0.06	-1.56	-2.61	0.42	-3.68	-4.74	0.21
S2	0.22	-0.76	-0.10	-0.34	-1.27	0.19	-0.61	-1.25	0.27	-1.76	-2.43	0.37
MAD	0.21	1.06	0.11	0.70	1.88	0.13	1.09	1.93	0.35	2.72	3.59	0.29
CBr4Bz												
S1	0.01	-1.30	0.20	-1.70	-2.63	0.39	-2.08	-2.83	0.64	-4.63	-5.21	0.54
S2	0.26	-0.71	0.23	-0.68	-1.47	0.51	-0.91	-1.50	0.60	-2.52	-3.06	0.71
MAD	0.13	1.00	0.22	1.19	2.05	0.45	1.50	2.16	0.62	3.57	4.14	0.62

kcal/mol	*APF*			*PBE0-DH*			*revDSD-PBEP86*			*PBE0*		
	DH-SVPD	Def2-TZVPP	Def2-TZVPP+D3	DH-SVPD	Def2-TZVPP	Def2-TZVPP+D3BJ	DH-SVPD	Def2-TZVPP	Def2-TZVPP+D3BJ	DH-SVPD	Def2-TZVPP	Def2-TZVPP+D3
Cl2Bz												
S1	-1.38	-2.31	0.55	-0.15	-1.28	0.43	0.46	-0.84	0.15	-0.76	-1.70	0.34
S2	-2.27	-2.98	0.52	-0.77	-1.69	0.22	0.19	-0.93	0.13	-1.55	-2.32	0.11
S3	-1.49	-1.80	0.30	-0.50	-0.96	0.20	0.18	-0.48	0.19	-0.93	-1.26	0.32
MAD	1.71	2.37	0.46	0.48	1.31	0.28	0.28	0.75	0.16	1.08	1.76	0.26
Br2Bz												
S1	-1.01	-1.91	1.50	0.23	-0.78	1.40	0.56	-0.45	0.80	-0.40	-1.27	0.97
S2	-2.86	-3.50	0.76	-1.19	-2.01	0.27	-0.28	-1.09	0.14	-2.14	-2.80	0.11
S3	-1.58	-2.03	0.53	-0.48	-1.08	0.31	0.14	-0.51	0.27	-1.01	-1.47	0.40
MAD	1.82	2.48	0.93	0.64	1.29	0.66	0.33	0.68	0.40	1.18	1.85	0.49
CCl4Bz												
S1	-3.04	-4.09	0.66	-1.16	-2.45	0.05	0.30	-1.37	0.00	-2.19	-3.28	0.00
S2	-1.57	-2.17	0.28	-0.49	-1.26	0.08	0.39	-0.70	0.05	-0.99	-1.61	0.24
MAD	2.30	3.13	0.47	0.82	1.85	0.07	0.35	1.03	0.03	1.59	2.45	0.12
CBr4Bz												
S1	-3.55	-4.37	1.00	-1.50	-2.58	0.24	-0.07	-1.35	0.16	-2.71	-3.55	0.18
S2	-2.00	-2.61	0.70	-0.66	-1.45	0.33	0.34	-0.67	0.31	-1.36	-1.98	0.47
MAD	2.77	3.49	0.85	1.08	2.01	0.29	0.21	1.01	0.23	2.04	2.77	0.32

kcal/mol	*M06*			*M06-L*			*TPSSh*			*CAM-B3LYP*		
Cl2Bz	DH-SVPD	Def2-TZVPP	Def2-TZVPP+D	DH-SVPD	Def2-TZVPP	Def2-TZVPP+D3	DH-SVPD	Def2-TZVPP	Def2-TZVPP+D3BJ	DH-SVPD	Def2-TZVPP	Def2-TZVPP+D3
S1	0.75	-0.45	0.08	0.72	0.04	0.26	-1.25	-2.33	0.41	-1.44	-2.25	0.06
S2	0.25	-0.47	0.24	0.01	-0.32	-0.13	-2.34	-3.15	0.15	-1.72	-2.44	0.20
S3	-0.09	-0.46	-0.04	-0.09	-0.38	-0.21	-1.51	-1.87	0.14	-0.95	-1.25	0.49
MAD	0.36	0.46	0.12	0.27	0.25	0.20	1.70	2.45	0.23	1.37	1.98	0.25
Br2Bz												
S1	1.65	-0.07	0.42	1.48	0.12	0.33	-0.78	-1.75	1.47	-1.83	-2.51	0.09
S2	0.27	-0.75	0.00	0.07	-0.59	-0.40	-2.95	-3.67	0.27	-2.70	-3.11	0.13
S3	0.17	-0.51	-0.06	0.02	-0.50	-0.31	-1.61	-2.11	0.30	-1.29	-1.58	0.53
MAD	0.69	0.44	0.16	0.52	0.40	0.35	1.78	2.51	0.68	1.94	2.40	0.25
CCl4Bz												
S1	0.46	-0.59	0.67	0.19	-0.31	0.14	-3.17	-4.24	0.23	-2.37	-3.53	-0.12
S2	-0.12	-0.66	0.05	-0.27	-0.69	-0.34	-1.60	-2.20	0.16	-1.00	-1.72	0.23
MAD	0.29	0.63	0.36	0.23	0.50	0.24	2.39	3.22	0.19	1.69	2.63	0.17
CBr4Bz												
S1	0.49	-0.72	0.58	0.35	-0.49	-0.02	-3.67	-4.54	0.52	-3.32	-3.99	0.01
S2	0.35	-0.43	0.44	0.14	-0.46	-0.07	-2.04	-2.67	0.52	-1.65	-2.24	0.37
MAD	0.42	0.58	0.51	0.25	0.47	0.05	2.86	3.61	0.52	2.48	3.11	0.19

kcal/mol	*ωB97X*		
	DH-SVPD	Def2-TZVPP	Def2-TZVPP+D
Cl2Bz			
S1	0.38	-0.43	-0.89
S2	0.43	-0.16	-0.41
S3	0.23	0.09	-0.25
MAD	0.35	0.23	0.52
Br2Bz			
S1	0.41	-0.50	-0.62
S2	0.24	-0.34	-0.22
S3	0.42	0.09	-0.01
MAD	0.36	0.31	0.28
CCl4Bz			
S1	0.32	-0.65	-0.38
S2	0.28	-0.25	-0.28
MAD	0.30	0.45	0.33
CBr4Bz			
S1	0.16	-0.67	0.01
S2	0.39	-0.22	0.16
MAD	0.27	0.44	0.08

Table S6.5. The errors (Er, kcal/mol) and MAD in the HXB set. (Units: kcal/mol)

	PBE-QIDH			*B2-PLYP*			*DSD-PBEP86*			*B3LYP*		
	DH-SVPD	Def2-TZVPP	Def2-TZVPP+D3BJ	DH-SVPD	Def2-TZVPP	Def2-TZVPP+D3	DH-SVPD	Def2-TZVPP	Def2-TZVPP+D3	DH-SVPD	Def2-TZVPP	Def2-TZVPP+D3
C6F6-C2F2	0.18	-1.29	-0.43	-0.61	-2.27	-0.07	-1.70	-2.86	0.40	-2.94	-4.51	-0.30
C6F6-C2F4	0.48	-1.61	-0.50	-0.88	-2.98	0.11	-2.57	-4.03	0.62	-4.58	-6.20	-0.24
C6F6-C2Cl2	0.42	-1.89	-0.48	-0.93	-3.22	0.12	-2.20	-3.95	0.58	-4.55	-6.48	-0.17
C6F6-C2Cl4	0.92	-2.53	-0.32	-1.56	-4.70	0.57	-3.63	-6.03	1.16	-7.51	-9.88	0.11
C6Cl6-C2F2	0.72	-1.58	-0.20	-0.65	-2.91	0.13	-1.85	-3.64	0.74	-4.18	-6.11	-0.18
C6Cl6-C2F4	1.25	-2.15	-0.41	-0.87	-3.90	0.27	-2.79	-5.18	0.90	-6.19	-8.30	-0.15
C6Cl6-C2Cl2	0.89	-2.45	-0.20	-1.31	-4.37	0.27	-2.61	-5.11	0.87	-6.39	-8.83	-0.05
C6Cl6-C2Cl4	1.46	-3.47	-0.01	-2.11	-6.44	0.59	-4.29	-7.76	1.45	-10.08	-13.27	0.05
MAD	0.79	2.12	0.32	1.11	3.85	0.27	2.70	4.82	0.84	5.80	7.95	0.16

	revDSD-PBEP86			*PBE0-DH*			*APF*			*PBE0*		
	DH-SVPD	Def2-TZVPP	Def2-TZVPP+D3BJ	DH-SVPD	Def2-TZVPP	Def2-TZVPP+D3BJ	DH-SVPD	Def2-TZVPP	Def2-TZVPP+D3	DH-SVPD	Def2-TZVPP	Def2-TZVPP+D3
C6F6-C2F2	0.33	-1.30	0.00	-1.04	-2.33	-0.09	-2.67	-3.95	0.99	-1.83	-3.12	-0.41
C6F6-C2F4	0.59	-1.71	0.07	-1.48	-3.12	-0.12	-4.14	-5.47	1.87	-2.93	-4.29	-0.43
C6F6-C2Cl2	0.59	-1.89	0.00	-1.50	-3.49	-0.16	-4.07	-5.82	0.94	-2.94	-4.73	-0.80
C6F6-C2Cl4	0.93	-2.67	0.24	-2.26	-5.15	0.01	-6.42	-8.77	1.86	-4.79	-7.23	-0.98
C6Cl6-C2F2	0.78	-1.61	0.18	-1.14	-3.14	0.01	-3.65	-5.42	1.24	-2.56	-4.37	-0.58
C6Cl6-C2F4	1.28	-2.24	0.15	-1.58	-4.31	-0.16	-5.40	-7.48	2.19	-3.87	-6.01	-0.79
C6Cl6-C2Cl2	0.89	-2.52	0.06	-1.82	-4.72	-0.01	-5.36	-7.80	0.96	-4.00	-6.53	-1.04
C6Cl6-C2Cl4	1.33	-3.68	0.21	-2.81	-7.01	0.11	-8.28	-11.65	1.74	-6.36	-9.88	-1.56
MAD	0.84	2.20	0.11	1.70	4.16	0.08	5.00	7.05	1.47	3.66	5.77	0.82

	M06			*M06-L*			*TPSSh*			*CAM-B3LYP*		
	DH-SVPD	Def2-TZVPP	Def2-TZVPP+D3	DH-SVPD	Def2-TZVPP	Def2-TZVPP+D3	DH-SVPD	Def2-TZVPP	Def2-TZVPP+D3	DH-SVPD	Def2-TZVPP	Def2-TZVPP+D3
C6F6-C2F2	0.02	-1.46	-0.56	0.70	-0.44	-0.17	-2.75	-4.05	-0.21	-1.62	-3.14	-0.24
C6F6-C2F4	-0.42	-1.70	-0.36	0.69	-0.25	0.15	-4.41	-5.68	-0.60	-2.57	-4.09	0.00
C6F6-C2Cl2	0.20	-1.87	-0.79	0.49	-1.18	-0.87	-4.31	-6.08	-0.32	-2.63	-4.65	-0.33
C6F6-C2Cl4	0.46	-1.43	0.30	0.96	-0.73	-0.27	-6.91	-9.34	-0.48	-4.55	-7.05	-0.24
C6Cl6-C2F2	0.45	-1.53	-0.33	1.31	-0.49	-0.18	-3.82	-5.62	-0.06	-2.36	-4.30	-0.30
C6Cl6-C2F4	0.46	-1.46	0.24	1.51	-0.17	0.27	-5.85	-7.85	-0.63	-3.53	-5.62	-0.12
C6Cl6-C2Cl2	0.38	-2.35	-0.83	0.36	-1.61	-1.23	-5.76	-8.25	0.04	-3.92	-6.61	-0.61
C6Cl6-C2Cl4	1.30	-1.41	0.89	0.64	-1.41	-0.81	-9.02	-12.53	0.02	-6.43	-9.97	-0.88
MAD	0.46	1.65	0.54	0.83	0.79	0.49	5.35	7.43	0.29	3.45	5.68	0.34

	ωB97X		
	DH-SVPD	Def2-TZVPP	Def2-TZVPP+D3
C6F6-C2F2	0.22	-0.91	0.00
C6F6-C2F4	-0.43	-1.50	-0.01
C6F6-C2Cl2	0.13	-1.50	-0.94
C6F6-C2Cl4	-0.40	-2.42	-1.40
C6Cl6-C2F2	0.08	-1.46	-0.52
C6Cl6-C2F4	-0.48	-2.22	-0.80
C6Cl6-C2Cl2	0.22	-2.06	-1.58
C6Cl6-C2Cl4	-0.29	-3.22	-2.32
MAD	0.28	1.91	0.95

Table S6.6. The errors (Er, kcal/mol) and MAD in the first 24 reaction extracted from X40×10 set at DH-SVPD basis set with different Double Hybrid functionals. (Units: kcal/mol)

PBE-QIDH	*R1*	*R2*	*R3*	*R4*	*R5*	*R6*	*R7*	*R8*	*R9*	*R10*	*R11*	*R12*	*R13*	*R14*	*R15*	*R16*	*R17*	*R18*	*R19*	*R20*	*R21*	*R22*	*R23*	*R24*
0.8	-0.09	-0.73	-0.23	-0.05	0.27	0.22	0.19	-0.27	-0.05	-0.21	-1.19	-1.96	-0.38	0.29	-0.41	-0.52	-0.16	-1.21	-0.39	0.16	-0.76	-1.17	-0.87	-1.91
0.85	-0.05	-0.52	-0.21	0.01	0.20	0.16	0.16	-0.21	-0.02	-0.21	-0.88	-1.52	-0.30	0.22	-0.25	-0.52	-0.18	-0.95	-0.34	0.12	-0.53	-1.18	-0.80	-1.78
0.9	-0.03	-0.36	-0.19	0.00	0.14	0.10	0.11	-0.21	-0.03	-0.22	-0.60	-1.14	-0.24	0.18	-0.14	-0.46	-0.17	-0.72	-0.29	0.10	-0.36	-1.08	-0.74	-1.54
0.95	-0.04	-0.27	-0.18	-0.03	0.09	0.05	0.06	-0.24	-0.07	-0.24	-0.38	-0.84	-0.22	0.15	-0.09	-0.39	-0.15	-0.54	-0.25	0.07	-0.25	-0.93	-0.68	-1.30
1	-0.05	-0.23	-0.17	-0.06	0.05	0.00	0.01	-0.27	-0.11	-0.26	-0.24	-0.65	-0.21	0.13	-0.07	-0.33	-0.14	-0.43	-0.25	0.05	-0.20	-0.78	-0.62	-1.09
1.05	-0.06	-0.22	-0.18	-0.09	0.01	-0.04	-0.02	-0.30	-0.15	-0.27	-0.18	-0.56	-0.20	0.10	-0.07	-0.30	-0.14	-0.36	-0.25	0.03	-0.18	-0.66	-0.56	-0.91
1.1	-0.07	-0.21	-0.19	-0.10	-0.01	-0.07	-0.05	-0.31	-0.17	-0.27	-0.16	-0.52	-0.20	0.06	-0.08	-0.28	-0.13	-0.33	-0.26	0.01	-0.18	-0.58	-0.50	-0.77
1.25	-0.07	-0.18	-0.20	-0.11	-0.05	-0.11	-0.08	-0.28	-0.18	-0.21	-0.14	-0.46	-0.17	-0.03	-0.11	-0.23	-0.14	-0.28	-0.21	-0.07	-0.17	-0.44	-0.36	-0.51
1.50	-0.03	-0.10	-0.15	-0.08	-0.05	-0.10	-0.04	-0.17	-0.13	-0.11	-0.18	-0.37	-0.09	-0.04	-0.06	-0.12	-0.12	-0.17	-0.07	-0.07	-0.10	-0.23	-0.26	-0.33
2	0.00	-0.02	-0.02	-0.01	0.00	-0.01	0.01	-0.01	-0.03	-0.04	0.05	0.03	-0.03	0.00	0.00	-0.05	-0.04	-0.03	-0.01	0.00	-0.01	-0.06	-0.03	-0.05
MAD	0.05	0.28	0.17	0.05	0.09	0.09	0.07	0.23	0.09	0.20	0.40	0.80	0.20	0.12	0.13	0.32	0.14	0.50	0.23	0.07	0.27	0.71	0.54	1.02

PBE-QIDH-D3(BJ)	*R1*	*R2*	*R3*	*R4*	*R5*	*R6*	*R7*	*R8*	*R9*	*R10*	*R11*	*R12*	*R13*	*R14*	*R15*	*R16*	*R17*	*R18*	*R19*	*R20*	*R21*	*R22*	*R23*	*R24*
0.80	-0.16	-0.98	-0.55	-0.47	0.06	-0.10	-0.02	-0.82	-0.20	-0.51	-3.25	-4.22	-0.65	-0.04	-0.82	-0.80	-0.48	-1.62	-0.90	-0.45	-1.48	-1.88	-1.76	-3.08
0.85	-0.12	-0.75	-0.51	-0.39	0.00	-0.14	-0.04	-0.73	-0.17	-0.48	-2.85	-3.68	-0.55	-0.09	-0.65	-0.78	-0.48	-1.35	-0.81	-0.45	-1.22	-1.84	-1.65	-2.89
0.90	-0.10	-0.58	-0.48	-0.38	-0.04	-0.18	-0.08	-0.69	-0.16	-0.47	-2.46	-3.18	-0.47	-0.12	-0.53	-0.70	-0.46	-1.10	-0.72	-0.44	-1.00	-1.69	-1.53	-2.59
0.95	-0.10	-0.47	-0.44	-0.38	-0.08	-0.22	-0.11	-0.68	-0.19	-0.47	-2.12	-2.74	-0.43	-0.12	-0.45	-0.61	-0.43	-0.90	-0.65	-0.42	-0.85	-1.49	-1.42	-2.29
1.00	-0.11	-0.42	-0.42	-0.39	-0.11	-0.25	-0.15	-0.67	-0.22	-0.47	-1.86	-2.41	-0.41	-0.13	-0.41	-0.54	-0.40	-0.77	-0.61	-0.40	-0.76	-1.30	-1.31	-2.01
1.05	-0.11	-0.40	-0.40	-0.38	-0.13	-0.27	-0.17	-0.65	-0.25	-0.46	-1.68	-2.17	-0.38	-0.14	-0.39	-0.49	-0.38	-0.68	-0.58	-0.39	-0.69	-1.13	-1.20	-1.78
1.10	-0.12	-0.37	-0.40	-0.37	-0.15	-0.27	-0.18	-0.62	-0.26	-0.44	-1.52	-1.98	-0.36	-0.16	-0.38	-0.46	-0.36	-0.63	-0.55	-0.37	-0.65	-1.00	-1.09	-1.57
1.25	-0.10	-0.29	-0.35	-0.30	-0.15	-0.25	-0.16	-0.48	-0.25	-0.33	-1.12	-1.49	-0.28	-0.18	-0.33	-0.37	-0.32	-0.51	-0.42	-0.36	-0.52	-0.74	-0.80	-1.12
1.50	-0.05	-0.16	-0.22	-0.16	-0.10	-0.17	-0.08	-0.26	-0.16	-0.17	-0.68	-0.88	-0.15	-0.11	-0.16	-0.19	-0.21	-0.29	-0.16	-0.22	-0.28	-0.39	-0.50	-0.66
2.00	0.00	-0.03	-0.04	-0.03	-0.01	-0.03	0.00	-0.03	-0.04	-0.05	-0.07	-0.09	-0.05	-0.02	-0.02	-0.07	-0.07	-0.06	-0.03	-0.03	-0.05	-0.10	-0.09	-0.14
MAD	0.10	0.45	0.38	0.32	0.08	0.19	0.10	0.56	0.19	0.39	1.76	2.29	0.37	0.11	0.41	0.50	0.36	0.79	0.54	0.35	0.75	1.16	1.13	1.81

PBE0-DH	R1	R2	R3	R4	R5	R6	R7	R8	R9	R10	R11	R12	R13	R14	R15	R16	R17	R18	R19	R20	R21	R22	R23	R24
0.80	0.03	-0.46	0.03	0.23	0.60	0.72	0.56	0.53	0.32	0.20	3.15	3.28	-0.07	0.61	-0.08	-0.21	0.15	-0.90	0.26	0.84	-0.12	-0.22	0.41	-0.32
0.85	0.07	-0.21	0.11	0.33	0.47	0.57	0.45	0.47	0.28	0.18	2.81	2.89	0.03	0.55	0.09	-0.19	0.16	-0.62	0.26	0.78	0.11	-0.33	0.33	-0.38
0.90	0.08	-0.05	0.13	0.34	0.35	0.44	0.33	0.36	0.22	0.13	2.51	2.52	0.06	0.51	0.20	-0.13	0.17	-0.38	0.25	0.71	0.25	-0.33	0.27	-0.32
0.95	0.06	0.01	0.13	0.30	0.26	0.32	0.23	0.23	0.14	0.05	2.21	2.18	0.05	0.46	0.24	-0.08	0.17	-0.21	0.22	0.63	0.32	-0.27	0.22	-0.22
1.00	0.04	0.01	0.11	0.24	0.19	0.23	0.15	0.11	0.05	-0.02	1.92	1.82	0.02	0.40	0.24	-0.06	0.15	-0.11	0.17	0.56	0.33	-0.20	0.18	-0.13
1.05	0.02	-0.02	0.07	0.18	0.13	0.15	0.09	0.01	-0.01	-0.07	1.60	1.46	-0.02	0.33	0.21	-0.06	0.13	-0.06	0.11	0.48	0.30	-0.16	0.16	-0.05
1.10	0.00	-0.04	0.03	0.14	0.09	0.08	0.04	-0.06	-0.06	-0.10	1.33	1.13	-0.05	0.25	0.17	-0.07	0.11	-0.05	0.05	0.41	0.25	-0.14	0.13	0.00
1.25	-0.01	-0.07	-0.06	0.04	0.02	-0.01	-0.01	-0.14	-0.10	-0.12	0.71	0.45	-0.08	0.08	0.06	-0.11	0.02	-0.08	-0.03	0.19	0.12	-0.17	0.06	0.03
1.50	0.00	-0.06	-0.08	-0.01	-0.01	-0.05	-0.01	-0.11	-0.08	-0.07	0.16	-0.02	-0.05	0.01	0.01	-0.06	-0.04	-0.07	0.01	0.05	0.04	-0.11	-0.06	-0.05
2.00	0.01	-0.01	-0.01	0.00	0.01	0.00	0.01	0.00	-0.02	-0.03	0.11	0.09	-0.02	0.01	0.01	-0.04	-0.02	-0.01	0.01	0.02	0.02	-0.03	0.01	0.01
MAD	0.03	0.09	0.07	0.18	0.21	0.26	0.19	0.20	0.13	0.10	1.65	1.58	0.04	0.32	0.13	0.10	0.11	0.25	0.14	0.47	0.19	0.20	0.18	0.15

PBE0-DH-D3(BJ)	*R1*	*R2*	*R3*	*R4*	*R5*	*R6*	*R7*	*R8*	*R9*	*R10*	*R11*	*R12*	*R13*	*R14*	*R15*	*R16*	*R17*	*R18*	*R19*	*R20*	*R21*	*R22*	*R23*	*R24*
0.80	-0.23	-1.39	-1.19	-1.36	-0.20	-0.50	-0.20	-1.33	-0.16	-0.75	-3.34	-4.02	-1.07	-0.63	-1.61	-1.16	-1.02	-2.38	-1.10	-0.86	-2.12	-2.17	-2.32	-4.12
0.85	-0.16	-1.03	-0.98	-1.04	-0.24	-0.48	-0.20	-1.09	-0.14	-0.66	-2.94	-3.54	-0.84	-0.58	-1.29	-1.04	-0.91	-1.98	-0.94	-0.75	-1.72	-2.04	-2.10	-3.77
0.90	-0.13	-0.78	-0.82	-0.84	-0.26	-0.45	-0.22	-0.93	-0.15	-0.60	-2.52	-3.06	-0.68	-0.50	-1.02	-0.89	-0.79	-1.61	-0.79	-0.65	-1.38	-1.81	-1.87	-3.31
0.95	-0.12	-0.62	-0.69	-0.69	-0.27	-0.43	-0.23	-0.83	-0.19	-0.57	-2.13	-2.61	-0.58	-0.40	-0.81	-0.75	-0.68	-1.29	-0.68	-0.55	-1.10	-1.55	-1.65	-2.83
1.00	-0.12	-0.52	-0.58	-0.58	-0.26	-0.41	-0.23	-0.75	-0.23	-0.54	-1.80	-2.24	-0.51	-0.31	-0.65	-0.64	-0.58	-1.05	-0.61	-0.47	-0.89	-1.30	-1.44	-2.39
1.05	-0.12	-0.46	-0.51	-0.48	-0.25	-0.39	-0.22	-0.68	-0.26	-0.51	-1.56	-1.96	-0.45	-0.25	-0.54	-0.56	-0.50	-0.86	-0.56	-0.40	-0.75	-1.10	-1.24	-2.00
1.10	-0.12	-0.41	-0.45	-0.41	-0.23	-0.36	-0.21	-0.62	-0.27	-0.46	-1.34	-1.73	-0.41	-0.22	-0.46	-0.50	-0.43	-0.73	-0.52	-0.35	-0.64	-0.94	-1.06	-1.67
1.25	-0.09	-0.28	-0.33	-0.25	-0.17	-0.27	-0.15	-0.44	-0.23	-0.32	-0.89	-1.23	-0.29	-0.17	-0.30	-0.36	-0.31	-0.48	-0.37	-0.28	-0.42	-0.65	-0.68	-1.00
1.50	-0.03	-0.14	-0.18	-0.12	-0.09	-0.15	-0.07	-0.22	-0.14	-0.15	-0.54	-0.73	-0.13	-0.08	-0.12	-0.17	-0.18	-0.23	-0.12	-0.15	-0.19	-0.33	-0.40	-0.51
2.00	0.00	-0.03	-0.03	-0.02	-0.01	-0.03	0.00	-0.03	-0.03	-0.05	-0.05	-0.07	-0.04	-0.01	-0.02	-0.06	-0.05	-0.05	-0.02	-0.02	-0.03	-0.08	-0.07	-0.10
MAD	0.11	0.57	0.58	0.58	0.20	0.35	0.17	0.69	0.18	0.46	1.71	2.12	0.50	0.32	0.68	0.61	0.55	1.07	0.57	0.45	0.92	1.20	1.28	2.17

B2-PLYP	*R1*	*R2*	*R3*	*R4*	*R5*	*R6*	*R7*	*R8*	*R9*	*R10*	*R11*	*R12*	*R13*	*R14*	*R15*	*R16*	*R17*	*R18*	*R19*	*R20*	*R21*	*R22*	*R23*	*R24*
0.80	-0.04	0.26	1.15	1.52	0.84	1.23	0.63	1.13	0.32	0.60	4.25	4.09	0.72	1.66	1.19	0.46	1.10	0.54	0.63	1.66	1.16	0.33	1.71	2.14
0.85	0.01	0.17	0.78	1.12	0.59	0.82	0.45	0.71	0.20	0.36	3.37	3.07	0.41	1.24	0.93	0.22	0.78	0.37	0.43	1.29	0.95	-0.02	1.18	1.35
0.90	0.03	0.13	0.53	0.81	0.43	0.57	0.32	0.40	0.11	0.19	2.72	2.36	0.22	0.94	0.74	0.10	0.57	0.28	0.31	1.01	0.80	-0.19	0.80	0.88
0.95	0.04	0.09	0.38	0.59	0.33	0.40	0.23	0.19	0.04	0.07	2.22	1.84	0.09	0.69	0.57	0.04	0.41	0.22	0.21	0.80	0.65	-0.25	0.53	0.58
1.00	0.04	0.05	0.27	0.43	0.25	0.28	0.16	0.05	-0.01	-0.01	1.79	1.41	0.01	0.51	0.43	0.00	0.30	0.16	0.12	0.63	0.52	-0.26	0.33	0.39
1.05	0.03	0.01	0.19	0.32	0.20	0.19	0.11	-0.04	-0.05	-0.05	1.40	1.03	-0.03	0.38	0.32	-0.03	0.22	0.10	0.05	0.50	0.40	-0.26	0.19	0.24
1.10	0.02	-0.02	0.12	0.24	0.15	0.13	0.06	-0.10	-0.07	-0.07	1.08	0.71	-0.06	0.28	0.24	-0.06	0.16	0.05	0.00	0.40	0.30	-0.26	0.10	0.14
1.25	0.00	-0.06	-0.01	0.09	0.06	0.02	-0.01	-0.17	-0.10	-0.08	0.43	0.11	-0.07	0.11	0.09	-0.08	0.05	-0.03	-0.05	0.18	0.13	-0.27	-0.05	-0.03
1.50	0.00	-0.06	-0.07	0.00	0.00	-0.05	-0.02	-0.15	-0.09	-0.06	-0.02	-0.19	-0.06	0.01	0.02	-0.06	-0.02	-0.04	-0.02	0.04	0.04	-0.17	-0.13	-0.12
2.00	0.01	-0.02	-0.01	0.00	0.01	-0.01	0.01	-0.01	-0.02	-0.02	0.06	0.06	-0.03	0.00	0.00	-0.04	-0.02	-0.01	0.00	0.01	0.01	-0.05	-0.02	-0.02
MAD	0.02	0.09	0.35	0.51	0.29	0.37	0.20	0.30	0.10	0.15	1.73	1.49	0.17	0.58	0.45	0.11	0.36	0.18	0.18	0.65	0.50	0.21	0.50	0.59

B2-PLYP-D3	*R1*	*R2*	*R3*	*R4*	*R5*	*R6*	*R7*	*R8*	*R9*	*R10*	*R11*	*R12*	*R13*	*R14*	*R15*	*R16*	*R17*	*R18*	*R19*	*R20*	*R21*	*R22*	*R23*	*R24*
0.80	-0.60	-0.58	0.33	0.72	-0.38	-0.39	-0.55	-1.32	-0.48	-0.35	-1.34	-2.24	0.08	1.02	0.55	-0.25	0.40	-0.11	-0.73	0.15	-0.30	-1.51	-0.64	-0.41
0.85	-0.50	-0.79	-0.22	0.13	-0.42	-0.62	-0.42	-1.26	-0.54	-0.64	-1.86	-2.74	-0.38	0.47	0.16	-0.54	0.02	-0.37	-0.82	-0.16	-0.50	-1.67	-1.01	-1.14
0.90	-0.36	-0.81	-0.55	-0.30	-0.36	-0.57	-0.33	-1.08	-0.50	-0.72	-2.00	-2.88	-0.64	0.06	-0.14	-0.67	-0.23	-0.52	-0.83	-0.34	-0.59	-1.64	-1.21	-1.51
0.95	-0.26	-0.72	-0.65	-0.50	-0.28	-0.47	-0.28	-0.92	-0.45	-0.69	-1.91	-2.73	-0.69	-0.24	-0.36	-0.70	-0.38	-0.60	-0.79	-0.44	-0.63	-1.52	-1.28	-1.65
1.00	-0.19	-0.61	-0.60	-0.52	-0.22	-0.38	-0.25	-0.80	-0.40	-0.61	-1.71	-2.46	-0.62	-0.34	-0.48	-0.67	-0.46	-0.65	-0.72	-0.47	-0.65	-1.38	-1.27	-1.65
1.05	-0.15	-0.50	-0.50	-0.44	-0.19	-0.33	-0.24	-0.72	-0.36	-0.52	-1.52	-2.17	-0.52	-0.31	-0.50	-0.60	-0.48	-0.67	-0.64	-0.46	-0.65	-1.22	-1.22	-1.58
1.10	-0.12	-0.41	-0.41	-0.35	-0.17	-0.30	-0.22	-0.66	-0.32	-0.44	-1.35	-1.93	-0.43	-0.24	-0.46	-0.52	-0.44	-0.66	-0.56	-0.41	-0.62	-1.07	-1.14	-1.47
1.25	-0.08	-0.27	-0.28	-0.19	-0.14	-0.25	-0.16	-0.49	-0.25	-0.29	-1.03	-1.44	-0.27	-0.14	-0.26	-0.33	-0.28	-0.45	-0.38	-0.28	-0.41	-0.74	-0.80	-1.07
1.50	-0.03	-0.15	-0.18	-0.12	-0.08	-0.16	-0.07	-0.27	-0.15	-0.15	-0.71	-0.90	-0.14	-0.09	-0.12	-0.16	-0.16	-0.21	-0.15	-0.17	-0.20	-0.38	-0.47	-0.58
2.00	0.00	-0.03	-0.03	-0.02	-0.01	-0.03	0.00	-0.03	-0.03	-0.04	-0.10	-0.09	-0.04	-0.02	-0.02	-0.06	-0.05	-0.05	-0.03	-0.03	-0.05	-0.10	-0.10	-0.13
MAD	0.23	0.49	0.37	0.33	0.22	0.35	0.25	0.76	0.35	0.44	1.35	1.96	0.38	0.29	0.31	0.45	0.29	0.43	0.57	0.29	0.46	1.12	0.91	1.12

DSD-PBEP86	R1	R2	R3	R4	R5	R6	R7	R8	R9	R10	R11	R12	R13	R14	R15	R16	R17	R18	R19	R20	R21	R22	R23	R24
0.80	0.75	1.16	2.01	2.05	0.93	1.44	0.71	1.43	0.69	1.14	9.40	11.08	1.67	2.89	2.10	1.08	1.83	0.76	1.49	2.89	2.16	2.15	4.37	4.46
0.85	0.51	0.73	1.26	1.38	0.57	0.86	0.48	0.86	0.39	0.63	6.87	7.78	0.93	2.00	1.46	0.55	1.16	0.37	1.03	2.11	1.58	1.25	3.14	3.19
0.90	0.36	0.46	0.78	0.91	0.35	0.51	0.34	0.47	0.20	0.31	5.07	5.48	0.51	1.39	1.01	0.25	0.71	0.13	0.72	1.55	1.17	0.72	2.23	2.28
0.95	0.25	0.29	0.48	0.60	0.22	0.30	0.24	0.22	0.05	0.09	3.77	3.87	0.26	0.92	0.70	0.07	0.41	-0.02	0.50	1.16	0.86	0.42	1.57	1.61
1.00	0.17	0.16	0.30	0.39	0.14	0.17	0.16	0.06	-0.05	-0.04	2.80	2.70	0.11	0.61	0.48	-0.03	0.22	-0.12	0.34	0.88	0.64	0.25	1.10	1.14
1.05	0.12	0.07	0.17	0.26	0.09	0.09	0.10	-0.03	-0.11	-0.11	2.04	1.82	0.03	0.43	0.32	-0.10	0.10	-0.19	0.22	0.69	0.46	0.14	0.77	0.80
1.10	0.08	0.02	0.09	0.18	0.05	0.04	0.06	-0.09	-0.15	-0.14	1.47	1.16	-0.02	0.31	0.22	-0.14	0.02	-0.23	0.14	0.54	0.34	0.06	0.55	0.56
1.25	0.03	-0.04	-0.03	0.06	0.00	-0.03	-0.01	-0.15	-0.18	-0.15	0.52	0.15	-0.06	0.12	0.08	-0.16	-0.07	-0.24	0.04	0.27	0.15	-0.09	0.21	0.17
1.50	0.01	-0.05	-0.06	0.00	-0.02	-0.06	-0.02	-0.13	-0.14	-0.09	0.02	-0.22	-0.04	0.03	0.03	-0.10	-0.09	-0.16	0.04	0.11	0.07	-0.07	0.00	-0.02
2.00	0.01	-0.01	-0.01	0.00	0.00	-0.01	0.01	-0.01	-0.05	-0.04	0.05	0.01	-0.02	0.01	0.01	-0.06	-0.05	-0.06	0.02	0.04	0.03	-0.02	0.02	0.01
MAD	0.23	0.30	0.52	0.59	0.24	0.35	0.21	0.35	0.20	0.28	3.20	3.43	0.36	0.87	0.64	0.25	0.47	0.23	0.45	1.02	0.75	0.52	1.40	1.42

DSD-PBEP86-D3	*R1*	*R2*	*R3*	*R4*	*R5*	*R6*	*R7*	*R8*	*R9*	*R10*	*R11*	*R12*	*R13*	*R14*	*R15*	*R16*	*R17*	*R18*	*R19*	*R20*	*R21*	*R22*	*R23*	*R24*
0.80	-0.34	-1.10	-0.57	-0.55	-0.39	-0.59	-0.46	-1.46	-0.38	-0.78	-4.71	-5.95	-0.70	0.00	-0.75	-0.76	-0.30	-1.22	-1.15	-0.49	-1.26	-2.11	-1.82	-2.85
0.85	-0.30	-1.03	-0.73	-0.66	-0.44	-0.68	-0.44	-1.40	-0.41	-0.83	-4.33	-5.44	-0.80	-0.26	-0.79	-0.90	-0.52	-1.23	-1.15	-0.66	-1.25	-2.15	-1.89	-2.94
0.90	-0.26	-0.91	-0.79	-0.71	-0.43	-0.67	-0.40	-1.31	-0.40	-0.82	-3.83	-4.81	-0.79	-0.39	-0.78	-0.90	-0.62	-1.16	-1.08	-0.73	-1.18	-2.04	-1.87	-2.81
0.95	-0.23	-0.80	-0.76	-0.71	-0.40	-0.63	-0.36	-1.19	-0.40	-0.77	-3.34	-4.17	-0.75	-0.44	-0.75	-0.85	-0.65	-1.07	-1.00	-0.75	-1.10	-1.84	-1.81	-2.61
1.00	-0.21	-0.70	-0.70	-0.67	-0.36	-0.58	-0.32	-1.06	-0.39	-0.71	-2.90	-3.60	-0.68	-0.44	-0.71	-0.77	-0.64	-0.97	-0.92	-0.73	-1.02	-1.63	-1.71	-2.37
1.05	-0.19	-0.61	-0.63	-0.61	-0.32	-0.52	-0.29	-0.93	-0.38	-0.64	-2.55	-3.13	-0.60	-0.40	-0.66	-0.69	-0.60	-0.89	-0.84	-0.69	-0.95	-1.43	-1.58	-2.15
1.10	-0.17	-0.53	-0.57	-0.53	-0.28	-0.46	-0.26	-0.82	-0.35	-0.56	-2.23	-2.75	-0.52	-0.36	-0.60	-0.62	-0.55	-0.81	-0.76	-0.63	-0.87	-1.25	-1.43	-1.93
1.25	-0.12	-0.34	-0.40	-0.34	-0.19	-0.32	-0.19	-0.54	-0.28	-0.35	-1.47	-1.83	-0.33	-0.24	-0.42	-0.41	-0.39	-0.58	-0.49	-0.48	-0.63	-0.86	-1.01	-1.36
1.50	-0.06	-0.17	-0.21	-0.15	-0.10	-0.18	-0.08	-0.28	-0.17	-0.17	-0.74	-0.90	-0.16	-0.11	-0.17	-0.18	-0.20	-0.28	-0.17	-0.23	-0.29	-0.40	-0.55	-0.72
2.00	0.00	-0.03	-0.04	-0.02	-0.01	-0.03	0.00	-0.03	-0.04	-0.05	-0.06	-0.07	-0.05	-0.02	-0.02	-0.07	-0.06	-0.05	-0.04	-0.03	-0.05	-0.10	-0.10	-0.13
MAD	0.19	0.62	0.54	0.50	0.29	0.47	0.28	0.90	0.32	0.57	2.62	3.26	0.54	0.27	0.56	0.62	0.45	0.83	0.76	0.54	0.86	1.38	1.38	1.99

revDSD-PBEP86	*R1*	*R2*	*R3*	*R4*	*R5*	*R6*	*R7*	*R8*	*R9*	*R10*	*R11*	*R12*	*R13*	*R14*	*R15*	*R16*	*R17*	*R18*	*R19*	*R20*	*R21*	*R22*	*R23*	*R24*
0.8	-0.04	-0.16	0.64	0.87	0.33	0.48	0.18	0.04	0.08	0.09	0.83	0.38	0.29	1.22	0.65	0.18	0.84	0.15	0.01	1.02	0.45	-0.41	0.62	0.42
0.85	-0.05	-0.26	0.26	0.49	0.16	0.19	0.08	-0.20	-0.02	-0.12	0.36	-0.14	-0.01	0.78	0.39	-0.11	0.46	-0.05	-0.17	0.62	0.24	-0.73	0.19	-0.14
0.9	-0.06	-0.28	0.02	0.22	0.05	0.03	0.01	-0.36	-0.09	-0.23	0.10	-0.42	-0.17	0.48	0.20	-0.25	0.21	-0.15	-0.26	0.35	0.09	-0.86	-0.12	-0.43
0.95	-0.07	-0.29	-0.11	0.03	0.00	-0.07	-0.03	-0.45	-0.14	-0.30	-0.06	-0.54	-0.26	0.24	0.06	-0.30	0.04	-0.22	-0.32	0.16	-0.03	-0.86	-0.34	-0.59
1	-0.07	-0.29	-0.17	-0.08	-0.04	-0.12	-0.06	-0.48	-0.18	-0.33	-0.18	-0.62	-0.29	0.10	-0.05	-0.32	-0.07	-0.27	-0.35	0.03	-0.13	-0.82	-0.48	-0.68
1.05	-0.08	-0.28	-0.21	-0.14	-0.06	-0.15	-0.08	-0.47	-0.20	-0.33	-0.29	-0.70	-0.29	0.01	-0.13	-0.32	-0.13	-0.31	-0.37	-0.05	-0.21	-0.76	-0.55	-0.73
1.1	-0.08	-0.27	-0.23	-0.16	-0.07	-0.16	-0.10	-0.45	-0.21	-0.31	-0.37	-0.75	-0.27	-0.03	-0.18	-0.31	-0.17	-0.34	-0.36	-0.10	-0.26	-0.70	-0.58	-0.75
1.25	-0.07	-0.20	-0.22	-0.15	-0.08	-0.15	-0.11	-0.35	-0.19	-0.22	-0.42	-0.72	-0.20	-0.08	-0.19	-0.25	-0.18	-0.33	-0.27	-0.17	-0.28	-0.54	-0.52	-0.68
1.50	-0.04	-0.12	-0.15	-0.08	-0.06	-0.12	-0.05	-0.21	-0.13	-0.12	-0.30	-0.46	-0.11	-0.05	-0.09	-0.12	-0.12	-0.18	-0.09	-0.10	-0.14	-0.27	-0.34	-0.44
2	0.00	-0.02	-0.02	-0.01	0.00	-0.02	0.01	-0.01	-0.03	-0.04	0.04	0.03	-0.04	-0.01	-0.01	-0.05	-0.04	-0.03	-0.02	-0.01	-0.01	-0.07	-0.04	-0.06
MAD	0.06	0.22	0.20	0.22	0.08	0.15	0.07	0.30	0.13	0.21	0.30	0.48	0.19	0.30	0.19	0.22	0.22	0.20	0.22	0.26	0.19	0.60	0.38	0.49

revDSD-PBEP86-D3(BJ)	*R1*	*R2*	*R3*	*R4*	*R5*	*R6*	*R7*	*R8*	*R9*	*R10*	*R11*	*R12*	*R13*	*R14*	*R15*	*R16*	*R17*	*R18*	*R19*	*R20*	*R21*	*R22*	*R23*	*R24*
0.80	-0.23	-0.82	-0.21	-0.17	-0.24	-0.36	-0.32	-1.14	-0.24	-0.56	-3.31	-4.30	-0.40	0.38	-0.34	-0.47	0.05	-0.81	-0.83	-0.04	-0.75	-1.61	-1.09	-1.94
0.85	-0.22	-0.82	-0.46	-0.37	-0.33	-0.51	-0.34	-1.16	-0.30	-0.66	-3.18	-4.13	-0.59	0.04	-0.47	-0.68	-0.24	-0.91	-0.90	-0.31	-0.84	-1.76	-1.30	-2.19
0.90	-0.20	-0.76	-0.58	-0.49	-0.35	-0.54	-0.32	-1.12	-0.33	-0.69	-2.91	-3.77	-0.64	-0.16	-0.53	-0.74	-0.40	-0.91	-0.88	-0.45	-0.85	-1.73	-1.40	-2.19
0.95	-0.19	-0.68	-0.61	-0.54	-0.33	-0.53	-0.30	-1.05	-0.34	-0.68	-2.59	-3.33	-0.64	-0.28	-0.55	-0.72	-0.48	-0.86	-0.84	-0.53	-0.84	-1.60	-1.43	-2.10
1.00	-0.17	-0.61	-0.58	-0.54	-0.31	-0.50	-0.28	-0.96	-0.35	-0.64	-2.29	-2.93	-0.60	-0.32	-0.56	-0.67	-0.51	-0.81	-0.80	-0.55	-0.81	-1.44	-1.40	-1.96
1.05	-0.16	-0.54	-0.54	-0.51	-0.28	-0.46	-0.26	-0.85	-0.34	-0.58	-2.05	-2.60	-0.54	-0.32	-0.54	-0.62	-0.50	-0.76	-0.74	-0.54	-0.78	-1.28	-1.33	-1.81
1.10	-0.15	-0.48	-0.50	-0.46	-0.25	-0.41	-0.24	-0.76	-0.33	-0.51	-1.83	-2.32	-0.47	-0.30	-0.52	-0.56	-0.47	-0.71	-0.68	-0.52	-0.74	-1.13	-1.24	-1.66
1.25	-0.11	-0.32	-0.37	-0.30	-0.18	-0.29	-0.18	-0.51	-0.27	-0.33	-1.26	-1.61	-0.31	-0.22	-0.38	-0.38	-0.36	-0.54	-0.45	-0.42	-0.56	-0.80	-0.91	-1.22
1.50	-0.05	-0.16	-0.20	-0.14	-0.10	-0.18	-0.08	-0.27	-0.16	-0.16	-0.66	-0.82	-0.15	-0.10	-0.15	-0.18	-0.19	-0.26	-0.15	-0.21	-0.26	-0.38	-0.51	-0.67
2.00	0.00	-0.03	-0.03	-0.02	0.00	-0.03	0.00	-0.03	-0.03	-0.04	-0.04	-0.05	-0.05	-0.02	-0.02	-0.07	-0.05	-0.05	-0.03	-0.03	-0.04	-0.10	-0.09	-0.12
MAD	0.15	0.52	0.41	0.35	0.24	0.38	0.23	0.78	0.27	0.48	2.01	2.59	0.44	0.21	0.41	0.51	0.32	0.66	0.63	0.36	0.65	1.18	1.07	1.59

Supporting materials of Chapter 7

Table S7.1 The parameters of the functionals used in GDV version.

C2	IOp(74)
C	-89 ... ωB97M-V
C	-88 ... B97M-V
C	-87 ... ωB97X-V
C	-85 ... VV10
C	-83 ... revM06
C	-82 ... revM06-L
C	-73 ... MN15.
C	-72 ... MN15-L
C	-66 ... M11L
C	-64 ... M11L

Table S7.2 The errors and MAD of the different functionals at aug-cc-pVTZ basi set for the reactants, transition states and products. (units:kcal/mol)

	MN15	*MN15-L*	*M11*	*M11L*	*DSD-PBEP86*	*MPW2PLYP-D*	*B97M-V*	*ωB97M-V*	*ωB97X-V*	*VV10*
1+7	0.00	0.00	0.00	0.00	0.00	0.00	0.00	0.00	0.00	0.00
TS5	-0.81	-6.37	4.68	-3.90	-8.26	-5.51	-6.97	2.83	4.33	-10.62
10	-2.80	3.11	-0.16	5.95	-1.04	4.70	5.90	-2.40	-5.15	10.50
TS7	-3.12	-7.54	4.44	-4.39	-8.08	-4.48	-7.29	0.24	0.42	-9.87
9	5.16	11.89	3.43	14.55	0.08	7.87	12.21	-0.37	-4.06	15.39
TS6	0.12	-4.16	6.52	-1.52	-7.28	-3.11	-4.31	3.33	3.78	-7.09
8	4.49	10.11	3.22	13.40	-0.56	6.95	10.89	-0.26	-3.84	14.16
TS9	-2.95	0.92	-2.23	5.35	-10.29	-0.60	2.98	-6.15	-9.01	4.15
12	3.10	8.89	4.86	16.52	-0.28	12.31	14.47	-1.67	-8.80	25.12
TS8	9.17	14.49	9.66	18.43	1.51	11.56	15.99	5.45	2.73	16.59
11	1.14	6.69	2.67	13.70	-1.99	10.45	12.56	-3.33	-10.52	23.11
MAD	3.29	7.41	4.19	9.77	3.94	6.75	9.36	2.61	5.27	13.67
	PBEPBE	*PBEPBE-D3*	*BLYP*	*B3LYP*	*B3LYP-D3*	*PBE0*	*M06*	*M06-L*	*M06-HF*	*M06-2X*
1+7	0.00	0.00	0.00	0.00	0.00	0.00	0.00	0.00	0.00	0.00
TS5	-3.54	-10.79	7.70	9.25	-2.31	1.35	-2.82	-6.21	3.04	0.23
10	9.68	5.13	26.99	18.38	11.19	2.75	3.72	10.29	-10.23	-0.90
TS7	-4.09	-11.10	9.63	10.15	-1.11	-0.05	-2.75	-5.59	2.09	0.44
9	18.25	11.78	36.54	26.83	16.52	10.04	8.40	16.32	-5.60	3.57
TS6	-0.70	-8.11	13.12	13.13	1.16	2.63	-0.42	-3.06	3.21	2.33
8	17.16	10.54	35.62	26.32	15.64	9.48	7.83	14.93	-5.57	3.46
TS9	3.50	-3.25	29.44	22.01	10.85	-1.12	1.99	8.38	-14.22	-1.87
12	20.81	14.67	52.77	37.27	27.35	7.05	10.87	20.95	-4.99	6.62
TS8	16.27	9.61	41.66	34.16	23.27	11.47	14.35	21.77	-3.32	10.11
11	18.49	12.22	50.89	35.41	25.14	4.83	8.85	18.23	-6.21	4.80
MAD	11.25	9.72	30.4	23.29	13.45	5.08	6.20	12.57	5.85	3.43

	B2-PLYP	*B2-PLYP-D3*	*PBE-QIDH*	*PBE-QIDH-D3(BJ)*	*rev-M06*	*rev-M06L*	*CAM-B3LYP*	*ωB97X-D*
1+7	0.00	0.00	0.00	0.00	0.00	0.00	0.00	0.00
TS5	0.16	-5.93	-5.19	-7.63	0.99	-1.51	11.51	1.19
10	10.57	6.76	-5.03	-6.51	1.44	7.37	7.70	0.68
TS7	1.09	-4.88	-6.05	-8.45	0.68	-1.81	9.80	-0.17
9	15.75	10.30	-1.39	-3.71	8.05	14.89	14.29	2.86
TS6	3.26	-3.08	-4.68	-7.20	3.20	1.34	13.32	2.34
8	15.09	9.41	-1.97	-4.30	7.63	13.84	14.35	2.65
TS9	7.55	1.57	-13.78	-16.13	0.69	7.86	11.70	-1.91
12	21.68	16.43	-8.38	-10.53	8.24	16.05	18.61	3.06
TS8	19.50	13.70	-1.43	-3.80	13.13	21.47	23.57	10.39
11	19.96	14.50	-10.41	-12.54	6.11	13.34	16.86	0.90
MAD	11.46	8.66	5.83	8.09	5.02	9.94	14.17	2.62

TableS7.3 All of the single-point energies (kcal/mol) at aug-cc-pVTZ basis set with the tested functionals.

aug-cc-pVTZ	*MN15*	*MN15-L*	*M11*	*M11L*	*DSD-PBEP86*	*mPW2PLYP-D*
1+7	0.00	0.00	0.00	0.00	0.00	0.00
TS5	19.29	13.73	24.78	16.20	11.84	14.59
10	-17.10	-11.19	-14.46	-8.35	-15.34	-9.60
TS7	19.88	15.46	27.44	18.61	14.92	18.52
9	-10.64	-3.91	-12.37	-1.25	-15.72	-7.93
TS6	16.82	12.54	23.22	15.18	9.42	13.59
8	-14.31	-8.69	-15.58	-5.40	-19.36	-11.85
TS9	11.95	15.82	12.67	20.25	4.61	14.30
12	-31.50	-25.71	-29.74	-18.08	-34.88	-22.29
TS8	18.57	23.89	19.06	27.83	10.91	20.96
11	-32.76	-27.21	-31.23	-20.20	-35.89	-23.45

aug-cc-pVTZ	***B97M-V***	***ωB97M-V***	***ωB97X-V***	***VV10***	***REV-M06***	***REV-M06L***
1+7	0.00	0.00	0.00	0.00	0.00	0.00
TS5	13.13	22.93	24.43	9.48	21.09	18.59
10	-8.40	-16.70	-19.45	-3.80	-12.86	-6.93
TS7	15.71	23.24	23.42	13.13	23.68	21.19
9	-3.59	-16.17	-19.86	-0.41	-7.75	-0.91
TS6	12.39	20.03	20.48	9.61	19.90	18.04
8	-7.91	-19.06	-22.64	-4.64	-11.17	-4.96
TS9	17.88	8.75	5.89	19.05	15.59	22.76
12	-20.13	-36.27	-43.40	-9.48	-26.36	-18.55
TS8	25.39	14.85	12.13	25.99	22.53	30.87
11	-21.34	-37.23	-44.42	-10.79	-27.79	-20.56

aug-cc-pVTZ	*PBEPBE*	*PBEPBE-D3*	*BLYP*	*B3LYP*	*B3LYP-D3*	*PBE0*

1+7	0.00	0.00	0.00	0.00	0.00	0.00
TS5	16.56	9.31	27.80	29.35	17.79	21.45
10	-4.62	-9.17	12.69	4.08	-3.11	-11.55
TS7	18.91	11.90	32.63	33.15	21.89	22.95
9	2.45	-4.02	20.74	11.03	0.72	-5.76
TS6	16.00	8.59	29.82	29.83	17.86	19.33
8	-1.64	-8.26	16.82	7.52	-3.16	-9.32
TS9	18.40	11.65	44.34	36.91	25.75	13.78
12	-13.79	-19.93	18.17	2.67	-7.25	-27.55
TS8	25.67	19.01	51.06	43.56	32.67	20.87
11	-15.41	-21.68	16.99	1.51	-8.76	-29.07

aug-cc-pVTZ	***CAM-B3LYP***	***ωB97X-D***	***M06***	***M06-L***	***M06-HF***	***M06-2X***
1+7	0.00	0.00	0.00	0.00	0.00	0.00
TS5	31.61	21.29	17.28	13.89	23.14	20.33
10	-6.60	-13.62	-10.58	-4.01	-24.53	-15.20
TS7	32.80	22.83	20.25	17.41	25.09	23.44
9	-1.51	-12.94	-7.40	0.52	-21.40	-12.23
TS6	30.02	19.04	16.28	13.64	19.91	19.03
8	-4.45	-16.15	-10.97	-3.87	-24.37	-15.34
TS9	26.60	12.99	16.89	23.28	0.68	13.03
12	-15.99	-31.54	-23.73	-13.65	-39.59	-27.98
TS8	32.97	19.79	23.75	31.17	6.08	19.51
11	-17.04	-33.00	-25.05	-15.67	-40.11	-29.10

aug-cc-pVTZ	***B2-PLYP***	***B2-PLYP-D3***	***PBE-QIDH***	***PBE-QIDH-D3(BJ)***
1+7	0.00	0.00	0.00	0.00
TS5	20.26	14.17	14.91	12.47
10	-3.73	-7.54	-19.33	-20.81
TS7	24.09	18.12	16.95	14.55
9	-0.05	-5.50	-17.19	-19.51
TS6	19.96	13.62	12.02	9.50
8	-3.71	-9.39	-20.77	-23.10
TS9	22.45	16.47	1.12	-1.23
12	-12.92	-18.17	-42.98	-45.13
TS8	28.90	23.10	7.97	5.60
11	-13.94	-19.40	-44.31	-46.44

TableS7.4. The substitued energies of the tested functionals at the aug-cc-pVTZ basis set (a=Cl, b=OMe)

a	*BLYP*	*BLYP-D3*	*PBEPBE*	*PBEPBE-D3*	*B3LYP*	*B3LYP-D3*	*CAM-B3LYP*	*B2PLYP*	*B2PLYP-D3*	*wB97X-D*	*PBE0*	*PBEQIDH*	*PBEQIDH-D3(BJ)*
1A+7	0.00	0.00	0.00	0.00	0.00	0.00	0.00	0.00	0.00	0.00	0.00	0.00	0.00
TS5A	29.23	13.85	18.15	10.36	30.43	18.07	32.40	20.93	14.42	21.57	22.62	15.54	12.87
10A	13.29	3.96	-3.31	-8.10	4.05	-3.52	-7.19	-3.85	-7.86	-14.27	-11.15	-19.38	-20.95
TS7A	33.26	18.35	20.06	12.53	33.57	21.53	33.18	24.43	18.06	22.72	23.79	17.66	15.04
9A	24.35	9.96	6.37	-0.81	13.93	2.34	0.53	1.51	-4.65	-11.19	-2.70	-15.85	-18.45
TS6A	31.61	15.49	18.04	10.02	31.18	18.22	30.90	20.82	13.96	19.48	20.82	12.85	10.09
8A	17.91	3.73	-0.37	-7.51	8.07	-3.39	-4.46	-3.58	-9.65	-16.66	-8.75	-20.86	-23.41
TS9A	44.42	28.84	18.56	11.00	36.31	23.67	25.35	20.79	14.00	11.02	13.18	-0.86	-3.49
12A	17.45	3.40	-14.04	-20.94	1.11	-10.18	-18.33	-15.47	-21.47	-34.26	-28.85	-45.70	-48.12
TS8A	50.44	35.44	25.63	18.26	42.34	30.16	31.16	26.58	20.08	17.71	20.08	5.68	3.03
11A	17.68	2.93	-14.33	-21.48	1.28	-10.63	-18.24	-15.49	-21.87	-34.54	-29.10	-46.14	-48.60

a	*M06*	*M06L*	*M062X*	*M06HF*	*rev-M06*	*rev-M06L*	*B97MV*	*wB97M-V*	*wB97X-V*	*VV10*	*M11*	*M11L*	*MN15*	*MN15L*	*DSD-PBEP86*	*mPW2PLYP-D*
1A+7	0.00	0.00	0.00	0.00	0.00	0.00	0.00	0.00	0.00	0.00	0.00	0.00	0.00	0.00	0.00	0.00
TS5A	17.71	14.73	20.80	23.51	21.67	19.54	13.88	23.21	24.54	10.43	25.06	17.54	19.85	14.33	12.15	14.99
10A	-10.40	-2.75	-15.23	-25.47	-12.55	-5.55	-7.65	-17.35	-20.36	-2.94	-14.69	-5.97	-16.95	-9.94	-15.60	-10.03
TS7A	20.17	17.78	23.79	25.62	24.00	21.72	15.99	23.40	23.38	13.55	27.57	19.64	20.35	15.84	15.37	18.62
9A	-5.97	3.59	-10.94	-21.62	-6.05	2.47	-1.57	-15.82	-19.19	1.92	-11.58	1.41	-9.66	-2.37	-15.36	-6.87
TS6A	16.90	14.84	19.55	20.07	20.60	19.42	13.39	20.20	20.53	10.85	23.41	16.72	17.40	13.37	9.86	14.10
8A	-10.79	-3.11	-15.56	-25.64	-11.05	-3.96	-7.39	-19.79	-23.42	-4.00	-16.09	-4.34	-14.44	-8.12	-19.75	-12.10
TS9A	14.78	22.01	11.21	-1.51	14.00	21.83	16.21	6.34	3.45	17.95	10.70	19.75	9.89	13.87	2.14	12.01
12A	-25.74	-14.49	-30.56	-43.60	-28.42	-19.47	-22.03	-39.81	-46.88	-10.98	-32.58	-19.56	-33.84	-27.61	-38.30	-25.39
TS8A	21.69	30.42	17.27	2.68	20.70	30.29	23.52	11.74	9.28	24.44	16.66	26.71	16.38	21.86	7.72	18.17
11A	-26.52	-15.44	-30.84	-43.42	-29.07	-20.32	-22.36	-40.01	-47.05	-11.34	-33.41	-20.30	-34.72	-28.50	-38.63	-25.66

b	*BLYP*	*BLYP-D3*	*PBEPBE*	*PBEPBE-D3*	*B3LYP*	*B3LYP-D3*	*CAM-B3LYP*	*B2PLYP*	*B2PLYP-D3*	*wB97X-D*	*PBE0*	*PBEQIDH*	*PBEQIDH-D3(BJ)*
1b+7	0.00	0.00	0.00	0.00	0.00	0.00	0.00	0.00	0.00	0.00	0.00	0.00	0.00
TS5b	32.61	15.92	21.61	13.17	33.85	20.42	35.75	24.10	16.99	24.43	26.23	18.79	16.05
10b	20.07	10.14	4.03	-1.11	10.82	2.75	-0.48	2.68	-1.61	-7.45	-3.93	-12.57	-14.21
TS7b	38.17	21.91	24.92	16.71	38.47	25.36	37.77	28.57	21.60	26.93	28.76	21.65	18.94
9b	30.65	14.56	12.78	4.76	19.73	6.80	5.59	7.01	0.13	-6.83	3.18	-10.47	-13.17
TS6b	34.93	17.72	21.64	13.02	34.70	20.87	34.70	24.12	16.79	22.80	24.73	16.41	13.58
8b	22.98	7.30	5.00	-2.95	12.71	0.11	-0.22	0.77	-5.90	-13.03	-3.89	-16.54	-19.22
TS9b	46.76	30.28	21.34	13.25	39.01	25.69	28.35	23.79	16.64	13.39	16.44	2.76	0.11
12b	22.70	7.47	-8.65	-16.19	5.94	-6.26	-14.05	-10.86	-17.34	-30.55	-23.92	-41.20	-43.68
TS8b	56.69	40.17	31.94	23.79	47.98	34.62	35.97	31.92	24.78	21.85	25.73	10.78	8.04
11b	23.48	7.90	-8.26	-15.91	6.74	-5.76	-13.23	-10.06	-16.73	-29.97	-23.42	-40.68	-43.16

b	*M06*	*M06L*	*M062X*	*M06HF*	*rev-M06*	*rev-M06L*	*B97MV*	*wB97M-V*	*wB97X-V*	*VV10*	*M11*	*M11L*	*MN15*	*MN15L*	*DSD-PBEP86*	*mPW2PLYP-D*
1b+7	0.00	0.00	0.00	0.00	0.00	0.00	0.00	0.00	0.00	0.00	0.00	0.00	0.00	0.00	0.00	0.00
TS5b	20.57	17.56	23.58	26.85	24.65	23.06	16.83	26.08	27.50	12.91	28.23	21.30	22.32	17.10	14.85	17.79
10b	-3.66	5.09	-8.71	-19.89	-5.66	2.44	-0.65	-11.22	-14.15	3.58	-7.43	1.67	-10.44	-2.55	-9.41	-3.57
TS7b	24.73	22.48	27.62	28.99	28.38	27.14	20.70	27.34	27.45	17.49	31.85	25.32	24.11	20.51	18.47	22.46
9b	-0.95	8.73	-7.07	-18.25	-1.56	7.49	3.27	-11.71	-15.12	7.10	-7.45	6.97	-5.61	1.62	-10.38	-2.38
TS6b	19.95	17.96	22.75	23.76	23.98	23.11	16.63	23.77	24.30	13.48	27.26	20.72	20.38	16.52	12.75	17.10
8b	-7.20	1.67	-12.21	-22.99	-7.41	0.57	-3.14	-16.56	-20.17	0.23	-12.15	0.52	-11.10	-4.74	-16.03	-8.24
TS9b	16.93	23.55	14.18	2.76	16.90	24.42	18.34	9.22	6.37	19.63	14.16	23.28	12.42	15.99	5.27	14.66
12b	-22.12	-9.78	-27.23	-40.86	-24.79	-15.23	-17.84	-36.44	-43.53	-6.68	-28.84	-14.48	-30.41	-24.19	-34.17	-21.47
TS8b	26.34	35.66	20.92	5.61	24.90	35.14	28.33	15.49	12.97	29.58	20.60	32.39	20.21	25.75	12.45	22.62
11b	-21.64	-9.98	-26.43	-39.45	-24.31	-15.19	-17.42	-35.68	-42.77	-6.20	-28.49	-14.50	-30.06	-23.89	-33.44	-20.84

Table S7.5. The optimized energies (kcal/mol) at the corresponding functionals with aug-cc-pVTZ basis set.

	B3LYP				*B3LYP-D3*				*B2PLYP*				*PBE0*			
	ΔE	Δ(E+ZPE)	ΔH	ΔG	ΔE	Δ(E+ZPE)	ΔH	ΔG	ΔE	Δ(E+ZPE)	ΔH	ΔG	ΔE	Δ(E+ZPE)	ΔH	ΔG
1+7	0.00	0.00	0.00	0.00	0.00	0.00	0.00	0.00	0.00	0.00	0.00	0.00	0.00	0.00	0.00	0.00
TS5	28.69	29.88	29.35	43.40	17.58	18.93	18.33	32.69	20.93	22.03	21.49	35.68	21.42	22.64	22.10	36.24
10	3.44	6.71	5.79	20.33	-3.52	-0.13	-1.10	13.68	-3.55	-0.17	-1.14	13.67	-11.78	-8.38	-9.36	5.44
TS7	31.93	33.74	32.87	47.50	21.79	23.89	22.90	38.00	25.00	26.89	25.94	40.96	22.67	24.64	23.69	38.71
9	10.37	14.36	13.30	28.79	0.21	4.31	3.24	18.77	0.17	4.26	3.20	18.72	-6.13	-1.99	-3.06	12.45
TS6	28.68	30.59	29.60	44.95	16.88	18.86	18.40	32.51	20.06	21.72	21.32	35.19	18.94	20.86	19.86	35.28
8	6.88	11.25	10.06	25.80	-3.68	0.83	-0.38	15.41	-3.48	0.96	-0.24	15.53	-9.72	-5.22	-6.42	9.35
TS9	36.42	40.09	38.23	55.63	25.38	29.22	27.32	44.80	22.83	26.51	24.66	42.05	13.52	17.36	15.50	32.92
12	1.67	7.71	5.56	23.42	-8.21	-2.07	-4.21	13.62	-13.03	-6.83	-8.99	8.87	-28.12	-21.75	-23.94	-6.03
TS8	42.96	46.49	44.68	61.92	32.16	35.79	33.96	51.23	29.19	32.73	30.93	48.14	20.62	24.34	22.53	39.77
11	0.55	6.55	4.38	22.36	-9.67	-3.52	-5.70	12.31	-14.03	-7.88	-10.06	7.94	-29.63	-23.32	-25.52	-7.48
TS6-TS8	-14.29	-15.90	-15.09	-16.97	-15.28	-16.93	-15.56	-18.72	-9.12	-11.00	-9.61	-12.95	-1.68	-3.49	-2.67	-4.49
TS6-TS9	-7.74	-9.51	-8.63	-10.68	-8.50	-10.36	-8.91	-12.29	-2.77	-4.79	-3.34	-6.86	5.42	3.49	4.36	2.37

	M06HF				*MN15*				*PBEPBED3*				*CAM-B3LYP*			
	ΔE	Δ(E+ZPE)	ΔH	ΔG	ΔE	Δ(E+ZPE)	ΔH	ΔG	ΔE	Δ(E+ZPE)	ΔH	ΔG	ΔE	Δ(E+ZPE)	ΔH	ΔG
1+7	0.00	0.00	0.00	0.00	0.00	0.00	0.00	0.00	0.00	0.00	0.00	0.00	0.00	0.00	0.00	0.00
TS5	20.43	21.96	21.10	36.40	19.15	20.17	19.59	33.97	9.39	10.67	10.11	24.67	31.41	32.65	32.05	46.36
10	-24.86	-21.46	-22.52	-7.25	-17.15	-13.79	-14.83	0.31	-9.35	-6.15	-7.14	8.12	-7.03	-3.56	-4.54	10.22
TS7	20.26	22.87	21.48	38.05	19.83	21.67	20.66	35.99	12.03	14.08	13.10	28.48	32.49	34.46	33.48	48.62
9	-21.18	-17.20	-18.32	-2.47	-10.64	-6.64	-7.67	7.78	-4.15	-0.33	-1.39	14.48	-2.10	2.23	1.12	16.74
TS6	15.23	17.63	16.32	32.76	16.58	18.29	17.29	32.77	9.15	11.25	10.21	26.09	29.65	31.62	30.58	46.12
8	-24.08	-19.68	-20.93	-4.85	-14.29	-9.97	-11.13	4.56	-8.48	-4.27	-5.47	10.68	-5.02	-0.35	-1.58	14.27
TS9	2.22	5.85	3.86	21.72	12.42	16.01	14.18	31.51	11.64	15.26	13.39	31.23	26.17	30.15	28.22	45.77
12	-39.12	-33.34	-35.50	-17.45	-31.04	-24.87	-27.00	-9.25	-20.14	-14.20	-16.37	1.91	-16.87	-10.43	-12.63	5.33
TS8	7.65	11.34	9.38	27.08	18.98	22.49	20.72	37.83	18.99	22.42	20.61	38.22	32.49	36.36	34.49	51.87
11	-39.64	-34.06	-36.22	-18.09	-32.25	-26.12	-28.28	-10.37	-21.84	-15.92	-18.12	0.33	-17.90	-11.52	-13.74	4.34
TS6-TS8	7.58	6.30	6.94	5.68	-2.40	-4.19	-3.43	-5.06	-9.84	-11.17	-10.40	-12.13	-2.84	-4.74	-3.91	-5.75
TS6-TS9	13.01	11.78	12.46	11.04	4.16	2.28	3.11	1.26	-2.49	-4.01	-3.18	-5.14	3.48	1.48	2.36	0.35

	DSDPBEP86				*wB97XV*				*M062X*			
	ΔE	Δ(E+ZPE)	ΔH	ΔG	ΔE	Δ(E+ZPE)	ΔH	ΔG	ΔE	Δ(E+ZPE)	ΔH	ΔG
1+7	0.00	0.00	0.00	0.00	0.00	0.00	0.00	0.00	0.00	0.00	0.00	0.00
TS5	12.92	14.05	13.46	27.85	24.23	25.45	24.80	39.40	20.56	21.69	21.05	35.55
10	-14.81	-11.29	-12.30	2.70	-19.70	-16.17	-17.19	-2.13	-15.55	-12.15	-13.17	1.83
TS7	16.16	18.25	17.20	32.63	22.70	24.09	22.77	38.93	23.46	25.26	24.24	39.60
9	-15.03	-10.76	-11.84	3.73	-20.20	-15.77	-16.89	-1.15	-12.62	-8.48	-9.58	6.05
TS6	10.38	12.18	11.15	26.72	19.58	21.82	20.66	36.61	19.01	20.77	19.74	35.30
8	-18.64	-14.06	-15.27	0.55	-22.95	-18.22	-19.47	-3.49	-15.72	-11.21	-12.43	3.41
TS9	5.55	9.38	7.49	24.99	5.70	9.78	7.85	25.50	12.99	16.84	14.91	32.47
12	-34.38	-27.93	-30.11	-12.21	-43.84	-37.25	-39.48	-21.40	-28.50	-22.30	-24.48	-6.58
TS8	11.83	15.53	13.70	30.98	11.96	15.96	14.07	31.57	19.42	23.17	21.31	38.65
11	-35.39	-28.98	-31.19	-13.13	-44.87	-38.35	-40.60	-22.39	-29.63	-23.50	-25.70	-7.66
TS6-TS8	-1.46	-3.36	-2.55	-4.27	7.62	5.85	6.59	5.04	-0.41	-2.40	-1.56	-3.36
TS6-TS9	4.83	2.79	3.67	1.72	13.88	12.03	12.81	11.11	6.01	3.94	4.83	2.83

				PBEQIDH			*M11*			*DLPNO-CCSD(T)*
	ΔE	Δ(E+ZPE)	ΔH	ΔG	ΔE	Δ(E+ZPE)	ΔH	ΔG	ΔG	ΔE
1+7	0.00	0.00	0.00	0.00	0.00	0.00	0.00	0.00	0	0
TS5	15.92	17.08	16.50	30.84	24.32	25.40	24.75	39.29	33	20.1
10	-19.07	-15.51	-16.53	-1.53	-15.43	-12.11	-13.16	2.02	1	-14.3
TS7	17.68	19.76	18.71	34.07	26.23	28.17	27.09	42.63	37.3	23
9	-16.87	-12.54	-13.63	1.94	-13.58	-9.52	-10.60	5.02	0.9	-15.8
TS6	12.60	14.48	13.43	29.03	22.15	23.99	22.90	38.67	31.1	16.7
8	-20.47	-15.83	-17.04	-1.22	-16.73	-12.35	-13.55	2.28	-1.5	-18.8
TS9	1.67	5.58	3.71	21.14	11.85	15.62	13.71	31.26	32.1	14.9
12	-42.96	-36.37	-38.55	-20.67	-31.11	-25.05	-27.21	-9.33	-14.2	-34.6
TS8	8.56	12.36	10.54	27.78	18.28	21.98	20.14	37.46	26.9	9.4
11	-44.31	-37.77	-39.99	-21.94	-32.59	-26.62	-28.81	-10.75	-13.8	-33.9
TS6-TS8	4.04	2.12	2.88	1.26	3.87	2.01	2.77	1.21	4.2	7.3
TS6-TS9	10.93	8.90	9.72	7.90	10.30	8.37	9.19	7.41	-1	1.8

Table S7.6 The percentage of exchange part and PT2 part of the different functionals.

Functional	*%EXX*	*%PT2*	*Functional*	*%EXX*	*%PT2*
GGA			***Global Hybrids***		
BLYP	0	0	*B3LYP*	20	0
PBE	0	0	*PBE0*	25	0
M06-L	0	0	*M06*	27	0
revM06-L	0	0	*revM06*	40.4	0
M11-L	0	0	*MN15*	44	0
MN15-L	0	0	*M06-2X*	54	0
B97M-V	0	0	*M06-HF*	100	0
VV10	0	0			
Range-Separated Hybrids			***Double Hybrids***		
ωB97M-V	15/100	0	*B2-PLYP*	53	27
ωB97X-V	16.7/100	0	*mPW2-PLYP-D*	55	25
CAM-B3LYP	19/65	0	*DSD-PBEP86*	69	22/52
ωB97X-D	22/100	0	*PBE-QIDH*	69.336	33.333
M11	42.8/100	0	*PBE-QIDH-D3BJ*	69.336	33.333

References

1 M. Born and R. Oppenheimer, Zur Quantentheorie der Molekeln, *Ann. Phys.*, 1927, **389**, 457–484.

2 P.-O. Löwdin, Exchange, Correlation, and Spin Effects in Molecular and Solid-State Theory, *Rev. Mod. Phys.*, 1962, **34**, 80–87.

3 L. H. Thomas, The calculation of atomic fields, *Math. Proc. Camb. Philos. Soc.*, 1927, **23**, 542–548.

4 E. Fermi, Statistical method to determine some properties of atoms, *Rendiconti Lincei*, 1927, **6**, 602–607.

5 Y. Tomishima, Thomas-Fermi-Dirac Theory with Correlation Correction, *Prog. Theor. Phys.*, 1959, **22**, 1–11.

6 P. A. M. Dirac, Note on Exchange Phenomena in the Thomas Atom, *Math. Proc. Camb. Philos. Soc.*, 1930, **26**, 376–385.

7 J. C. Slater, A Simplification of the Hartree-Fock Method, *Phys. Rev.*, 1951, **81**, 385–390.

8 P. Hohenberg and W. Kohn, Inhomogeneous Electron Gas, *Phys. Rev.*, 1964, **136**, B864–B871.

9 W. Kohn and L. J. Sham, Self-Consistent Equations Including Exchange and Correlation Effects, *Phys. Rev.*, 1965, **140**, A1133–A1138.

10 W. Kohn and M. C. Holthausen, A Chemist's Guide to Density Functional Theory, 2nd Edition | Wiley.

11 F. Jensen, Introduction to Computational Chemistry, 2nd Edition | Wiley.

12 E. J. Baerends and O. V. Gritsenko, A Quantum Chemical View of Density Functional Theory, *J. Phys. Chem. A*, 1997, **101**, 5383–5403.

13 A. D. Becke, A multicenter numerical integration scheme for polyatomic molecules, *J. Chem. Phys.*, 1988, **88**, 2547–2553.

14 S. H. Vosko, L. Wilk and M. Nusair, Accurate spin-dependent electron liquid correlation energies for local spin density calculations: a critical analysis, *Can. J. Phys.*, 1980, **58**, 1200–1211.

15 A. D. Becke, Density-functional exchange-energy approximation with correct asymptotic behavior, *Phys. Rev. A*, 1988, **38**, 3098–3100.

16 J. P. Perdew, K. Burke and M. Ernzerhof, Generalized Gradient Approximation Made Simple, *Phys. Rev. Lett.*, 1996, **77**, 3865–3868.

17 J. P. Perdew, Density-functional approximation for the correlation energy of the inhomogeneous electron gas, *Phys. Rev. B*, 1986, **33**, 8822–8824.

18 A. D. Becke, A new mixing of Hartree–Fock and local density-functional theories, *J. Chem. Phys.*, 1993, **98**, 1372–1377.

19 L. A. Curtiss, K. Raghavachari, P. C. Redfern and J. A. Pople, Assessment of Gaussian-2 and density functional theories for the computation of enthalpies of formation, *J. Chem. Phys.*, 1997, **106**, 1063–1079.

20 C. Adamo and V. Barone, Toward reliable density functional methods without adjustable parameters: The PBE0 model, *J. Chem. Phys.*, 1999, **110**, 6158–6170.

21 A. D. Becke, Density-functional thermochemistry. III. The role of exact exchange, *J. Chem. Phys.*, 1993, **98**, 5648–5652.

22 Y. Zhao and D. G. Truhlar, The M06 suite of density functionals for main group thermochemistry, thermochemical kinetics, noncovalent interactions, excited states, and transition elements: two new functionals and systematic testing of four M06-class functionals and 12 other functionals, *Theor. Chem. Acc.*, 2008, **120**, 215–241.

23 M. E. Casida, in *Recent Advances in Computational Chemistry*, WORLD SCIENTIFIC, 1995, vol. 1, pp. 155–192.

24 L. Bernasconi, M. Sprik and J. Hutter, Time dependent density functional theory study of charge-transfer and intramolecular electronic excitations in acetone–water systems, *J. Chem. Phys.*, 2003, **119**, 12417–12431.

25 A. Görling and M. Levy, Correlation-energy functional and its high-density limit obtained from a coupling-constant perturbation expansion, *Phys. Rev. B*, 1993, **47**, 13105–13113.

26 A. Görling and M. Levy, Exact Kohn-Sham scheme based on perturbation theory, *Phys. Rev. A*, 1994, **50**, 196–204.

27 A. Szabo and N. S. Ostlund, *Modern Quantum Chemistry: Introduction to Advanced Electronic Structure Theory*, Dover Publications Inc., Mineola, New York, New edition., 1996.

28 Y. Zhao, B. J. Lynch and D. G. Truhlar, Doubly Hybrid Meta DFT: New Multi-Coefficient Correlation and Density Functional Methods for Thermochemistry and Thermochemical Kinetics, *J. Phys. Chem. A*, 2004, **108**, 4786–4791.

29 S. Grimme, Semiempirical hybrid density functional with perturbative second-order correlation, *J. Chem. Phys.*, 2006, **124**, 034108.

30 D. C. Langreth and J. P. Perdew, The exchange-correlation energy of a metallic surface, *Solid State Commun.*, 1975, **17**, 1425–1429.

31 O. Gunnarsson and B. I. Lundqvist, Exchange and correlation in atoms, molecules, and solids by the spin-density-functional formalism, *Phys. Rev. B*, 1976, **13**, 4274–4298.

32 O. Gunnarsson and B. I. Lundqvist, Erratum: Exchange and correlation in atoms, molecules, and solids by the spin-density-functional formalism, *Phys. Rev. B*, 1977, **15**, 6006–6006.

33 D. C. Langreth and J. P. Perdew, Exchange-correlation energy of a metallic surface: Wave-vector analysis, *Phys. Rev. B*, 1977, **15**, 2884–2901.

34 K. Sharkas, J. Toulouse and A. Savin, Double-hybrid density-functional theory made rigorous, *J. Chem. Phys.*, 2011, **134**, 064113.

35 J. Toulouse, K. Sharkas, E. Brémond and C. Adamo, Communication: Rationale for a new class of double-hybrid approximations in density-functional theory, *J. Chem. Phys.*, 2011, **135**, 101102.

36 S. M. O. Souvi, K. Sharkas and J. Toulouse, Double-hybrid density-functional theory with meta-generalized-gradient approximations, *J. Chem. Phys.*, 2014, **140**, 084107.

37 A. Görling and M. Levy, Correlation-energy functional and its high-density limit obtained from a coupling-constant perturbation expansion, *Phys. Rev. B*, 1993, **47**, 13105–13113.

38 M. Levy and J. P. Perdew, Hellmann-Feynman, virial, and scaling requisites for the exact universal density functionals. Shape of the correlation potential and diamagnetic susceptibility for atoms, *Phys. Rev. A*, 1985, **32**, 2010–2021.

39 S. Kozuch and J. M. L. Martin, DSD-PBEP86: in search of the best double-hybrid DFT with spin-component scaled MP2 and dispersion corrections, *Phys. Chem. Chem. Phys.*, 2011, **13**, 20104.

40 S. Grimme, Improved second-order Møller–Plesset perturbation theory by separate scaling of parallel- and antiparallel-spin pair correlation energies, *J. Chem. Phys.*, 2003, **118**, 9095–9102.

41 S. Kozuch, D. Gruzman and J. M. L. Martin, DSD-BLYP: A General Purpose Double Hybrid Density Functional Including Spin Component Scaling and Dispersion Correction, *J. Phys. Chem. C*, 2010, **114**, 20801–20808.

42 A. Karton, A. Tarnopolsky, J.-F. Lamère, G. C. Schatz and J. M. L. Martin, Highly Accurate First-Principles Benchmark Data Sets for the Parametrization and Validation of Density Functional and Other Approximate Methods. Derivation of a Robust, Generally Applicable, Double-Hybrid Functional for Thermochemistry and Thermochemical Kinetics, *J. Phys. Chem. A*, 2008, **112**, 12868–12886.

43 W. Kohn, Y. Meir and D. E. Makarov, van der Waals Energies in Density Functional Theory, *Phys. Rev. Lett.*, 1998, **80**, 4153–4156.

44 T. van Mourik and R. J. Gdanitz, A critical note on density functional theory studies on rare-gas dimers, *J. Chem. Phys.*, 2002, **116**, 9620–9623.

45 A. D. Becke, Density-functional thermochemistry. IV. A new dynamical correlation functional and implications for exact-exchange mixing, *J. Chem. Phys.*, 1996, **104**, 1040–1046.

46 T. Van Voorhis and G. E. Scuseria, A novel form for the exchange-correlation energy functional, *J. Chem. Phys.*, 1998, **109**, 400–410.

47 A. D. Becke, Simulation of delocalized exchange by local density functionals, *J. Chem. Phys.*, 2000, **112**, 4020–4026.
48 A. D. Boese and N. C. Handy, New exchange-correlation density functionals: The role of the kinetic-energy density, *J. Chem. Phys.*, 2002, **116**, 9559–9569.
49 J. Tao, J. P. Perdew, V. N. Staroverov and G. E. Scuseria, Climbing the Density Functional Ladder: Nonempirical Meta–Generalized Gradient Approximation Designed for Molecules and Solids, *Phys. Rev. Lett.*, 2003, **91**, 146401.
50 M. Lein, J. F. Dobson and E. K. U. Gross, Toward the description of van der Waals interactions within density functional theory, *J. Comput. Chem.*, 1999, **20**, 12–22.
51 Q. Wu and W. Yang, Empirical correction to density functional theory for van der Waals interactions, *J. Chem. Phys.*, 2002, **116**, 515–524.
52 M. Dion, H. Rydberg, E. Schröder, D. C. Langreth and B. I. Lundqvist, Van der Waals Density Functional for General Geometries, *Phys. Rev. Lett.*, 2004, **92**, 246401.
53 J. F. Dobson and T. Gould, Calculation of dispersion energies, *J. Phys. Condens. Matter*, 2012, **24**, 073201.
54 K. Lee, É. D. Murray, L. Kong, B. I. Lundqvist and D. C. Langreth, Higher-accuracy van der Waals density functional, *Phys. Rev. B*, 2010, **82**, 081101.
55 O. A. Vydrov and T. Van Voorhis, Nonlocal van der Waals Density Functional Made Simple, *Phys. Rev. Lett.*, 2009, **103**, 063004.
56 O. A. Vydrov and T. Van Voorhis, Nonlocal van der Waals density functional: The simpler the better, *J. Chem. Phys.*, 2010, **133**, 244103.
57 S. Grimme, S. Ehrlich and L. Goerigk, Effect of the damping function in dispersion corrected density functional theory, *J. Comput. Chem.*, 2011, **32**, 1456–1465.
58 K. T. Tang and J. P. Toennies, An improved simple model for the van der Waals potential based on universal damping functions for the dispersion coefficients, *J. Chem. Phys.*, 1984, **80**, 3726–3741.
59 E. R. Johnson and A. D. Becke, A post-Hartree-Fock model of intermolecular interactions: Inclusion of higher-order corrections, *J. Chem. Phys.*, 2006, **124**, 174104.
60 A density-functional model of the dispersion interaction: The Journal of Chemical Physics: Vol 123, No 15, https://aip.scitation.org/doi/abs/10.1063/1.2065267, (accessed March 24, 2022).
61 S. Grimme, J. Antony, S. Ehrlich and H. Krieg, A consistent and accurate *ab initio* parametrization of density functional dispersion correction (DFT-D) for the 94 elements H-Pu, *J. Chem. Phys.*, 2010, **132**, 154104.
62 K. E. Yousaf and E. N. Brothers, Applications of Screened Hybrid Density Functionals with Empirical Dispersion Corrections to Rare Gas Dimers and Solids, *J. Chem. Theory Comput.*, 2010, **6**, 864–872.
63 D. Bousquet, E. Brémond, J. C. Sancho-García, I. Ciofini and C. Adamo, Non-parametrized functionals with empirical dispersion corrections: A happy match?, *Theor. Chem. Acc.*, 2015, **134**, 1602.
64 J. C. Sancho-García, É. Brémond, M. Savarese, A. J. Pérez-Jiménez and C. Adamo, Partnering dispersion corrections with modern parameter-free double-hybrid density functionals, *Phys. Chem. Chem. Phys.*, 2017, **19**, 13481–13487.
65 J. C. Slater, Analytic Atomic Wave Functions, *Phys. Rev.*, 1932, **42**, 33–43.
66 Electronic wave functions - I. A general method of calculation for the stationary states of any molecular system, *Proc. R. Soc. Lond. Ser. Math. Phys. Sci.*, 1950, **200**, 542–554.
67 K. B. Lipkowitz and D. B. Boyd, *Reviews in computational chemistry*, Wiley, New York, 2002.
68 J. G. Hill, Gaussian basis sets for molecular applications, *Int. J. Quantum Chem.*, 2013, **113**, 21–34.
69 F. Weigend and R. Ahlrichs, Balanced basis sets of split valence, triple zeta valence and quadruple zeta valence quality for H to Rn: Design and assessment of accuracy, *Phys. Chem. Chem. Phys.*, 2005, **7**, 3297–3305.
70 T. H. Dunning, Gaussian basis sets for use in correlated molecular calculations. I. The atoms boron through neon and hydrogen, *J. Chem. Phys.*, 1989, **90**, 1007–1023.
71 A. J. Sadlej, Medium-size polarized basis sets for high-level-correlated calculations of molecular electric properties, *Theor. Chim. Acta*, 1991, **81**, 45–63.

72 W. Kutzelnigg, U. Fleischer and M. Schindler, in *Deuterium and Shift Calculation*, eds. U. Fleischer, W. Kutzelnigg, H.-H. Limbach, G. J. Martin, M. L. Martin and M. Schindler, Springer, Berlin, Heidelberg, 1991, pp. 165–262.

73 P. Hobza, H. L. Selzle and E. W. Schlag, Abinitio calculations on the structure, stabilization, and dipole moment of benzene···Ar complex, *J. Chem. Phys.*, 1991, **95**, 391–394.

74 G. Berthier, R. Savinelli and A. Pullman, Theoretical study of the binding of the chloride anion to water and alcohols, *Int. J. Quantum Chem.*, 1997, **63**, 567–574.

75 J. Makarewicz, Well-balanced basis sets for second-order Møller–Plesset treatment of argon-aromatic molecule complexes, *J. Chem. Phys.*, 2004, **121**, 8755–8768.

76 S. Lucidi and M. Sciandrone, A Derivative-Free Algorithm for Bound Constrained Optimization, *Comput. Optim. Appl.*, 2002, **21**, 119–142.

77 A. Karton, A computational chemist's guide to accurate thermochemistry for organic molecules, *WIREs Comput. Mol. Sci.*, 2016, **6**, 292–310.

78 J. M. L. Martin, in *Annual Reports in Computational Chemistry*, Elsevier, 2005, vol. 1, pp. 31–43.

79 D. A. Dixon, D. Feller and K. A. Peterson, in *Annual Reports in Computational Chemistry*, Elsevier, 2012, vol. 8, pp. 1–28.

80 J. A. Pople, M. Head-Gordon, D. J. Fox, K. Raghavachari and L. A. Curtiss, Gaussian-1 theory: A general procedure for prediction of molecular energies, *J. Chem. Phys.*, 1989, **90**, 5622–5629.

81 J. M. L. Martin and G. de Oliveira, Towards standard methods for benchmark quality ab initio thermochemistry—W1 and W2 theory, *J. Chem. Phys.*, 1999, **111**, 1843.

82 L. Goerigk, A. Hansen, C. Bauer, S. Ehrlich, A. Najibi and S. Grimme, A look at the density functional theory zoo with the advanced GMTKN55 database for general main group thermochemistry, kinetics and noncovalent interactions, *Phys. Chem. Chem. Phys.*, 2017, **19**, 32184–32215.

83 J. A. Pople, Nobel Lecture: Quantum chemical models, *Rev. Mod. Phys.*, 1999, **71**, 1267–1274.

84 A. Sengupta and K. Raghavachari, Solving the Density Functional Conundrum: Elimination of Systematic Errors To Derive Accurate Reaction Enthalpies of Complex Organic Reactions, *Org. Lett.*, 2017, **19**, 2576–2579.

85 N. Mardirossian and M. Head-Gordon, Thirty years of density functional theory in computational chemistry: an overview and extensive assessment of 200 density functionals, *Mol. Phys.*, 2017, **115**, 2315–2372.

86 L. A. Curtiss, P. C. Redfern and K. Raghavachari, Gaussian-4 theory, *J. Chem. Phys.*, 2007, **126**, 084108.

87 A. Tajti, P. G. Szalay, A. G. Császár, M. Kállay, J. Gauss, E. F. Valeev, B. A. Flowers, J. Vázquez and J. F. Stanton, HEAT: High accuracy extrapolated *ab initio* thermochemistry, *J. Chem. Phys.*, 2004, **121**, 11599–11613.

88 A. Karton, E. Rabinovich, J. M. L. Martin and B. Ruscic, W4 theory for computational thermochemistry: in pursuit of confident sub-kJ/mol predictions, *J. Chem. Phys.*, 2006, **125**, 144108.

89 J. H. Thorpe, C. A. Lopez, T. L. Nguyen, J. H. Baraban, D. H. Bross, B. Ruscic and J. F. Stanton, High-accuracy extrapolated ab initio thermochemistry. IV. A modified recipe for computational efficiency, *J. Chem. Phys.*, 2019, **150**, 224102.

90 Á. Ganyecz, M. Kállay and J. Csontos, Moderate-Cost *Ab Initio* Thermochemistry with Chemical Accuracy, *J. Chem. Theory Comput.*, 2017, **13**, 4193–4204.

91 B. Chan and L. Radom, W3X: A Cost-Effective Post-CCSD(T) Composite Procedure, *J. Chem. Theory Comput.*, 2013, **9**, 4769–4778.

92 Y. Zhao, L. Xia, X. Liao, Q. He, M. X. Zhao and D. G. Truhlar, Extrapolation of high-order correlation energies: the WMS model, *Phys. Chem. Chem. Phys.*, 2018, **20**, 27375–27384.

93 D. G. Liakos, Y. Guo and F. Neese, Comprehensive Benchmark Results for the Domain Based Local Pair Natural Orbital Coupled Cluster Method (DLPNO-CCSD(T)) for Closed- and Open-Shell Systems, *J. Phys. Chem. A*, 2020, **124**, 90–100.

94 F. Ballesteros, S. Dunivan and K. U. Lao, Coupled cluster benchmarks of large noncovalent complexes: The L7 dataset as well as DNA–ellipticine and buckycatcher–fullerene, *J. Chem. Phys.*, 2021, **154**, 154104.

95 W. C. McKee and P. von R. Schleyer, Correlation Effects on the Relative Stabilities of Alkanes, *J. Am. Chem. Soc.*, 2013, **135**, 13008–13014.

96 S. Grimme, Accurate description of van der Waals complexes by density functional theory including empirical corrections, *J. Comput. Chem.*, 2004, **25**, 1463–1473.

97 J. C. Sancho-García and C. Adamo, Double-hybrid density functionals: merging wavefunction and density approaches to get the best of both worlds, *Phys. Chem. Chem. Phys.*, 2013, **15**, 14581.

98 L. Goerigk and S. Grimme, Double-hybrid density functionals, *WIREs Comput. Mol. Sci.*, 2014, **4**, 576–600.

99 É. Brémond, M. Savarese, Á. J. Pérez-Jiménez, J. C. Sancho-García and C. Adamo, Systematic Improvement of Density Functionals through Parameter-Free Hybridization Schemes, *J. Phys. Chem. Lett.*, 2015, **6**, 3540–3545.

100 N. Q. Su, Z. Zhu and X. Xu, Doubly hybrid density functionals that correctly describe both density and energy for atoms, *Proc. Natl. Acad. Sci.*, 2018, **115**, 2287–2292.

101 E. Brémond, I. Ciofini, J. C. Sancho-García and C. Adamo, Nonempirical Double-Hybrid Functionals: An Effective Tool for Chemists, *Acc. Chem. Res.*, 2016, **49**, 1503–1513.

102 J. M. L. Martin and G. Santra, Empirical Double-Hybrid Density Functional Theory: A 'Third Way' in Between WFT and DFT, *Isr. J. Chem.*, 2020, **60**, 787–804.

103 E. Semidalas and J. M. L. Martin, Canonical and DLPNO-Based G4(MP2)XK-Inspired Composite Wave Function Methods Parametrized against Large and Chemically Diverse Training Sets: Are They More Accurate and/or Robust than Double-Hybrid DFT?, *J. Chem. Theory Comput.*, 2020, **16**, 4238–4255.

104 N. Mehta, M. Casanova-Páez and L. Goerigk, Semi-empirical or non-empirical double-hybrid density functionals: which are more robust?, *Phys. Chem. Chem. Phys.*, 2018, **20**, 23175–23194.

105 D. Bakowies, Assessment of Density Functional Theory for Thermochemical Approaches Based on Bond Separation Reactions, *J. Phys. Chem. A*, 2013, **117**, 228–243.

106 J. S. García, É. Brémond, M. Campetella, I. Ciofini and C. Adamo, Small Basis Set Allowing the Recovery of Dispersion Interactions with Double-Hybrid Functionals, *J. Chem. Theory Comput.*, 2019, **15**, 2944–2953.

107 É. Brémond, I. Ciofini, J. C. Sancho-García and C. Adamo, Double-Hybrid Functionals and Tailored Basis Set: Fullerene (C_{60}) Dimer and Isomers as Test Cases, *J. Phys. Chem. A*, 2019, **123**, 10040–10046.

108 B. Tirri, I. Ciofini, J. C. Sancho-García, C. Adamo and É. Brémond, Computation of covalent and noncovalent structural parameters at low computational cost: Efficiency of the DH-SVPD method, *Int. J. Quantum Chem.*, 2020, **120**, e26233.

109 A. J. C. Varandas, Zeroth-order exchange energy as a criterion for optimized atomic basis sets in interatomic force calculations. Application to He2, *Chem. Phys. Lett.*, 1980, **69**, 222–224.

110 R. A. Kendall, T. H. Dunning and R. J. Harrison, Electron affinities of the first-row atoms revisited. Systematic basis sets and wave functions, *J. Chem. Phys.*, 1992, **96**, 6796–6806.

111 Y. Zhao and D. G. Truhlar, A new local density functional for main-group thermochemistry, transition metal bonding, thermochemical kinetics, and noncovalent interactions, *J. Chem. Phys.*, 2006, **125**, 194101.

112 C. Adamo and V. Barone, Toward reliable density functional methods without adjustable parameters: The PBE0 model, *J Chem Phys*, , DOI:10.1063/1.478522.

113 T. Yanai, D. P. Tew and N. C. Handy, A new hybrid exchange–correlation functional using the Coulomb-attenuating method (CAM-B3LYP), *Chem. Phys. Lett.*, 2004, **393**, 51–57.

114 J.-D. Chai and M. Head-Gordon, Long-range corrected hybrid density functionals with damped atom–atom dispersion corrections, *Phys. Chem. Chem. Phys.*, 2008, **10**, 6615.

115 E. Brémond and C. Adamo, Seeking for parameter-free double-hybrid functionals: The PBE0-DH model, *J. Chem. Phys.*, 2011, **135**, 024106.

116 É. Brémond, J. C. Sancho-García, Á. J. Pérez-Jiménez and C. Adamo, Communication: Double-hybrid functionals from adiabatic-connection: The QIDH model, *J. Chem. Phys.*, 2014, **141**, 031101.

117 G. Santra, N. Sylvetsky and J. M. L. Martin, Minimally Empirical Double-Hybrid Functionals Trained against the GMTKN55 Database: revDSD-PBEP86-D4, revDOD-PBE-D4, and DOD-SCAN-D4, *J. Phys. Chem. A*, 2019, **123**, 5129–5143.

118 A. D. Becke and E. R. Johnson, Exchange-hole dipole moment and the dispersion interaction revisited, *J. Chem. Phys.*, 2007, **127**, 154108.

119 C. R. Kemnitz, J. L. Mackey, M. J. Loewen, J. L. Hargrove, J. L. Lewis, W. E. Hawkins and A. F. Nielsen, Origin of Stability in Branched Alkanes, *Chem. - Eur. J.*, 2010, **16**, 6942–6949.

120 S. Gronert, Electron Delocalization Is Not a Satisfactory Explanation for the Preference for Branching in the Alkanes, *Chem. - Eur. J.*, 2013, **19**, 11090–11092.

121 Y. Zhao and D. G. Truhlar, A Density Functional That Accounts for Medium-Range Correlation Energies in Organic Chemistry, *Org. Lett.*, 2006, **8**, 5753–5755.

122 A. Karton, D. Gruzman and J. M. L. Martin, Benchmark Thermochemistry of the $C_n H_{2n+2}$ Alkane Isomers (n = 2−8) and Performance of DFT and Composite Ab Initio Methods for Dispersion-Driven Isomeric Equilibria, *J. Phys. Chem. A*, 2009, **113**, 8434–8447.

123 J.-W. Song, T. Tsuneda, T. Sato and K. Hirao, Calculations of Alkane Energies Using Long-Range Corrected DFT Combined with Intramolecular van der Waals Correlation, *Org. Lett.*, 2010, **12**, 1440–1443.

124 S. Grimme, *n* -Alkane Isodesmic Reaction Energy Errors in Density Functional Theory Are Due to Electron Correlation Effects, *Org. Lett.*, 2010, **12**, 4670–4673.

125 H. Krieg and S. Grimme, Thermochemical benchmarking of hydrocarbon bond separation reaction energies: Jacob's ladder is not reversed!, *Mol. Phys.*, 2010, **108**, 2655–2666.

126 E. R. Johnson, J. Contreras-García and W. Yang, Density-Functional Errors in Alkanes: A Real-Space Perspective, *J. Chem. Theory Comput.*, 2012, **8**, 2676–2681.

127 W. J. Hehre, R. Ditchfield, L. Radom and J. A. Pople, Molecular orbital theory of the electronic structure of organic compounds. V. Molecular theory of bond separation, *J. Am. Chem. Soc.*, 1970, **92**, 4796–4801.

128 M. Modrzejewski, G. Chałasiński and M. M. Szczęśniak, Range-Separated meta-GGA Functional Designed for Noncovalent Interactions, *J. Chem. Theory Comput.*, 2014, **10**, 4297–4306.

129 M. D. Wodrich, C. Corminboeuf and P. von R. Schleyer, Systematic Errors in Computed Alkane Energies Using B3LYP and Other Popular DFT Functionals, *Org. Lett.*, 2006, **8**, 3631–3634.

130 https://www.chemie.uni-bonn.de/pctc/mulliken-center/software/GMTKN.

131 Frisch, M. J.; Trucks, G. W.; Schlegel, H. B.; Scuseria, G. E.; Robb, M. A.; Cheeseman, J. R.; Scalmani, G.; Barone, V.; Petersson, G. A.; Nakatsuji, H.; Li, X.; Caricato, M.; Marenich, A. V.; Bloino, J.; Janesko, B. G.; Gomperts, R.; Mennucci, B.; Hratchian, H. P.; Ortiz, J. V.; Izmaylov, A. F.; Sonnenberg, J. L.; Williams-Young, D.; Ding, F.; Lipparini, F.; Egidi, F.; Goings, J.; Peng, B.; Petrone, A.; Henderson, T.; Ranasinghe, D.; Zakrzewski, V. G.; Gao, J.; Rega, N.; Zheng, G.; Liang, W.; Hada, M.; Ehara, M.; Toyota, K.; Fukuda, R.; Hasegawa, J.; Ishida, M.; Nakajima, T.; Honda, Y.; Kitao, O.; Nakai, H.; Vreven, T.; Throssell, K.; Montgomery, J. A., Jr.; Peralta, J. E.; Ogliaro, F.; Bearpark, M. J.; Heyd, J. J.; Brothers, E. N.; Kudin, K. N.; Staroverov, V. N.; Keith, T. A.; Kobayashi, R.; Normand, J.; Raghavachari, K.; Rendell, A. P.; Burant, J. C.; Iyengar, S. S.; Tomasi, J.; Cossi, M.; Millam, J. M.; Klene, M.; Adamo, C.; Cammi, R.; Ochterski, J. W.; Martin, R. L.; Morokuma, K.; Farkas, O.; Foresman, J. B.; Fox, D. J., *Gaussian 16, Revision C.01*, Gaussian, Inc, Wallingford CT, 2016.

132 B. Ruscic, R. E. Pinzon, M. L. Morton, G. von Laszevski, S. J. Bittner, S. G. Nijsure, K. A. Amin, M. Minkoff and A. F. Wagner, Introduction to Active Thermochemical Tables: Several "Key" Enthalpies of Formation Revisited, *J. Phys. Chem. A*, 2004, **108**, 9979–9997.

133 Active Thermochemical Tables - Home, https://atct.anl.gov/, (accessed February 22, 2022).

134 N. O. of D. and Informatics, NIST Chemistry WebBook, https://webbook.nist.gov/chemistry/, (accessed February 23, 2022).

135 É. Brémond, M. Savarese, N. Q. Su, Á. J. Pérez-Jiménez, X. Xu, J. C. Sancho-García and C. Adamo, Benchmarking Density Functionals on Structural Parameters of Small-/Medium-Sized Organic Molecules, *J. Chem. Theory Comput.*, 2016, **12**, 459–465.

136 A. Najibi and L. Goerigk, The Nonlocal Kernel in van der Waals Density Functionals as an Additive Correction: An Extensive Analysis with Special Emphasis on the B97M-V and ωB97M-V Approaches, *J. Chem. Theory Comput.*, 2018, **14**, 5725–5738.

137A. Karton, Can density functional theory 'Cope' with highly fluxional shapeshifting molecules?, *Chem. Phys.*, 2021, **540**, 111013.

138 H. Li, B. Tirri, E. Brémond, J. C. Sancho-García and C. Adamo, Beyond Chemical Accuracy for Alkane Thermochemistry: The DHthermo Approach, *J. Org. Chem.*, 2021, **86**, 5538–5545.

139 Y.-M. Chang, Y.-S. Wang and S. D. Chao, A minimum quantum chemistry CCSD(T)/CBS dataset of dimeric interaction energies for small organic functional groups, *J. Chem. Phys.*, 2020, **153**, 154301.
140 T. Schwabe and S. Grimme, Double-hybrid density functionals with long-range dispersion corrections: higher accuracy and extended applicability, *Phys. Chem. Chem. Phys.*, 2007, **9**, 3397.
141 C. Riplinger and F. Neese, An efficient and near linear scaling pair natural orbital based local coupled cluster method, *J. Chem. Phys.*, 2013, **138**, 034106.
142 F. Neese, Software update: the ORCA program system, version 4.0, *WIREs Comput. Mol. Sci.*, 2018, **8**, e1327.
143 D. G. Liakos, M. Sparta, M. K. Kesharwani, J. M. L. Martin and F. Neese, Exploring the Accuracy Limits of Local Pair Natural Orbital Coupled-Cluster Theory, *J. Chem. Theory Comput.*, 2015, **11**, 1525–1539.
144 T. Helgaker, W. Klopper, H. Koch and J. Noga, Basis-set convergence of correlated calculations on water, *J. Chem. Phys.*, 1997, **106**, 9639–9646.
145 A. Karton, How reliable is DFT in predicting relative energies of polycyclic aromatic hydrocarbon isomers? comparison of functionals from different rungs of jacob's ladder, *J. Comput. Chem.*, 2017, **38**, 370–382.
146 J. Řezáč and P. Hobza, Describing Noncovalent Interactions beyond the Common Approximations: How Accurate Is the "Gold Standard," CCSD(T) at the Complete Basis Set Limit?, *J. Chem. Theory Comput.*, 2013, **9**, 2151–2155.
147A. Karton, Can density functional theory 'Cope' with highly fluxional shapeshifting molecules?, *Chem. Phys.*, 2021, **540**, 111013.
148 M. Savarese, É. Brémond and C. Adamo, Exploring the limits of recent exchange–correlation functionals in modeling lithium/benzene interaction, *Theor. Chem. Acc.*, 2016, **135**, 99.
149 K. Tonigold and A. Groß, Dispersive interactions in water bilayers at metallic surfaces: A comparison of the PBE and RPBE functional including semiempirical dispersion corrections, *J. Comput. Chem.*, 2012, **33**, 695–701.
150 F. Di Meo, I. Bayach, P. Trouillas and J.-C. Sancho-García, Unraveling the performance of dispersion-corrected functionals for the accurate description of weakly bound natural polyphenols, *J. Mol. Model.*, 2015, **21**, 291.
151 C. W. Bauschlicher and S. R. Langhoff, Quantum Mechanical Calculations to Chemical Accuracy, *Science*, 1991, **254**, 394–398.
152 K. N. Houk and F. Liu, Holy Grails for Computational Organic Chemistry and Biochemistry, *Acc. Chem. Res.*, 2017, **50**, 539–543.
153 A. Karton, N. Sylvetsky and J. M. L. Martin, W4-17: A diverse and high-confidence dataset of atomization energies for benchmarking high-level electronic structure methods, *J. Comput. Chem.*, 2017, **38**, 2063–2075.
154 B. Chan, How to computationally calculate thermochemical properties objectively, accurately, and as economically as possible, *Pure Appl. Chem.*, 2017, **89**, 699–713.
155 P. Pinski, C. Riplinger, E. F. Valeev and F. Neese, Sparse maps—A systematic infrastructure for reduced-scaling electronic structure methods. I. An efficient and simple linear scaling local MP2 method that uses an intermediate basis of pair natural orbitals, *J. Chem. Phys.*, 2015, **143**, 034108.
156 C. Riplinger, P. Pinski, U. Becker, E. F. Valeev and F. Neese, Sparse maps—A systematic infrastructure for reduced-scaling electronic structure methods. II. Linear scaling domain based pair natural orbital coupled cluster theory, *J. Chem. Phys.*, 2016, **144**, 024109.
157 Y. Guo, C. Riplinger, U. Becker, D. G. Liakos, Y. Minenkov, L. Cavallo and F. Neese, Communication: An improved linear scaling perturbative triples correction for the domain based local pair-natural orbital based singles and doubles coupled cluster method [DLPNO-CCSD(T)], *J. Chem. Phys.*, 2018, **148**, 011101.
158 H. S. Yu, S. L. Li and D. G. Truhlar, Perspective: Kohn-Sham density functional theory descending a staircase, *J. Chem. Phys.*, 2016, **145**, 130901.
159 A. D. Becke, Perspective: Fifty years of density-functional theory in chemical physics, *J. Chem. Phys.*, 2014, **140**, 18A301.
160 N. Q. Su and X. Xu, The XYG3 type of doubly hybrid density functionals, *WIREs Comput. Mol. Sci.*, 2016, **6**, 721–747.

161 É. Brémond, Á. J. Pérez-Jiménez, J. C. Sancho-García and C. Adamo, Range-separated hybrid density functionals made simple, *J. Chem. Phys.*, 2019, **150**, 201102.
162 M. Casanova-Páez, M. B. Dardis and L. Goerigk, ωB2PLYP and ωB2GPPLYP: The First Two Double-Hybrid Density Functionals with Long-Range Correction Optimized for Excitation Energies, *J. Chem. Theory Comput.*, 2019, **15**, 4735–4744.
163 É. Brémond, M. Savarese, Á. J. Pérez-Jiménez, J. C. Sancho-García and C. Adamo, Range-Separated Double-Hybrid Functional from Nonempirical Constraints, *J. Chem. Theory Comput.*, 2018, **14**, 4052–4062.
164 I. Y. Zhang and X. Xu, Reaching a Uniform Accuracy for Complex Molecular Systems: Long-Range-Corrected XYG3 Doubly Hybrid Density Functional, *J. Phys. Chem. Lett.*, 2013, **4**, 1669–1675.
165 É. Brémond, M. Savarese, J. C. Sancho-García, Á. J. Pérez-Jiménez and C. Adamo, Quadratic integrand double-hybrid made spin-component-scaled, *J. Chem. Phys.*, 2016, **144**, 124104.
166 I. Y. Zhang, N. Q. Su, É. A. G. Brémond, C. Adamo and X. Xu, Doubly hybrid density functional xDH-PBE0 from a parameter-free global hybrid model PBE0, *J. Chem. Phys.*, 2012, **136**, 174103.
167 I. Y. Zhang, X. Xu, Y. Jung and W. A. Goddard, A fast doubly hybrid density functional method close to chemical accuracy using a local opposite spin ansatz, *Proc. Natl. Acad. Sci.*, 2011, **108**, 19896–19900.
168 A. Najibi, M. Casanova-Páez and L. Goerigk, Analysis of Recent BLYP- and PBE-Based Range-Separated Double-Hybrid Density Functional Approximations for Main-Group Thermochemistry, Kinetics, and Noncovalent Interactions, *J. Phys. Chem. A*, 2021, **125**, 4026–4035.
169 C. Puzzarini and V. Barone, Diving for Accurate Structures in the Ocean of Molecular Systems with the Help of Spectroscopy and Quantum Chemistry, *Acc. Chem. Res.*, 2018, **51**, 548–556.
170 G. L. Stoychev, A. A. Auer and F. Neese, Efficient and Accurate Prediction of Nuclear Magnetic Resonance Shielding Tensors with Double-Hybrid Density Functional Theory, *J. Chem. Theory Comput.*, 2018, **14**, 4756–4771.
171 J. L. Bao, L. Gagliardi and D. G. Truhlar, Self-Interaction Error in Density Functional Theory: An Appraisal, *J. Phys. Chem. Lett.*, 2018, **9**, 2353–2358.
172 A. J. Cohen, P. Mori-Sánchez and W. Yang, Insights into Current Limitations of Density Functional Theory, *Science*, 2008, **321**, 792–794.
173 G. Santra, M. Cho and J. M. L. Martin, Exploring Avenues beyond Revised DSD Functionals: I. Range Separation, with *x* DSD as a Special Case, *J. Phys. Chem. A*, 2021, **125**, 4614–4627.
174 A. Tarnopolsky, A. Karton, R. Sertchook, D. Vuzman and J. M. L. Martin, Double-Hybrid Functionals for Thermochemical Kinetics, *J. Phys. Chem. A*, 2008, **112**, 3–8.
175 V. K. Prasad, Z. Pei, S. Edelmann, A. Otero-de-la-Roza and G. A. DiLabio, BH9, a New Comprehensive Benchmark Data Set for Barrier Heights and Reaction Energies: Assessment of Density Functional Approximations and Basis Set Incompleteness Potentials, *J. Chem. Theory Comput.*, 2022, **18**, 151–166.
176 F. Neese, F. Wennmohs, U. Becker and C. Riplinger, The ORCA quantum chemistry program package, *J. Chem. Phys.*, 2020, **152**, 224108.
177 D. Rappoport and F. Furche, Property-optimized Gaussian basis sets for molecular response calculations, *J. Chem. Phys.*, 2010, **133**, 134105.
178 F. Neese, F. Wennmohs, A. Hansen and U. Becker, Efficient, approximate and parallel Hartree–Fock and hybrid DFT calculations. A 'chain-of-spheres' algorithm for the Hartree–Fock exchange, *Chem. Phys.*, 2009, **356**, 98–109.
179 A. Karton and L. Goerigk, Accurate reaction barrier heights of pericyclic reactions: Surprisingly large deviations for the CBS-QB3 composite method and their consequences in DFT benchmark studies, *J. Comput. Chem.*, 2015, **36**, 622–632.
180 J.-D. Chai and M. Head-Gordon, Long-range corrected double-hybrid density functionals, *J. Chem. Phys.*, 2009, **131**, 174105.
181 D. Bousquet, E. Brémond, J. C. Sancho-García, I. Ciofini and C. Adamo, Non-parametrized functionals with empirical dispersion corrections: A happy match?, *Theor. Chem. Acc.*, 2014, **134**, 1602.
182 S. Kozuch and J. M. L. Martin, Spin-component-scaled double hybrids: An extensive search for the best fifth-rung functionals blending DFT and perturbation theory, *J. Comput. Chem.*, 2013, **34**, 2327–2344.

183 L. Goerigk and S. Grimme, A thorough benchmark of density functional methods for general main group thermochemistry, kinetics, and noncovalent interactions, *Phys. Chem. Chem. Phys.*, 2011, **13**, 6670.
184 S. Grimme, J. Antony, S. Ehrlich and H. Krieg, A consistent and accurate *ab initio* parametrization of density functional dispersion correction (DFT-D) for the 94 elements H-Pu, *J. Chem. Phys.*, 2010, **132**, 154104.
185 N. Mardirossian and M. Head-Gordon, ωB97X-V: A 10-parameter, range-separated hybrid, generalized gradient approximation density functional with nonlocal correlation, designed by a survival-of-the-fittest strategy, *Phys. Chem. Chem. Phys.*, 2014, **16**, 9904.
186 Y. Zhao, N. E. Schultz and D. G. Truhlar, Design of Density Functionals by Combining the Method of Constraint Satisfaction with Parametrization for Thermochemistry, Thermochemical Kinetics, and Noncovalent Interactions, *J. Chem. Theory Comput.*, 2006, **2**, 364–382.
187 H. S. Yu, X. He, S. L. Li and D. G. Truhlar, MN15: A Kohn–Sham global-hybrid exchange–correlation density functional with broad accuracy for multi-reference and single-reference systems and noncovalent interactions, *Chem. Sci.*, 2016, **7**, 5032–5051.
188 M. Ernzerhof and G. E. Scuseria, Assessment of the Perdew–Burke–Ernzerhof exchange-correlation functional, *J. Chem. Phys.*, 1999, **110**, 5029–5036.
189 A. D. Becke and E. R. Johnson, A unified density-functional treatment of dynamical, nondynamical, and dispersion correlations, *J. Chem. Phys.*, 2007, **127**, 124108.
190 E. R. Johnson, P. Mori-Sánchez, A. J. Cohen and W. Yang, Delocalization errors in density functionals and implications for main-group thermochemistry, *J. Chem. Phys.*, 2008, **129**, 204112.
191 J. C. Sancho-García, É. Brémond, M. Savarese, A. J. Pérez-Jiménez and C. Adamo, Partnering dispersion corrections with modern parameter-free double-hybrid density functionals, *Phys. Chem. Chem. Phys.*, 2017, **19**, 13481–13487.
192 A. Gosset, Š. N. Lachmanová, S. Cherraben, G. Bertho, J. Forté, C. Perruchot, H.-P. J. de Rouville, L. Pospíšil, M. Hromadová, É. Brémond and P. P. Lainé, On the Supra-LUMO Interaction: Case Study of a Sudden Change of Electronic Structure as a Functional Emergence, *Chem. – Eur. J.*, 2021, **27**, 17889–17899.
193 H. Li, E. Brémond, J. C. Sancho-García and C. Adamo, Pairing double hybrid functionals with a tailored basis set for an accurate thermochemistry of hydrocarbons, *RSC Adv.*, 2021, **11**, 26073–26082.
194 J. P. Perdew, in *AIP Conference Proceedings*, AIP, Antwerp (Belgium), 2001, vol. 577, pp. 1–20.
195 M. Ernzerhof, Construction of the adiabatic connection, *Chem. Phys. Lett.*, 1996, **263**, 499–506.
196 J. Klimeš and A. Michaelides, Perspective: Advances and challenges in treating van der Waals dispersion forces in density functional theory, *J. Chem. Phys.*, 2012, **137**, 120901.
197 Y. Zhao and D. G. Truhlar, Density Functionals with Broad Applicability in Chemistry, *Acc. Chem. Res.*, 2008, **41**, 157–167.
198 B. Brauer, M. K. Kesharwani, S. Kozuch and J. M. L. Martin, The S66x8 benchmark for noncovalent interactions revisited: explicitly correlated ab initio methods and density functional theory, *Phys. Chem. Chem. Phys.*, 2016, **18**, 20905–20925.
199 J. Řezáč, K. E. Riley and P. Hobza, S66: A Well-balanced Database of Benchmark Interaction Energies Relevant to Biomolecular Structures, *J. Chem. Theory Comput.*, 2011, **7**, 2427–2438.
200 R. Sedlak, T. Janowski, M. Pitoňák, J. Řezáč, P. Pulay and P. Hobza, Accuracy of Quantum Chemical Methods for Large Noncovalent Complexes, *J. Chem. Theory Comput.*, 2013, **9**, 3364–3374.
201 Z. Ni, Y. Guo, F. Neese, W. Li and S. Li, Cluster-in-Molecule Local Correlation Method with an Accurate Distant Pair Correction for Large Systems, *J. Chem. Theory Comput.*, 2021, **17**, 756–766.
202 M. Feyereisen, G. Fitzgerald and A. Komornicki, Use of approximate integrals in ab initio theory. An application in MP2 energy calculations, *Chem. Phys. Lett.*, 1993, **208**, 359–363.
203 F. Neese, F. Wennmohs and A. Hansen, Efficient and accurate local approximations to coupled-electron pair approaches: An attempt to revive the pair natural orbital method, *J. Chem. Phys.*, 2009, **130**, 114108.
204 F. Neese, The ORCA program system, *WIREs Comput. Mol. Sci.*, 2012, **2**, 73–78.
205 F. Neese, Software update: the ORCA program system, version 4.0, *WIREs Comput. Mol. Sci.*, , DOI:10.1002/wcms.1327.
206 F. Weigend, Accurate Coulomb-fitting basis sets for H to Rn, *Phys. Chem. Chem. Phys.*, 2006, **8**, 1057.

207 B. Brauer, M. K. Kesharwani and J. M. L. Martin, Some Observations on Counterpoise Corrections for Explicitly Correlated Calculations on Noncovalent Interactions, *J. Chem. Theory Comput.*, 2014, **10**, 3791–3799.
208 J. Calbo, E. Ortí, J. C. Sancho-García and J. Aragó, Accurate Treatment of Large Supramolecular Complexes by Double-Hybrid Density Functionals Coupled with Nonlocal van der Waals Corrections, *J. Chem. Theory Comput.*, 2015, **11**, 932–939.
209 Z. Ni, W. Li and S. Li, Fully optimized implementation of the cluster-in-molecule local correlation approach for electron correlation calculations of large systems: Fully Optimized Implementation of the Cluster-in-Molecule Local Correlation Approach for Electron Correlation Calculations of Large Systems, *J. Comput. Chem.*, 2019, **40**, 1130–1140.
210 J. Calbo, J. C. Sancho-García, E. Ortí and J. Aragó, DLPNO-CCSD(T) scaled methods for the accurate treatment of large supramolecular complexes, *J. Comput. Chem.*, 2017, **38**, 1869–1878.
211 D. Wu and D. G. Truhlar, How Accurate Are Approximate Density Functionals for Noncovalent Interaction of Very Large Molecular Systems?, *J. Chem. Theory Comput.*, 2021, **17**, 3967–3973.
212 Y. S. Al-Hamdani, P. R. Nagy, A. Zen, D. Barton, M. Kállay, J. G. Brandenburg and A. Tkatchenko, Interactions between large molecules pose a puzzle for reference quantum mechanical methods, *Nat. Commun.*, 2021, **12**, 3927.
213 E. Caldeweyher, S. Ehlert, A. Hansen, H. Neugebauer, S. Spicher, C. Bannwarth and S. Grimme, A generally applicable atomic-charge dependent London dispersion correction, *J. Chem. Phys.*, 2019, **150**, 154122.
214 G. Cavallo, P. Metrangolo, R. Milani, T. Pilati, A. Priimagi, G. Resnati and G. Terraneo, The Halogen Bond, *Chem. Rev.*, 2016, **116**, 2478–2601.
215 P. Politzer, P. Lane, M. C. Concha, Y. Ma and J. S. Murray, An overview of halogen bonding, *J. Mol. Model.*, 2007, **13**, 305–311.
216 K. E. Riley and P. Hobza, Investigations into the Nature of Halogen Bonding Including Symmetry Adapted Perturbation Theory Analyses, *J. Chem. Theory Comput.*, 2008, **4**, 232–242.
217 P. Politzer, J. S. Murray and T. Clark, Halogen bonding and other σ-hole interactions: a perspective, *Phys. Chem. Chem. Phys.*, 2013, **15**, 11178.
218 G. R. Desiraju, P. S. Ho, L. Kloo, A. C. Legon, R. Marquardt, P. Metrangolo, P. Politzer, G. Resnati and K. Rissanen, Definition of the halogen bond (IUPAC Recommendations 2013), *Pure Appl. Chem.*, 2013, **85**, 1711–1713.
219 R. Wilcken, M. O. Zimmermann, A. Lange, A. C. Joerger and F. M. Boeckler, Principles and Applications of Halogen Bonding in Medicinal Chemistry and Chemical Biology, *J. Med. Chem.*, 2013, **56**, 1363–1388.
220 M. R. Scholfield, C. M. V. Zanden, M. Carter and P. S. Ho, Halogen bonding (X-bonding): A biological perspective: Halogen Bonding (X-Bonding), *Protein Sci.*, 2013, **22**, 139–152.
221 S. Kawai, A. Sadeghi, F. Xu, L. Peng, A. Orita, J. Otera, S. Goedecker and E. Meyer, Extended Halogen Bonding between Fully Fluorinated Aromatic Molecules, *ACS Nano*, 2015, **9**, 2574–2583.
222 R. Bertani, P. Sgarbossa, A. Venzo, F. Lelj, M. Amati, G. Resnati, T. Pilati, P. Metrangolo and G. Terraneo, Halogen bonding in metal–organic–supramolecular networks, *Coord. Chem. Rev.*, 2010, **254**, 677–695.
223 V. V. Sivchik, A. I. Solomatina, Y.-T. Chen, A. J. Karttunen, S. P. Tunik, P.-T. Chou and I. O. Koshevoy, Halogen Bonding to Amplify Luminescence: A Case Study Using a Platinum Cyclometalated Complex, *Angew. Chem.*, 2015, **127**, 14263–14266.
224 P. Politzer and J. S. Murray, Halogen Bonding: An Interim Discussion, *ChemPhysChem*, 2013, **14**, 278–294.
225 P. Politzer, J. S. Murray and T. Clark, Halogen bonding: an electrostatically-driven highly directional noncovalent interaction, *Phys. Chem. Chem. Phys.*, 2010, **12**, 7748.
226 P. Hobza, K. Müller-Dethlefs, and Royal Society of Chemistry (Great Britain), *Non-covalent interactions: theory and experiment*, RSC Pub., Cambridge, U.K., 2010.
227 T. Brinck, J. S. Murray and P. Politzer, Surface electrostatic potentials of halogenated methanes as indicators of directional intermolecular interactions, *Int. J. Quantum Chem.*, 1992, **44**, 57–64.
228 T. Clark, M. Hennemann, J. S. Murray and P. Politzer, Halogen bonding: the σ-hole: Proceedings of "Modeling interactions in biomolecules II", Prague, September 5th–9th, 2005, *J. Mol. Model.*, 2007, **13**, 291–296.

229 J. S. Murray, K. E. Riley, P. Politzer and T. Clark, Directional Weak Intermolecular Interactions: σ-Hole Bonding, *Aust. J. Chem.*, 2010, **63**, 1598.
230 J. M. L. Martin and G. de Oliveira, Towards standard methods for benchmark quality *ab initio* thermochemistry—W1 and W2 theory, *J. Chem. Phys.*, 1999, **111**, 1843–1856.
231 C. Corminboeuf, Minimizing Density Functional Failures for Non-Covalent Interactions Beyond van der Waals Complexes, *Acc. Chem. Res.*, 2014, **47**, 3217–3224.
232 K. E. Riley, M. Pitoňák, P. Jurečka and P. Hobza, Stabilization and Structure Calculations for Noncovalent Interactions in Extended Molecular Systems Based on Wave Function and Density Functional Theories, *Chem. Rev.*, 2010, **110**, 5023–5063.
233 J.-D. Chai and M. Head-Gordon, Long-range corrected hybrid density functionals with damped atom–atom dispersion corrections, *Phys. Chem. Chem. Phys.*, 2008, **10**, 6615.
234 S. Grimme, Accurate description of van der Waals complexes by density functional theory including empirical corrections, *J. Comput. Chem.*, 2004, **25**, 1463–1473.
235 J.-D. Chai and M. Head-Gordon, Systematic optimization of long-range corrected hybrid density functionals, *J. Chem. Phys.*, 2008, **128**, 084106.
236 J. C. Sancho-García and C. Adamo, Double-hybrid density functionals: merging wavefunction and density approaches to get the best of both worlds, *Phys. Chem. Chem. Phys.*, 2013, **15**, 14581.
237 L. Goerigk, A. Hansen, C. Bauer, S. Ehrlich, A. Najibi and S. Grimme, A look at the density functional theory zoo with the advanced GMTKN55 database for general main group thermochemistry, kinetics and noncovalent interactions, *Phys. Chem. Chem. Phys.*, 2017, **19**, 32184–32215.
238 L. Goerigk and S. Grimme, Double-hybrid density functionals: Double-hybrid density functionals, *Wiley Interdiscip. Rev. Comput. Mol. Sci.*, 2014, **4**, 576–600.
239 B. S. D. R. Vamhindi and A. Karton, Can DFT and ab initio methods adequately describe binding energies in strongly interacting C6X6···C2X π–π complexes?, *Chem. Phys.*, 2017, **493**, 12–19.
240 T. H. Dunning, A Road Map for the Calculation of Molecular Binding Energies, *J. Phys. Chem. A*, 2000, **104**, 9062–9080.
241 B. Brauer, M. K. Kesharwani, S. Kozuch and J. M. L. Martin, The S66x8 benchmark for noncovalent interactions revisited: explicitly correlated ab initio methods and density functional theory, *Phys. Chem. Chem. Phys.*, 2016, **18**, 20905–20925.
242 P. Hobza, H. L. Selzle and E. W. Schlag, *A b i n i t i o* calculations on the structure, stabilization, and dipole moment of benzene···Ar complex, *J. Chem. Phys.*, 1991, **95**, 391–394.
243 J. Makarewicz, Well-balanced basis sets for second-order Møller–Plesset treatment of argon-aromatic molecule complexes, *J. Chem. Phys.*, 2004, **121**, 8755–8768.
244 J. S. García, É. Brémond, M. Campetella, I. Ciofini and C. Adamo, Small Basis Set Allowing the Recovery of Dispersion Interactions with Double-Hybrid Functionals, *J. Chem. Theory Comput.*, 2019, **15**, 2944–2953.
245 J. Řezáč, K. E. Riley and P. Hobza, Benchmark Calculations of Noncovalent Interactions of Halogenated Molecules, *J. Chem. Theory Comput.*, 2012, **8**, 4285–4292.
246 I. S. Youn, D. Y. Kim, W. J. Cho, J. M. L. Madridejos, H. M. Lee, M. Kołaski, J. Lee, C. Baig, S. K. Shin, M. Filatov and K. S. Kim, Halogen−π Interactions between Benzene and X_2 /CX_4 (X = Cl, Br): Assessment of Various Density Functionals with Respect to CCSD(T), *J. Phys. Chem. A*, 2016, **120**, 9305–9314.
247 F. Weigend and R. Ahlrichs, Balanced basis sets of split valence, triple zeta valence and quadruple zeta valence quality for H to Rn: Design and assessment of accuracy, *Phys. Chem. Chem. Phys.*, 2005, **7**, 3297.
248 K. E. Riley, M. Vazquez, C. Umemura, C. Miller and K.-A. Tran, Exploring the (Very Flat) Potential Energy Landscape of R−Br···π Interactions with Accurate CCSD(T) and SAPT Techniques, *Chem. – Eur. J.*, 2016, **22**, 17690–17695.
249 G. Santra, N. Sylvetsky and J. M. L. Martin, Minimally Empirical Double-Hybrid Functionals Trained against the GMTKN55 Database: revDSD-PBEP86-D4, revDOD-PBE-D4, and DOD-SCAN-D4, *J. Phys. Chem. A*, 2019, **123**, 5129–5143.
250 A. Austin, G. A. Petersson, M. J. Frisch, F. J. Dobek, G. Scalmani and K. Throssell, A Density Functional with Spherical Atom Dispersion Terms, *J. Chem. Theory Comput.*, 2012, **8**, 4989–5007.

251 L. A. Burns, Á. V.- Mayagoitia, B. G. Sumpter and C. D. Sherrill, Density-functional approaches to noncovalent interactions: A comparison of dispersion corrections (DFT-D), exchange-hole dipole moment (XDM) theory, and specialized functionals, *J. Chem. Phys.*, 2011, **134**, 084107.

252 M. K. Kesharwani, D. Manna, N. Sylvetsky and J. M. L. Martin, The X40×10 Halogen Bonding Benchmark Revisited: Surprising Importance of (*n* –1)d Subvalence Correlation, *J. Phys. Chem. A*, 2018, **122**, 2184–2197.

253 J. K. Nørskov, F. Abild-Pedersen, F. Studt and T. Bligaard, Density functional theory in surface chemistry and catalysis, *Proc. Natl. Acad. Sci.*, 2011, **108**, 937–943.

254 L. Rao, X. Xu and C. Adamo, Theoretical Investigation on the Role of the Central Carbon Atom and Close Protein Environment on the Nitrogen Reduction in Mo Nitrogenase, *ACS Catal.*, 2016, **6**, 1567–1577.

255 F. Himo, T. Lovell, R. Hilgraf, V. V. Rostovtsev, L. Noodleman, K. B. Sharpless and V. V. Fokin, Copper(I)-Catalyzed Synthesis of Azoles. DFT Study Predicts Unprecedented Reactivity and Intermediates, *J. Am. Chem. Soc.*, 2005, **127**, 210–216.

256 P.-F. Loos, N. Galland and D. Jacquemin, Theoretical 0–0 Energies with Chemical Accuracy, *J. Phys. Chem. Lett.*, 2018, **9**, 4646–4651.

257 L. Goerigk and S. Grimme, A General Database for Main Group Thermochemistry, Kinetics, and Noncovalent Interactions − Assessment of Common and Reparameterized (*meta* -)GGA Density Functionals, *J. Chem. Theory Comput.*, 2010, **6**, 107–126.

258 L. Goerigk and S. Grimme, Efficient and Accurate Double-Hybrid-Meta-GGA Density Functionals—Evaluation with the Extended GMTKN30 Database for General Main Group Thermochemistry, Kinetics, and Noncovalent Interactions, *J. Chem. Theory Comput.*, 2011, **7**, 291–309.

259 G. Talarico, P. H. M. Budzelaar, V. Barone and C. Adamo, A theoretical study of the competition between ethylene insertion and chain transfer in cationic aluminum systems, *Chem. Phys. Lett.*, 2000, **329**, 99–105.

260 D. H. Ess, S. E. Wheeler, R. G. Iafe, L. Xu, N. Çelebi-Ölçüm and K. N. Houk, Bifurcations on Potential Energy Surfaces of Organic Reactions, *Angew. Chem. Int. Ed.*, 2008, **47**, 7592–7601.

261 Z. Yang, X. Dong, Y. Yu, P. Yu, Y. Li, C. Jamieson and K. N. Houk, Relationships between Product Ratios in Ambimodal Pericyclic Reactions and Bond Lengths in Transition Structures, *J. Am. Chem. Soc.*, 2018, **140**, 3061–3067.

262 X.-S. Xue, C. S. Jamieson, M. Garcia-Borràs, X. Dong, Z. Yang and K. N. Houk, Ambimodal Trispericyclic Transition State and Dynamic Control of Periselectivity, *J. Am. Chem. Soc.*, 2019, **141**, 1217–1221.

263 H.-H. Chuang, D. J. Tantillo and C.-P. Hsu, Construction of Two-Dimensional Potential Energy Surfaces of Reactions with Post-Transition-State Bifurcations, *J. Chem. Theory Comput.*, 2020, **16**, 4050–4060.

264 S. Lee and J. M. Goodman, Rapid Route-Finding for Bifurcating Organic Reactions, *J. Am. Chem. Soc.*, 2020, **142**, 9210–9219.

265 C. S. Jamieson, A. Sengupta and K. N. Houk, Cycloadditions of Cyclopentadiene and Cycloheptatriene with Tropones: All *Endo* -[6+4] Cycloadditions Are Ambimodal, *J. Am. Chem. Soc.*, 2021, **143**, 3918–3926.

266 N. Mardirossian and M. Head-Gordon, *ω* B97M-V: A combinatorially optimized, range-separated hybrid, meta-GGA density functional with VV10 nonlocal correlation, *J. Chem. Phys.*, 2016, **144**, 214110.

267 M. J. Frisch, G. W. Trucks, H. B. Schlegel, G. E. Scuseria, M. A. Robb, J. R. Cheeseman, G. Scalmani, V. Barone, G. A. Petersson, H. Nakatsuji, X. Li, A. V. Marenich, M. Caricato, J. Bloino, B. G. Janesko, J. Zheng, R. Gomperts, B. Mennucci, H. P. Hratchian, J. V. Ortiz, A. F. Izmaylov, J. L. Sonnenberg, D. Williams-Young, F. Ding, F. Lipparini, F. Egidi, J. Goings, B. Peng, A. Petrone, T. Henderson, D. Ranasinghe, V. G. Zakrzewski, J. Gao, N. Rega, G. Zheng, W. Liang, M. Hada, M. Ehara, K. Toyota, R. Fukuda, J. Hasegawa, M. Ishida, T. Nakajima, Y. Honda, O. Kitao, H. Nakai, T. Vreven, K. Throssell, J. A. Montgomery, Jr., J. E. Peralta, F. Ogliaro, M. J. Bearpark, J. J. Heyd, E. N. Brothers, K. N. Kudin, V. N. Staroverov, T. A. Keith, R. Kobayashi, J. Normand, K. Raghavachari, A. P. Rendell, J. C. Burant, S. S. Iyengar, J. Tomasi, M. Cossi, J. M. Millam, M. Klene, C. Adamo, R. Cammi, J. W. Ochterski, R. L. Martin, K. Morokuma, O. Farkas, J. B. Foresman, and D. J. Fox, Gaussian, Inc., Wallingford CT, 2020.M. J. Frisch, G. W. Trucks, H. B. Schlegel, G. E. Scuseria, M. A. Robb, J. R. Cheeseman, G. Scalmani, V. Barone, G. A. Petersson, H. Nakatsuji, X. Li, A. V. Marenich, M. Caricato, J. Bloino, B. G. Janesko, J. Zheng, R. Gomperts, B. Mennucci, H. P. Hratchian, J. V. Ortiz, A. F. Izmaylov, J. L. Sonnenberg, D. Williams-Young, F. Ding, F. Lipparini, F. Egidi, J. Goings, B. Peng, A. Petrone,

T. Henderson, D. Ranasinghe, V. G. Zakrzewski, J. Gao, N. Rega, G. Zheng, W. Liang, M. Hada, M. Ehara, K. Toyota, R. Fukuda, J. Hasegawa, M. Ishida, T. Nakajima, Y. Honda, O. Kitao, H. Nakai, T. Vreven, K. Throssell, J. A. Montgomery, Jr., J. E. Peralta, F. Ogliaro, M. J. Bearpark, J. J. Heyd, E. N. Brothers, K. N. Kudin, V. N. Staroverov, T. A. Keith, R. Kobayashi, J. Normand, K. Raghavachari, A. P. Rendell, J. C. Burant, S. S. Iyengar, J. Tomasi, M. Cossi, J. M. Millam, M. Klene, C. Adamo, R. Cammi, J. W. Ochterski, R. L. Martin, K. Morokuma, O. Farkas, J. B. Foresman, and D. J. Fox., *Gaussian Development Version, Revision J.19,* Gaussian, Inc., Wallingford CT, 2020, 2021.

268 T. H. Dunning, Gaussian basis sets for use in correlated molecular calculations. I. The atoms boron through neon and hydrogen, *J. Chem. Phys.*, 1989, **90**, 1007–1023.

269 É. Brémond, H. Li, Á. J. Pérez-Jiménez, J. C. Sancho-García and C. Adamo, Tackling an accurate description of molecular reactivity with double-hybrid density functionals, *J. Chem. Phys.*, 2022, **156**, 161101.

270 J. L. Bao, Y. Wang, X. He, L. Gagliardi and D. G. Truhlar, Multiconfiguration Pair-Density Functional Theory Is Free From Delocalization Error, *J. Phys. Chem. Lett.*, 2017, **8**, 5616–5620.

271 C. Li, X. Zheng, N. Q. Su and W. Yang, Localized orbital scaling correction for systematic elimination of delocalization error in density functional approximations, *Natl. Sci. Rev.*, 2018, **5**, 203–215.

RÉSUMÉ

La détermination des interactions faibles dominées par la dispersion, est un enjeu majeur pour la bonne description des molécules de van der Waals, des forces à longue portée et de certains systèmes complexes. Une nouvelle classe de fonctionnelle « double hybride » (DH), a récemment été développée pour remédier à certaines des difficultés rencontrées par les modèles DFT traditionnelles, pour la définition de ces interactions non-covalentes. L'objectif de cette thèse est de mieux comprendre les interactions non-covalentes calculées à partir de fonctionnelles non empiriques. Grâce à un protocole de calcul alliant une fonctionnelle double hybride (PBE-QIDH ou B2-PLYP), une correction empirique de dispersion (D3) et une petite base à valence séparée développée spécialement pour les interactions non-covalentes (DH-SVPD), nous avons calculé les énergies de « bond separation reaction » avec une erreur inférieure à 1,0 kcal/mol. Ce protocole, appelé DH*thermo*, a pu être transféré à d'autres systèmes pour calculer, entre autres, les énergies de réaction ainsi que les enthalpies des réactions isodesmiques, produisant à nouveau une très faible erreur par rapport aux résultats expérimentaux et aux méthodes quantiques plus avancées. Ce protocole opératoire a ensuite été élargi avec succès aux systèmes halogénés. Ainsi, ce travail montre l'avenir prometteur des fonctionnelles non-empiriques dans la modélisation des interactions non covalentes.

MOTS CLÉS

Interactions non covalentes, Fonctionnelles double-hybrides, Modélisation, Précision chimique

ABSTRACT

Weak interactions dominated by dispersion are important for van der Waals molecules, long-range forces, and some complex systems. A new class of functionals, called Double Hybrids (DH), have been developed more recently, to cure some of the difficulties encountered by more traditional DFT models. The purpose of this thesis is to better understand the non-covalent interactions with the non-empirical functionals. Firstly, an accuracy on Bond Separation Reaction (BSR) energies beyond the commonly-accepted threshold for chemical applications (errors ≤ 1.0 kcal/mol) can be obtained using a protocol combining a double-hybrid functional, such as PBE-QIDH or B2PLYP, with a D3-like empirical correction and a small split-valence basis set, DH-SVPD. This protocol, which is named DH*thermo*, is not further tuned on the selected systems and is able to correctly reproduce, with exceptionally low errors, both reaction energies and enthalpies for selected isodesmic reactions. And further tests on some difficult systems on this proposed protocol, also show the reliability of this protocol, then, we enlarged this protocol to the Halogen systems. The study of these cases confirms that the nonempirical functionals show a promising future in modeling noncovalent interactions.

KEYWORDS

Non-covalent interactions, Double-hybrid Functionals, Modelling, Chemical accuracy